DOE/BC/14938-16
(OSTI ID: 776907)

ADVANCED RESERVOIR CHARACTERIZATION IN THE ANTELOPE SHALE TO ESTABLISH THE VIABILITY OF CO_2 ENHANCED OIL RECOVERY IN CALIFORNIA'S MONTEREY FORMATION SILICEOUS SHALES

Annual Report
February 7, 2000-February 6, 2001

By:
Pasquale R. Perri

Date Published: April 2001

Work Performed Under Contract No. DE-FC22-95BC14938

Chevron USA Production Company
Bakersfield, California

National Energy Technology Laboratory
National Petroleum Technology Office
U.S. DEPARTMENT OF ENERGY
Tulsa, Oklahoma

DOE/BC/14938-16
Distribution Category UC-122

Advanced Reservoir Characterization in the Antelope Shale to Establish the Viability of Co_2 Enhanced Oil Recovery in California's Monterey Formation Siliceous Shales

By
Pasquale R. Perri

April 2001

Work Performed Under Contract DE-FC22-95BC14938

Prepared for
U.S. Department of Energy
Assistant Secretary for Fossil Energy

Gary D. Walker, Project Manager
National Petroleum Technology Office
P.O. Box 3628
Tulsa, OK 74101

Prepared by
Chevron USA Production Company
5001 California Avenue
Bakersfield, CA 93309

TABLE OF CONTENTS

LIST OF FIGURES

LIST OF TABLES

ABSTRACT

This report describes the evaluation, design, and implementation of a DOE funded CO_2 pilot project in the Lost Hills Field, Kern County, California. The pilot consists of four inverted (injector-centered) 5-spot patterns covering approximately 10 acres, and is located in a portion of the field, which has been under waterflood since early 1992. The target reservoir for the CO_2 pilot is the Belridge Diatomite. The pilot location was selected based on geology, reservoir quality and reservoir performance during the waterflood. A CO_2 pilot was chosen, rather than full-field implementation, to investigate uncertainties associated with CO_2 utilization rate and premature CO_2 breakthrough, and overall uncertainty in the unproven CO_2 flood process in the San Joaquin Valley.

A summary of the design and objectives of the CO_2 pilot are included along with an overview of the Lost Hills geology, discussion of pilot injection and production facilities, and discussion of new wells drilled and remedial work completed prior to commencing injection.

Actual CO_2 injection began on August 31, 2000 and a comprehensive pilot monitoring and surveillance program has been implemented. This report summarizes the injection and production performance and the monitoring results to date including oil geochemistry, CO_2 injection tracers, crosswell electromagnetic surveys, crosswell seismic, CO_2 injection profiling, cased hole resistivity, tiltmetering results, and corrosion monitoring results. The results presented in this report may be applicable to evaluate and design other potential San Joaquin Valley CO_2 floods.

ACKNOWLEDGMENTS

I would like to thank the following individuals for their help and participation on this project: John Cooney, William Fong, Dale Julander, Gregg Molesworth, Michael Morea, Deborah Piceno, and Renee Stahl of Chevron U.S.A. Production Company; Mark Emanuele and Dieuhang Tran of Chevron Petroleum Technology Company; Rong Hwang of Chevron Research and Technology Company; Michael Wilt of EMI, Inc.; Earuch Broacha of ProTechnics; Barry Kirkendall and Jeffery Roberts of Lawrence Livermore National Laboratory; Sally Benson, Roland Gritto, Thomas Daley, Michael Hoversten, and Ernest Majer of Lawrence Berkeley National Laboratory; David Cole of Oak Ridge National Laboratory and Eric Davis of Pinnacle Technologies, Inc.

EXECUTIVE SUMMARY

Introduction:
The primary objective of our project was to conduct advanced reservoir characterization and modeling studies in the Antelope Shale of the Buena Vista Hills Field. Work was subdivided into two phases or budget periods. The first phase of the project would focus on a variety of advanced reservoir characterization techniques to determine the production characteristics of the Antelope Shale reservoir. Simulation models based on the results of the characterization work would then be used to evaluate how the reservoir would respond to enhanced oil recovery (EOR) processes such as of CO_2 flooding. The second phase of the project would be to implement and evaluate a CO_2 flood in the Buena Vista Hills Field. A successful project would demonstrate the economic viability and widespread applicability of CO_2 flooding in siliceous shale reservoirs of the San Joaquin Valley.

However, it was decided not to proceed with a Phase II field trial in Buena Vista Hills because of its very low oil saturation, lithologic heterogeneity and relatively few natural fractures in the siliceous shale reservoirs. Although Buena Vista Hills turned out to be a poor CO_2 EOR candidate, our reservoir characterization has demonstrated that under the right conditions, CO_2 is a viable enhanced recovery process for other siliceous shales. Therefore, the Phase II CO_2 pilot was moved to Lost Hills Field, about 30 miles north of Buena Vista Hills with the DOE's concurrence.

Lost Hills Field:
The target reservoir at Lost Hills is the Belridge Diatomite of the Monterey Formation. The Belridge Diatomite is a diatomaceous mudstone and is not present at Buena Vista Hills. The diatomite has high oil saturation (50%) and high porosity (45 - 70%), but its low permeability (<1 millidarcy) has led to low primary oil recovery (3 - 4% of OOIP). Due to the low primary recovery and large amount of remaining oil in place, Lost Hills presents an attractive target for EOR. In addition to the large resource base, there is technical and economic justification for CO_2 flooding that was developed through our reservoir characterization and simulation efforts. CO_2 flood production forecasts were generated using Chevron's proprietary reservoir simulation software. The simulation results indicate a tremendous oil response associated with CO_2 flooding. This is mainly due to the improved injectivity with CO_2. CO_2 injectivity is at least two to three times greater than that of water or steam. Two other favorable mechanisms associated with CO_2 injection are reservoir oil viscosity reduction and increased fluid expansion.

Preliminary economics for full-scale implementation of a CO_2 Flood in Lost Hills has identified several key uncertainties, which will be evaluated as part of the pilot demonstration. The main economic uncertainties that can only be further evaluated by the pilot are oil response, and the corresponding CO_2 utilization required for such a response. The pilot has been designed and implemented to significantly reduce the range of uncertainty for these two key items.

Funding is also included in this project to further evaluate the feasibility and cost of local long-term CO_2 supplies. Since it is very unlikely that a CO_2 pipeline to California will be built anytime soon, success of a full-scale CO_2 flood will depend on utilization of CO_2 entrained in local produced gas and flue gas. Global warming and future world emission trading of CO_2 credits may drastically increase the availability and lower the cost of CO_2 in California. As part of project scoping, the CO_2 Team will continue to track developments for global warming.

Background & Present Situation:

The Lost Hills Field, located 45 miles northwest of Bakersfield, California, was discovered in 1910. Reserves in the shallow sands, diatomite, and chert pools were developed using slotted liner completion techniques until the late 1970's. From the late 1970's to 1987, small volume hydrofracture completions were performed covering the entire Belridge Diatomite.

Advances in hydraulic fracturing technology in the late 1980's resulted in increased oil recovery that led to a more aggressive development program by Chevron. From 1987 to the present, high volume hydrofracture completions have been performed across the entire Belridge Diatomite and the Upper Brown Shale resulting in significant production increases. The Lost Hills Field is developed on a 5 acre (siliceous shale) to 1.25 acre (diatomite) well spacing. There are over 2.2 billion barrels of oil in place in the Belridge Diatomite in Lost Hills. To date only 112 million barrels have been produced, or approximately 5% of the original oil in place (OOIP).

Chevron initiated a pilot diatomite waterflood project in December 1990 and began full-project development in April 1992. Since 1992, two hundred and eight 2-1/2 acre patterns have been put on water injection spanning parts of four sections (Sections 4, 5, 32 Fee, and 33). Since the initiation of first project water injection in April 1992, production has increased approximately 4,000 BOPD from 6,400 BOPD to the current rate of 10,400 BOPD.

CO_2 Pilot Installation:

During the year 2000, Chevron installed a four-pattern, 2.5 acre pilot on Section 32 Fee to evaluate the potential of CO_2 flooding the Lost Hills Diatomite. The pilot installation included remedial work to evaluate and upgrade the tubing and packers in the existing injectors. Two existing injection wells were successfully repaired. Three observation wells and two replacement injection wells were drilled and completed. In 2000, the CO_2 facility construction was completed for the well gauging and the liquid CO_2 injection facilities. The pilot construction and all associated well work were completed and CO_2 injection commenced on August 31, 2000. A comprehensive CO_2 monitoring program has been put in place and baseline surveys taken prior to the injection of CO_2. The pilot will be evaluated for a period of approximately 18 months or until February 28, 2002.

Objectives:
A CO_2 a pilot was installed in Section 32 Fee of the Lost Hills field to test the technical and economic viability of CO_2 flooding the low permeability diatomite resource. A full-scale CO_2 project is economically justified by an incremental analysis and comparison to the current base case waterflood. Incremental tertiary reserves are estimated to be 80 MMBOEG and are technically supported by reservoir simulation. However, the project is only marginally economic and considerable uncertainty exists in the magnitude of predicted CO_2 recoveries. Installing a pilot will provide us with an opportunity to gather and analyze the pertinent geologic, reservoir, and production data and gather facilities design information necessary to commit to a full-field project. In addition, the pilot capital and operating costs will take advantage of available DOE funding of nearly 2.7 million dollars. The following are the main objectives of the recently installed CO_2 pilot:

- Gain information that could benefit other drive mechanisms in Diatomite such as steamflooding and fireflooding.
- Learn how injecting a gas (very low viscosity fluid) differs from injecting water into the diatomite in terms of fracture azimuth, injectivity, and areal and vertical sweep.
- Mitigation measures for CO_2 breakthrough problems can be applied to other IOR operations.
- Learn how much of the diatomite pay zone can effectively be processed. This knowledge can be applied to other IOR process designs.
- Learn how to mitigate and/or control hydrofracture growth (vertically and areally).
- Potential Federal Regulations may make CO_2 a "free" commodity 5 to 10 years down the road. Injecting CO_2 may be used to offset emissions from other nearby Chevron facilities.

Pilot Operation:
CO_2 injection commenced on August 31, 2000. CO_2 injection began slowly at 50 MCF/D per injector as we de-bugged and became acquainted with the new facilities. We continued to increase CO_2 injection rates slowly to the target rate of 500 MSCF/D per injector to prevent any premature CO_2 breakthrough. Through December 31, 2000, 116,460 MCF of CO_2 has been injected at the average rate of 239 MCF/D per injector. An initial oil response was observed in one well (11-8E) as a result of the CO_2 injection. Pre-mature breakthrough has not been a problem since we have completed nearly four months of continuos injection without any producer showing a significant increase in the concentration of CO_2 production in the produced gas. However, the initial oil response in well 11-8E has been curtailed due to a recent sanding problem with it and several other pilot producers. It appears that the CO_2 injection may have played a role in the sanding problems. These wells remain shut-in as remediation programs are being developed to correct these problems.

Pilot Monitoring and Surveillance:
In order to gauge the CO_2 pilot's performance, a comprehensive monitoring and surveillance program has been developed. The following discussion summarizes the major accomplishments in 2000 as a result of the comprehensive CO_2 monitoring program.

An interwell tracer program is being carried out by ProTechnics in the CO_2 pilot area. Four gas phase interwell tracers were injected into four CO_2 injection wells. A review of the analyses performed on the collected produced gas samples from the thirteen producing wells in the Lost Hills CO_2 pilot area program indicates that tracer has arrived at six of these wells. These low tracer recoveries for the first 38 days of the program tend to indicate that no direct, large scale channeling of the injected CO_2 is occurring in the pilot area.

An electromagnetic (EM) survey was conducted by Electromagnetic Instruments, Inc., from August 2-3, 2000 at the Lost Hills CO_2 pilot area. The crosswell EM survey provided an excellent baseline resistivity distribution prior to the CO_2 flood. We can clearly see which layers the water has penetrated and also deduce what rates it is moving. The survey also clearly indicates the effect of the waterflood on the section showing that it has concentrate largely in the diatomite units and has largely bypassed the silts. It is also clearly more effective in deeper horizons indicating that the penetration is probably a function of the pressure. This suggests that the present waterflood penetrates quite slowly and could be effectively monitored by one or two measurements per year at most. However, the effect of the CO_2 flooding is largely unknown and the first repeat measurement will be approximately six months after full-scale injection has begun.

In August 2000, crosswell electromagnetic (EM) imaging was deployed by Lawrence Livermore National Laboratory (LLNL) at the Lost Hills CO_2 pilot area. The objective of their research project is to develop the ability to image subsurface injected CO_2 during EOR processes while simultaneously discriminating between pre-existing petroleum and water deposits. They are currently combining laboratory and field methods to image a pilot CO_2 sequestration EOR site using the cross-borehole EM technique, improve the inversion process in CO_2 studies by coupling results with petrophysical laboratory measurements, and focus on new gas interpretation techniques. This project directly addresses energy issues in two ways: 1) the development of field and laboratory techniques to improve in-situ analysis of oil and gas enhanced recovery operations and 2) provides a tool for in-situ analysis of CO_2 sequestration, a technical issue of growing importance. In April 2001, this deployment will be duplicated and the data will be processed and compared to show any change in the subsurface between the two dates. After the April 2001 deployment, LLNL will be able to compare laboratory and field data to suggest an initial procedure to interpreting CO_2 sequestration with electromagnetic induction techniques.

Geochemical characterization has been conducted on produced oils that were sampled periodically from selected producing wells located in the CO_2 flood pilot area of the Lost Hills field. The objective is to determine if formation of solids, specifically elemental sulfur, has been induced by CO_2 injection to the reservoir. The analytical results of the recent oil samples (second set) taken in December 2000 and in January 2001 are comparable to those of the earlier samples (first set) taken in August 2000 shortly before the start of CO_2 injection. Little changes in bulk properties of the oils including API gravity, total sulfur %,

and asphaltene % indicate that there are no significant changes in oil chemistry caused by CO_2 injection for over 3 months. Elemental sulfur is absent in all the oils produced from wells in the pilot area prior to CO_2 injection. No elemental sulfur was found in the second set of oil samples either. Thus, CO_2 injection has so far not caused formation of elemental sulfur. The results indicate that the oils in the pilot area, based on bulk properties, have remained virtually unchanged after CO_2 injection for over three months. This suggests the interaction between oil and CO_2 in the reservoir has been fairly weak.

Oak Ridge National Laboratory (ORNL) participates in the GEO-SEQ project funded jointly by NETL to LBNL, LLNL, and ORNL. The overall goal of the ORNL effort is to provide methods that utilize the power of natural and introduced tracers to decipher the fate and transport of CO_2 injected into the subsurface. The resulting data will be used to calibrate and validate predictive models used for (1) estimating CO_2 residence time, reservoir storage capacity, and storage mechanisms; (2) testing injection scenarios for process optimization; and (3) assessing the potential leakage of CO_2 from the reservoir. In order to use the stable isotope compositions of carbon and oxygen in CO_2 as effective tracers during the injection tests we need to understand how these isotopes partition as a consequence of different process pathways (e.g., mineral reactions; sorption; aqueous dissolution). In 2000, ORNL investigated one important isotopic partitioning pathway, that of CO_2 interacting with hydrocarbon-saturated rock (an EOR injection scenario). They obtained hydrocarbon-bearing core from Chevron's Lost Hills field (Well OB-7). Four samples were selected for study. The preliminary conclusion drawn is that a light isotopic component of CO_2 may be retained in the reservoir leading to progressively heavier isotopic CO_2 farther down the flow path. Clearly, more effort is needed to quantify how these isotopes fractionate as a function of temperature, PCO_2, surface area, hydrocarbon composition, mineral composition, solid to volatile mass ratios, and presence of H_2O.

Injection profiles were run in all four injectors in September 2000 to determine vertical conformance of CO_2. Profiles indicate where CO_2 is exiting the wellbore. An "excellent" profile would be one that had CO_2 exiting all the perforations in equal amounts of CO_2. A "poor" injection profile would be one that had uneven distribution or portions of the wellbore receiving no CO_2. Two injectors (wells 11-8WR and 12-8W) have poor injection profiles with most of the CO_2 exiting the upper perforations. Two injectors (wells 11-8WAR and 12-7W) had good profiles. Well 12-7W has the best injection profile of the four injectors, clearly showing that CO_2 has no preference for silt-rich or diatom-rich lithologies. The poorer injection profiles in the other wells could be due to blocked perforations, preference for lower pressure zones, or poor hydraulic fractures.

In January 2001 resistivity logs were run in the fiberglass cased OB-C1 and OB-C2 observation wells. The purpose of this logging was to compare these logs with the baseline surveys that were taken in both wells prior to CO_2 injection, and to monitor changes in resistivity due to CO_2 injection. The OB-C1 is located 60 feet (bottom hole location), and the OB-C2 is located 30 feet (bottom hole location) on either side of the 11-8WR injector. Both wells are situated perpendicular to 11-8WR's hydraulic propped fracture azimuth. A comparison of the open and cased hole logs in OB-C2 showed that there had been a subtle change in resistivity (~1 unit reduction in oil saturation) due to CO_2 injection. A similar

comparison using open and cased hole logs in OB-C1 showed that there were larger changes in the deep resistivity curves in some intervals. These changes in resistivity equate to oil reductions in the 1 to 4 saturation unit range. Two preliminary observations that can be made: 1) CO_2 has reduced the oil saturation in both diatomite and sandy diatomite, and 2) CO_2 has made its way out of the injection interval (FF – L) and migrated up into the C unit. What is interesting about the log monitoring surveys in the two observation wells is that OB-C1 is twice as far away from the injector 11-8WR as OB-C2, and CO_2 has caused a greater oil saturation reduction in OB-C1 than OB-C2. Subsequent monitoring efforts (cased hole logs, electromagnetics, etc.) will help to further understand the distribution pattern of CO_2 in the reservoir.

Lawrence Berkeley National Laboratory (LBNL) has collected three borehole seismic data sets in the Lost Hills CO2 pilot area using the observation wells OB-C1 and OB-C2. In general, diatomite has a fairly complicated seismic wave propagation due to the high porosity and mixed pore fluid (oil, water and gas). The detection and delineation of CO_2 will be combined with understanding the overall wave propagation properties of diatomite. LBNL's goal is to demonstrate through field testing, techniques for imaging subsurface CO_2 and for monitoring geologic sequestration. CO_2 has been used by the oil industry for many years to enhance oil production. Previous studies in carbonate reservoirs have shown that seismic velocity changes are caused by CO_2 injection and that these changes can be spatially mapped using crosswell seismic surveys. The seismic velocity change can be up to 10%, which is easily detectable and mappable with modern crosswell seismic surveys. Therefore, borehole seismic surveys hold great promise for mapping and long term monitoring of sequestered CO_2. LBNL has obtained preliminary 2-D tomographic images of velocity for both pre-injection seismic crosswell experiments. The most important aspect of these data sets is that they represent a baseline measurement of reservoir properties before CO_2 injection. The complexities of the diatomite reservoir make direct measurement of one property (such as CO_2 concentration) very difficult. However, time-lapse changes measured against this baseline survey, should be controlled by CO_2 injection and flow properties. The post-injection surveys should begin in spring of 2001. It is the time-lapse changes in seismic properties that should be most useful in monitoring and mapping CO_2 in the subsurface.

As part of LBNL's work on carbon sequestration in geologic formations, they are conducting numerical modeling and field data acquisition of crosswell seismic and electromagnetic (EM) data at Chevron's Lost Hills CO_2 injection pilot. Numerical forward models have been generated from reservoir flow simulations provided by Chevron. The objective of the modeling works is to provide an understanding of the relationships between the reservoir parameters, the fluid and CO_2 saturations and the observed geophysical data that will be used to monitor the injection process. The relationships developed through forward modeling will then be used to interpret the field data in terms of fluid saturations and CO_2 content. LBNL is only in the initial stages of forward and inverse modeling. So far they are working with the pre-injection model to explore the relations between the reservoir flow simulations and the geophysical data taken prior to injection. Future work will include modeling the geophysical response to CO_2 injection.

A dedicated pressure observation well was drilled and completed for the CO_2 pilot (OB-C3). It contains a "short string" and a "long string" to monitor average reservoir pressure changes during the pilot. We have been measuring reservoir pressure on a monthly basis since commencing CO_2 injection on August 31, 2000. We are perplexed why the short string (shallower) reads higher that the long string (deeper). In addition, the pressure observation well readings are significantly lower than RFT pressure data taken from pilot producer 12-8D in 1999. A recent tracer injection test into the pressure observation well indicated the possibility of a poor cement bond. We hope to substantiate these results and possibly implement cement-squeezing techniques to rectify the problem.

In December of 2000 a series of shut-ins were conducted on each of the four injection wells (11-8WR, 11-WAR, 12-8W and 12-7W) to determine the tilt signal that would be induced by a closing fracture system. This type of analysis requires that all activities in other wells continue as normal, so that the "background signal" from these other activities remains the same. If only one CO_2-injection well is shut-in at the time, the change in tilt signal will reflect the "image" of the closing fracture. Unfortunately, these conditions were NOT met due to accidental power outages that occurred quickly after each of the four shut-ins, which is the period used for background data. The power outages caused ALL of the field injection and production activities to suddenly stop. These power outages, where all injection and production activities in the field suddenly stop, largely "overwhelm" the changes in surface tilt signals that are induced by the shut-in at individual CO_2-injection wells. As a result, the azimuth and dip uncertainties generated by these power outages are much larger than normal. Therefore, there is higher uncertainty in the tilt induced from the shut-in in the individual well. As a result, the vector maps for the CO_2 injectors, which comprise the tilt from multiple surface tilt sites, do not show the familiar pattern associated with hydraulic fracture growth.

A corrosion monitoring program has been implemented to determine the impact of produced CO_2, in higher concentrations, on our existing facilities. It will help us determine what facilities and flowlines would need to be replaced or upgraded, due to CO_2 corrosion, if the pilot is successful. If excessive corrosion is detected, we will attempt to mitigate it utilizing chemicals. If necessary, some flowlines and facilities will be replaced. Mitigation measures will be scaled up to evaluate facility costs (capital and operating expenditures) for full-field CO_2 development.

The following report is a complete summary of the CO_2 pilot activities in 2000 including an overview of the Lost Hills geology, current field development plans, CO_2 pilot installation and facilities, early pilot performance, reservoir simulation, and a discussion of the comprehensive pilot monitoring and surveillance program that has been implemented.

SECTION 1

GEOLOGY

1.1 GEOLOGIC OVERVIEW OF LOST HILLS

Michael F. Morea
Chevron USA Production Company

Structure:
Lost Hills Field was discovered in 1910 and is located 40 miles northwest of Bakersfield, CA (Figures 1.1-1 and 2). Productive intervals include Middle to Upper Miocene chert, porcelanite, siliceous shale, and diatomite, and Plio-Pleistocene sands. The field is situated along a northwest-southeast trending series of structural highs that begins with the Coalinga Anticline to the northwest and culminates with the Lost Hills Anticline to the southeast. This series of highs roughly parallels folds of similar age on the westside of the San Joaquin Valley. These folds are oriented nearly parallel to the trend of the San Andreas Fault to the west and approximately perpendicular to the direction of regional compression.

Lost Hills oil is trapped at the crest and along the southeast plunge of the anticline (Figures 1.1-3 and 4). In this portion of the field where the pilot is located, the structural plunge varies from 2 to 6° toward the southeast. Dips along the northeast flank average around 30° while those on the southwest flank average around 15 to 20°. This asymmetry in dips in the NE-SW direction is consistent with a fault-bend fold model (Medwedeff, 1989). Evidence from onlapping sediments shows the Lost Hills Anticline began to grow during the deposition of the Etchegoin Formation and continued into the Holocene. The resulting anticline is perched above a ramp thrust that is located around 13,000 feet below the surface. Numerous northeast-southwest trending normal faults with throws rarely exceeding 40 feet cut the Lost Hills structure. These faults do not appear to have a major impact on production.

Stratigraphy and Sedimentation:
The stratigraphy at Lost Hills is shown in Figures 1.1-5 and 6. The Monterey Formation is comprised of the Devilwater/Gould Shale, McLure Shale and Reef Ridge members. The Devilwater/Gould consists of clay shales and siliceous shales. It is slightly phosphatic. The McLure is subdivided into the McDonald Shale and the Antelope Shale. The McDonald consists of interbedded porcelanites and siliceous shales. It is also slightly phosphatic. The Antelope is comprised of finely laminated cherts and porcelanites. The uppermost member of the Monterey Formation is the Reef Ridge and it is subdivided into the Brown Shale and Belridge Diatomite. The Brown Shale is made up of interbedded siliceous shale, shale, and silt. The Belridge Diatomite consists of interbedded diatomaceous mudstone, fine-grained, argillaceous sands/silts, and porcelanite.

Based on regional studies of late Miocene paleogeography and paleobathymetry, the rocks of the Monterey Formation were mainly deposited in a deep marine environment (Graham and Williams, 1985). In the San Joaquin Basin, the late Miocene environment was such that: water depths were bathyal (between 600 and 3,000 feet), cool water temperatures and upwelling in the upper 200 feet supported large diatom populations, and the deeper basin waters were oxygen poor. Two primary sedimentation processes were active in the basin at that time. First, hemipelagic sedimentation: the settling of diatom frustules and clay-sized

particles onto the basin floor from the overlying water column. And second, turbidite sedimentation: the deposition of sand, silt, and clay-sized particles carried into the basin by density currents (usually originating along the basin margins).

This combination of environmental conditions and sedimentation processes led to the accumulation of thick deposits of organic-rich, laminated, diatomaceous sediments which occasionally are interrupted by thin-bedded, clastic-rich turbidite deposits. However, compared to the southwestern San Joaquin Basin, sandy turbidites at Lost Hills are not common. The Monterey Formation in the San Joaquin Basin differs from the coastal and offshore Monterey in that it is much more clastic rich.

The composition of the Monterey can be described in terms of three primary components: biogenic silica, clay, and silt/sand. As shown in Table 1.1-1, there is a fair amount of vertical compositional variation within the stratigraphic column at Lost Hills. The Devilwater contains 27% biogenic silica, 50% clay, and 23% silt/sand. The McDonald is slightly richer in biogenic silica, roughly comparable in clay, and slightly lower in silt/sand. The Antelope is very rich in biogenic silica, poor in clay, and poor in silt/sand. The Brown Shale is clay rich. The Belridge Diatomite has roughly equal amounts of biogenic silica, clay and silt/sand. The overlying Etchegoin Formation is rich in silt/sand and clay, and almost totally lacking in biogenic silica.

Table 1.1-1. Average rock compositions from Well 166, Section 32, T26S/R21E.

Rock Unit	Average. % Biogenic Silica	Average % Clay	Average % Silt/Sand	Number of Samples
Etchegoin	4	38	58	8
Belridge Diatomite	33	36	31	19
Brown Shale	26	47	27	28
Antelope Shale	61	18	21	14
McDonald Shale	34	47	19	24
Devilwater/Gould Shale	27	50	23	8

Diagenesis:

As hemipelagic and occasional turbidite deposits in the Lost Hills area were buried by the overlying Etchegoin and Tulare sediments, the diatomaceous sediments of the Monterey Formation gradually lithified into the highly porous (50-60% or more) but low permeability (0.1-10.0 millidarcy) rock termed diatomite. As discussed above, anywhere from 26% to 61% of this diatomite was composed of diatom frustules. Diatom frustules consist of a form of silica called opal-A, which is an unstructured mineral (essentially a solidified gel) usually containing 3-10% water. As this diatomite is buried deeper and reaches greater temperatures (~ 45° C), the opal-A material in the diatom frustule becomes unstable and undergoes a phase transition (Keller and Issacs, 1985) to opal-CT (Figures 1.1-7 and 8). This form of silica is more structured than opal-A and has released much of its water. Porosity is reduced to about 40%. At still greater depths and higher temperatures (~ 80° C), the opal-CT undergoes a final phase transition to a form of quartz with only a trace of water left. The Monterey Formation at Lost Hills is presently comprised of opal-A rocks at shallow depths ($\pm$ 2,300 feet or shallower), opal-CT rocks at intermediate depths ($\pm$2,300 to $\pm$ 4,300 feet), and quartz phase rocks below $\pm$ 4300 feet.

The exact temperatures at which the opal-A to opal-CT and opal-CT to quartz phase changes occur is governed by the amount of biogenic silica (diatoms) in the rock. Opal-A rocks rich in biogenic silica convert to opal-CT at lower temperatures (and therefore shallower depths) than those poor in biogenic silica. Conversely, opal-CT rocks rich in biogenic silica convert to quartz phase at higher temperatures (and greater depths) than those poor in biogenic silica (higher clay content). For this reason, an interval of rocks whose laminations vary in their biogenic silica content create a transition zone (~ 100') of alternating phase changes near the phase transition temperature. These alternating beds of opal-A and opal-CT or opal-CT and quartz (particularly where the beds are thin) may be especially susceptible to natural fracturing, thereby enhancing system permeability. Volume reduction and water expulsion associated with the phase changes probably adds to the fracturing in these zones. In general, hydrocarbons are found in all three (opal-A, opal-CT, and quartz) phases. Also production is enhanced in the opal-A to opal-CT and, in particular, the opal-CT to quartz phase transition zones.

Petroleum Geochemistry:
Geochemical analyses have demonstrated that Monterey Formation rocks in Lost Hills are typically composed of 1% to 6% total organics, making them fair to good hydrocarbon source rocks. Studies of kerogen maturation have shown that the Monterey rocks are immature (i.e., they have not been buried deep enough to generate oil) within the confines of the Lost Hills Field. However, studies of samples taken from down-flank wells indicate that these rocks are mostly mature in the syncline to the east of Lost Hills and possibly below the ramp thrust immediately beneath the Lost Hills Anticline. Because the Monterey Formation kerogens and the produced oils at Lost Hills have similar isotopic compositions, and because they contain similar concentrations of sulfur, it is believed that Lost Hills oil was sourced from the Monterey Formation itself.

Hydrocarbons migrated into the low permeability Monterey rocks at Lost Hills by way of faults, fractures and thin sands. Also the opal-A to opal-CT and opal-CT to quartz phase transition zones with their higher fracture density probably served as pathways for hydrocarbons to migrate from source beds down-structure to their ultimate resting place in the crest of the anticline.

In the McDonald Shale and Lower Brown Shale/Antelope Shale pools, hydrocarbons are confined fairly well within or immediately below the fractured opal-CT to quartz phase transition rocks. In the Upper Brown Shale, fracturing also helps to make it productive. Because the McDonald, Antelope, and Brown shales have such low matrix permeability, most of the oil produced from these rocks comes out of the fractures. In the Belridge Diatomite with its relatively higher matrix permeability, hydrocarbons have saturated the uppermost opal-CT, the opal-A to opal-CT transition, and most of the opal-A rocks. Most of the oil produced from the diatomite comes from the matrix. Lastly, oil has also migrated into the overlying Etchegoin and Tulare Formations.

Belridge Diatomite at Lost Hills:
The Belridge Diatomite is comprised of varying amounts of biogenic silica, clay, and silt/sand, and ranges in depth from 800 to 3,000 feet (Figure 1.1-9). The diatomite has high

porosity (40 - 65%) and low permeability (<1 – 10 millidarcies). Oil saturation ranges from 40% to 65% in opal-A, and from 10% to 30% in opal-CT (Table 1.1-2). Oil gravity ranges from 28 to 18° API.

Table 1.1-2. Comparison of rock types at the pilot location (Lost Hills) and at the original location in Buena Vista Hills.

Parameter	Lost Hills Pilot	Buena Vista Hills Pilot
Rock Unit	Belridge Diatomite	Upper Antelope Shale
Age	Uppermost Miocene	Upper Miocene
Depositional Environment	Hemipelagic; Progradational Slope	Hemipelagic-Turbidite; Basin
Rock Type	Diatomaceous Mudstone	Siliceous Shale
Silica Phase	Opal-A	Opal-CT
Percent Sand Beds	30%	5%
Sand Description	5-60 feet thick, fine-grained, argillaceous, bioturbated	<1 inch thick, fine-grained, non-bioturbated
Depth to Top of Unit	1,400 feet	4,200 feet
Thickness	700 feet	600 feet
Porosity	50%	29%
Permeability	0.1 – 10.0 millidarcies	<0.1 millidarcies
Oil Saturation	50%	14%

At Lost Hills, the Belridge Diatomite (opal-A) is informally subdivided into three lithology types: clean, sandy, and clayey diatomite (Fast and others, 1993). These designations are based on bulk density log cutoffs and are supported by core and rock geochemistry. Clean diatomite has bulk density values 1.6 gm/cc or less. Sandy diatomite has bulk density values greater than 1.75 gm/cc. Clayey diatomite has bulk density values between 1.6 and 1.75 gm/cc.

The clean and clayey portions of the Belridge Diatomite are finely laminated. In general these laminations alternate between a more detritus-rich lamina and a more diatomaceous-rich lamina. The laminations reflect cyclic variations in yearly runoff (detritus-rich) and upwelling (diatomaceous-rich).

The clean and clayey diatomites were deposited under oxygen poor to anoxic conditions that could sustain only a limited sediment-dwelling fauna. Thus laminations are preserved in the diatomites (Figures 1.1-10 and 11). Sandy diatomites, on the other hand, were deposited under oxygen poor to oxygenated conditions. Sandy diatomites were originally deposited as interlaminated sands and clays but shortly after deposition were heavily bioturbated.

Superimposed on the yearly depositional cycling was the deposition of sedimentary packages that reflect changes in relative sea level. During the Late Miocene, diatomaceous sediments were deposited from the outer shelf to the basin floor in the San Joaquin Basin. At Lost Hills, diatom frustules and clay particles settled onto the upper slope environment from the overlying water column. As sea level rose, diatomaceous rich deposits were deposited further up on the slope. As sea level fell, sandy diatomite deposits prograded down the slope. (In the northern half of Lost Hills Field, the Belridge Diatomite grades into the shallow water clastics of the Etchegoin Formation.) These fluctuations in sea level caused the larger scale deposition of sedimentary units of clean diatomite, clayey diatomite, and sandy diatomite.

Lastly, superimposed on these relative sea level changes was the overall progradation and coarsening upward of the Belridge Diatomite and the eventual filling in of the basin in the Pliocene.

The fluctuations in relative sea level led to the deposition of a series of parasequences (Perri and others, 2000). Lithologic and trace fossil evidence from cores indicates that at least three sequence boundaries, or their equivalents, can be recognized in the Belridge Diatomite (Figure 1.1-12): L PT (base Belridge Diatomite), BH PT, and D PT (top Belridge Diatomite).

Fractures and Thief Zones:
There are two types of fractures in Lost Hills: natural and man-made. In general, all diatomite wells are hydraulically propped-fractured in order to increase production from the low permeability, diatomite reservoir. To efficiently develop the field, surface tiltmeters have been used to determine hydraulic fracture azimuths. The average fracture azimuth is N50E and ideally, wells are placed along a grid pattern that is aligned to that azimuth. Occasionally hydraulic fracturing of a new producer causes an existing producer to sand-up or there is an increase in water production if an injection well communicates with a producer. Hydraulic fractures intersecting existing wells can be the result of many factors. These include: 1) wells closely spaced and in fracture alignment; 2) presence of existing faults/fractures; and 3) localized areas of depletion due to production, or localized areas of re-pressurization from injection that cause the hydraulic fracture to propagate at an azimuth that is not aligned with the natural stress field.

Recent analysis of natural fractures by D. Julander using Electrical Micro Imaging (EMI) logs from the OB-7 and 12-8D wells allowed for observations to be made regarding their abundance and distribution (Figures 1.1-13 - 14). The EMI from the CO_2 injectivity test well 12-8D is fairly representative of this part of the Lost Hills Field. It shows a fracture frequency between 1 and 3 fractures per 10 feet of vertical interval. This fracture frequency includes all observable fractures: open, closed (clay-filled), and fractures of undeterminable type (due to being poorly imaged). This data indicates that the diatomite is not highly fractured in this part of the field.

With regards to thief zones, i.e., high permeability sands interbedded within the diatomite, there does not appear to be much evidence to support this idea. Recent data from the nearby OB-7 well (1,160 feet SW of 12-8D) clearly exemplifies this. OB-7 was drilled and cored only 20 feet (perpendicular to fracture azimuth) from a water injection well (10-9W) that was drilled in 1994. Core PKS data clearly showed that the sandy diatomites from OB-7 do not have highly reduced oil saturations as compared to the original nearby injector. This would be expected from a sand bed that was close to an injector and highly permeable. As stated above and illustrated in Figures 1.1-12 and 13, the sandy diatomites are clay rich and bioturbated. These features make it very difficult to behave as a thief zone. Also, the CO_2 injection profiles from wells 12-8D (injectivity test) and 12-7W also showed that CO_2 does not have a strong preference for the sandy diatomites.

In summary, while there are fractures and faults present in the diatomite, the reservoir should not be considered a highly fractured reservoir. However it should also be said that based on

CO_2 and waterflood tracers, it appears that fractures and faults do play a role in the unpredictable distribution of low viscosity fluids at low injection rates.

Overview of Field Development:
Development of the Lost Hills Field has evolved over the years. From 1910 to the late 1970's, slotted liner completions were used in the upper Belridge Diatomite. From the late 1970's to 1987, small volume, hydrofrac completions were performed covering the entire Belridge Diatomite. From 1987 to the present, high volume hydrofrac completions have been performed across the entire Belridge Diatomite and the Upper Brown Shale. Since 1992 a portion of the diatomite has been under waterflood. The field is developed on a 5 acre (siliceous shale) to 0.625-acre (diatomite) well spacing. There are over 2 billion barrels of oil in place in the Belridge Diatomite in Lost Hills. Due to the reservoir's low permeability less than 7% of this oil has been produced.

Subsidence:
Due to the high compressibility of diatomite, the removal of fluids, and the de-pressurizing of the reservoir, Lost Hills has experienced subsidence over a portion of the field. Figure 1.1-15 is a map showing cumulative subsidence between 1989 and 2000. Based on ground positioning satellite (GPS) data, the field has subsided over 8 feet in 12 years. In order to mitigate the subsidence and reduce related wells failures, waterflooding was initiated in the diatomite in the early 1990's. This has greatly reduced the rate of subsidence in the field.

CO_2 Pilot Location:
The pilot is located in Section 32 T26S/R21E. The target reservoir is the FF – L interval of the Belridge Diatomite (Figures 1.1-16 - 18). In the pilot area, the diatomite is in opal-A phase. A fault zone runs NE-SW through the center of the 10-acre pilot. The pilot is divided into four 2.5 acre patterns with four injector and ten producers. There are three observation wells to monitor the pilot.

References:
Fast, R. E., Murer, A. S., and Zambrano, L. G., 1993, Lost Hills Diatomite Simulation Study: Predicting Waterflood Performance in a Low Permeability, Compacting Reservoir, SPE 26627.

Graham, S. A., and Williams, L. A., 1985, Tectonic, depositional, and Diagenetic History of Monterey Formation (Miocene), Central San Joaquin Basin, California, AAPG Bulletin, v. 69, n. 3, p. 385-411.

Keller, M. A., and Issacs, C. M., 1985, An Evaluation of Temperature Scales for Silica Diagenesis in Diatomaceous Sequences Including a New Approach Based on the Miocene Monterey Formation, California, Geo-Marine Letters, v. 5, p. 31-35.

Medwedeff, D. A., 1989, Growth Fault-Bend Folding at Southeast Lost Hills, San Joaquin Valley, California, AAPG Bulletin, v. 73, n. 1, p. 54-67.

Perri, P. R., Emanuele, M. A., Fong, W. S., and Morea, M. F., 2000, Lost Hills CO_2 Pilot: Evaluation, Design, Injectivity Test Results, and Implementation, SPE 62526.

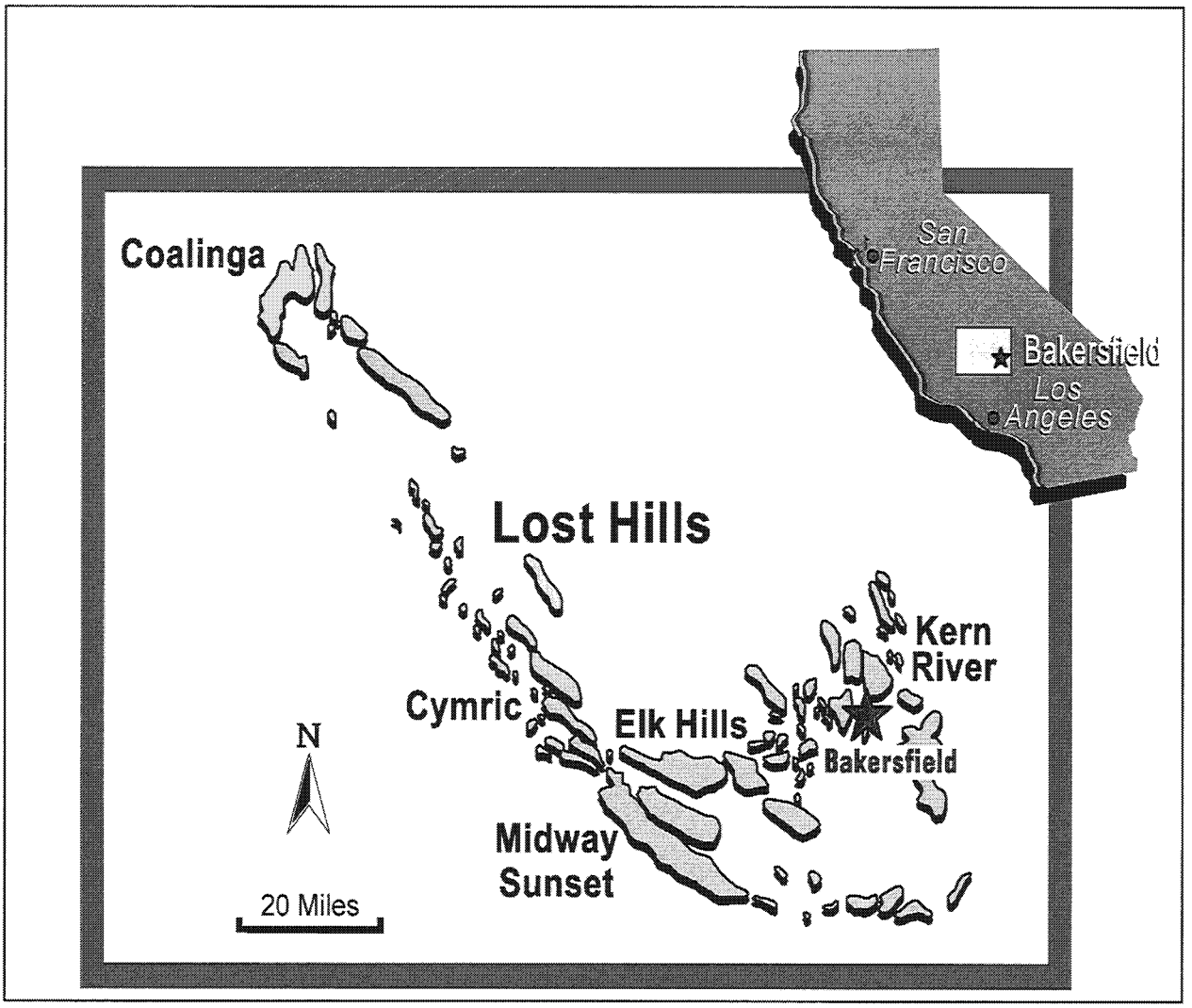

Figure 1.1-1. Location map of major oil fields in the southern San Joaquin Valley. Lost Hills Field is highlighted.

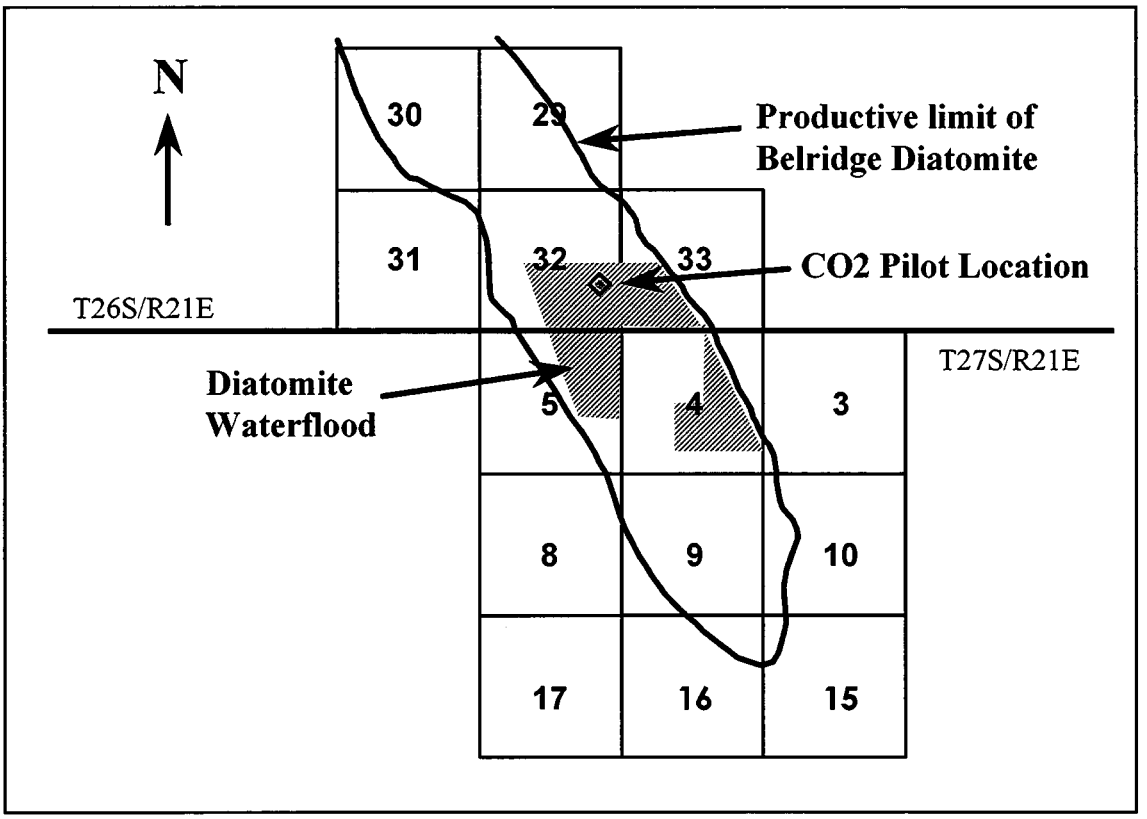

Figure 1.1-2. Productive limits of Belridge Diatomite follows trend of southeast plunge of the Lost Hills Anticline. Chevron diatomite waterflood and CO_2 pilot are also illustrated.

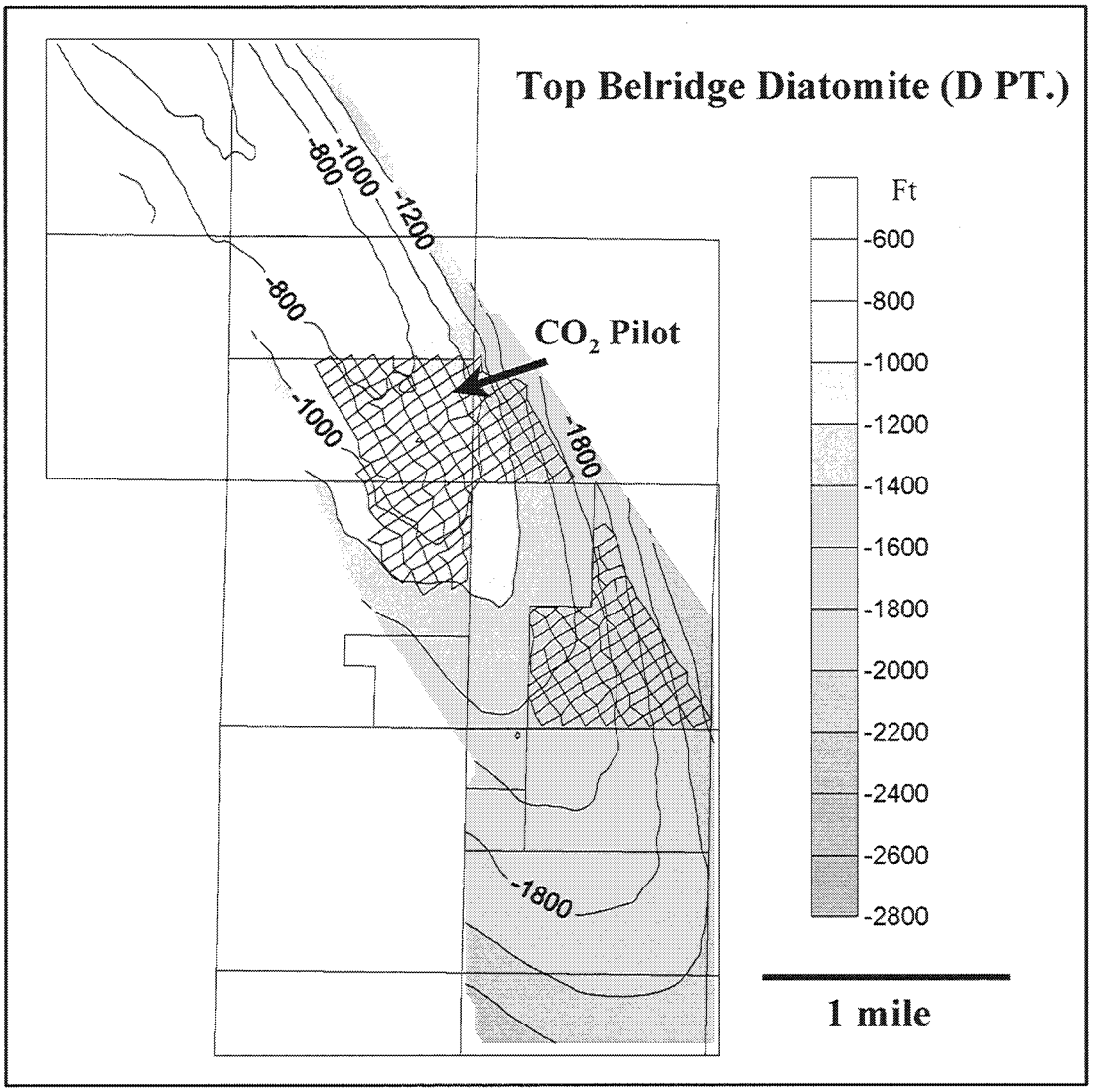

Figure 1.1-3. Lost Hills Top Belridge Diatomite (D Point) Structure Map. Contour Interval 200 Feet.

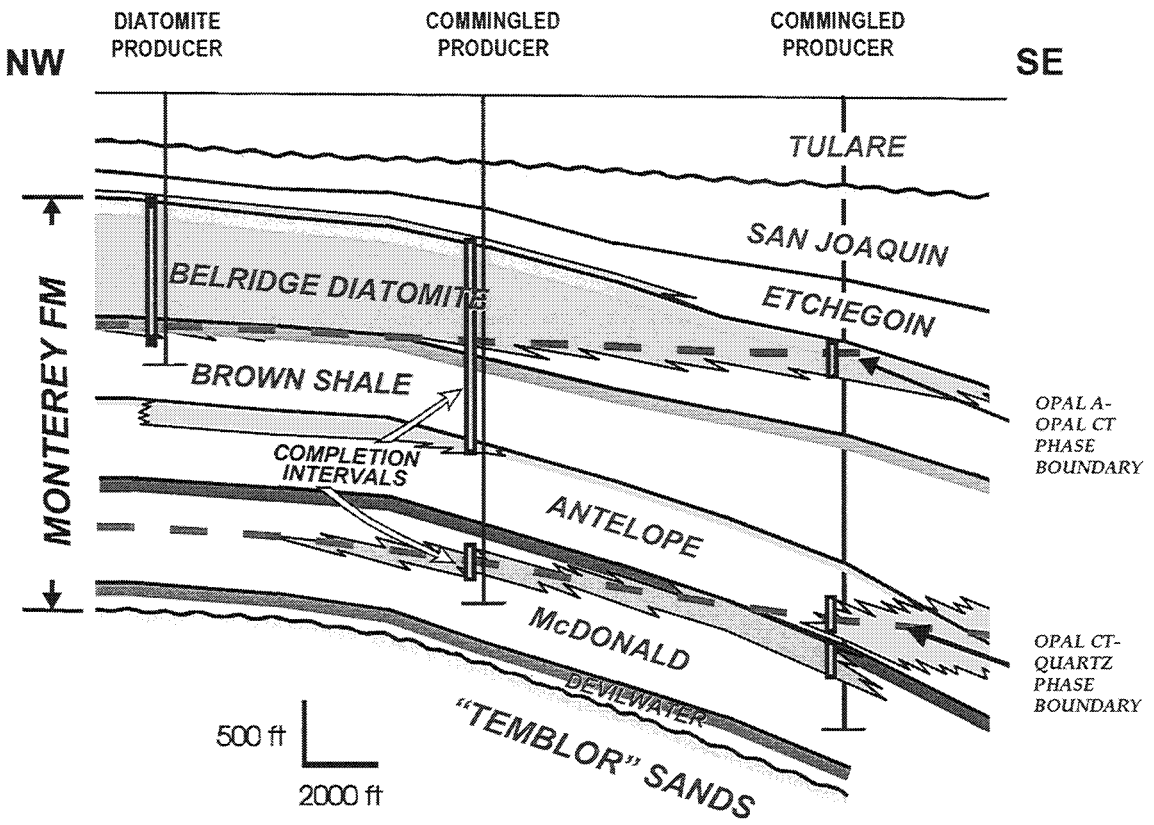

Figure 1.1-4. Generalized cross section along the crest of the southeast plunge of Lost Hills. The Belridge Diatomite is the objective of the CO_2 pilot project.

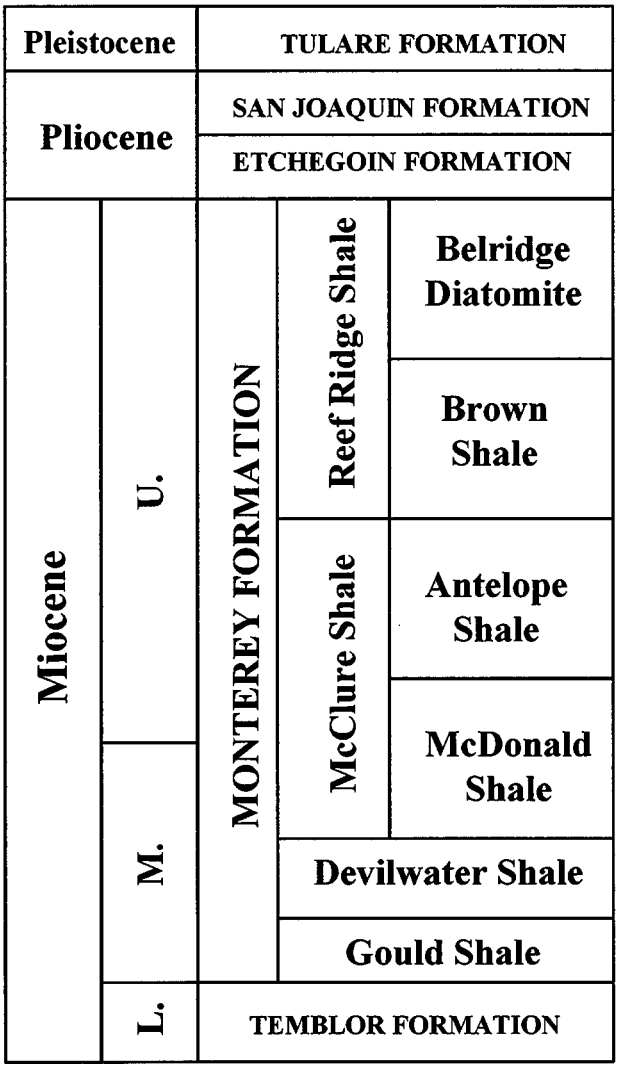

Figure 1.1-5. Monterey Formation stratigraphic column. In the Lost Hills area, the Devilwater and Gould members are undifferentiated and the Reef Ridge is subdivided into the Brown Shale and the Belridge Diatomite. The CO_2 pilot is in the Belridge Diatomite.

Lost Hills Type Log
166 Sec 32 26S/21E

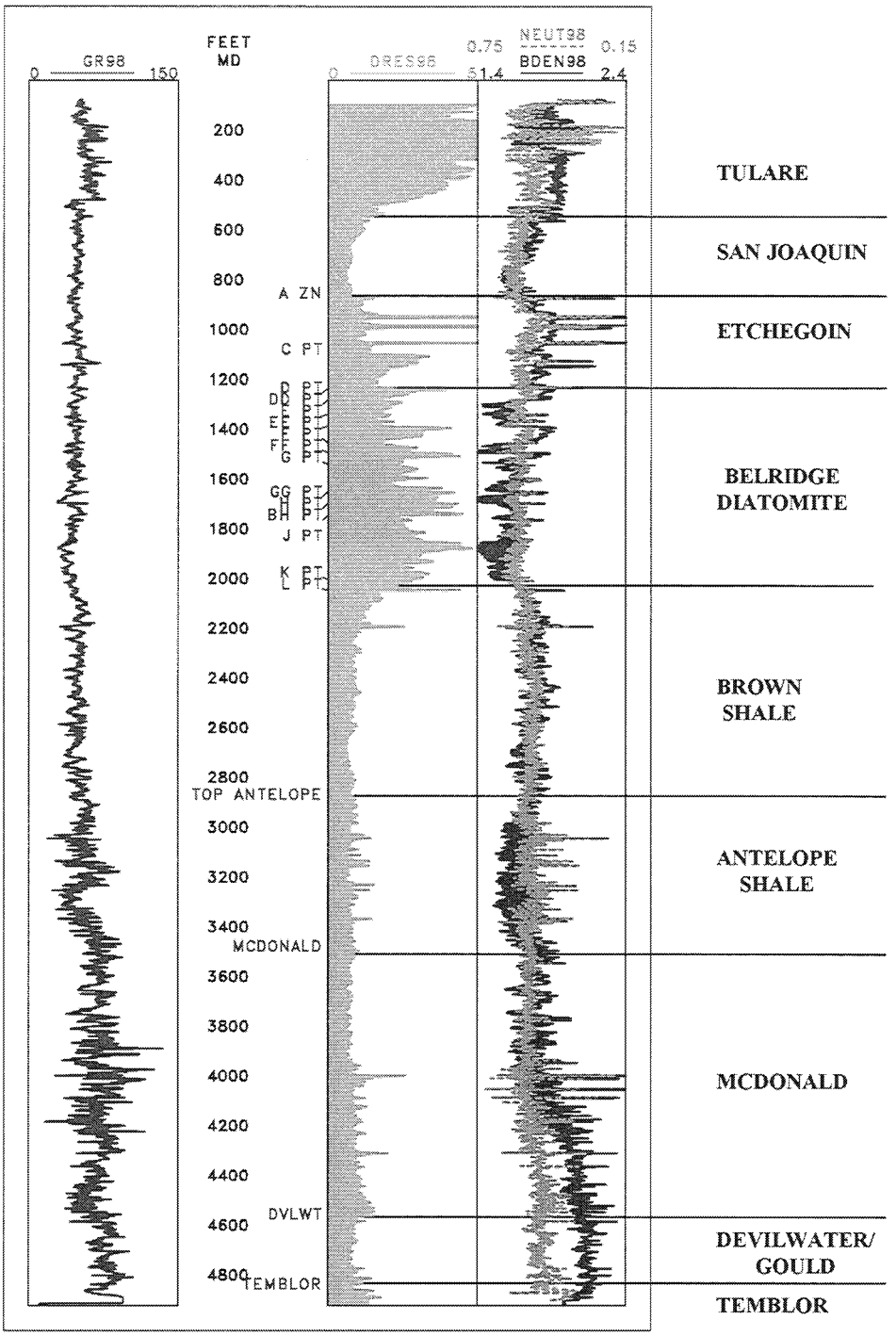

Figure 1.1-6. Lost Hills Type Log. Log tracks from left to right are gamma ray; measured depth; geologic markers; deep resistivity; neutron, and bulk density.

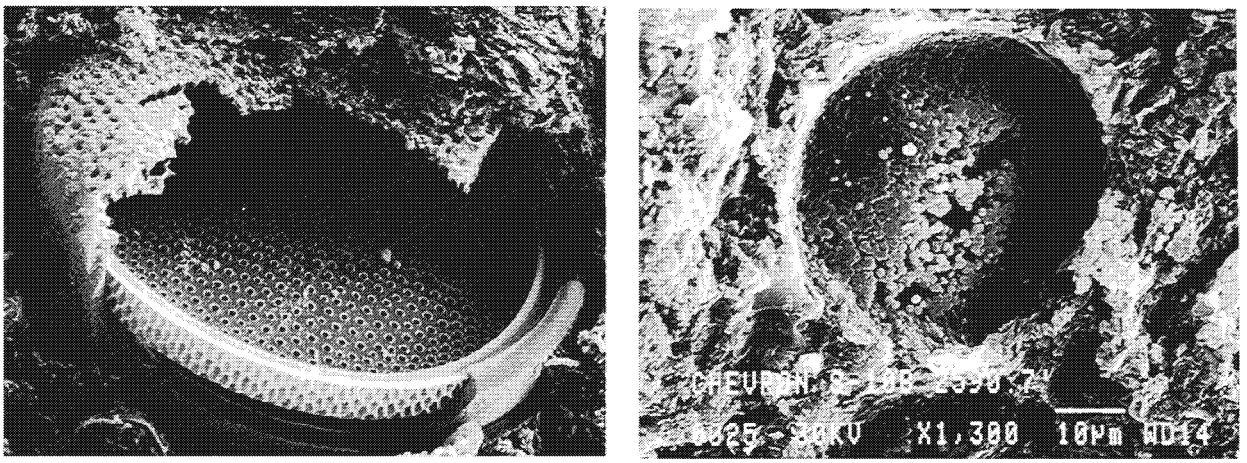

Figure 1.1-7. SEM photomicrographs of opal-A frustule starting to convert to opal-CT (left), and frustule converted to opal-CT (right). 1,300X magnification.

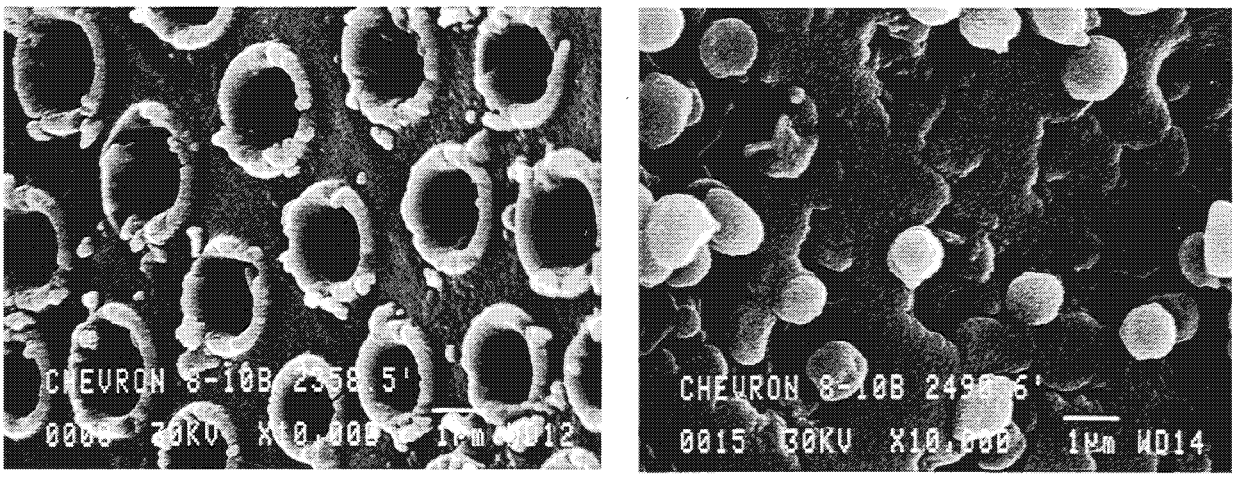

Figure 1.1-8. Opal-A frustule initiating conversion to opal-CT (left), and a frustule after its conversion to opal-CT. SEM photomicrographs, 10,000X magnification.

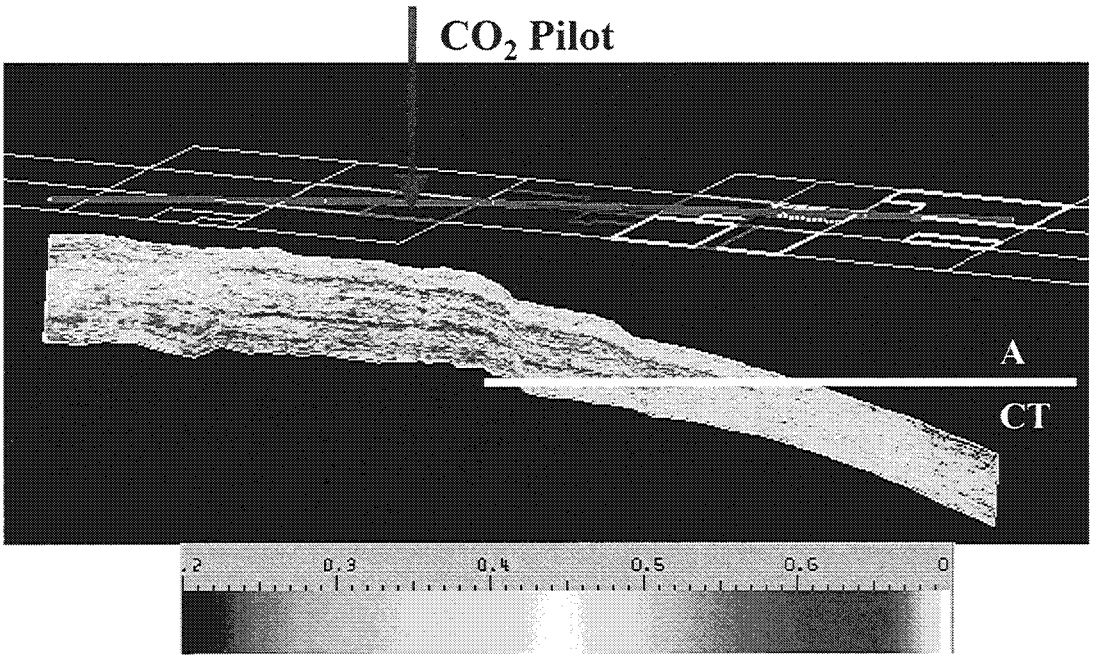

Figure 1.1-9. Cross section showing Belridge Diatomite geostatistical porosity distribution across the southern portion of Lost Hills Field. The overlying map shows the location of the cross section (blue) and the location of the CO_2 pilot in relation to the field. High porosity (red) represents opal-A. The lower porosity (green/yellow on the left, northwest) represents silt/sand. The lower porosity (green/yellow on the right, southeast) represents the conversion from opal-A to opal-CT. From 3D earth model by W. Fong.

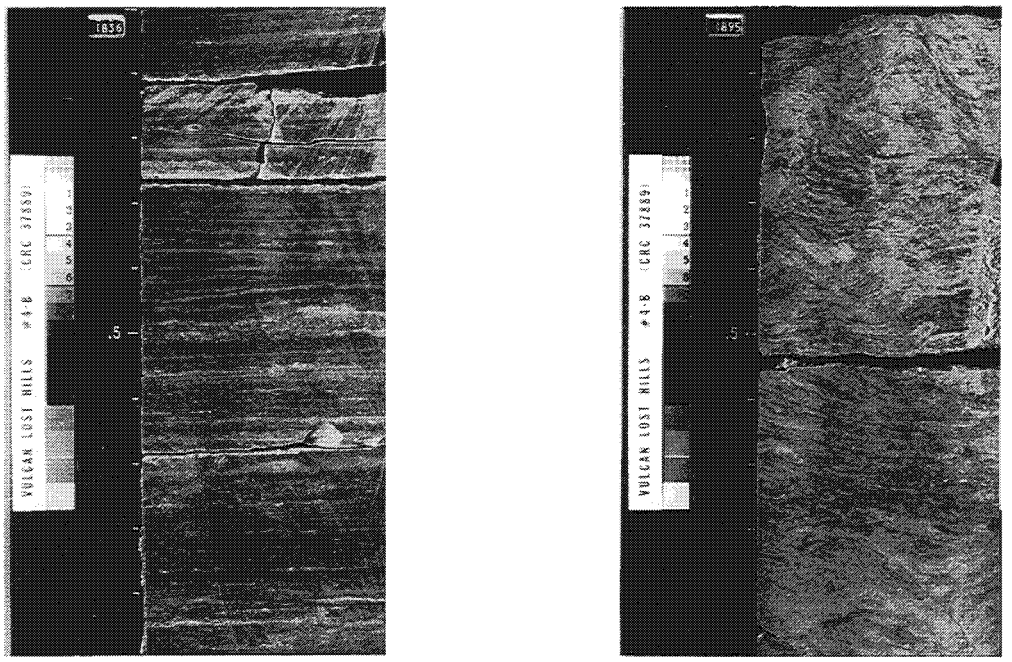

Figure 1.1-10. Slabbed core of laminated diatomite (left), and bioturbated sandy diatomite (right).

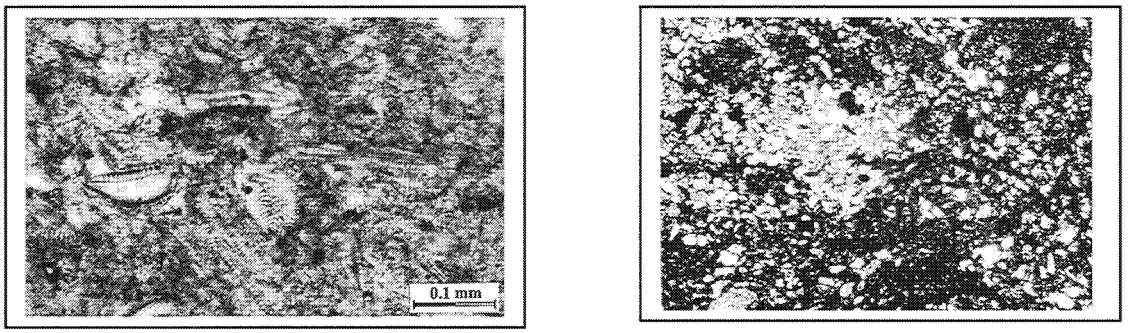

Figure 1.1-11. Thin section photomicrographs of a clean diatomite from the J Unit (left; 200X) and a sandy diatomite from the GG Unit (right; 40X, unpolarized and polarized light). The J unit thin section shows diatoms and porosity in blue. The GG Unit shows "blotchy" sand and porosity due to bioturbation.

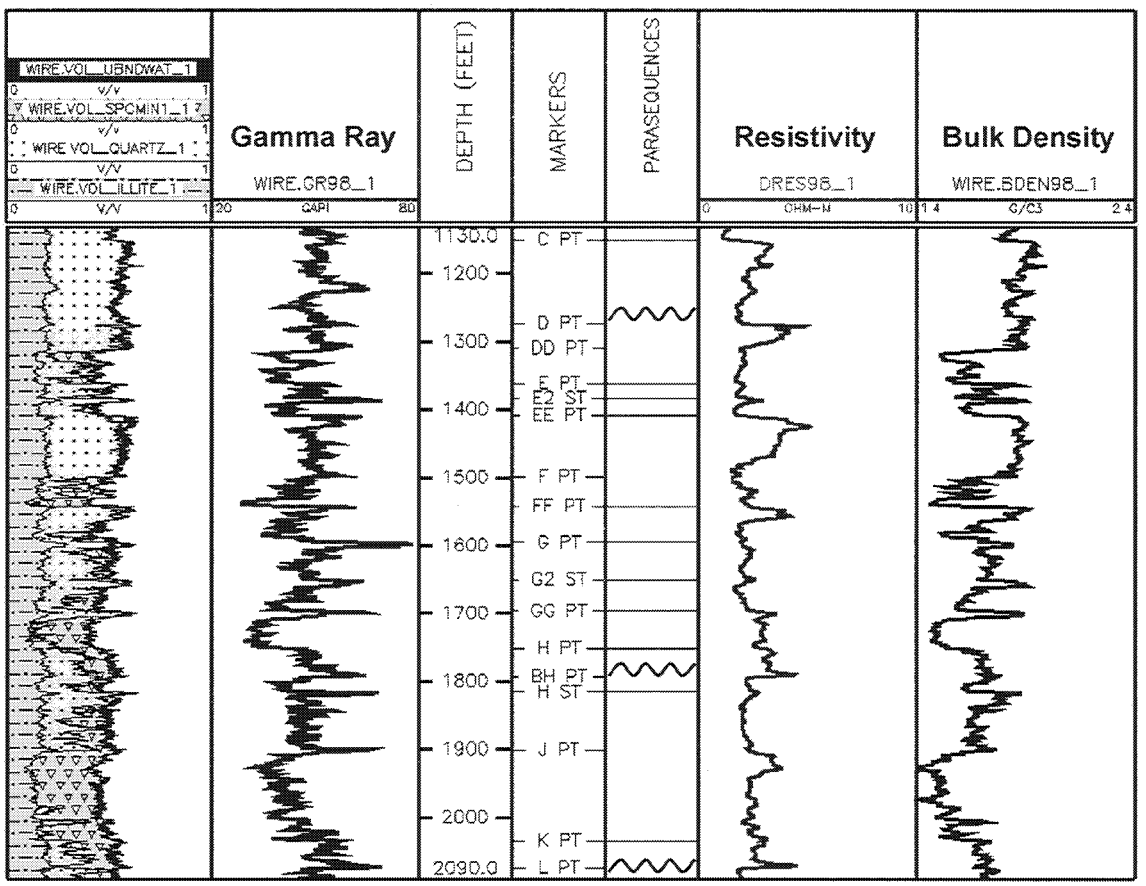

Figure 1.1-12. Log of Well 12-7W illustrating parasequences of the Belridge Diatomite in the Lost Hills pilot location. Log tracks from left to right are % lithology (clay silt/sand, and opal-A); gamma ray; measured depth; geologic markers; parasequence (straight line) and sequence (wavy line) boundaries; deep resistivity, and bulk density.

Figure 1.1-13. Azimuths of natural fractures as measured from the 12-8D EMI log. The CO_2 pilot will target the F-L interval. Note the increase in fractures and change in fracture azimuth in the Upper Brown Shale versus the F-J and J-L intervals. Data is from D. Julander and H. Wu.

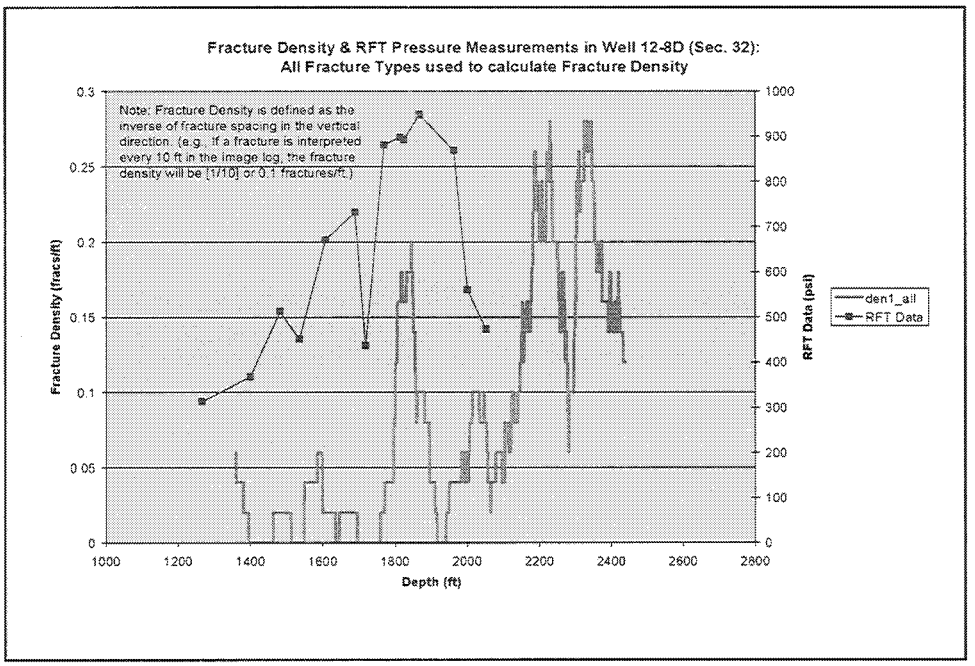

Figure 1.1-14. Halliburton Formation Tester measurements (upper curve) and fracture densities calculated from well 12-8D EMI log. Fracture data is from D. Julander.

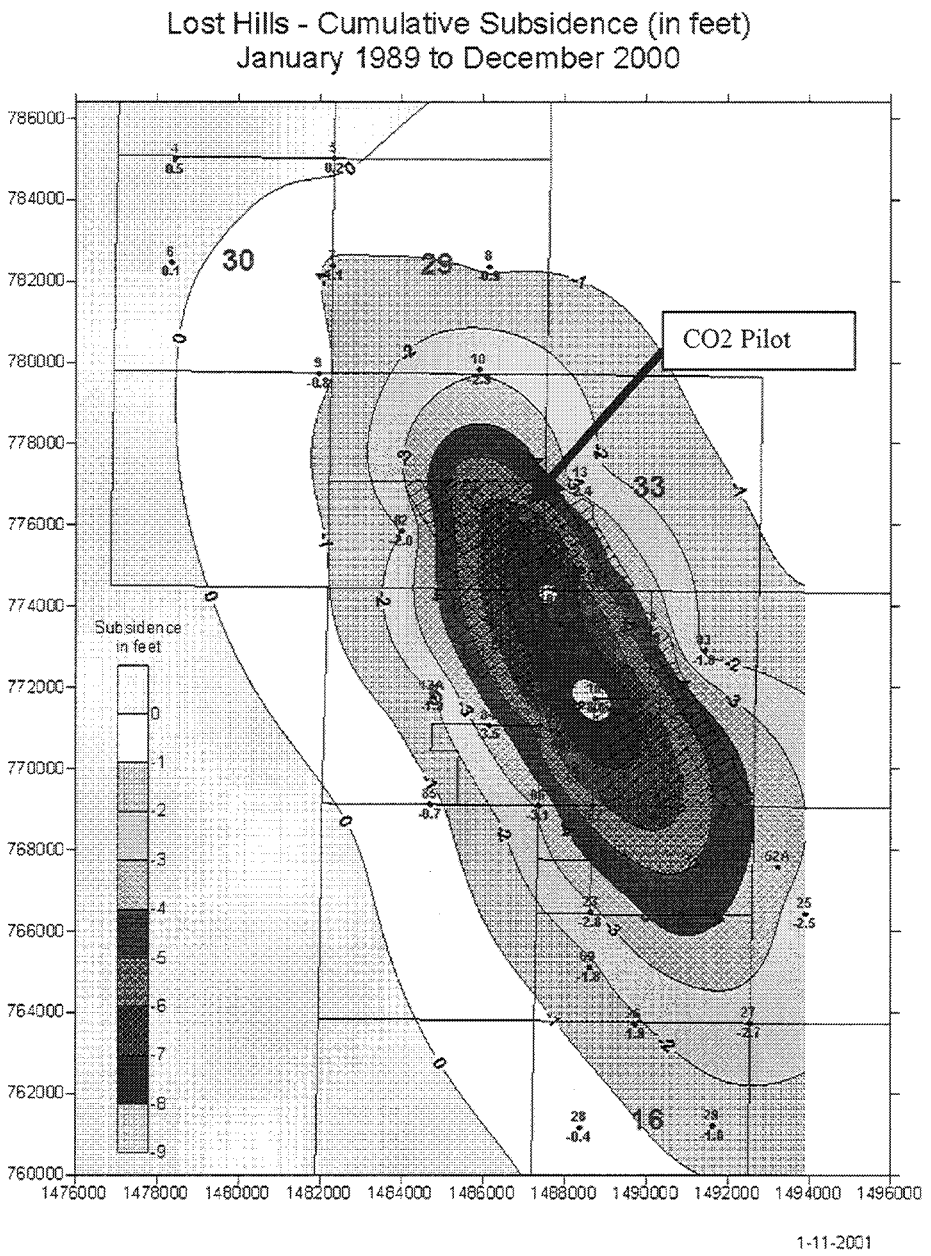

Figure 1.1-15. Map of cumulative subsidence (from N. Wildman). Lost Hills has subsided over 8 feet in 12 years. Waterflooding has greatly helped in reducing the subsidence rate and in reducing well failures due to subsidence.

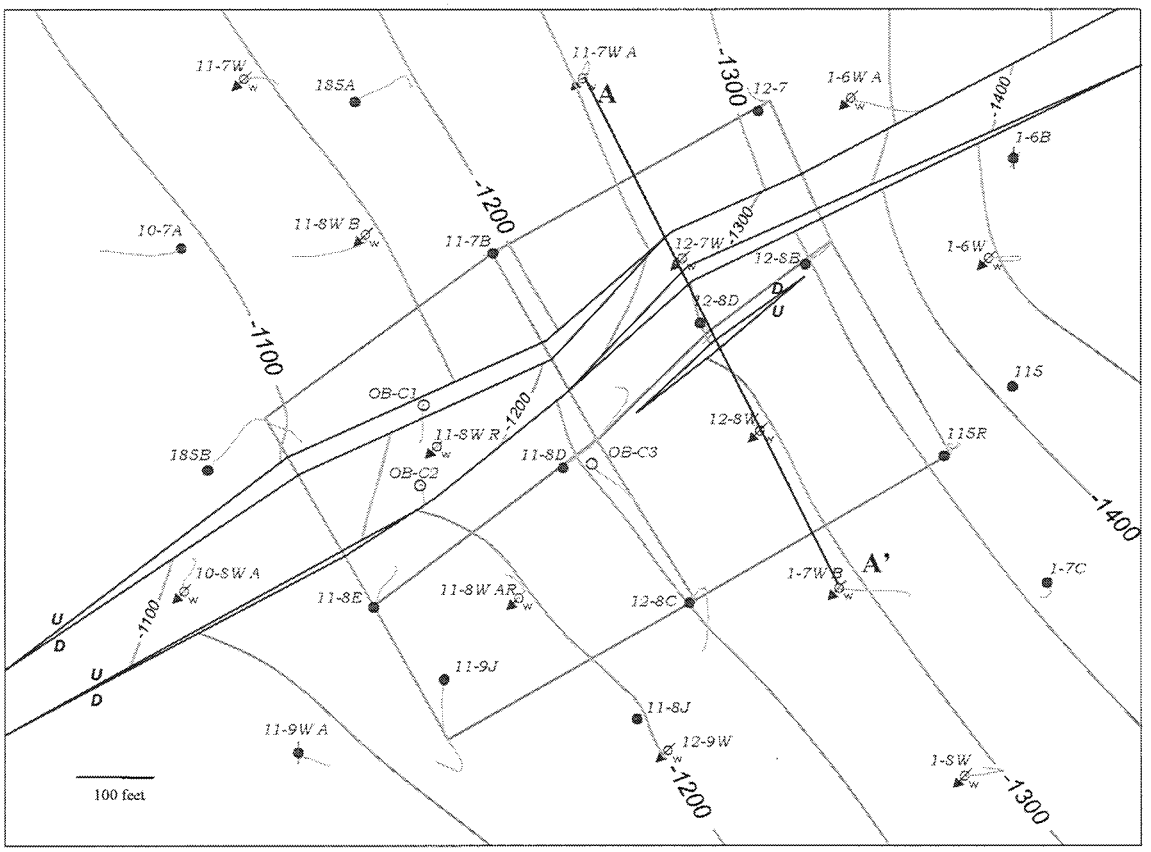

Figure 1.1-16. Lost Hills CO_2 pilot base map. Structure contours on FF Point (top of injection interval).

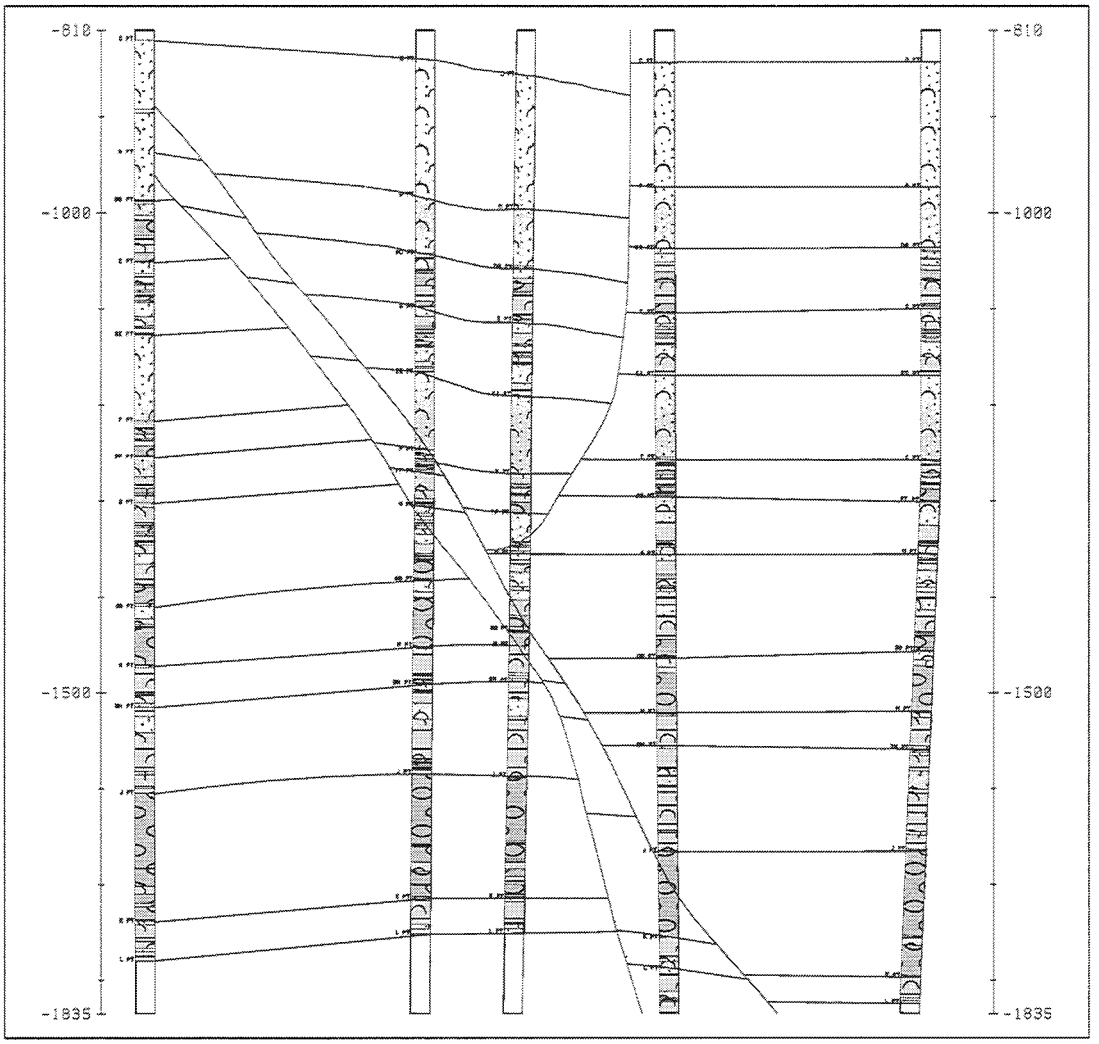

Figure 1.1-17. Cross Section A – A' through pilot area showing fault zone. The wells are from left to right are 11-7WA, 12-7W, 12-8D, 12-8W, and 1-7WB. Predominant lithologies (end members) shown: sandy diatomite (half circles and dots), clean diatomite (ovals), and clayey diatomite (half circles). CO_2 injection will be in the FF through L interval which is predominantly clean and clayey diatomite.

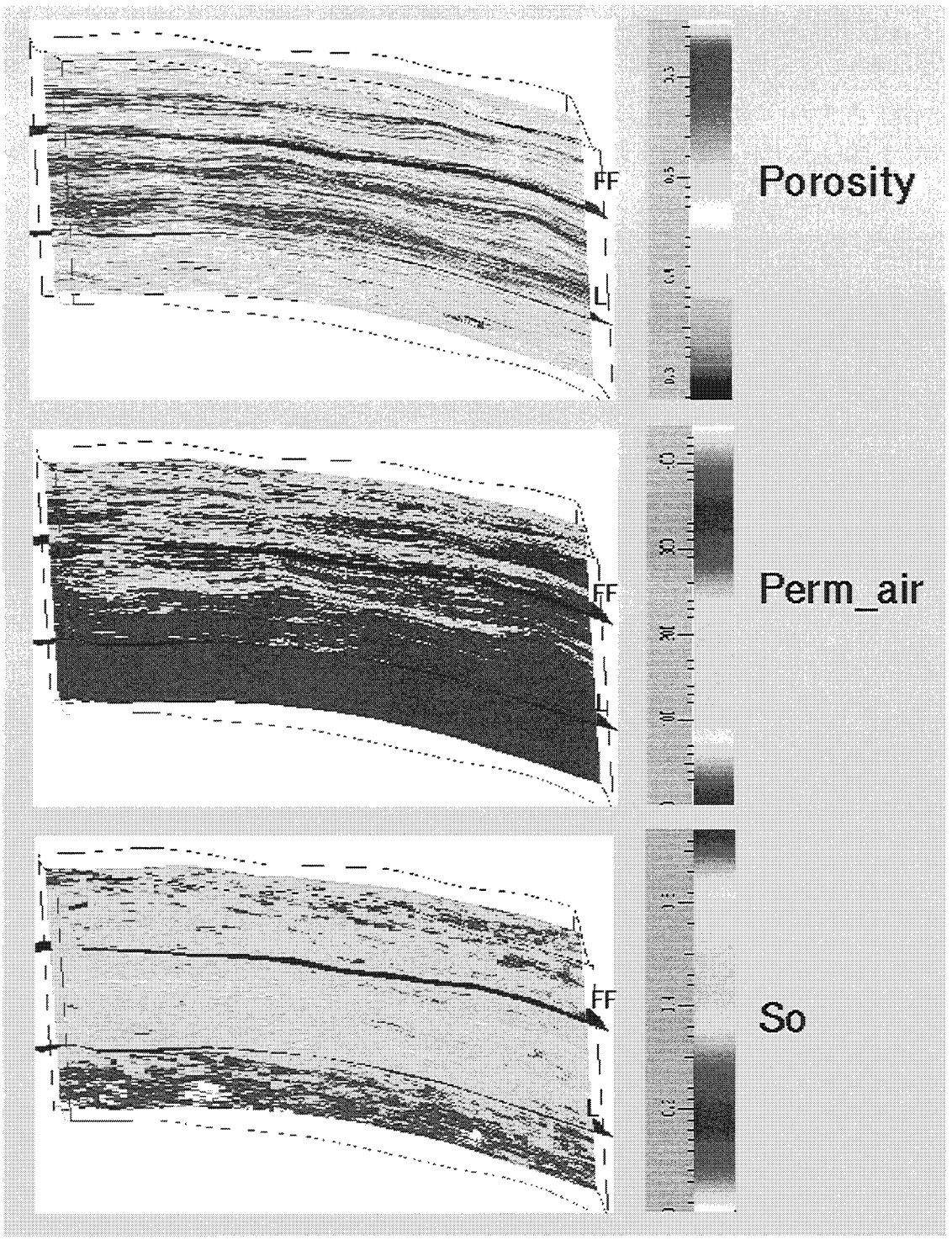

Figure 1.1-18. Cross-sections of porosity, air permeability, and oil saturation of the C Point to Upper Brown Shale interval from W. Fong's 3D Earth Model. The view is SW-NE and the length extends across 4 patterns (one on either side of the pilot). The proposed CO_2 injection interval, FF - L, is highlighted. This is the same interval as the current waterflood.

1.2 FRACTURE INTERPRETATION OF WELL 12-8D FROM HALLIBURTON EMI LOG, CO_2 PILOT AREA

D. R. Julander
Chevron USA Production Company

In December 1998, a Halliburton Electrical Micro Image (EMI) log was acquired in well 12-8D (Sec 32, T26S, R21E) in the Lost Hills Field. The logged interval extended from 1100' to 2510' MD and covered the bottom 284' of the Pliocene Etchegoin Formation, the entire Belridge Diatomite, and the upper 360' of the Upper Brown Shale. The log also covered the entire opal-A section and the uppermost 219' of opal-CT (the base of the opal-A is estimated to be at 2291').

Unfortunately, quality of the EMI data was degraded to some extent by excessive tool rotation during logging (greater than 4 rotations per 100 feet). The Halliburton logging engineers attempted multiple logging passes in the lower portion of the well in order to reduce the tool rotation but were unsuccessful. They eventually concluded that the rotation must be due to hole conditions and proceeded to log the rest of the well. High rates of tool rotation occurred sporadically throughout the entire logged interval. Fortunately, except for occasional thin zones (1 to 2 feet) where the tool rotation is extreme, the log was interpretable.

Z&S Recall software was used to interpret the EMI data. Bed boundaries were picked every 10 to 20 feet on average, and all recognizable fractures were picked in the interpretation. Each pick contains information about location, strike, dip, and type of event. Five fracture types with the following characteristics were interpreted from the image log data:

(1) *Open and clay-filled fractures:* high confidence picks which are resistive (usually black colored) compared to background image.
(2) *Faults:* high confidence picks with apparent offset.
(3) *Mineralized fractures:* high confidence picks which are conductive (usually yellow colored) compared to background image.
(4) *Poor fractures:* medium confidence picks which are predominantly open or clay-filled.
(5) *? Fractures:* lowest confidence picks which may be open, clay-filled, or mineralized.

Figures 1.2-1 through 4 show examples of EMI data from different intervals in the 12-8D well. In each figure, the left half shows the raw, uninterpreted data, while the right half shows the same data with its corresponding interpretation. In these examples, open and clay-filled fractures, faults, and bed boundaries have been interpreted from the image logs. Figure 1.2-1 shows an example of a fault in the H – BH interval. Figure 1.2-2 shows a fault-bound interval in the J – K interval (approximately 2028' to 2037') in which bedding is dipping at a significantly higher rate (~45° in the N50°-55° direction) than the beds above and below (~15° in the N50° to 55° direction). The lower bounding fault in Figure 1.2-2 appears to be a bedding-plane fault. Figure 1.2-3 shows a pair of faults in the Upper Brown Shale that have similar strikes (approximately east – west) but dip in opposite directions (the upper one 36°

to the south and the lower one 54° to the north). Figure 1.2-4 shows another pair of faults in the Upper Brown Shale with orientations of N2°E/49°ESE and S35°E/42°SW, respectively.

The fractures interpreted from the EMI data were used to calculate fracture density curves for the 12-8D well. Note that fracture density has units of fractures/ft, and is defined as the inverse of fracture spacing. Thus, as an example, if a fracture were interpreted every 10 feet from an image log, the fracture density in fractures/ft would be the inverse of 10 - - or 0.1. Two fracture density curves were calculated for 12-8D: one in which all of the above listed fracture types were included (blue curve in Figure 1.2-5), and one in which only fracture types 1 and 3 were used (magenta curve in Figure 1.2-5). A 50-foot averaging window was used to convert the irregularly sampled fracture picks to regularly sampled fracture density curves.

Figure 1.2-5 shows a fracture density trend that is similar to others observed in the Section 32 area of Lost Hills. Fracture densities calculated for all fracture types generally fall in the 0 to 0.1 fractures/ft range for the lower Etchegoin and Belridge Diatomite (1100' - 2140' interval). This is equivalent to fracture spacing in the vertical direction of roughly 10 feet or greater. For the Upper Brown Shale (2140' – 2510' interval), the fracture densities for all fracture types are in the 0.2 to 0.3 range. (Fracture densities of this magnitude correspond to vertical fracture spacings of roughly 3 to 5 ft.) The only significant anomaly in the data for the 12-8D well is the interval around 1800' – 1850' (Figure 1.2-5) where fracture densities are unusually high due to a concentration of fractures and faults between 1816' and 1836'. (See Figure 1.2-6 which shows both the uninterpreted [left] and interpreted [right] EMI data for the 1816' – 1836' interval.) This concentration of fractures and faults may coincide with an interval that appears to be anomalously thin based on correlations of the 12-8D open-hole logs to surrounding wells (M.F. Morea, personal communication). Table 1.2-1 provides a summary of orientation data for the faults in the 1816' – 1836' interval which may prove useful in the structural interpretation of the CO_2 pilot area.

The rapid increase in fracture density around the top of the Brown Shale is consistent with other fracture density trends in the Section 32 area. However, it remains uncertain whether this increase is primarily a lithology effect associated with the formation change or an opal phase change effect (due to the fact that the opal-A/CT transition usually occurs near the top of the Brown Shale in this part of the field).

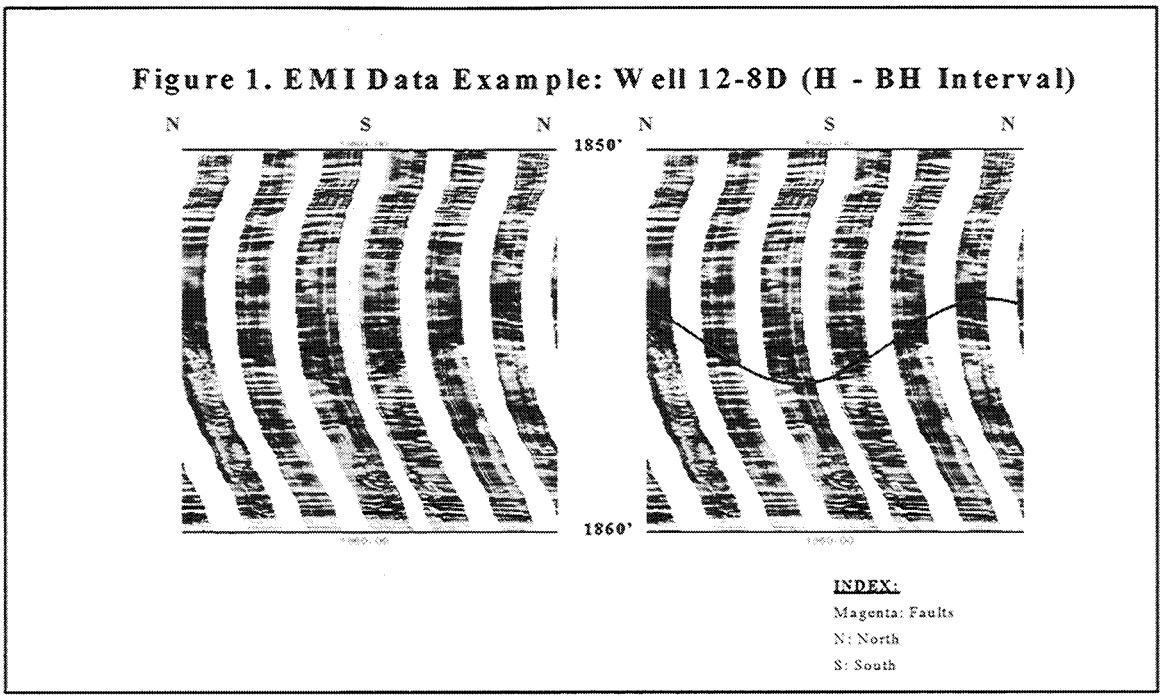

Figure 1.2-1. EMI data example from the H – BH interval inWell 12-8D.

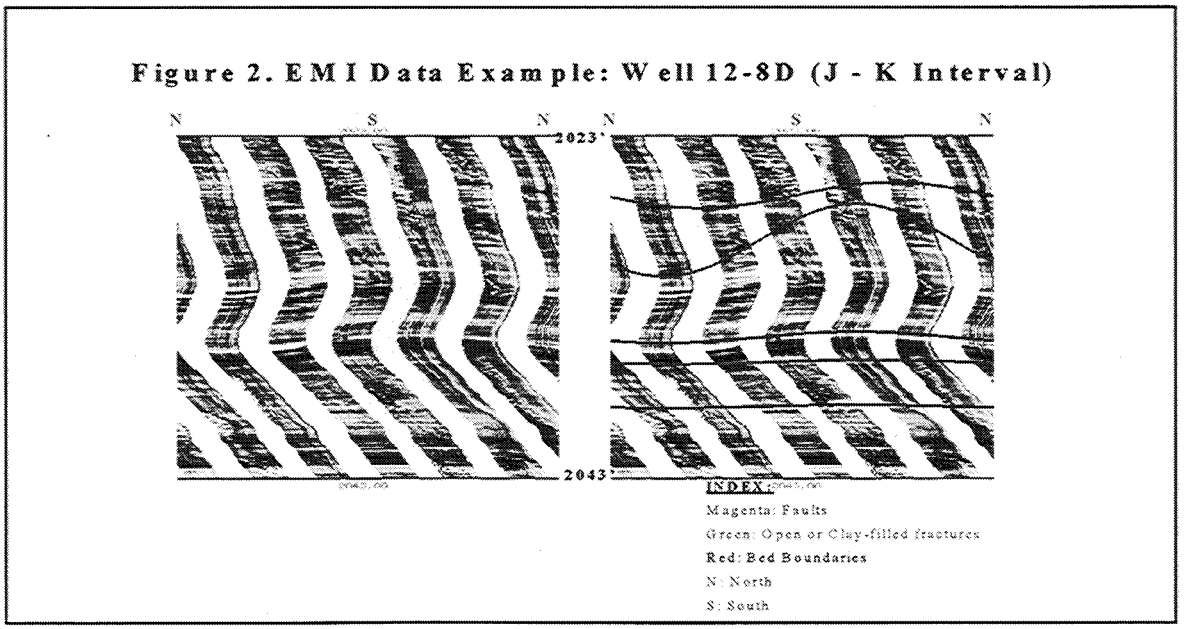

Figure 1.2-2. EMI data example from the J – K interval in Well 12-8D.

Figure 3. EMI Data Example: Well 12-8D (U. Brown Shale)

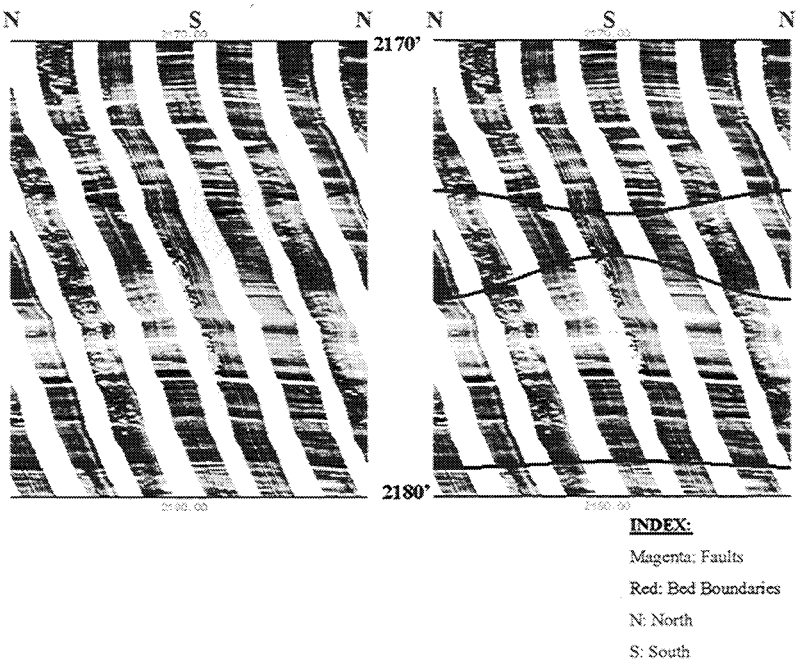

Figure 1.2-3. EMI data example 1 from the Upper Brown Shale interval in Well 12-8D.

Figure 4. EMI Data Example: Well 12-8D (U. Brown Shale)

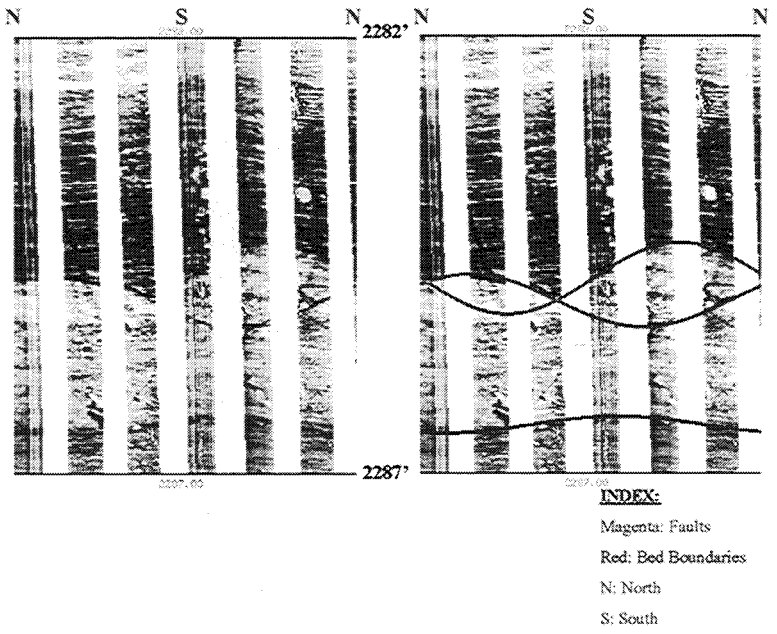

Figure 1.2-4. EMI data example 2 from the Upper Brown Shale interval in Well 12-8D.

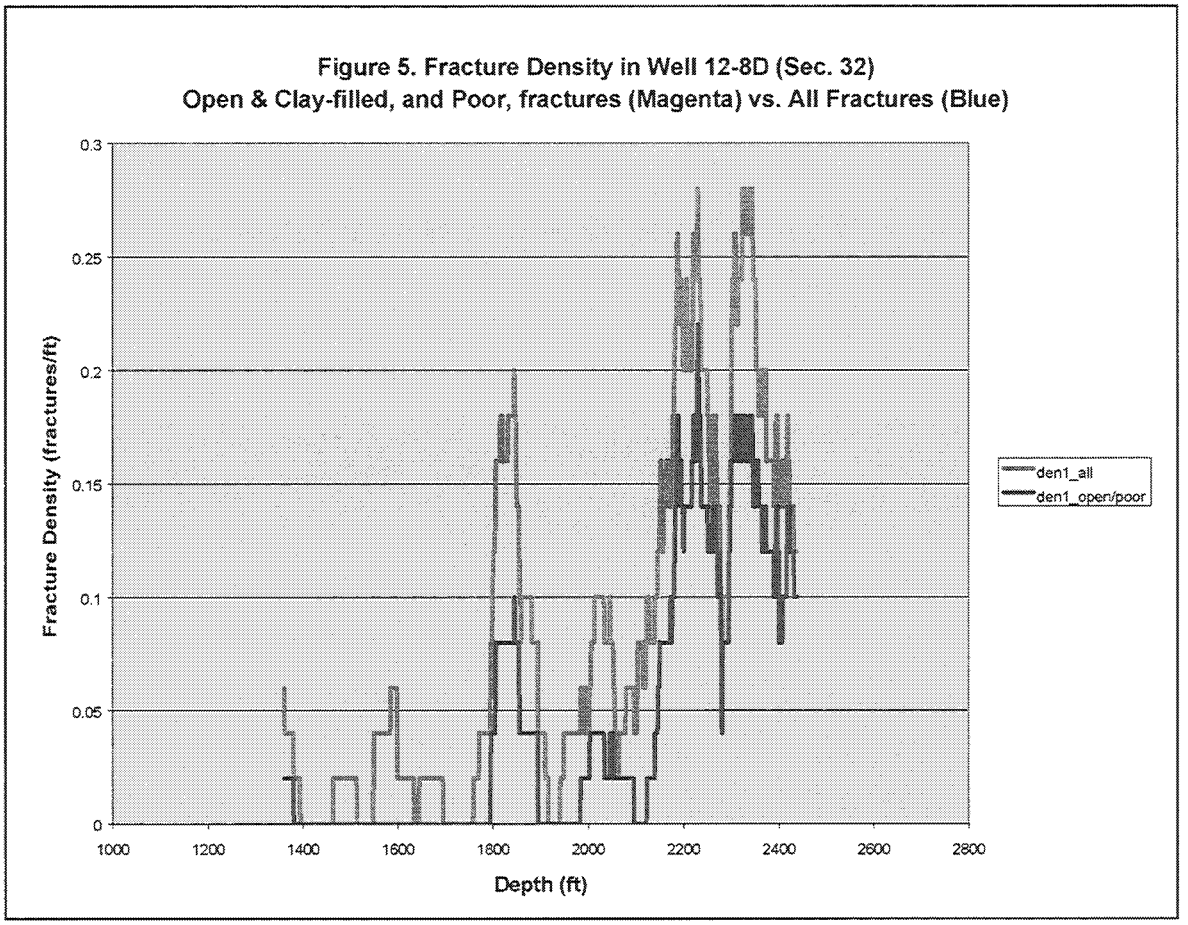

Figure 1.2-5. Fracture density in well 12-8D.

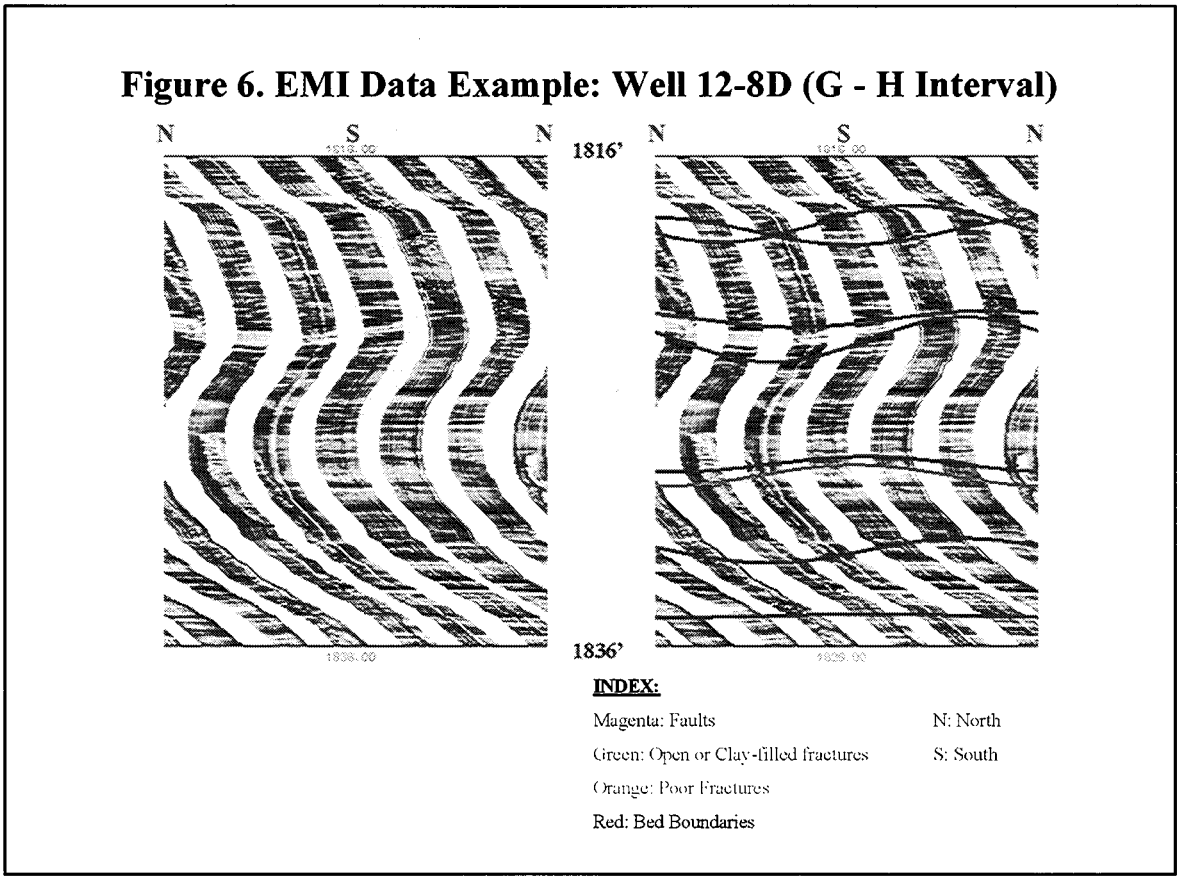

Figure 1.2-6. EMI data example from the G – H interval in well 12-8D.

Table 1.2-1. Fault data in the 1818 – 1832 ft interval in well 12-8D.

Table 1. Fault Data in the 1818' - 1832' Interval			
Depth	Strike	Dip (degrees)	Dip Direction
1822'	N41E	43	SE
1823'	N20E	69	SE
1832'	N16E	56	SE

SECTION 2

CO_2 PILOT INSTALLATION

2. CO_2 PILOT INSTALLATION

John F. Cooney, Gregg R. Molesworth, and Pasquale R. Perri
Chevron USA Production Company

2.1 CURRENT DEVELOMENT

Lost Hills Primary Development:
The Lost Hills Field, located 45 miles northwest of Bakersfield, California, (see Figure 2.1-1) was discovered in 1910. Reserves in the shallow sands, diatomite, and chert pools (Figure 2.1-2) were developed using slotted liner completion techniques until the late 1970's. From the late 1970's to 1987, small volume hydrofracture completions were performed covering the entire Belridge Diatomite.

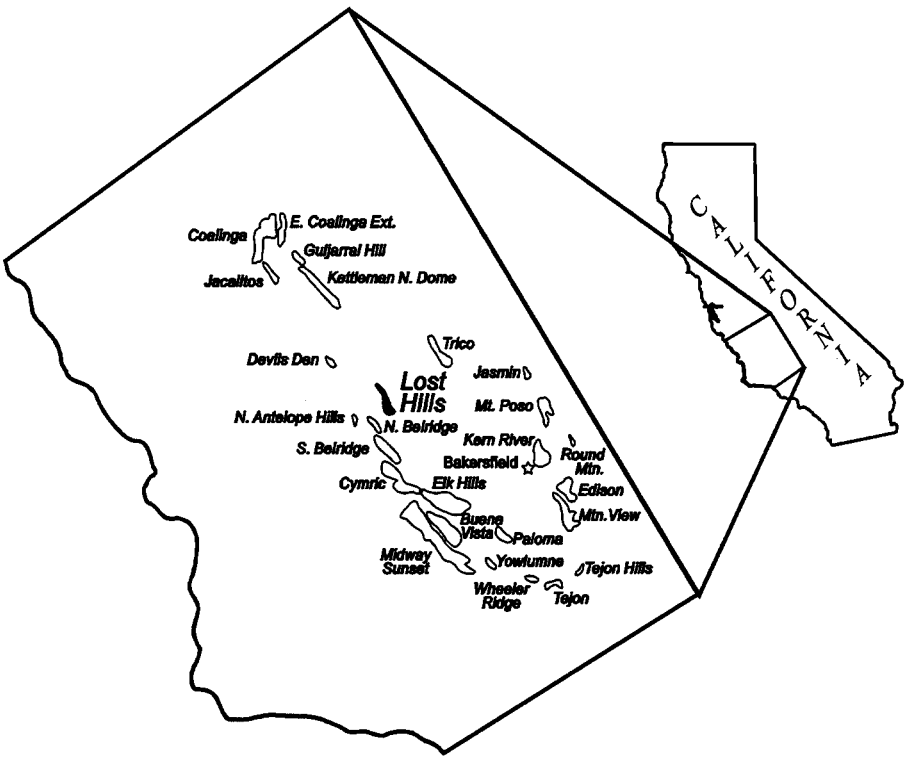

Figure 2.1-1. Lost Hills Field Location Map.

Advances in hydraulic fracturing technology in the late 1980's resulted in increased oil recovery that led to a more aggressive development program by Chevron. From 1987 to the present, high volume hydrofracture completions have been performed across the entire Belridge Diatomite and the Upper Brown Shale resulting in significant production increases as shown in Figure 2.1-3.

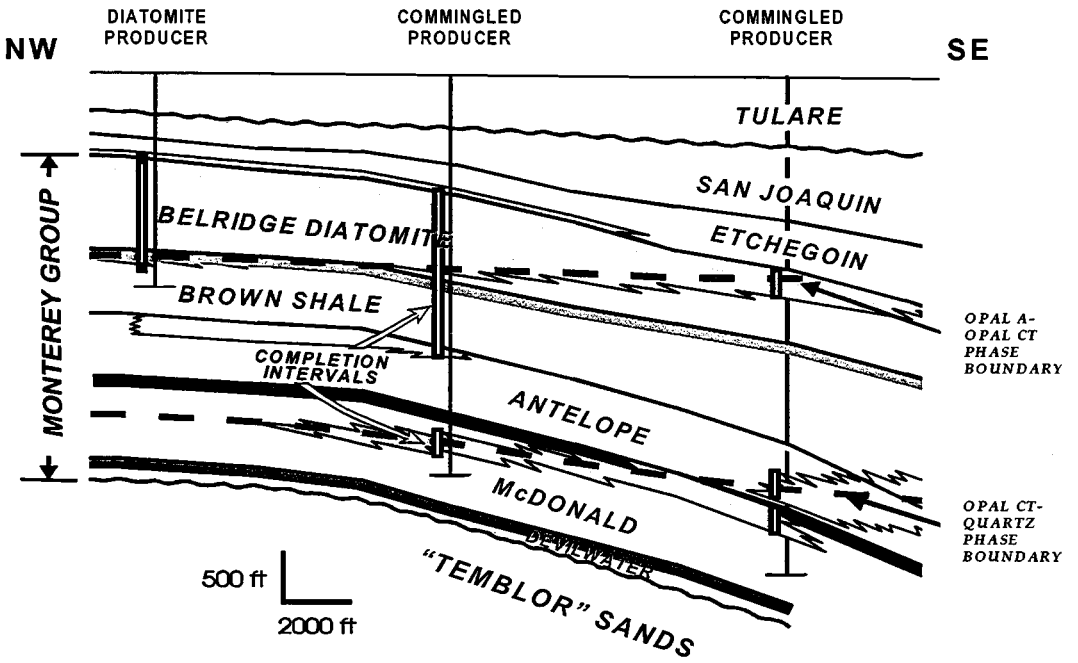

Figure 2.1-2. Lost Hills Field Regional Cross-Section.

The Lost Hills Field is developed on a 5 acre (siliceous shale) to 1.25 acre (diatomite) well spacing. There are over 2.2 billion barrels of oil in place in the Belridge Diatomite in Lost Hills. To date only 112 million barrels have been produced, or approximately 5% of the original oil in place (OOIP).

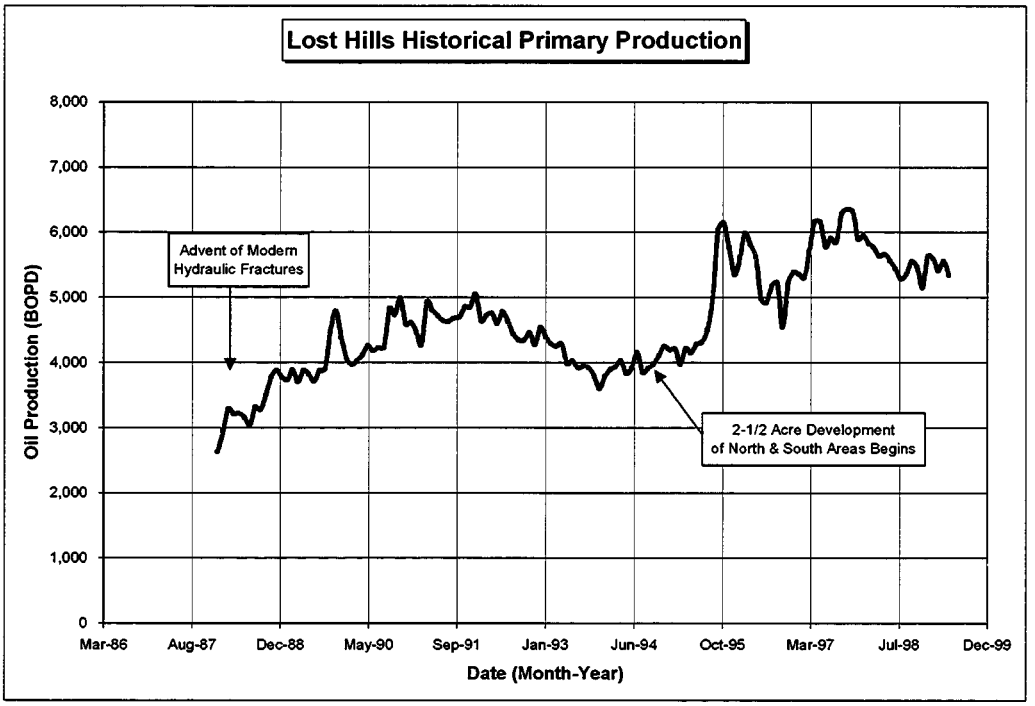

Figure 2.1-3. Lost Hills Historical Primary Production.

Diatomite Waterflood Development:

Chevron initiated a pilot diatomite waterflood project in December 1990 and began full-project development in April 1992. Since 1992, two hundred and eight 2-1/2 acre patterns have been put on water injection spanning parts of four sections (Sections 4, 5, 32 Fee, and 33) as shown in Figure 2.1-4. The historical performance of the Lost Hills waterflood performance can be seen in Figure 2.1-5. Since the initiation of first project water injection in April 1992, production has increased approximately 4,000 BOPD from 6,400 BOPD to the current rate of 10,400 BOPD.

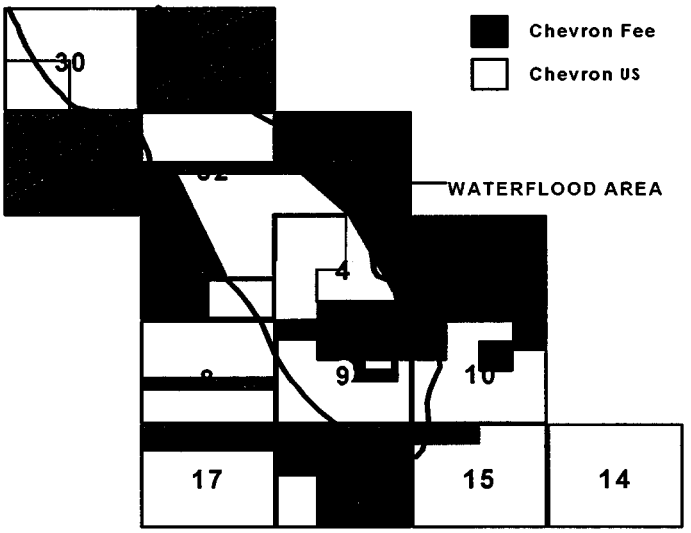

Figure 2.1-4. Lost Hills Waterflood Project Location Map.

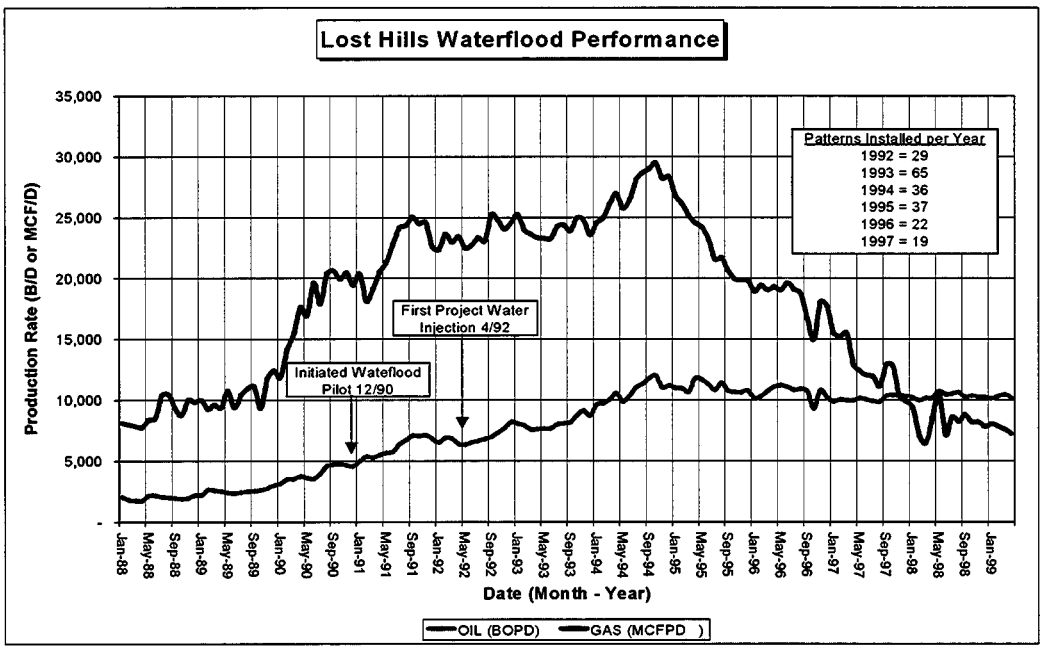

Figure 2.1-5. Lost Hills Waterflood Performance.

In terms of recovery efficiency, Figure 2.1-6 compares the estimated primary and secondary (waterflood) recoveries for each of the 4 sections under waterflood to the original Lost Hills waterflood project estimate (GO-36) on a per pattern basis. The height of the bars in Figure 2.1-6 represent the average pattern OOIP. Estimated ultimate waterflood recovery from the Lost Hills diatomite is 8.1% of OOIP, which is considerably less than the original project estimate of 19.6% of OOIP.

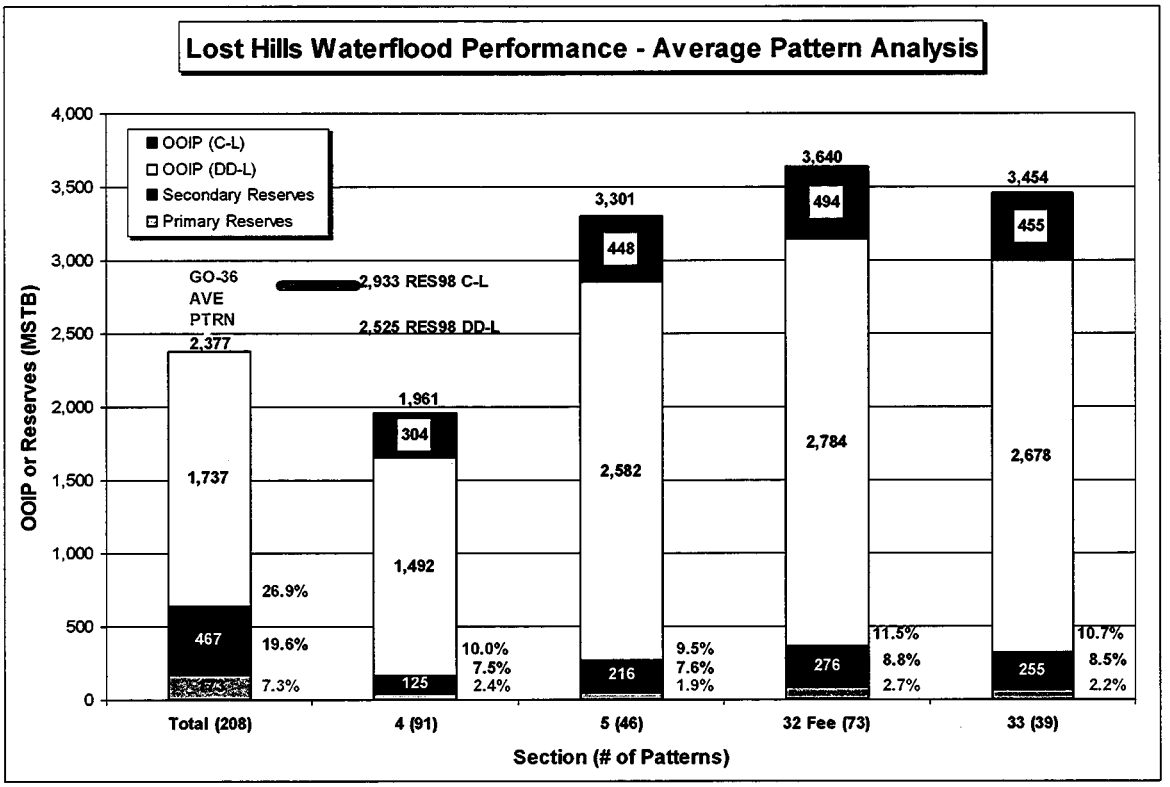

Figure 2.1-6. Lost Hills Estimated Waterflood Reserves and Recovery Factors.

Infill Primary Pilot:

An infill primary pilot was initiated by Chevron in Section 32 U.S. in 1998 to test the economic viability of improving primary recovery (3 – 4 % of OOIP to date) by infill drilling from the current 2-1/2 acre development down to 1-1/4 acre spacing. A total of 11 infill producers have been drilled and completed as part of the pilot test to date. The results have been disappointing and keeping the wells on production due to excessive sanding continues to be a problem.

Infill Waterflood Pilot:

Installation of an infill waterflood pilot began in late 1998 by Chevron in Section 32 Fee to test the potential of waterflooding with 1-1/4 acre "direct line-drive" patterns compared to the current 2-1/2 acre "staggered" patterns. To date, 28 wells (9 injectors and 19 producers) have been drilled on 1-1/4 acre spacing to determine if the current waterflood recovery can be accelerated, or better yet, if incremental waterflood reserves can be obtained by infill drilling.

Diatomite Steamflood Pilot:
Chevron initiated a diatomite steamflood/cyclic steam pilot in the southern portion of Section 29 in October 1998. The steamflood pilot consists of 7 injectors targeting the J – L "clean" diatomite intervals. A single pattern cyclic steam pilot consisting of 4 producers targeting the more permeable EE – F "sandy" diatomite was initiated concurrently. Both pilots are still under evaluation.

Horizontal Wells:
In 1997 Chevron began experimenting with horizontal wells to try to exploit the flanks of the field where vertical wells could not be economically justified due to the reduced oil column. Through December 2000, four horizontal wells have been drilled with mixed results. Figure 2.1-7 is a summary of the Lost Hills horizontal well performance to date.

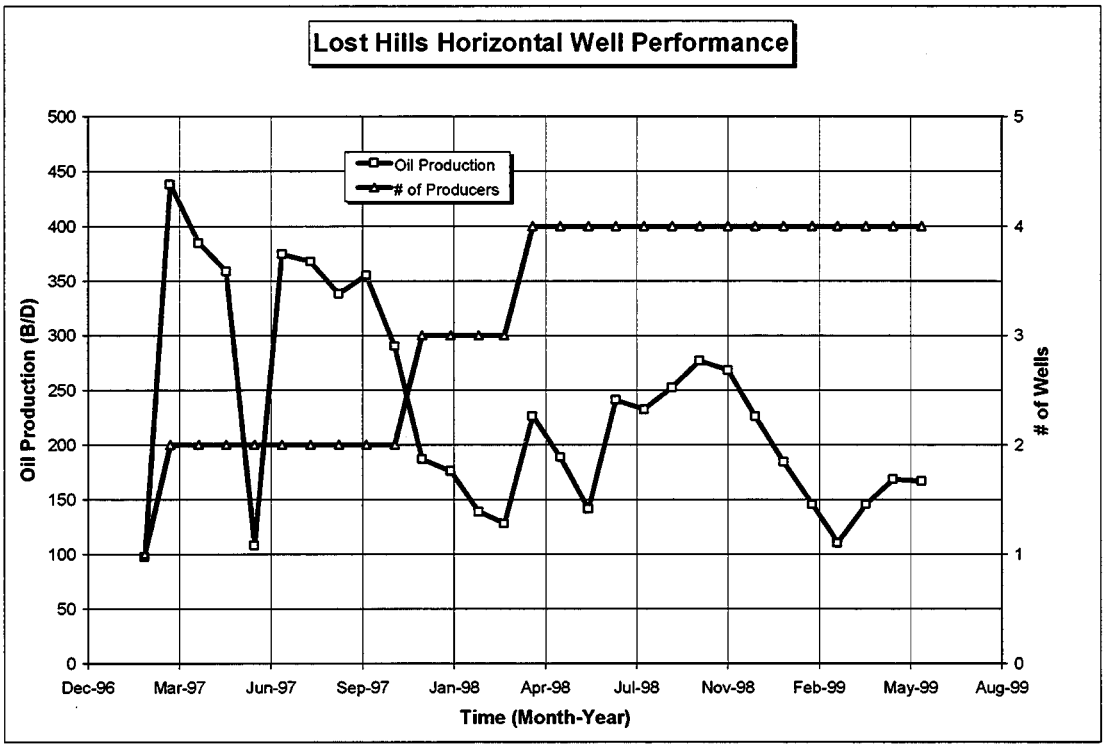

Figure 2.1-7. Lost Hills Horizontal Well Performance.

2.2 CO_2 PILOT LOCATION

The CO_2 Pilot is located in the southeast quarter-section of Section 32, T.26S., R.21E. of the Lost Hills Field as shown in Figure 2.2-1. A four-pattern pilot has been installed. The pilot area is enlarged in Figure 2.2-2 showing the four existing waterflood patterns (10-8WA, 11-8WA, 12-7W, and 12-8W) which were converted to CO_2 injection.

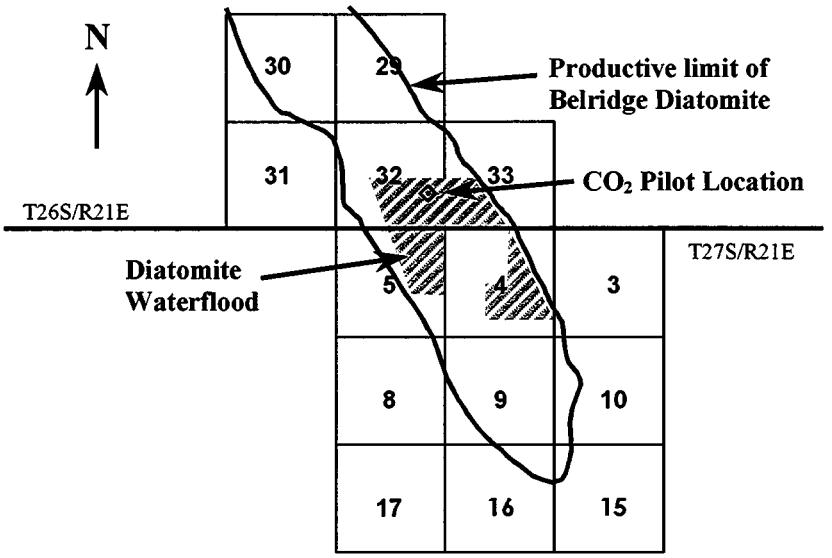

Figure 2.2-1. Lost Hills CO_2 Pilot Location Map.

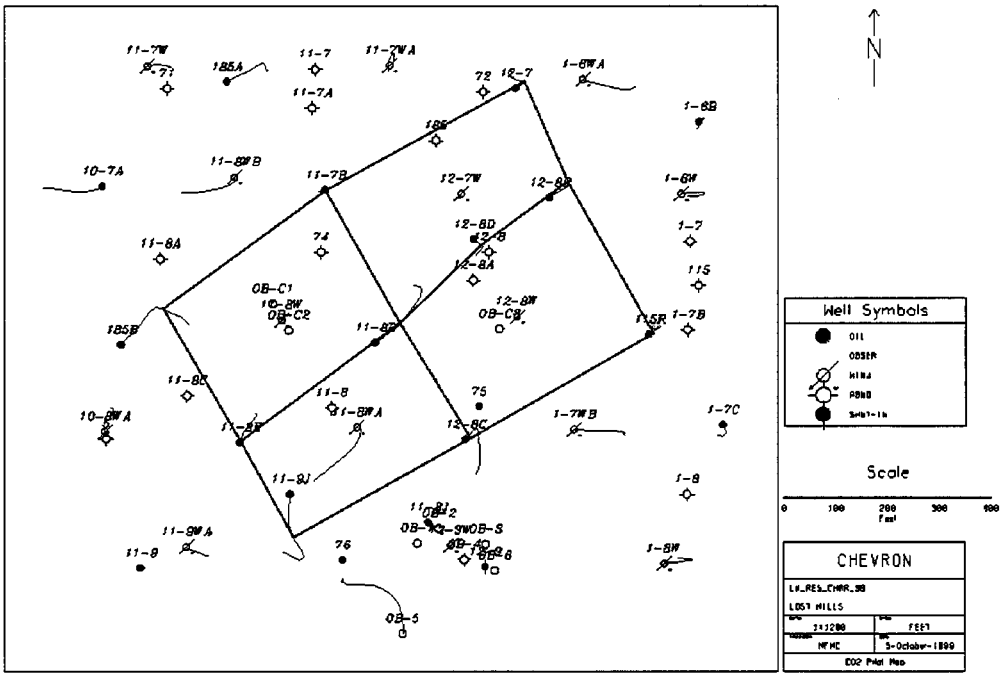

Figure 2.2-2. Lost Hills CO_2 Pilot Pattern Map.

Two of the existing injectors (10-8WA and 11-8WA) had to be replaced due to poor mechanical conditions of the wellbore. The two new injectors are 10-8WAR and 11-8WAR.

2.3 CO_2 PILOT DESIGN AND OBJECTIVES

Objectives:

The Lost Hills CO_2 Pilot was designed with the following goals and objectives in mind:

- Test the technical and economic viability of CO_2 flooding the low permeability Diatomite resource, which is one member of California's siliceous shale reservoirs of the Monterey Formation.
- Test the technical and economic viability of CO_2 flooding the Diatomite resource in a timely manner (3 years or less).
- Install a configuration that enhances the chance of process success (oil response).
- Install a configuration that minimizes the likelihood of premature CO_2 breakthrough.
- Provide an opportunity to gather and analyze reservoir, geologic, and production data and gather facilities design information necessary to commit to a full-field project.
- Install a CO_2 Pilot in Lost Hills safely, without incident, and in accordance with all county, state, and federal environmental rules and regulations.

With the foregoing objectives in mind, a four pattern (2.5 acre each) CO_2 pilot configuration was chosen as shown in Figure 2.3-1. This configuration confines one producer (11-8D) and reduces the risk of premature breakthrough that a 5/8 acre pilot configuration would likely incur.

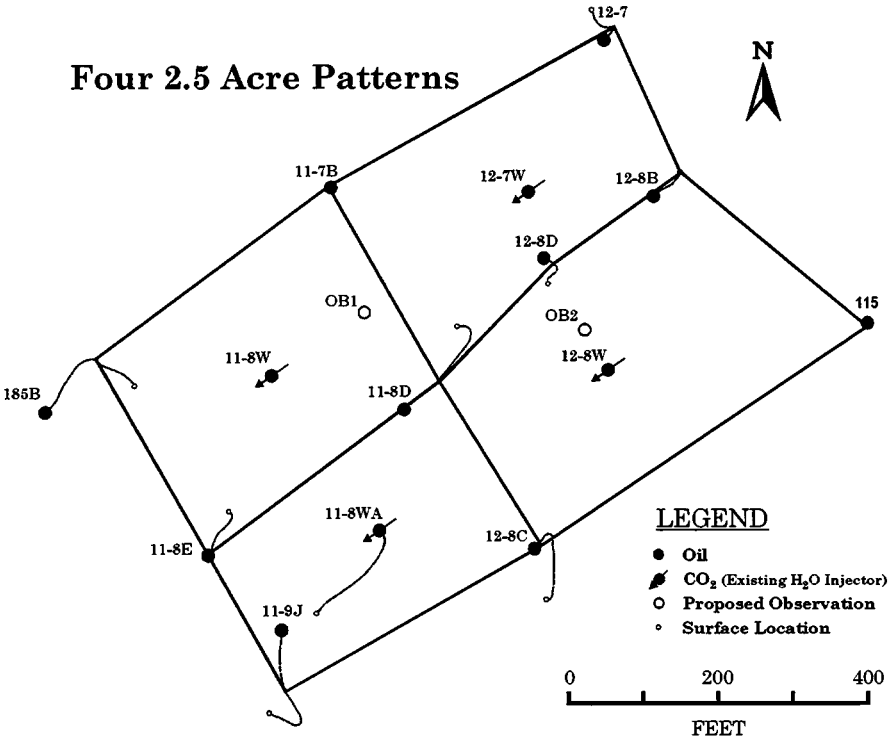

Figure 2.3-1. Four 2.5 Acre Patterns Pilot Configuration.

2.4 Pilot Facilities

Design Basis:
The facilities were designed to support four 2.5 acre patterns with the following as the design basis:

- Four injection wells (existing water injectors) requiring a maximum pressure of 1200 psig. The equipment will be able to deliver a CO_2 rate as low as 100 mscfd per well, and as high as 500 MSCF/D per well. This range is based on the results of the March 1999 injectivity test.
- Ten producing wells

A phased approach is being taken to establish early baseline data from the existing producing wells in the CO_2 pilot.

Phase 1 – New Gauging Facilities:
It should be noted that the existing gauge setting can handle and monitor the production associated with the pilot. However, if the pilot is sustained it would be advantageous to install the new gauge setting to improve metering accuracy and to minimize corrosion damage to existing facilities.

The new gauging facilities started operating in early May 2000 in order to establish good baseline production data prior to starting injection. A picture of the new gauging facilities are shown in Figure 2.4-1. They are designed to handle and monitor the increased CO_2 production associated with the CO_2 pilot. The key objective of these facilities will be to isolate and handle the wet gases high in CO_2 to prevent excessive corrosion of the existing gathering system. The time lag between phase 1 and 2 facilities will be minimal (2 to 4 months). Since these gauging facilities will have salvage value to Chevron, regardless of the outcome of the pilot, the DOE is paying only 25% for this portion.

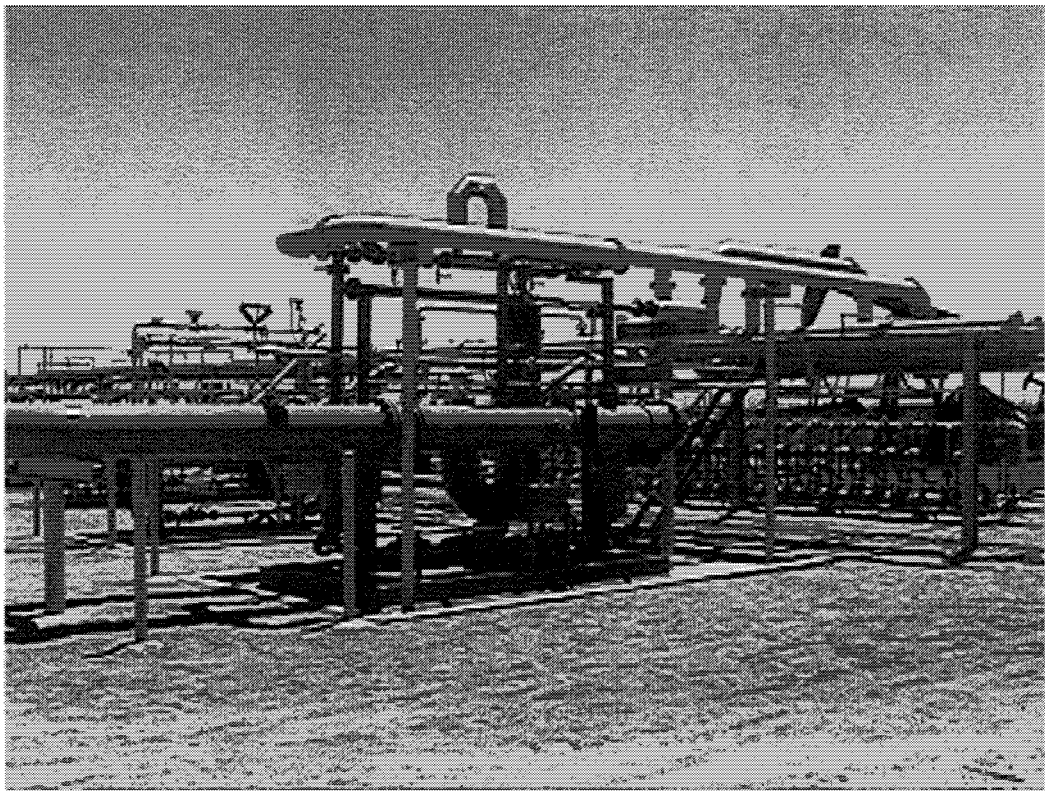

Figure 2.4-1. CO_2 pilot gauging facilities.

Some of the existing flow lines were utilized for the producers, while others were replaced with cement lined piping. Funding was included in the AFE to tie additional wells into the pilot dedicated gauge setting should they also experience CO_2 breakthrough outside the immediate pilot patterns. The facilities also include monitoring equipment, such as density meters and online corrosion monitors, to help detect CO_2 breakthrough.

Phase 2 - Injection Facilities:
The injection equipment is being leased and consists of; storage tanks, injection pumps, heaters, monitoring equipment, and injection lines. It will be very similar to the equipment utilized for the March 1999 injectivity test but with a greater capacity. SCADA equipment was installed to enable the existing infrastructure to gather and compile the data from the pilot.

Figure 2.4-2 is a picture of the CO_2 injection header and CO_2 storage vessel. Figure 2.4-3 is a picture of the CO_2 storage tanks. Figure 2.4-4 is a picture of the CO_2 injection pumps and heater.

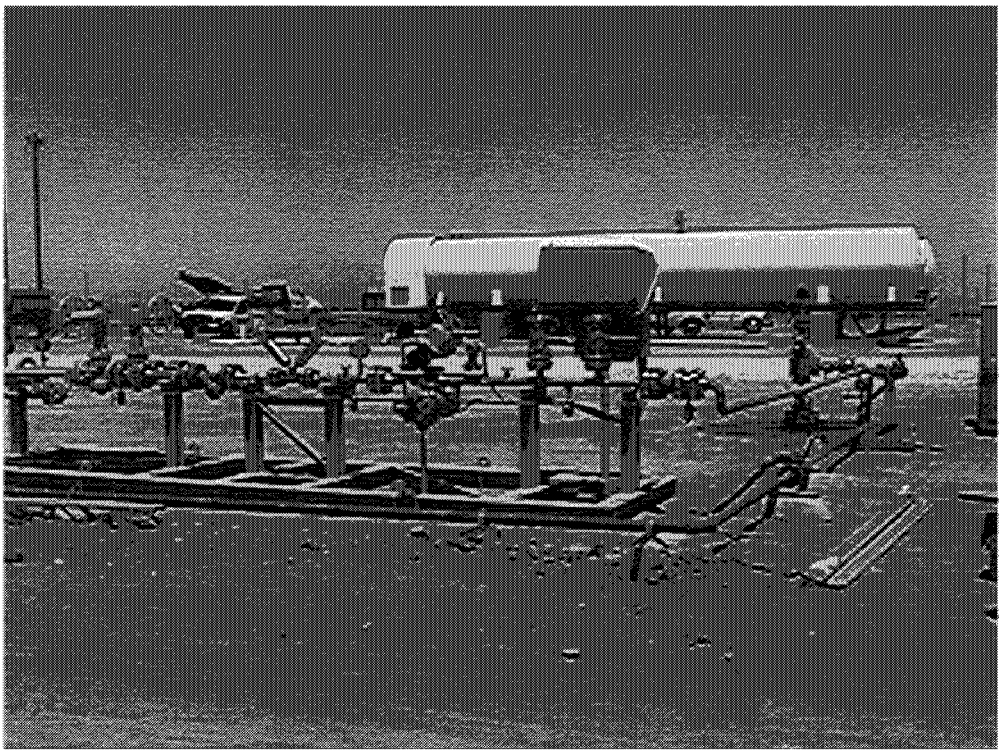

Figure 2.4-2. CO_2 Pilot Injection Header.

All major components of the pilot facilities have been operational since August 31, 2000. We have been getting excellent run time out of the injection equipment. However, due to the power availability situation in California we have been required to shut down injection pumps when a stage 2 alert occurs. Cold weather spells result in several shut downs each week, that affect the entire Lost Hills Field, and last several hours.

As injection proceeds we continue to monitor and control all critical process parameters. Due to higher produced gas rates from well 11-8E, we had trouble gauging oil production for approximately one month. In early November 2000, we saw oil from this well increase from roughly 80 BOPD to over 100 BOPD. Unfortunately, the higher gas rates that occurred simultaneously prevented us from verifying the encouraging gauge. The gas-metering bottleneck has been eliminated but the well has been down due to sanding problems ever since. The next describes the remedial action that will be taken to return this well (11-8E) to production.

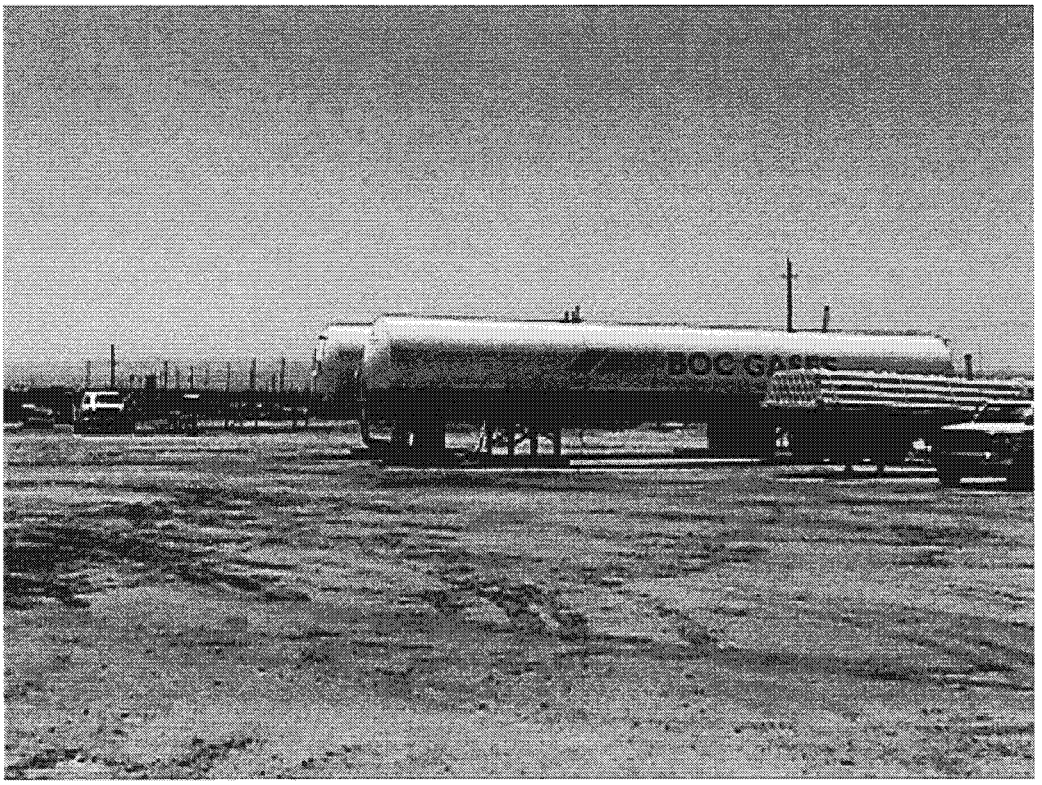

Figure 2.4-3. CO_2 storage facilities.

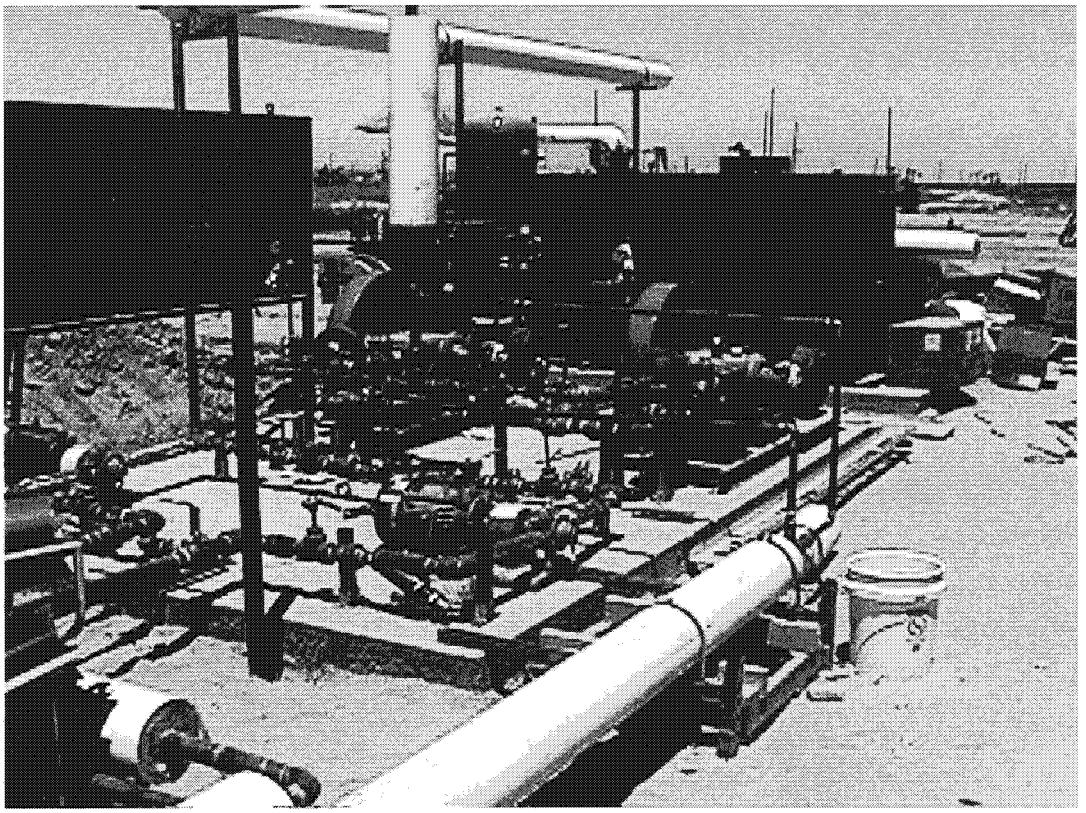

Figure 2.4-4. CO_2 injection pumps with heater in the background.

2.5 New Wells and Remedial Work

Introduction:
The well work completed in 2000 for the Lost Hills CO_2 Pilot included attempts to remediate four existing waterflood injectors and to drill and complete three observation wells. The four proposed injection wells had known mechanical problems and had existing completion equipment that was not compatible with CO_2 injection. At the start of this remedial program, it was unknown if any of the existing injection wells could be repaired and used in the CO_2 Pilot. Project funds were available for four replacement injection wells should the remedial work prove to be unsuccessful. Of the three observation wells to be drilled, two are to be used for a cased hole logging program to monitor reservoir conditions during the CO_2 Pilot, and a third observation well is to be used for monitoring reservoir pressure.

Summary:

1) Well work in the CO_2 Pilot area was started in March 2000 and was completed in early August 2000.

2) Of the four original injectors, two had successful remedial programs completed and two injectors were found with severe casing damage within the completion interval and were abandoned. Replacement injectors were drilled following the abandonment of the original injectors.

3) The three pilot observation wells were drilled and completed.

4) The total cost for all well work associated with the CO_2 Pilot was $1,567,000.

Well Histories (Injection Wells):
The original injection wells (11-8W, 11-8WA, 12-7W and 12-8W) had been drilled and completed in 1994 and 1995, as water injectors in the Lost Hills Waterflood project. The wells had been hydraulically fractured upon completion (two hydraulically fractured stages per well) and three of the four had been completed with dual packers and injection strings.

The existing completion equipment in these wells was not compatible with CO_2 injection and needed to be replaced to prevent corrosion problems and possible communication with the tubing-casing annulus. With known subsidence related shallow casing problems throughout Lost Hills, it was important to insure mechanical integrity in these CO_2 pilot injectors. All three wells completed with dual injection strings had mechanical problems that did allow injection surveys to be run. The single string injector (12-7W) had reported shallow casing problems (~500') and had a known packer leak. Prior to starting this remedial effort it was unclear as to the amount of mechanical damage that existed in these wells and whether they could be used for CO_2 injection or should be abandoned and replacement wells drilled.

Job Execution – Injection Wells:

Well 12-8W: Rig work was started on the subject well on March 13, 2000. The short string, long string and dual packer were successfully recovered from the well, leaving only the permanent packer in the hole. A 5-¾" mill, that was to used to mill over and recover the permanent packer at 1926', stopped at 494'. Attempts to work through this bad spot were unsuccessful. The rig moved off the well while *Engineering* and *the Well Development Team* discussed alternative completion strategies. A sinker bar run had indicated no fill in the well and the sealbore through the permanent packer was open. Perforations below the packer were also uncovered. On May 25, 2000 the rig moved back over the well and completion equipment was run and cemented into place. An inflatable packer, located at 1600', and a stage collar were used to cement the tubing string in place. The top of cement in the annulus was estimated at approximately 1000'. The well was ready to be returned to injection on May 30, 2000.

Well 11-8W: Rig work was started on the subject well on March 20, 2000. The short string was pulled successfully from the well, but there was difficulty in killing the well and in setting plugs in the long string due to tubing restrictions. A cement plug was set in the long string and a snubbing unit was moved onto the well. A total of 8 rig days were required before the long string and dual packer were recovered from the well. The well continued to flow following the recovery of the long string (water and formation sand). Attempts to snub back in with 6"wash pipe stopped at 448'. A 2-7/8" workstring was snubbed into the hole and tagged fill at 1583'. Fill was circulated out to 1587' (the top of perforations) where no further progress was made (damaged casing). The rig was moved off and an abandonment program was prepared.

On May 18, 2000 the rig was moved back onto the subject well for abandonment. The well could not be killed, even after 100 barrels of 15 ppg mud was spotted. A cement plug was spotted in the well. The following day the well was still flowing. It is believed that the cement plug did not set up. Surface cement samples confirmed this. A second plug was spotted in the wellbore that successfully killed the well and the final abandonment of the well was completed on May 24, 2000.

Well 11-8WA: The rig was moved onto the subject well on April 5, 2000. The short string, long string and dual packer were successfully pulled from the well without incident. While pulling out of the well with the dual packer, tight spots in the casing were encountered at 1474', 1434' and 450'. The tubing below the dual packer was also severely pitted and corroded. A 6" washpipe run into the well, in an attempt to mill over the permanent packer at 1858', stopped due to a casing restriction at 441'. The 2-7/8" workstring was run into the well and tagged solid at 1754'(damaged casing). Formation rocks were circulated from the well. The rig was moved off the well and an abandonment program was prepared. On May 24, 2000 the rig was moved back onto the subject well. The abandonment was completed on June 2, 2000 without incident.

Well 12-7W: The rig was moved onto the subject well on April 7, 2000. The well was flowed into a pit until it died. The packer was released and the single tubing string was

recovered from the well. The rig was moved off the well to complete other Lost Hills work on April 11, 2000. The rig returned to the subject well on April 17, 2000. A 2-7/8" workstring was run and tagged fill at 2195' (120' of fill). The fill was circulated from the well and the casing above the perforations was tested to 1500 psi successfully. Completion equipment was run into the well (see attached Wellbore Schematic No. 3). The rig was moved off and the well ready for injection on April 19, 2000.

In August 2000, annulus pressure was discovered in the subject well. It was determined that the packer was leaking. On August 7, 2000 the workover rig was moved back onto 12-7W, the packer was reset and the well returned to injection on August 9, 2000.

Job Execution – Observation Well:

Well OB-C1: Observation well OB-C1 was spud on June 7, 2000. It was drilled to a depth of 2235' and logged. The well was completed with 7" fiberglass casing cemented across the pay interval. The rig was released on June 11, 2000.

Well OB-C2: Observation well OB-C2 was spud on May 31, 2000. There was significant difficulty in controlling the well as mud weight was built up to 12.5 ppg in an attempt to control flow. Open hole logs were not run in the well due to well control problems. During cementing operations the 7" fiberglass casing was damaged. The drilling rig was released on June 6, 2000.

On June 26, 2000 the workover rig was moved onto the subject well. Damage to the fiberglass casing was confirmed at 1614'. A casing patch was run and cemented into place (1606'-1628') to isolate the damaged area. The internal diameter of the casing patch is 4.187". Rig work was completed on the subject well on July 13, 2000. See attached Wellbore Schematic No. 4 for additional details. An additional $52,000 was spent to install the casing patch and isolate the damaged casing.

Well OB-C3: Observation well OB-C3 was spud on June 11, 2000. It was drilled to a depth of 2220' and logged. The well was completed with dual strings of 2-7/8" Duoline tubing cemented into place. The drilling rig was released on June 15, 2000.

On July 18-19, 2000 the subject well was perforated using Schlumberger 1-11/16" perforating guns and Power Orienting Tool (see attached Wellbore Schematic No. 5). On August 1, 2000 during routine pressure buildup work, debris was discovered in both tubing string covering the perforations. Coiled tubing was moved onto the well and both tubing strings were successfully cleaned out.

Job Execution – Replacement Injectors:

Well 11-8WAR: Replacement injector 11-8WAR was spud on June 20,2000. The well was drilled to a depth of 2337' and logged. 7", 23#, K-55 casing was run and cemented into the hole. The drilling rig was released on June 23, 2000.

On 7/15/00, the subject well was hydraulically fractured. Two frac stages were completed and 807,300 lbs. of proppant was placed into the formation. On July 21, 2000 the workover rig was moved onto the well. Fill was circulated out and completion equipment was run (see attached Wellbore Schematic No. 2). The rig work was completed on July 26, 2000.

Well 11-8WR: Replacement injector 11-8WR was spud on June 16, 2000. The well was drilled to a depth of 2240' and logged. 7", 23#, K-55 casing was run and cemented into the hole. The drilling rig was released on June 19, 2000.

On July 15, 2000, the subject well was hydraulically fractured. Two frac stages were completed and 714,900 lbs. of proppant was placed into the formation. On July 17, 2000, the workover rig was moved onto the well. Fill was circulated out of the wellbore. The well was unable to be killed, even though 22% KCl water was used as a kill fluid). A snubbing unit was moved in and completion equipment was run (see attached Wellbore Schematic No.1). The rig work was completed on July 21, 2000.

Tiltmetering Work:

The hydraulic fracture completions of both new injectors, 11-8WAR and 11-8WR, were tiltmetered. The results are shown in tabular form in Table 1 below and graphically in map view in Figure 2.5-1.

Table 2.5-1. Surface tiltmeter fracture mapping results for 11-8WAR and 11-8WR.

Well Name	Stage #	Job Date mm/dd/yy	Perforation Interval (ft)	Fracture Azimuth	Fracture Dip	Vol. % Horizontal Component
11-8WAR	1	07/15/00	1898 - 2105	N 67° E ± 3°	88° down to the SE ±2°	24%
	2	07/15/00	1605 - 1785	N 79° E ±2°	88° down to the NW ±2°	35%
11-8WR	1	07/15/00	1847 - 2035	N 65 E ± 2°	85° down to the NW ±2°	24%
	2	07/15/00	1605 - 1785	N 60 E ± 2°	80° down to the SE ± 2°	21%
Average				**N 68°E**	**89° down to the SE**	**26%**

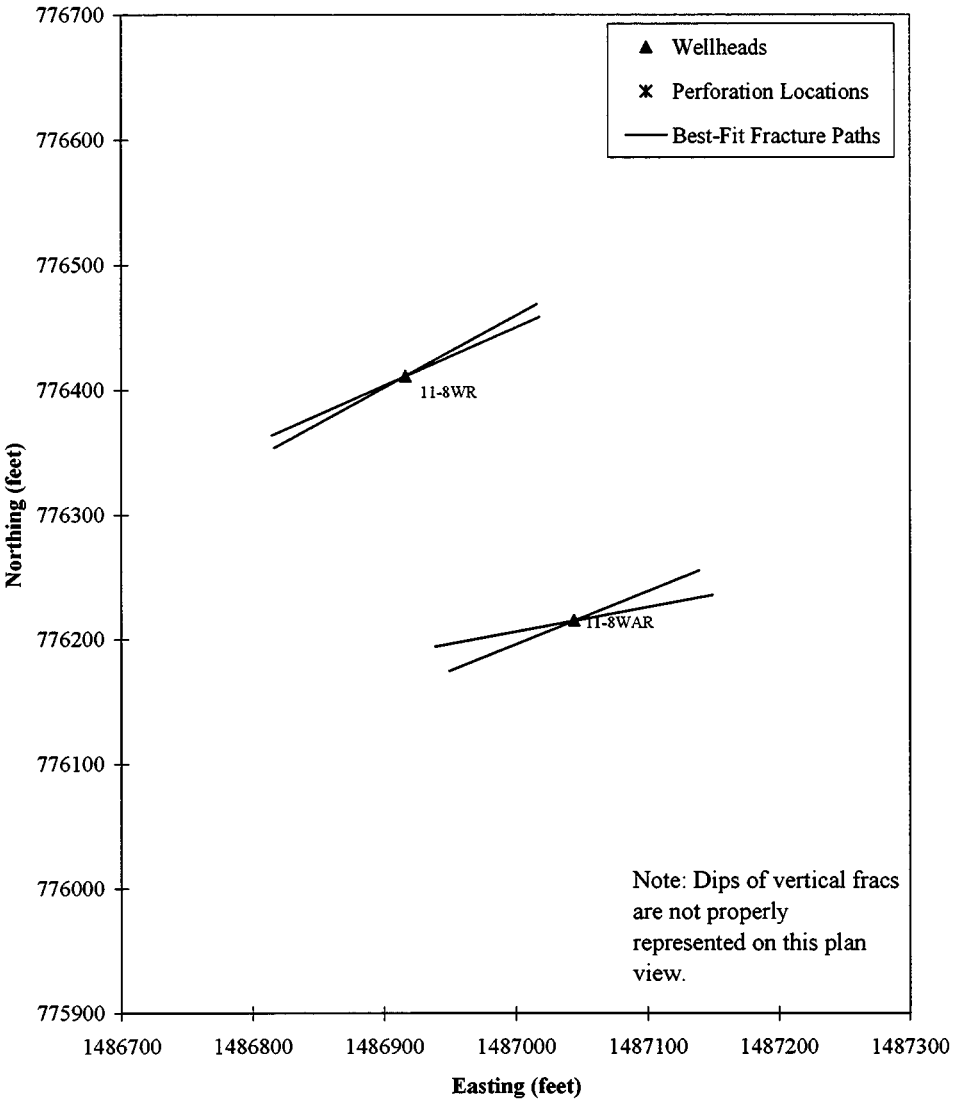

Figure 2.5-1. Tiltmetering results for new injectors 11-8WR and 11-8WAR.

Post-Job Analysis - Well Review:

The *CO_2 Pilot* team and the *Well Development* team were able to successfully salvage two of the four existing injection wells. The average cost to remediate wells 12-7W and 12-8W was approximately $75,000 per well. The average cost to drill and complete replacement injectors 11-8WR and 11-8WAR was approximately $298,000 per well. Salvaging wells 12-7W and 12-8W, resulted in a savings of approximately $450,000 in lieu of drilling two new replacement injectors.

At the start of this remedial effort, shallow casing problems (approximately at 500') created by subsidence issues had been identified. A remedial strategy had been prepared to take into account these shallow casing issues. However, it was discovered during these remedial operations that casing problems actually existed across the completion interval (approximately at 1600'). The casing problems encountered within the completion intervals

were the driving factors in the abandonments of injectors 11-8W and 11-8WA. Future injector remedial work at Lost Hills should be prepared for both shallow (approximately at 500') and deeper (approximately at 1600') casing problems.

Well 12-8W was a successful remedial candidate in spite of significant shallow casing problems that would not allow the permanent packer to be milled out or a completion packer to be run below 494'. In this situation, an inflatable packer and stage collar were utilized to help cement the tubing string into place and return the well to injection.

All four injection wells are completed with CO_2 compatible completion equipment. Duoline (internally coated with fiberglass) tubing was run. The packers are both internally and externally coated, as is all completion equipment below the packer.

Post-Job Cost Analysis:
Total appropriations for all well work including remedial, abandonments and new wells was $1,623,140. Expenditures through September 30, 2000 are $1,567,000 (with all work completed as of August 8, 2000).

Producer Sanding Problems:
Sanding problems developed in CO_2 Pilot producers, 11-8D, 11-8E, 12-8D and 12-8C in mid-December 2000. These sanding problems developed after an increase in CO_2 injection rates which occurred on November 30, 2000 (all 4 injectors were increased to a rate of ~500/mcfd per injector). The sanding problems resulted in these four wells being shut-in, the wellbores cleaned out, and in certain cases, the pump depths being raised. The end result has been a decline in production due to well downtime and increased hydrostatic pressure on the formation due to the raised pump depths. To date, three of the four wells have been returned to production.

The fourth well, 11-8E, will require additional remedial efforts to resolve its current sand control problems. A Halliburton Services treatment know as *"Sand Wedge"* will be attempted within the next few weeks in an effort to control sand inflow into this well. A caliper log run in well 11-8D indicated potentially damaged perforations at a depth of ~1200 feet. The log also appeared to indicate that deeper perforations, across the lower half of the CO_2 injection interval were plugged off, possibly with scale.

A tracer survey was run on CO_2 Pilot Pressure Observation well OB-C3 in January 2001. The survey indicated communication between the short and long strings through the annulus which likely means poor cement bond behind pipe. Until remedial efforts are completed to isolate the short and long strings, well OB-C3 will not be used for any pressure monitoring.

The CO_2 Technical Team will focus on the following remedial efforts in the next few months:

1. Identify possible reasons for the increase in sand production in these problem wells. Note: In all (4) problem wells, there was no significant increase in gas production prior to the initiation of sand production.
2. The plugged off perforations in well 11-8D. How many other CO_2 Pilot producers have this problem? What is the best remedial/stimulation method to eliminate the plugging problem and effectively produce from the entire completion interval?
3. How to successfully isolate the short and long strings in observation well OB-C3?

Well No:	11-8WR	**Section:**	32 Fee	**API No.:**	030-15353
Drilled:	Jun-00	**DF Elev.:**	388.74	**DF:**	12.0'
TD:	2240'	**ED:**	2182'		

Existing Condition as of: **7/20/2000**

Casing/Liner Detail:

Size	Weight	Grade	Depth	Cmt'd
9 5/8"	32#	K-55	0-342"	100 sks.
7"	23#	K-55	0-2231'	345 sks.

Perforation Detail:

	Depth	Hole Size	Density	Phasing	Markers
Stage #1	2035'-2032'	0.5"	1jh/ft, (4)	0 deg.	J
Stage #1	1974'-1970'	0.5"	1jh/ft, (5)	0 deg.	J
Stage #1	1912'-1909'	0.5"	1jh/ft, (4)	0 deg.	J
Stage #1	1851'-1847'	0.5"	1jh/ft, (5)	0 deg.	Hsb
Stage #2	1785'-1782'	0.5"	1jh/ft, (4)	0 deg.	Bh
Stage #2	1727'-1723'	0.5"	1jh/ft, (5)	0 deg.	H
Stage #2	1667'-1664'	0.5"	1jh/ft, (4)	0 deg.	GG
Stage #2	1609'-1605'	0.5"	1jh/ft, (5)	0 deg.	G2st

Tubing Detail:

Size	Weight	Grade	Depth	ID
2 3/8"	4.6#	Duoline	at 1568'	**1.74"**

Completion Equipment:

Packer	Profile Nipple
Baker "A-3"	"x" Nipple
Lok-Set	**(1.5" ID)**
at 1557'	at 1567'

Markers	**Markers**	**Markers**	**Markers**	**Markers**
FF-1572'	G1sb-1596'	GG-1665'	BH-1769'	J-1878'
FFsb-1579'	G2st-1623'	GGsb-1681'	Hst-1793'	K-2005'
G-1592'	G2sb-1626'	H-1723'	Hsb-1813'	L-2035'

Tubing	2 3/8" Duoline	
x-over	2 3/8 x 2 7/8	
Baker A-3	Lok-Set Pkr	at 1557'
x-over	2 7/8 x 2 3/8	
6' pup joint	2 3/8" Duoline	
x-nipple	9 Chrome, (1.5")	at 1567'
6' pup joint	2 3/8" Duoline	
Entry Guide	at 1568'	

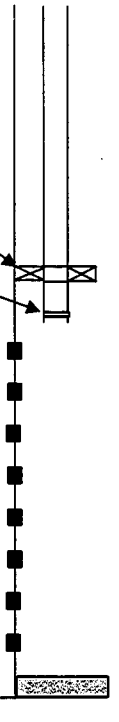

Wellbore Schematic No. 1: Injector 11-8WR

Well No:	11-8WAR	**Section:**	32 Fee	**API No.:**	030-15352
Drilled:	Jun-00	**DF Elev.:**	390.9	**DF:**	12.0'
TD:	2337'	**ED:**	2316'		

Existing Condition as of: 7/26/2000

Casing/Liner Detail:

Size	Weight	Grade	Depth	Cmt'd
9 5/8"	36#	K-55	0-327'	86 sks.
7"	23#	K-55	0-2332'	310 sks.

Perforation Detail:

	Depth	Hole Size	Density	Phasing	Markers
Stage #2	2105'-2102'	0.5"	1jh/ft, (4)	0 deg.	K
Stage #2	2038'-2034'	0.5"	1jh/ft, (5)	0 deg.	J
Stage #2	1970'-1967'	0.5"	1jh/ft, (4)	0 deg.	J
Stage #2	1902'-1898'	0.5"	1jh/ft, (5)	0 deg.	Hsb
Stage #1	1830'-1827'	0.5"	1jh/ft, (4)	0 deg.	BH
Stage #1	1764'-1760'	0.5"	1jh/ft, (5)	0 deg.	GGsb
Stage #1	1697'-1694'	0.5"	1jh/ft, (4)	0 deg.	G2sb
Stage #1	1631'-1627'	0.5"	1jh/ft, (5)	0 deg.	FFsb

Tubing Detail:

Size	Weight	Grade	Depth	ID
2 3/8"	4.6#	Duoline	at 1,576'	1.74"

Completion Equipment:

Packer	Nipple Profile
Baker "A-3" Lok-Set at 1,544'	"x" nipple (1.5" ID) at 1,569'

Markers	Markers	Markers	Markers	Markers
FF-1589'	G1sb-1642'	GG-1737'	BH-1835'	J-1937'
FFsb-1609'	G2st-1684'	GGsb-1750'	Hst-1849'	K-2068'
G-1635'	G2sb-1693'	H-1795'	Hsb-1875'	L-2106'

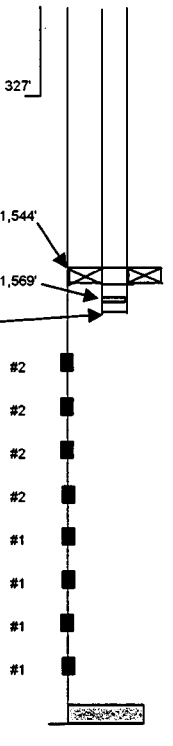

Wellbore Schematic No. 2: Injector 11-8WAR

Well No:	12-7W	**Section:**	32 Fee	**API No.:**	030-03565
Drilled:	Feb-95	**DF Elev.:**	379.24'	**DF:**	12.0'
TD:	2,368'	**ED:**	2,315'		

Existing Condition as of: 8/8/2000

Casing/Liner Detail:

Size	Weight	Grade	Depth	Cmt'd
9 5/8"	36#	K-55	0-487'	150 sks.
7"	23#	K-55	0-2359'	220 sks.

Perforation Detail:

	Depth	Hole Size	Density	Phasing	Markers
Stage #1	2140'-1930'	0.5"	1jh/5'	0 deg.	J-L
Stage #2	1880'-1670'	0.5"	1jh/5'	0 deg.	FF-BH

Tubing Detail:

Size	Weight	Grade	Depth	ID
2 3/8"	4.6#	Duoline	1606'	**1.74"**

Completion Equipment:

Packer	Profile Nipple
Baker "A-3" Lok-Set (1.5" ID) at 1592'	"x" Nipple at 1600'

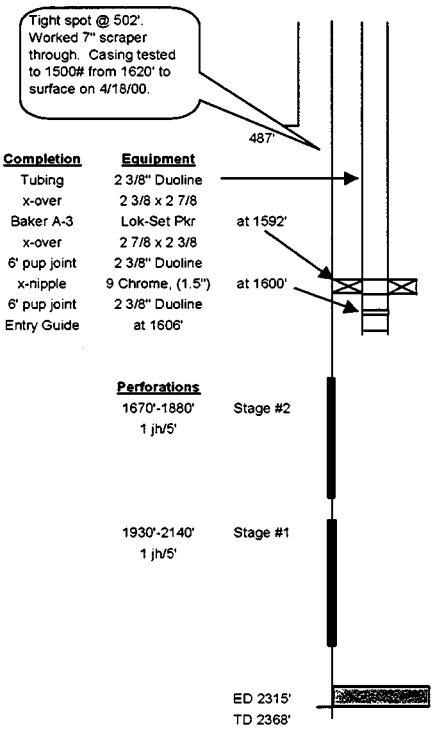

Wellbore Schematic No. 3: Injector 12-7W

Well No:	OB-C2	**Section:**	32 Fee	**API No.:**	030-15273
Drilled:	Jun-00	**DF Elev.:**	392'	**DF:**	12.0'
TD:	2240'	**ED:**	2201'		

Existing Condition as of: 7/13/2000

Casing/Liner Detail:	Size	Weight	Grade	Depth	Cmt'd
Intermediate	9 5/8"	36#	K-55	0-337'	141 cu. ft.
Completion	7"	23#	K-55	0-1055'	460 cu. ft.
	7"	"1010"	Fiberglass	1055'-2155'	
	7"	23#	K-55	2155'-2232'	
Bestline Casing Patch	4.187" ID			1606'-1628'	281 cu. ft.

Markers (Hole problems, no logs)
FF-
H-
BH-
J-
K-
L-

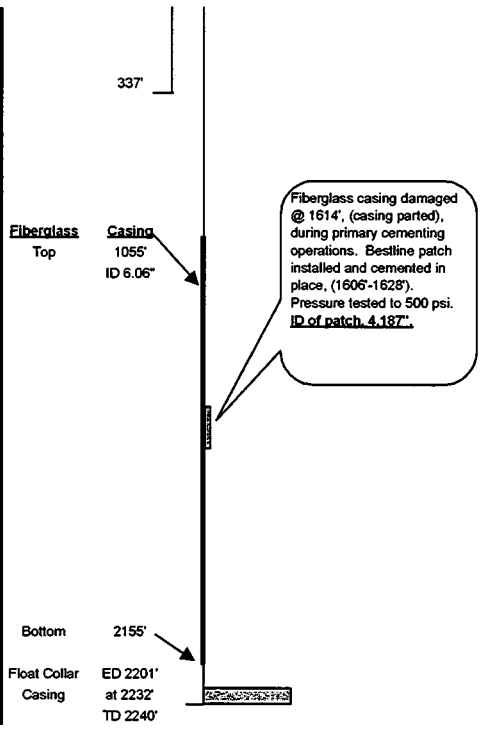

Wellbore Schematic No. 4: Observation Well OB-C2

Well No:	OB-C3	**Section:**	32 Fee	**API No.:**	030-15325
Drilled:	Jun-00	**DF Elev:**	388.2'	**DF:**	12.0'
TD:	2,220'	**ED:**	2,202'		

Existing Condition as of: 8/28/2000

Casing Detail	Size	Weight	Grade	Depth	Cmt'd
	10 3/4"	40.5#	K-55	0-320'	144 cu. ft.

Tubing Detail:	Size	Weight	Grade	Depth	ID
Long String, (cemented)	2 7/8"	6.4#	Duoline	2,213'	2.14"
Short String, (cemented)	2 7/8"	6.4#	Duoline	2,203'	2.14"

Perforation Detail:	Depth	Hole Size	Density	Phasing	Markers
Long String	1885'-2080'	.20"	1 jh/5'	0 deg.	Hst-L
Short String	1650'-1845'	.20"	1 jh/5'	0 deg.	FF-H

Markers	**Markers**
FF-1649'	H-1829'
FFsb-1671'	BH-1868'
G-1684'	Hst-1883'
G1sb-1693'	Hsb-1897'
G2st-1734'	J-1943'
G2sb-1746'	K-2040'
GG-1785'	L-2078'
GGsb-1793'	

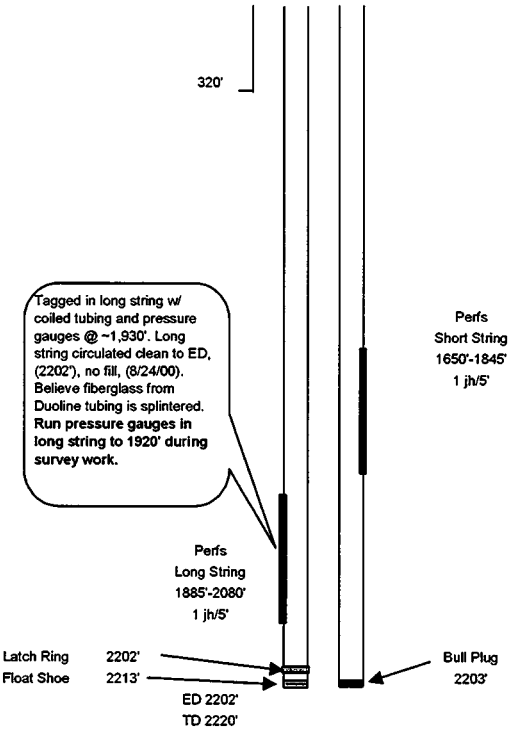

Wellbore Schematic No. 5: Observation Well OB-C3

SECTION 3

PILOT PERFORMANCE

3. PILOT PERFORMANCE

Pasquale R. Perri
Chevron USA Production Company

3.1 Injection Performance:

CO_2 injection commenced on August 31, 2000 into the four pilot injectors. CO_2 injection began slowly at 50 MCF/D per injector as we de-bugged and became acquainted with the new facilities. CO_2 injection was slowly ramped up from 50 MCF/D per injector to approximately 475 MSCF/D per injector prior to experiencing sanding problems in four producers. Figures 3.1-1 through 3.1-4 are the individual water/CO_2 injection plots for the four pilot injectors. Sanding problems developed in CO_2 pilot producers 11-8D, 11-8E, 12-8D and 12-8C in mid-December 2000. CO_2 injection has been suspended as we try to figure out the root cause of the sanding problems and how we plan to remediate the wells.

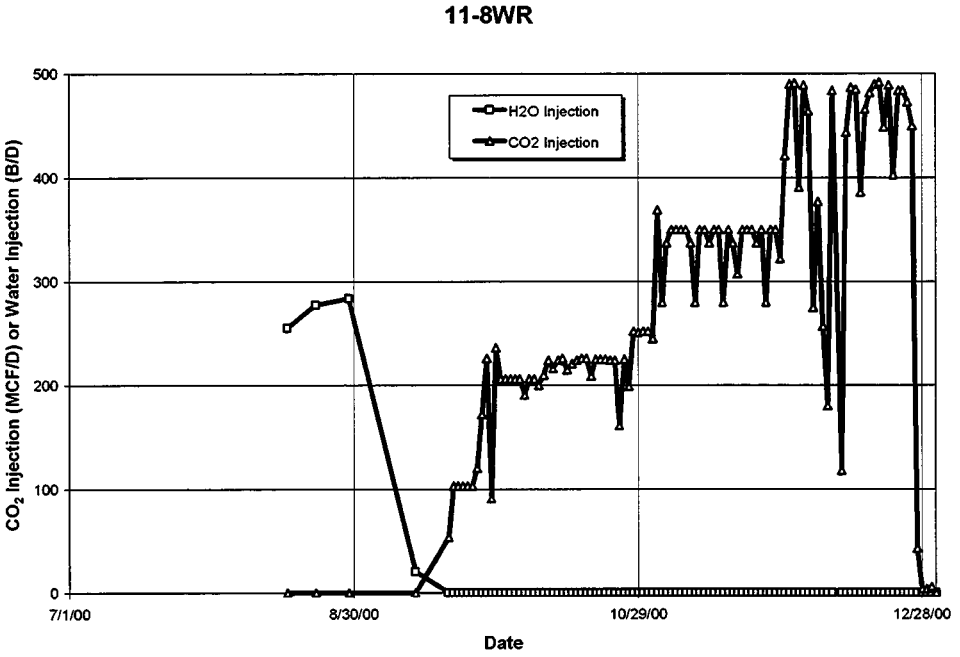

Figure 3.1-1. Injection Plot for CO_2 Injector 11-8WR.

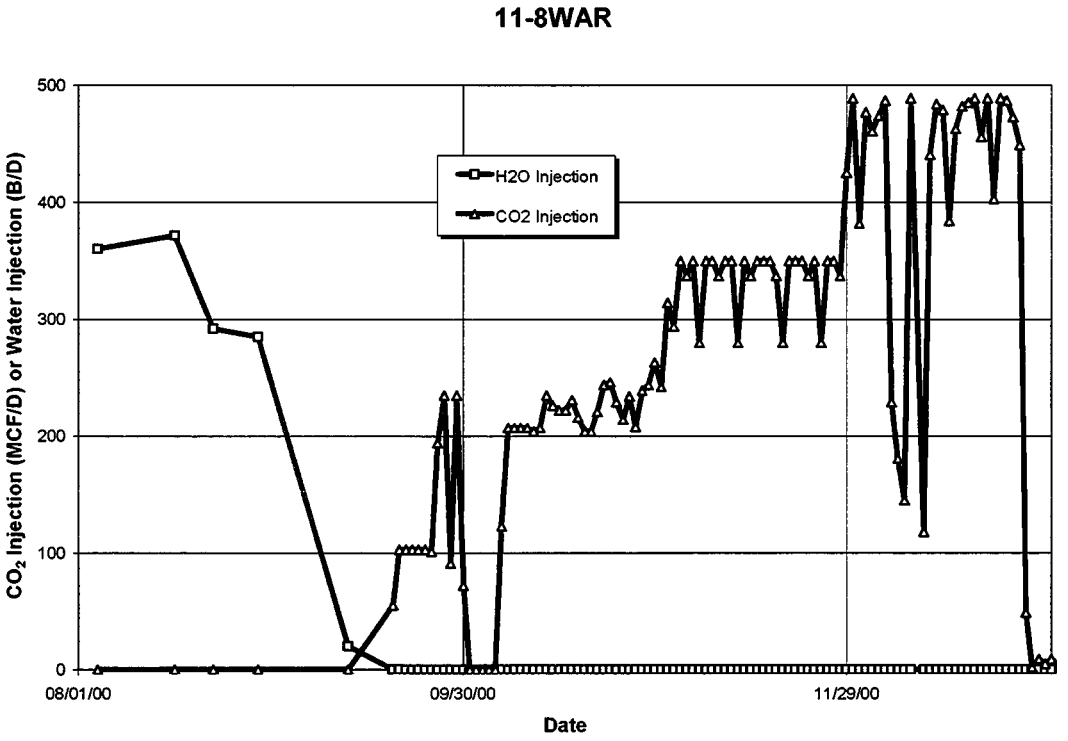

Figure 3.1-2. Injection Plot for CO_2 Injector 11-8WAR.

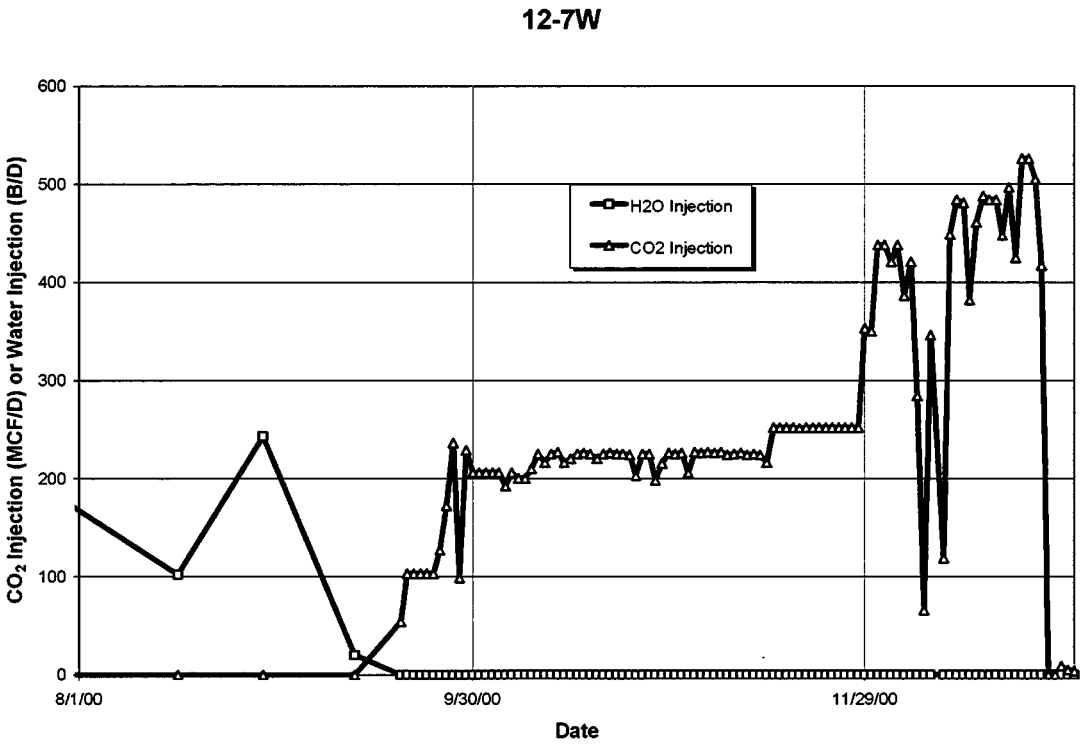

Figure 3.1-3. Injection Plot for CO_2 Injector 12-7W.

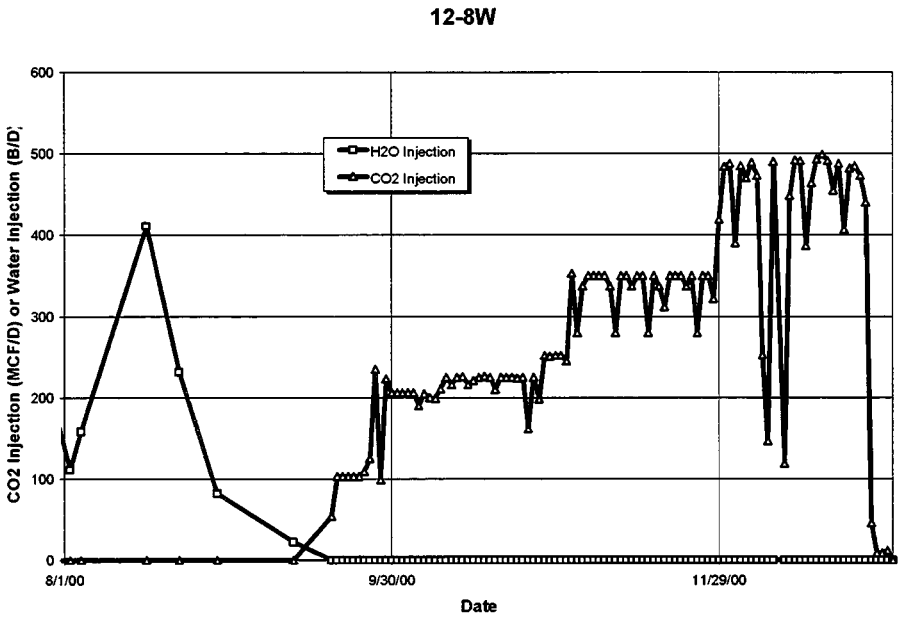

Figure 3.1-4. Injection Plot for CO_2 Injector 12-8W.

Figure 3.1-5 is the composite or total CO_2 injection for the pilot. Table 3.1-1 summarizes the cumulative CO_2 injected for the pilot through December 31, 2000. Since August 31, 2000, we have injected 116,460 MCF of CO_2 at the average rate of 239 MCF/D per injector. This equates to a HCPV of CO_2 injected of only 0.0155.

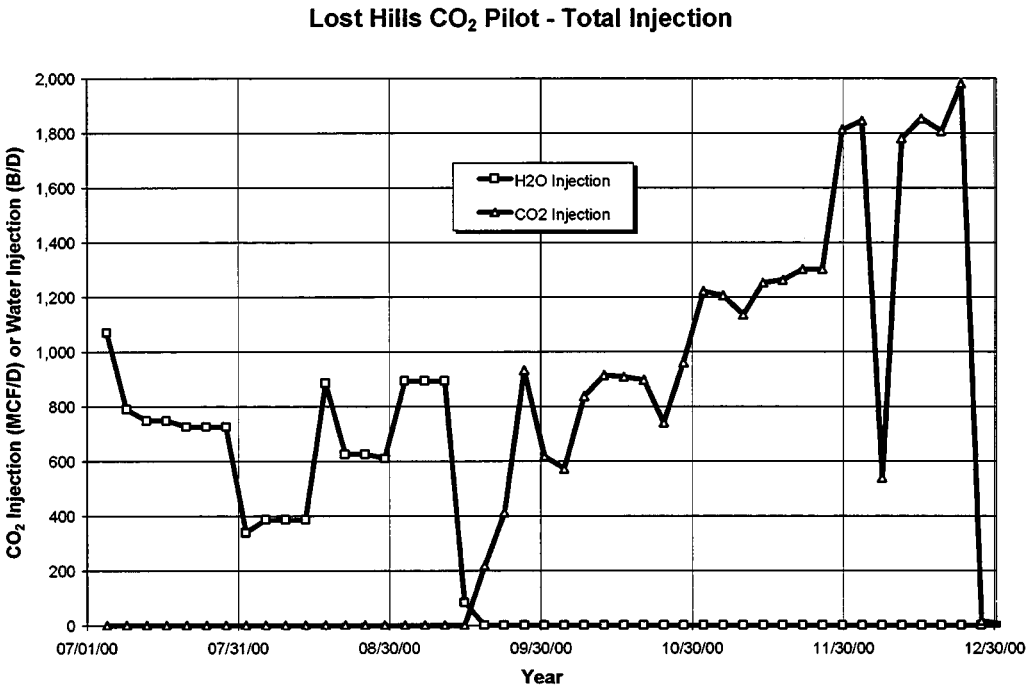

Figure 3.1-5. Total Injection Plot for CO_2 Pilot.

Table 3.1-1. Cumulative Pilot CO_2 Injection through December 31, 2000.

Injector	MCF	HCPV
11-8WR	30,677	0.0153
11-8WAR	30,677	0.0200
12-7W	24,119	0.0133
12-8W	30,987	0.0142
Total	**116,460**	**0.0155**

3.2 Production Performance:

The pilot project contains ten producers in addition to the four pilot injectors. Figures 3.2-1 through 3.2-10 are the individual production plot for the ten pilot producers. Figure 3.2-11 is the total production performance plot for the ten producers since the initiation of CO_2 injection on August 31, 2000. Note that we started to see an oil response in mid-November 2000 in well 11-8E (see Figure 3.2-5). However, at approximately the same point in time we began experiencing sanding problems and pilot production subsequently, declined. Eventually four producers had to be shut-in due to extensive sanding. These wells remain shut-in as remediation programs are being developed to correct these problems.

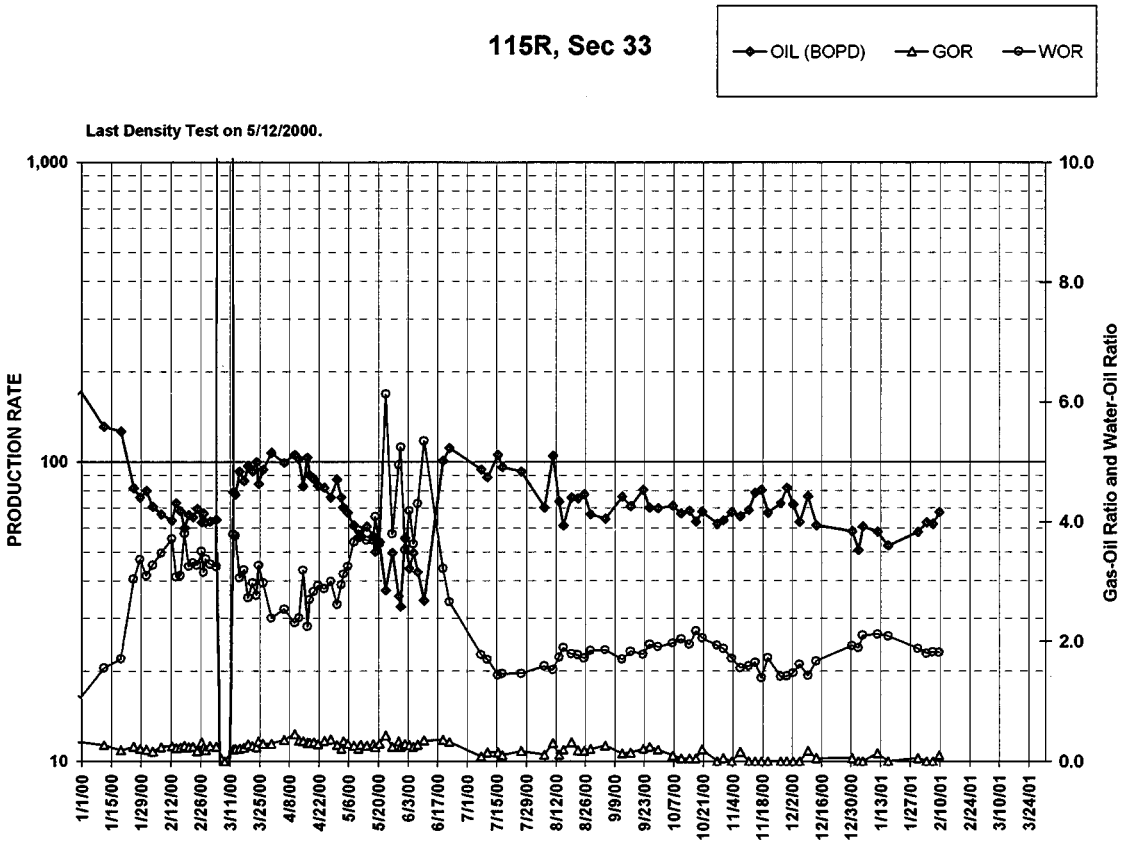

Figure 3.2-1. Production Plot for CO_2 Producer 115R, Section 33.

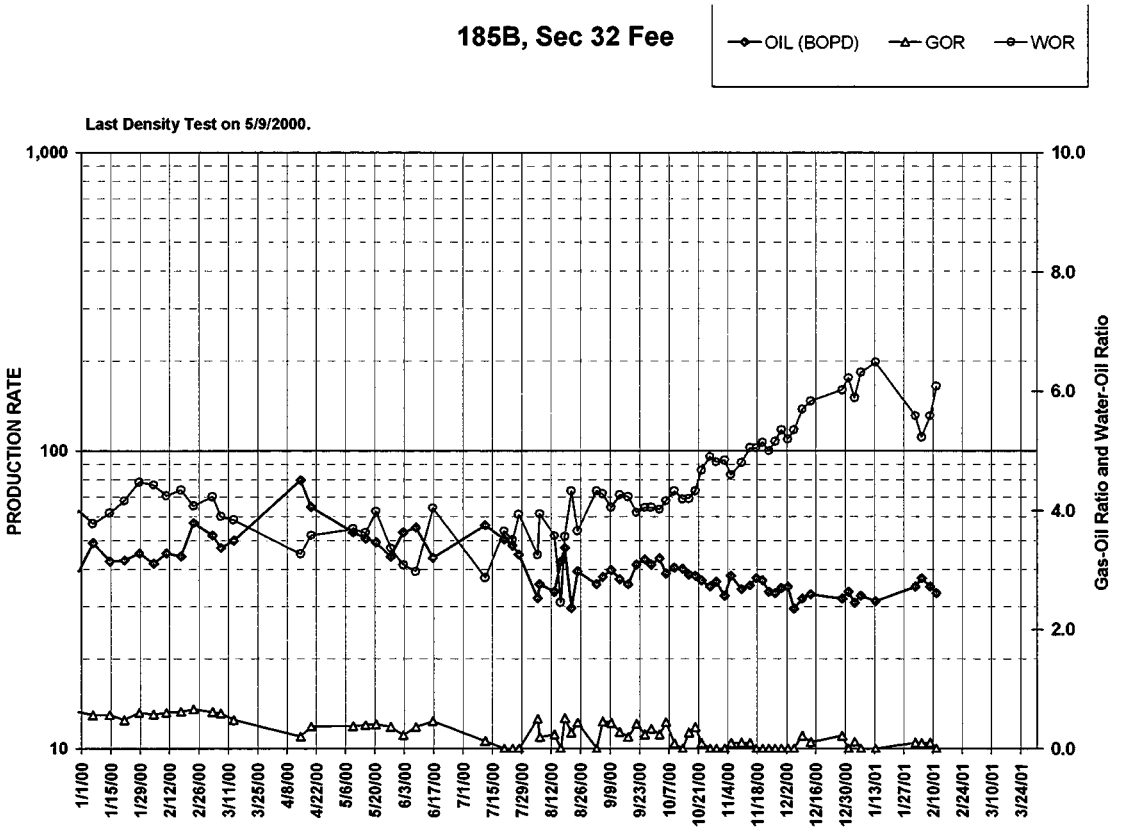

Figure 3.2-2. Production Plot for CO_2 Producer 185B, Section 32 Fee.

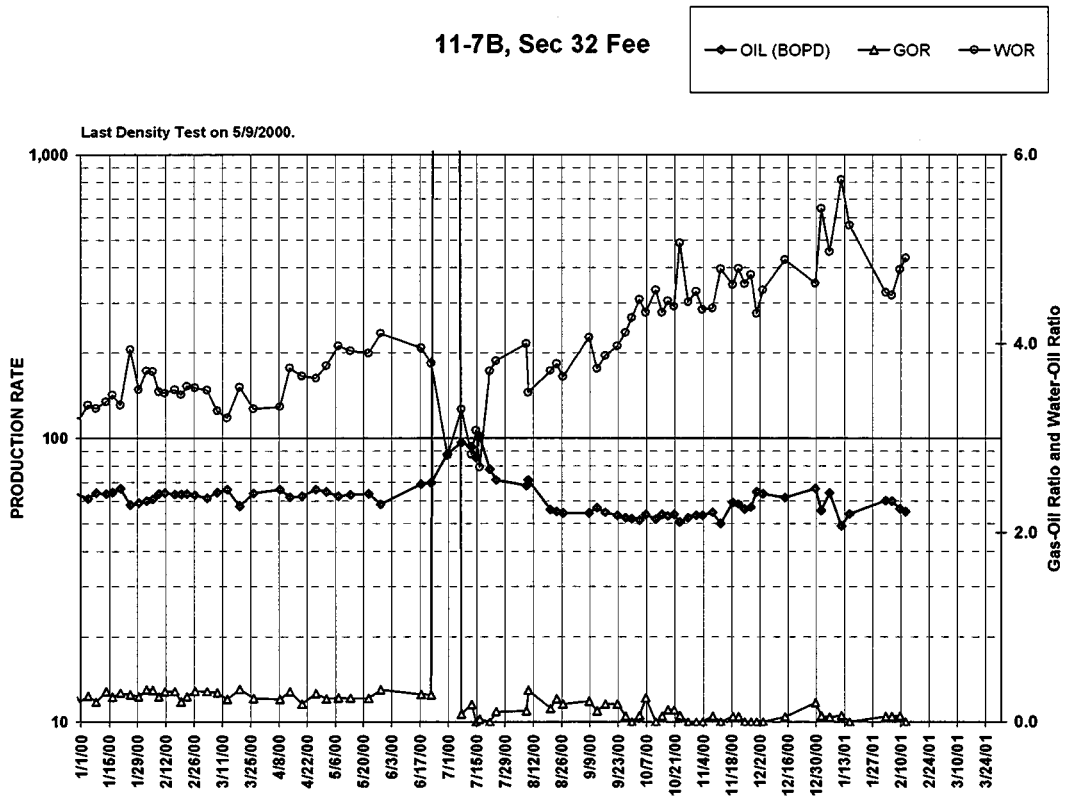

Figure 3.2-3. Production Plot for CO_2 Producer 11-7B, Section 32 Fee.

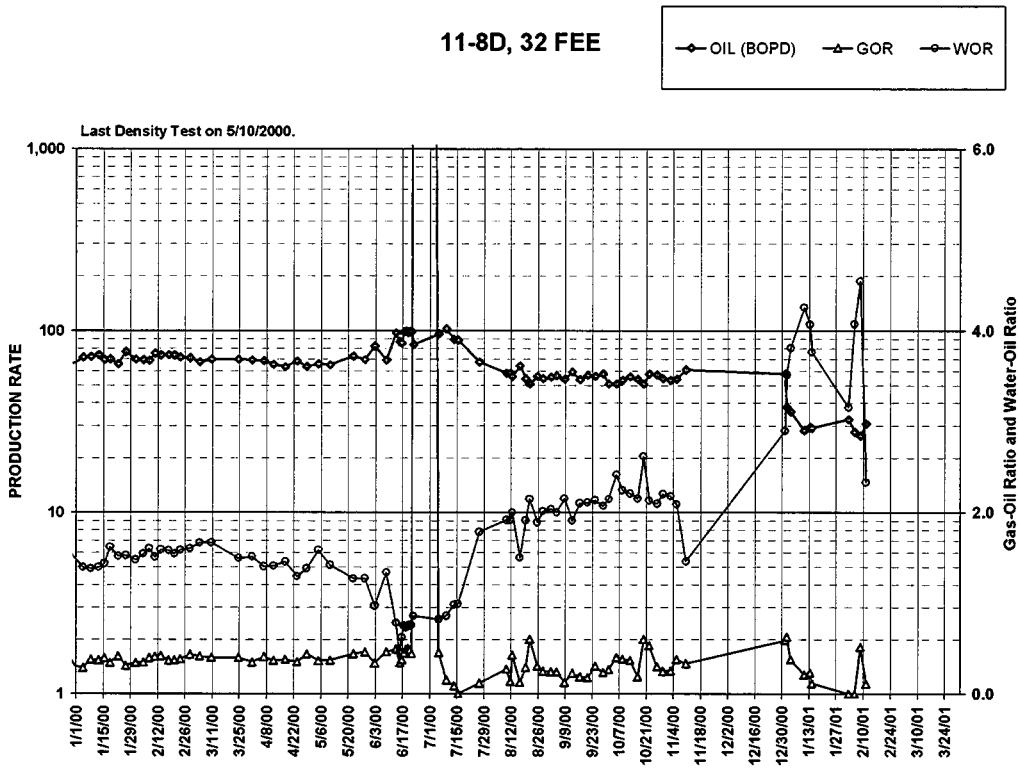

Figure 3.2-4. Production Plot for CO_2 Producer 11-8D, Section 32 Fee.

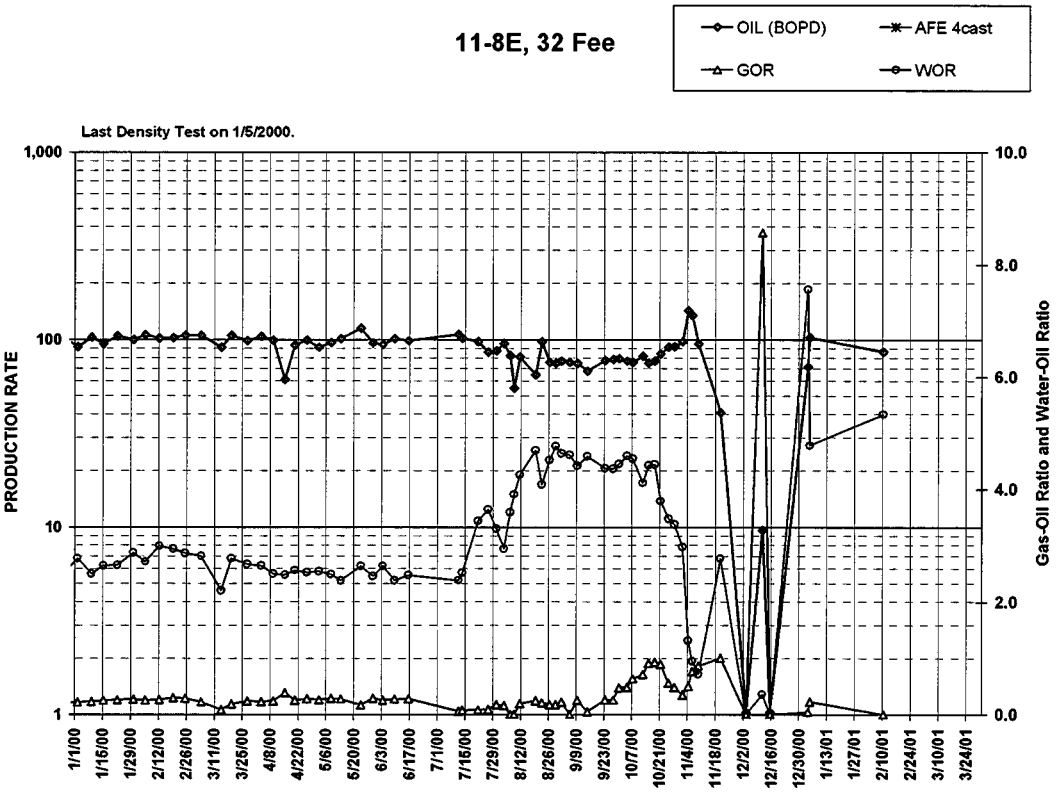

Figure 3.2-5. Production Plot for CO_2 Producer 11-8E, Section 32 Fee.

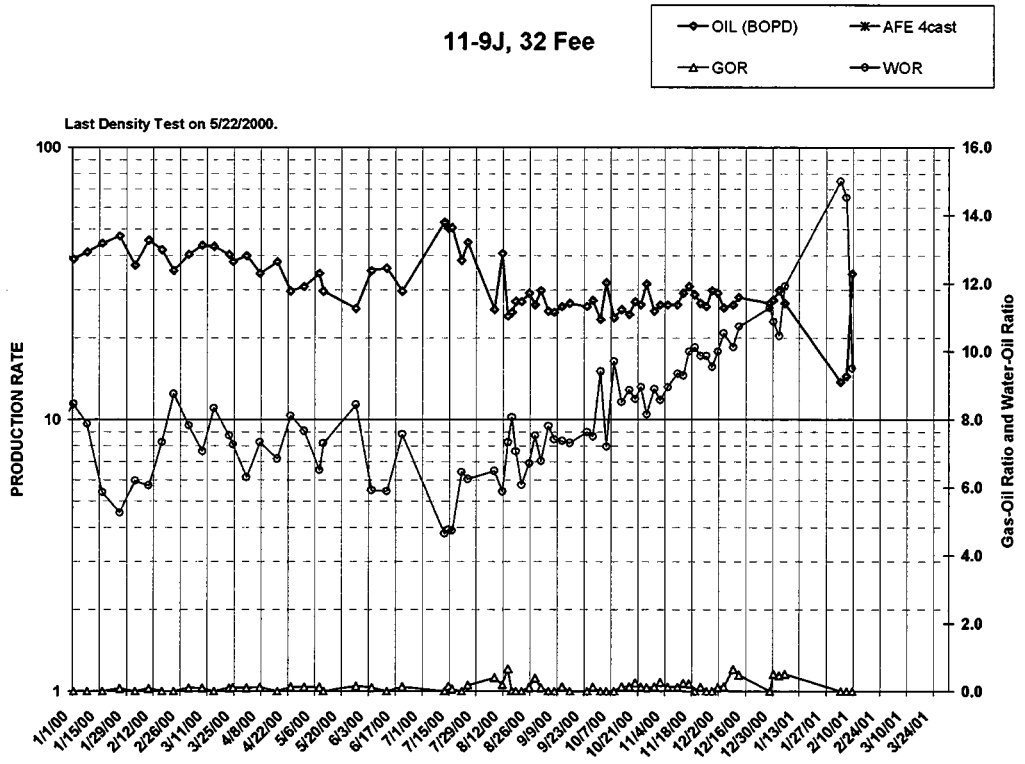

Figure 3.2-6. Production Plot for CO_2 Producer 11-9J, Section 32 Fee.

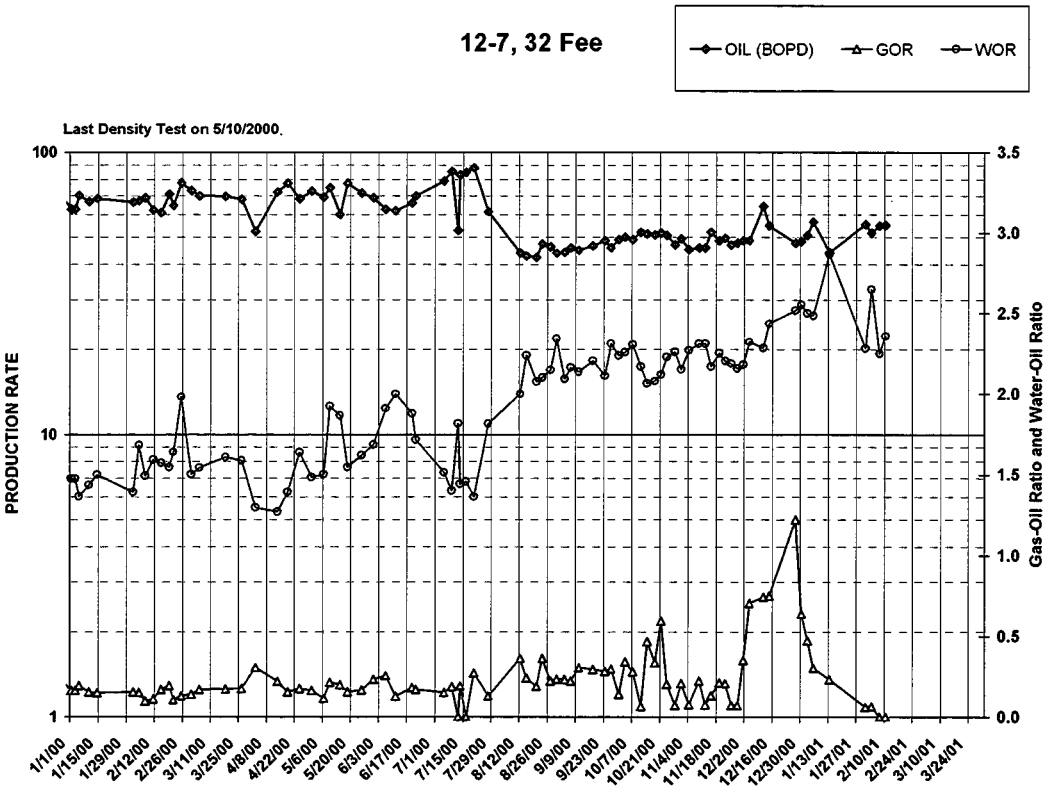

Figure 3.2-7. Production Plot for CO_2 Producer 12-7, Section 32 Fee.

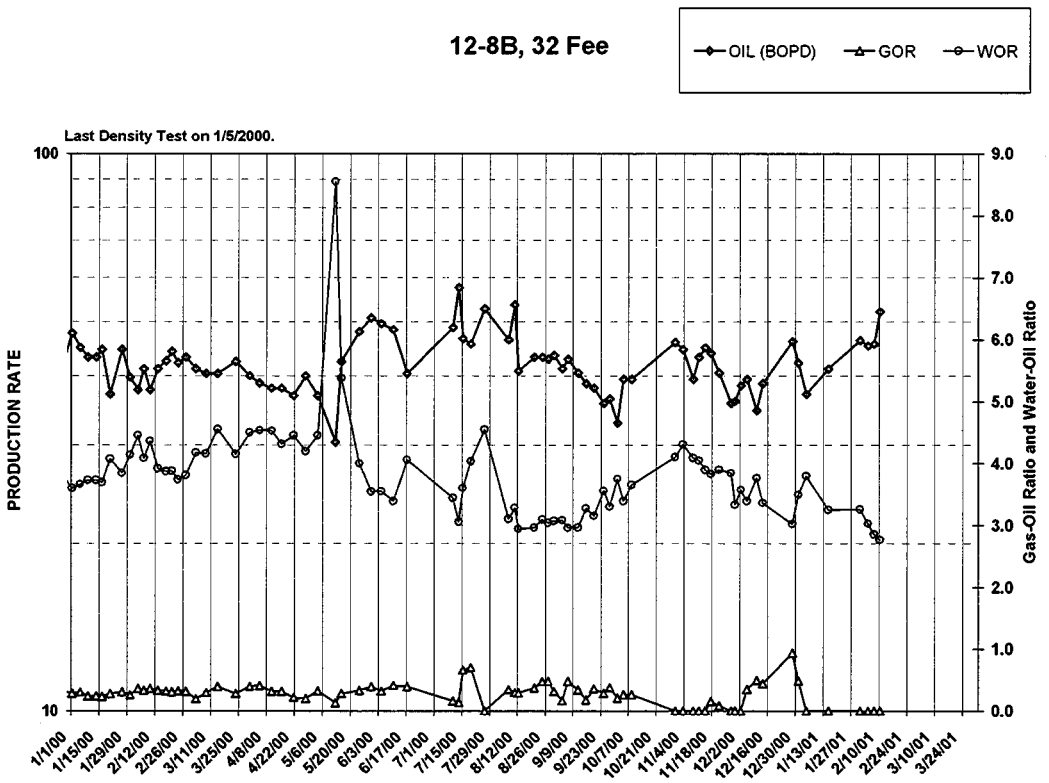

Figure 3.2-8. Production Plot for CO_2 Producer 12-8B, Section 32 Fee.

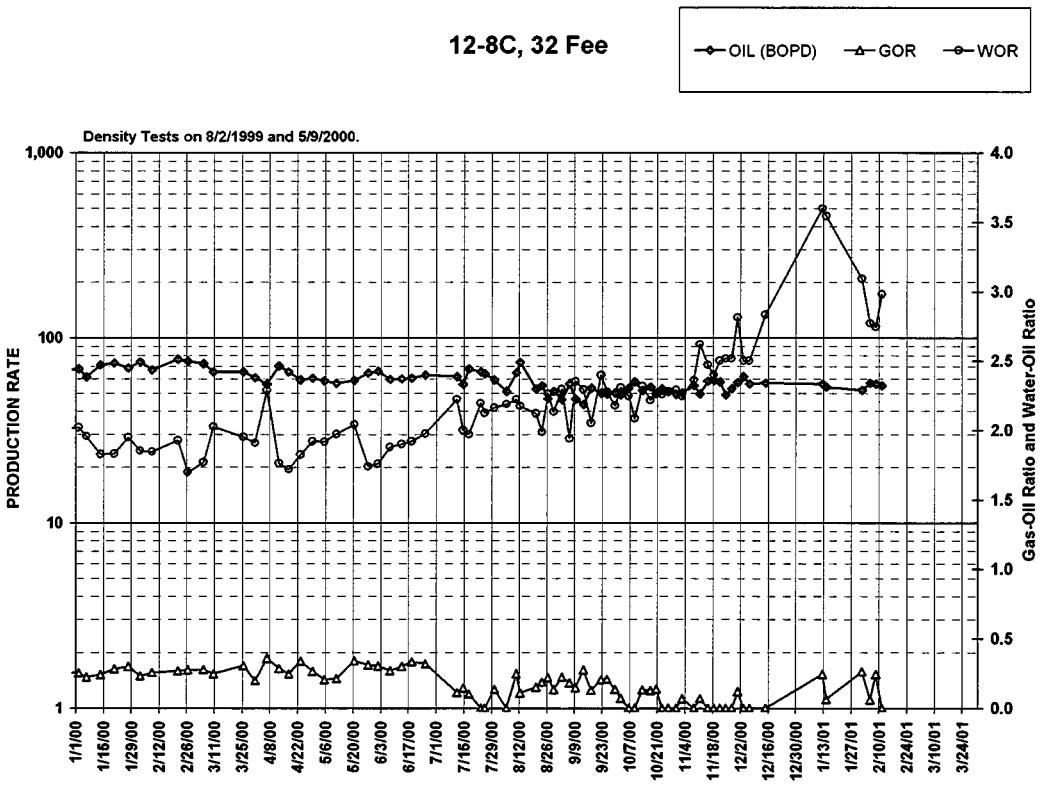

Figure 3.2-9. Production Plot for CO_2 Producer 12-8C, Section 32 Fee.

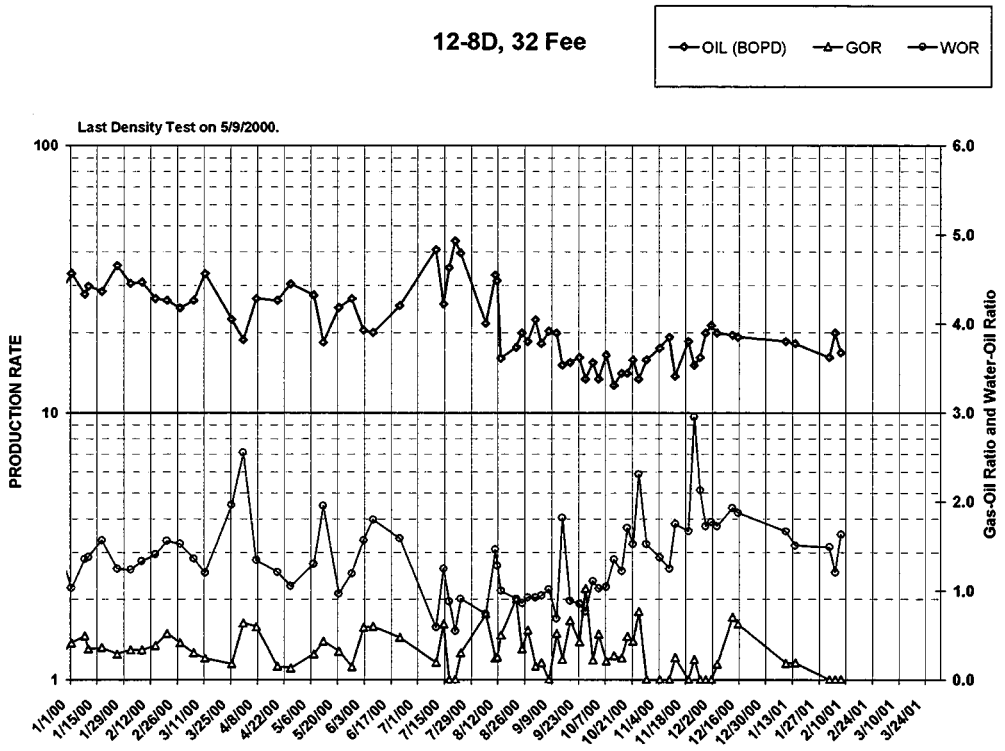

Figure 3.2-10. CO_2 Producer 12-8D, Section 32 Fee.

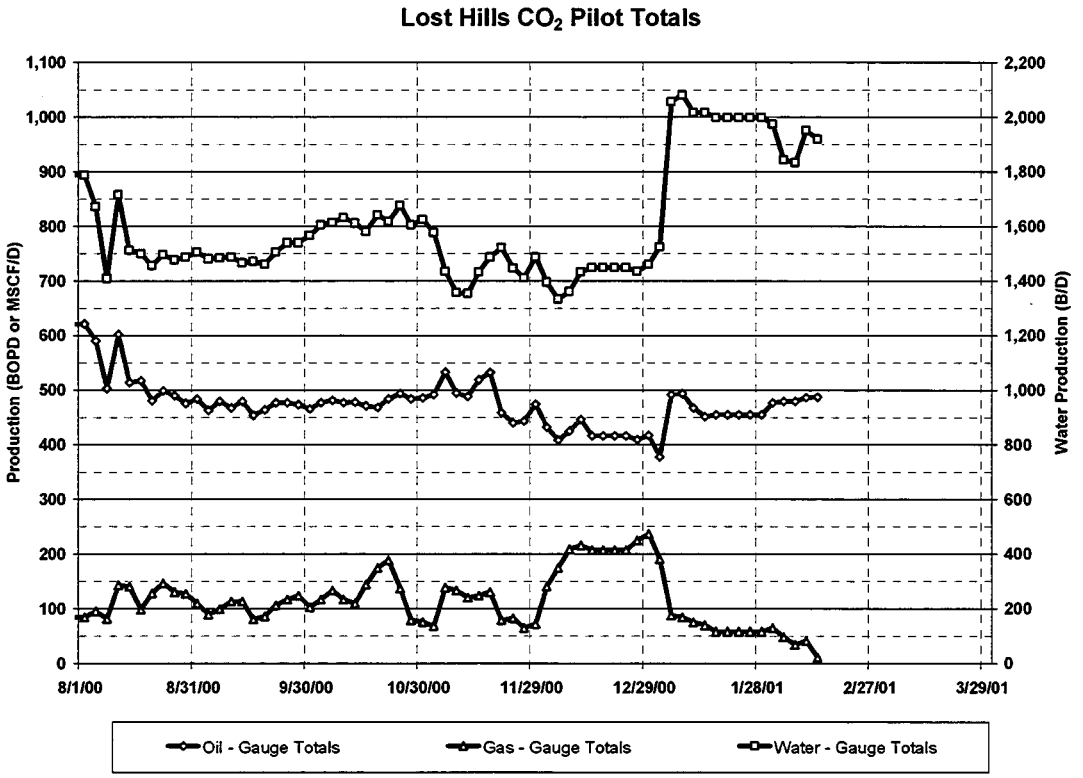

Figure 3.2-11. Total Production Plot for CO_2 Pilot.

3.3 PILOT OPERATING STRATEGY

John F. Cooney, Pasquale R. Perri
Chevron USA Production Company

WAG Optimization:
Based on the industry experience with West Texas CO_2 floods, we anticipate having to deal with CO_2 breakthrough. Therefore the operating strategy for the pilot centers around the need to control breakthrough individually for each pattern, on a moments notice.

The following table depicts the planned strategy for dealing with breakthrough:

Table 3.3-1. CO_2 Pilot WAG Operating Strategy.

Injectants	CO_2 / Water Injection Rate	CO_2 Injection Duration	Water Injection Duration	WAG Cycle Times	Synchronize Patterns ? (i.e. same injectant at all times?)
CO_2 Alt. With Water	Start with low of 100 mscfd per well and work up to 500 mscfd max.	Inject until breakthrough is detected (breakthrough defined by detection of tracer gases in one producer)	Either: • Inject until desired HCPVSI is achieved. or • If there is a production kick, "ride it out".	Continue with cycles until desired cumulative HCPVSI is achieved.	Control patterns individually. Some may be under CO_2 injection while others under water injection

By applying the above strategies, we hope to arrive at the optimal process for controlling CO_2 breakthrough while monitoring for an oil kick. As noted before, the above strategies will be tested before facilities to handle high CO_2 are installed. We are risking shutting down injection for a while but it reduces the capital investment risked up-front. If the cumulative CO_2 percentage for the area of the pilot stays low enough to avoid corrosion, injection will not be stopped to wait on facilities.

3.4 RESERVOIR SIMULATION

William S. Fong
Chevron USA Production Company

Simulation Model – History Match:
This section discusses the results of history matching the past 50 years of production in the CO_2 pilot area. Wells that started producing in the 1950's were non-hydraulically fractured wells. These wells produced until the late 1980's. From 1989 to present day, new hydraulically fractured wells, each year, have been put on production. Water injection also was initiated in the early 1990's. The history match was therefore made in two stages:

1. **Primary production match** with no hydraulic fractures in the model from 1949 - 1991.
2. **Waterflood match** in which all new wells are hydraulically fractured from 1991 - 1999.

To model hydraulic fractures, thin planes of cells were added to the simulation grid as shown in Figure 3.4-1.

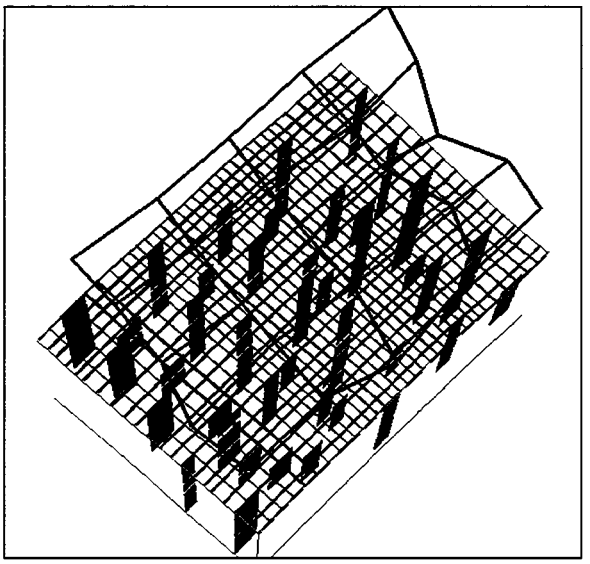

Figure 3.4-1. 16 pattern model showing hydraulic fractures. The CO_2 Pilot is encompassed by the center 4 patterns.

Primary Production History Match:
The result of the primary, or non-hydraulic fracturing, stage history match is considered satisfactory. Figures 3.4-2 and 3.4-3 are comparison plots of oil production and GOR history (lines) compared to simulation results (squares). By 1992, some water injection has already taken place, resulting in a decrease in GOR.

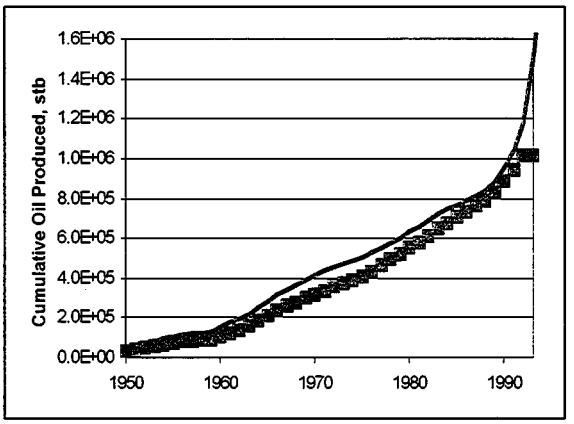

Figure 3.4-2. Cumulative oil match–primary.

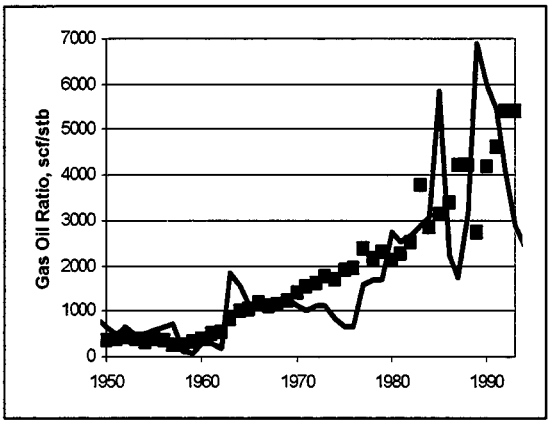

Figure 3.4-3. Gas-oil ratio match–primary.

Waterflood History Match:

The pressure, oil bubble point and saturations of the primary, or non-hydraulic fracturing, model at timestep 1991 was output to construct a model with hydraulic fractures at the newer wells for the waterflood history match. All the adjustments in the primary model were carried over to this model. We assumed all the wells that were put on production after 1991 are all hydraulically fractured at 1991 in the model. The history match was then continued.

Initially, due to the numerous hydraulic fractures in the model, the model ran very slow. A few adjustments were made, including (a) a reduction in fracture permeability from 1000 md to 250 md, and (b) a test a case in which the hydraulic fractures in the outer boundary of the 16-pattern model were inactive. The results were very satisfactory. Simulation run time was reduced to less than 1.5 cpu days. When the hydraulic fractures on the outer boundary were taken out, the model ran in 14 cpu hours.

Results from the following two cases are discussed here:

1. All the hydraulic fractures are retained (all_t6 case).
2. Hydraulic fractures in the outer boundary of the 16-pattern model are inactive (fhm5 case).

Figure 3.4-4 shows the oil production match for both cases. For both of the above models, the predicted oil matches historical production until later times (1996 – 2000) when the predicted oil is lower than actual oil production. This is because the model boundary patterns do not get enough pressure support, especially in the "fhm5" case, where the hydraulic fractures are inactive. The water-oil ratio (WOR) and gas-oil ratio (GOR) matches are shown in Figures 3.4-5 and 3.4-6, respectively, and are reasonably close.

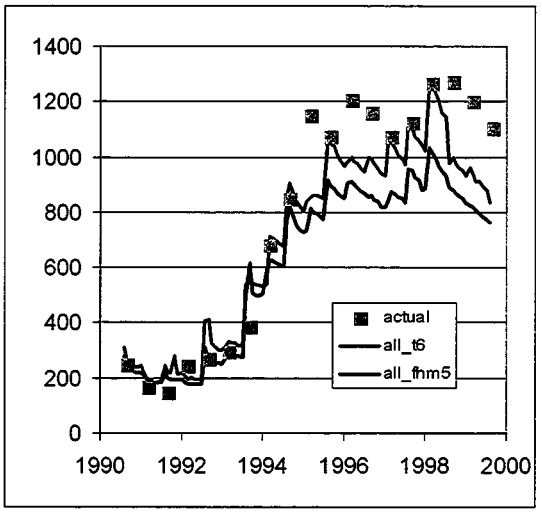

Fig. 3.4-4. Oil rate (bbl/d) match–waterflood.

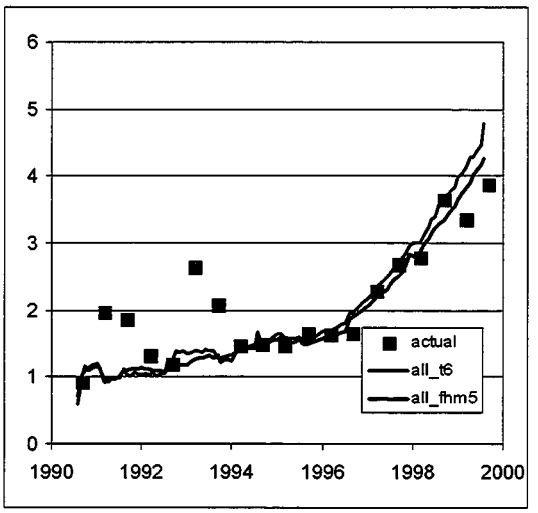

Figure 3.4-5. WOR (bbl/bbl) ratio match–waterflood.

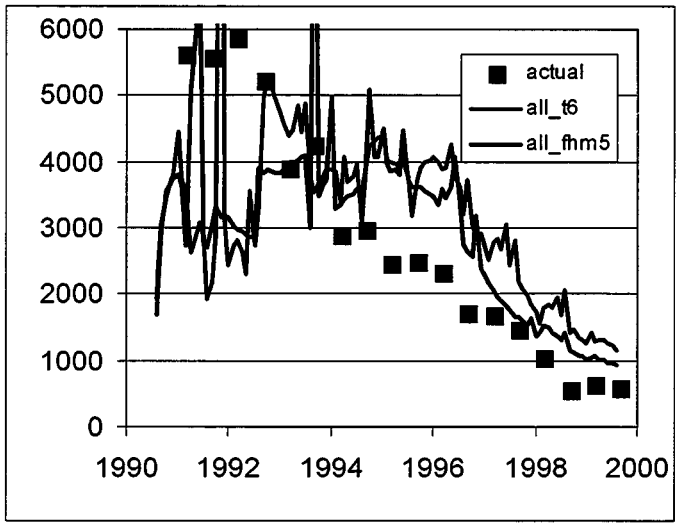

Figure 3.4-6. GOR (scf/stb) ratio match–waterflood.

The purpose of modeling sixteen patterns is to make sure the center four patterns (CO_2 pilot area) have accurate boundary conditions for the CO_2 simulation predictive runs. If we just plot the history match for the center four patterns only, then the quality of match improves, as shown in Figures 3.4-7 to 3.4-9. The oil history match (Figure 3.4-7) and the water production history match (Figure 3.4-8) are very good. However, the simulated GOR (Figure 3.4-9) still does not decrease as fast as the actual GOR. This could be due to the fact that all hydraulic fractures were turned on at the beginning of simulation in 1991, while in actuality, a number of new wells are added and fractured through 1994.

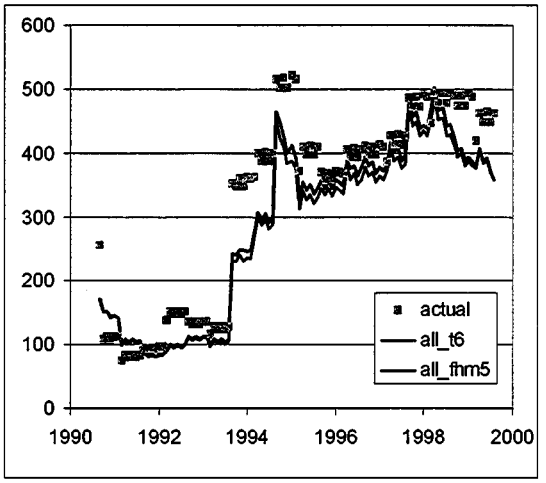

Fig. 3.4-7. Oil rate (bbl/d) match – center 4 patterns waterflood.

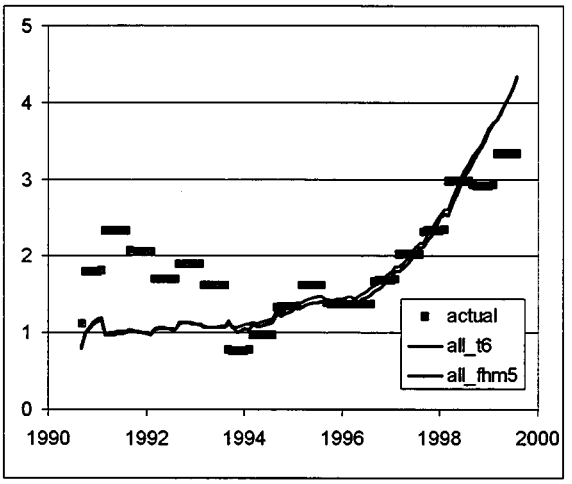

Figure 3.4-8. WOR (bbl/bbl) ratio - center 4 patterns waterflood.

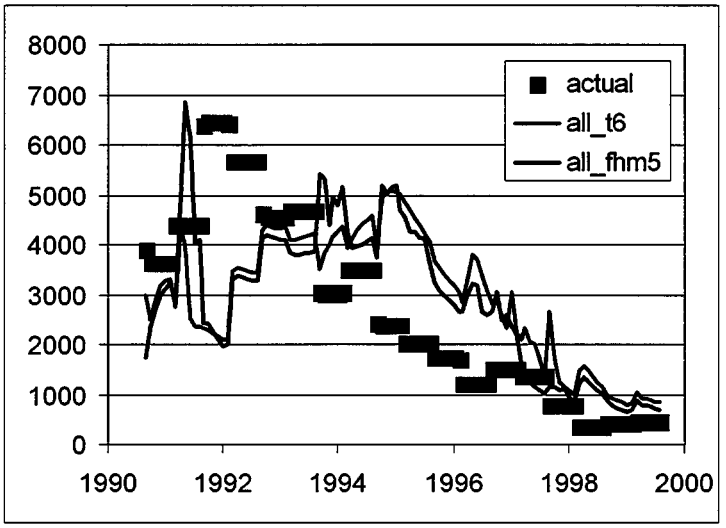

Figure 3.4-9. GOR (scf/stb) ratio match – center 4 patterns waterflood.

Figure 3.4-10 shows the changes in water saturation since initiating the waterflood in 1991. Figure 3.4-11 shows current pressure support due to waterflooding. The diamond symbols are cumulative water injection into each pattern. Figure 3.4-12 shows swept oil ellipsoids from each injector. Our next simulation step is to output pressure and saturation information from the waterflood run to a compositional version of the same model for subsequent CO_2 pilot history matching and CO_2 injection prediction runs.

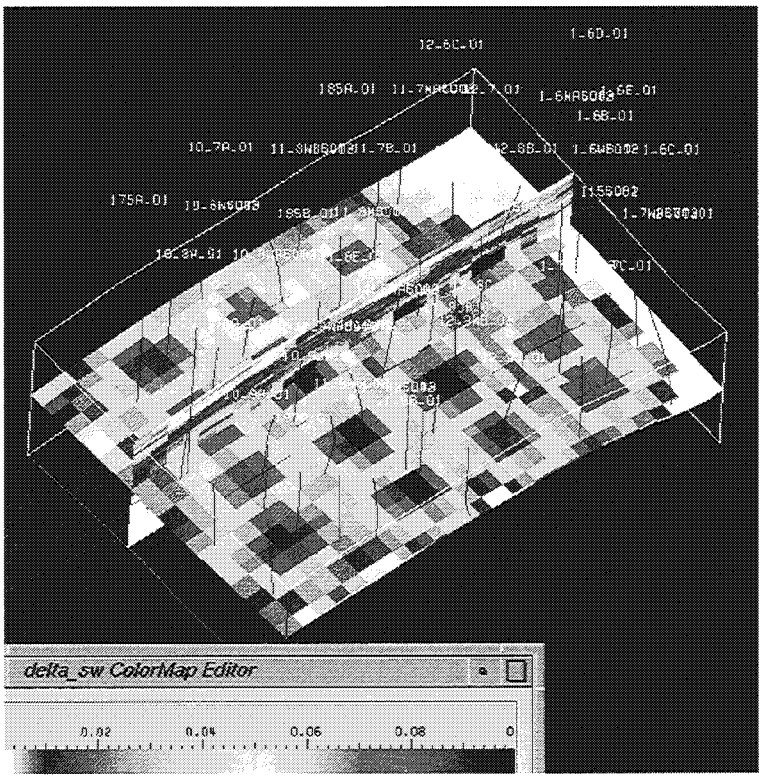

Figure 3.4-10. Change in water saturation from 1991 to 2000.

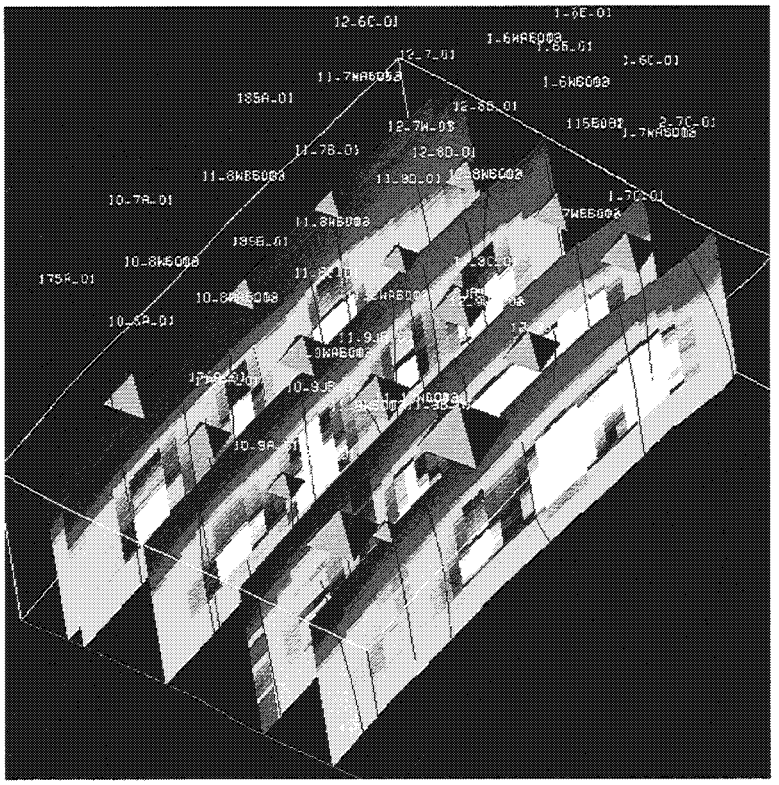

Figure 3.4-11. Current reservoir pressure showing waterflood support.

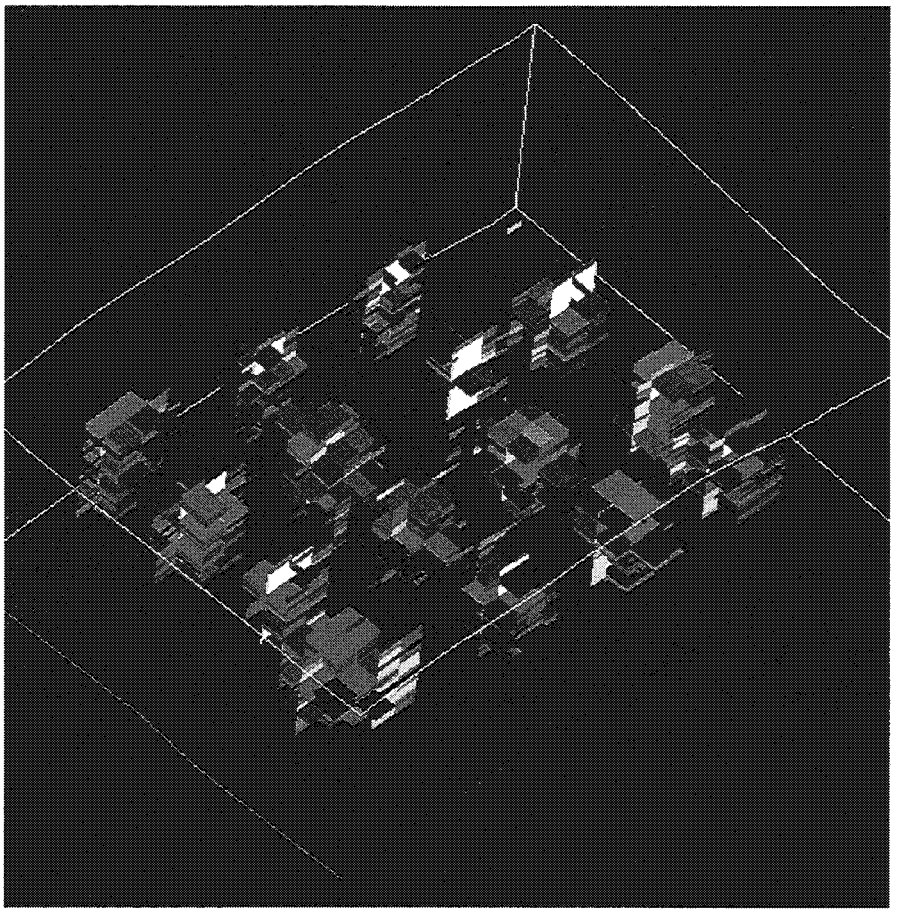

Figure 3.4-12. Decrease in oil saturation from 1991 to 2000. Showing sells with changes from 0.07 – 0.15.

SECTION 4

PILOT MONITORING AND SURVEILLANCE

4.1 RESULTS OF CO_2 INTERWELL TRACER PROGRAM

Earuch F. Broacha
ProTechnics
Gregg Molesworth and Michael F. Morea
Chevron USA Production Company

An interwell tracer program is being carried out by ProTechnics in the pilot area. Four gas phase interwell tracers (Perfluoromethylcyclopentane, Perfluorodimethyl-cyclohexane, Perfluoroethylcyclohexane, and Perfluorodimethylcyclobutane) were injected into four CO_2 injection wells per the following schedule (4.1-Table 1):

Table 4.1-1. Interwell Tracer Program.

Injection Well	Tracer Material	Date of Injection	Injection Time	Amount Tracer
11-8WR	PMCP	9-12-00	4 hrs.	0.50 kg
11-8WAR	PDMCH	9-12-00	4 hrs.	0.50 kg
12-8W	PMCH	9-13-00	5 hrs.	0.50 kg
12-7W	PDMCB	9-13-00	5 hrs.	0.50 kg

A review of the analyses performed on the collected produced gas samples from the thirteen producing wells in the Lost Hills CO_2 pilot area program indicates that tracer has arrived at six of these wells (Figure 4.1-1). Tracer breakthrough is being observed in wells 11-7B, 11-8D, 11-8E, 11-9J, 12-7 and 12-8D. The time required for initial tracer breakthrough to occur ranged from as little as 8 days to as long as 36 days following tracer injection. Seven of the producing wells being sampled in the program have shown no tracer breakthrough as of the last sample date analyzed (10-19-00). In the wells where tracer breakthrough is being observed, none of the tracer material introduced into injection well 12-8W has been detected.

Tracer mass balance calculations were performed on five of the six wells where breakthrough is currently occurring. The results of these calculations are summarized in Tables 4.1-2 and 3. As may be observed in these tables, very little of the injected tracers have been recovered as of the last sample analyzed.

These low tracer recoveries for the first 38 days of the program tend to indicate that no direct, large scale channeling of the injected CO_2 is occurring in the pilot area. This is assuming that all the injected CO_2 remained in the study area as defined by the thirteen producing wells currently being sampled. The small amount of tracer breakthrough currently being observed is insignificant as compared to the volume of CO_2 being injected into the pilot area. However, significant CO_2 and tracer breakthrough could occur in the near future as long as injection into the pilot area continues.

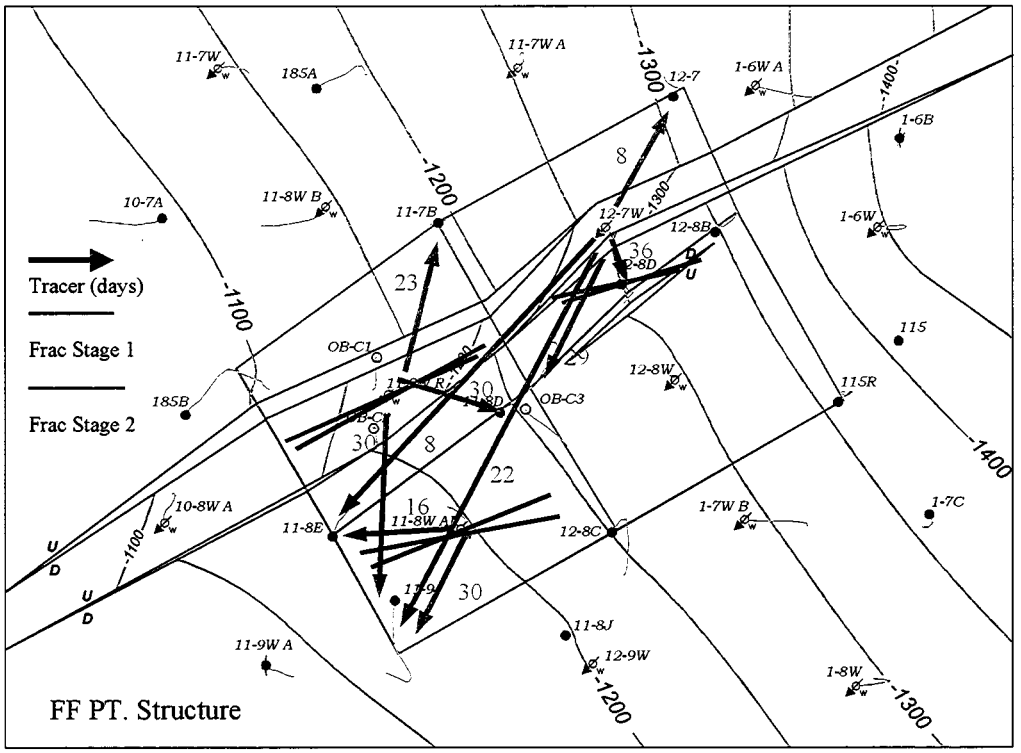

Figure 4.1-1. Structure map with faults (red) of the pilot area. The green arrows show the interwell connectivity between injectors and producers, as of 10/09/00, as determined from the tracers. The numbers next to the arrows represent the number of days it took the injection tracer to reach the producer. Tracer from 12-8W has not been observed in any of the 13 sampled producers. The pink and blue lines represent hydraulic propped fracture azimuths in 3 wells (the length of the line only represents azimuth, not fracture length).

Table 4.1-2. Tracer Mass Balance Calculations for Lost Hills Diatomite CO_2 Pilot Area.

Well Name	Amount of Injected Tracer Material Recovered (grams)			
	PMCP	PDMCB	PMCH	PDMCH
11-7B	0.425	0	0	0
11-8D	0.607	0.109	0	0
11-8E	0	12.430	0	8.488
11-9J	0.225	1.249	0	0.155
12-7	0	4.562	0	0
Total	1.257	18.350	0	8.643

Table 4.1-3. Percent Recovery of Injected Tracers for Lost Hills Diatomite CO_2 Pilot Area.

Well Name	Percent Recovery of Injected Tracer Material			
	PMCP	PDMCB	PMCH	PDMCH
11-7B	0.085%	0%	0%	0%
11-8D	0.121%	0.022%	0%	0%
11-8E	0%	2.49%	0%	1.70%
11-9J	0.045%	0.25%	0%	0.031%
12-7	0%	0.912%	0%	0%
Total	0.25%	3.67%	0%	1.73%

4.2 CROSSWELL EM AT THE CO_2 PILOT AREA, LOST HILLS FIELD, CA

Michael Wilt
Electromagnetic Instruments, Inc.
Michael F. Morea
Chevron USA Production Company

Introduction:

In this report we describe results from a crosswell EM survey at the CO_2 injection pilot at the Lost Hills field, Kern County, California. The survey was conducted from August 2-3, 2000. We first describe the field site, provide details on the data collection, data processing and discuss the results. We finally display the 2D interwell resistivity distributions and interpret these results in terms of known or deduced geology and ongoing reservoir processes.

Field Setting and Background:

The Lost Hills field is located at the western margin of the San Joaquin basin in Kern County, California. Production is concentrated in the Pliocene Etchegoin Formation and Miocene Monterey Formation, which combined, account for original oil in place in excess of 2 billion barrels within a 1000 foot thick reservoir. The principal reservoir rock is diatomaceous shale characterized by very low matrix permeability (0.1 to 1 millidarcies) and a slightly higher permeability siltstone. Both rocks are characterized by high porosity and oil saturation.

Most recovery operations at Lost Hills use induced fractures, for better reservoir contact, and waterflooding, for pressure maintenance. Wells are hydraulically propped fractured, in up to 5 intervals within the production zone. Low flow rates and inefficient sweep have historically characterized oil recovery operations at Lost Hills.

The CO_2 pilot area represents an effort to test CO_2 injection technology to improve oil recovery efficiency at Lost Hills (Figure 4.2-1). The existing waterflood has been effective in mitigating subsidence but it has been less effective in producing the remaining oil.

For the pilot, two observation wells (Figure 4.2-2) were drilled that straddle an abandoned water injector (11-8W) and an adjacent newly drilled well for CO_2 injection (11-8WR). Well 11-8W had been injecting water at the rate of 500 barrels/day throughout the production interval (~1400-2000 feet) since 1994.

The injected water is a combination of produced water and make-up water from a shallower and less saline Tulare Formation source. The overall fluid is 30 percent more resistive than the formation water but the injected fluid will still dramatically reduce the formation resistivity as it fills up void space or mobilizes oil or gas.

EM Field Survey:

EMI deployed the XBH2000 crosswell system in August 2000 using well OB-C1 for the transmitter tool and OB-C2 for the receiver. Data were collected within the depth range from

1250-2100 ft, or the entire depth range completed with fiberglass well casing. A 4 level vertical receiver string was deployed in well OB-C2 and the transmitter in well OB-C1 (See appendix for a description of these tools). Data are collected in individual profiles where the receiver remains fixed and the transmitter moves between the depth ranges, broadcasting continuously while moving. After the profile is complete the receivers are re-positioned and the process is repeated until all source and receiver positions are occupied. The receivers are spaced every 17 feet and the transmitters spaced every 4 feet within the depths of interest. Data were collected using a frequency of 760 Hz; the signal was stacked 500 cycles for each measurement.

Each profile required roughly 55 minutes to collect and re-position the sensors. The entire data set was collected in about 12 hours, including calibration and a repeated section for quality control. Data quality was exceptional, with data profiles repeating to 0.5 percent or better. Sample observed and calculated data profiles are shown in Figure 4.2- 5.

One challenge for this survey was the combination of small well separation (less than 100 feet) and long profile lengths (more than 800 feet). Due to the variation of source receiver separation this combination results in signal levels that varied by more than 10^4 for each profile. To compensate for this we installed an automatic gain ranging system in data collection to automatically adjusts the amplifier gain according to the incoming signal level. This adjustment makes a large difference in data quality and we were typically able to maintain data integrity even at the lowest signal levels.

Another aspect of the close well spacing is that we have increased sensitivity to position errors caused by well deviation. Fortunately well deviation surveys were measured and these were made available by Chevron and used in the data processing.

Data Processing and Inversion:
The first steps in data processing are to remove spikes and outliers from individual profiles, apply calibration corrections and re-sample the profiles so that the sampling interval is uniform. The combined data set is then gathered as a single file and then plotted in a contour form. At this point the data should form a continuous surface and any further errors, miscalibrations or outliers can be easily identified. The present data set required no further adjustments except for removal of outliers and application of calibration constants. In fact, the entire data reduction was complete in about four hours.

The crosshole data were interpreted with a two dimensional inverse code developed at Sandia National Laboratory and adapted by EMI (Alumbaugh and Newman, 1996). The code uses a finite difference solution to the 2D EM problem and a regularized inversion to fit observed data to a 2D interwell resistivity distribution.

The code requires a starting model before the inversion begins. We normally use the induction logs in the two wells to construct a smoothed 2D cross-section. If a dipping section is required this can be input manually. We also weight the data according to the magnitude of the fields and apply a horizontal smoothing constraint to emphasize layered structures.

In Figure 4.2-3 we show a contour plot of the observed and calculated data after 7 iterations of the inversion code. The contour plots display the entire data set with the transmitter position on horizontal axis, the receiver position on the vertical axis and the data value contoured at their intersection. The figure plots in-phase (real) and out-of-phase (imaginary) with respect to the transmitter signal. The difference plot at the base of the figure indicates an average data fit to within one percent for the more than 2000 data points. Large misfits are evident only where the field curves cross zero. The inversion required about 12 hours on a DEC Alpha workstation.

In Figure 4.2-4 we show sample profile plots in log scale. The plots indicate a close fit of observed and calculated data throughout the profile length with the exception of the peaked areas, which indicate zero crossings. The data quality and subsequent fit for this survey was truly exceptional. The result is that we have a good confidence in the accuracy and resolution of the final model.

Data Interpretation:
Interpretation of the crosswell EM data follows the same principles as a single-well induction log interpretation. That is, the resistivity is interpreted in terms of formation porosity, clay content, and fluid saturation. In this case, the formation and injected water are good electrical conductors, whereas, the formation oil is an insulator. We therefore feel that the biggest influence of the resistivity is the water saturation. For example, regions of high water saturation would typically indicate relatively low resistivity, and higher resistivity zones might indicate lower water saturations. In addition, fronts of injected water would appear as low resistivity zones, and undersaturated or gas filled zones would appear as areas of higher resistivity.

The reservoir stratigraphy at this site consists of a series of 10-80 foot thick layers dipping slightly from north to south. (OB-C1 to OB-C2). Stratigraphic profiles indicate that the section consists of a relatively constant percentage of shale (illite) and variable amounts of silt and diatomite. Prior to waterflooding the siltier sections tended to have lower resistivities, 1.5-2.5 ohm-m, and the diatomite sections have resistivities that range from 2.5-4.0 ohm-m, suggesting higher initial oil saturation.

The reservoir section has been divided into approximately 15 correlatable units chosen for differences in composition and log responses. Several of the prominent markers are also shown on the crosswell resistivity section in Figure 4.2-5.

In Figure 5 we show the deep induction logs from wells 11-8W and 11-8WR, which are adjacent and situated roughly at the 40 foot mark on the cross-section (Figure 4.2-2). Well 11-8W was drilled in 1994 to supply water for the waterflood pilot, and well 11-8WR was drilled in June 2000 to supply CO_2 to the same layers (FF-L). We have also plotted the depths of some of the marker horizons adjacent to the logs.

The logs from these adjacent wells can be used to measure changes in resistivity that has occurred during the past 6 years. We can see that layers H and J have significantly changed

during the flooding operations. These are 100 foot thick layers of predominantly diatomite. The change is largest in layer H, which shows a more than 50 percent reduction in resistivity over the 6-year period. This corresponds to a 12 percent replacement of void space (or oil) by the injected salt water. In layers F and J there is a corresponding, but less dramatic, reduction. In other layers, for example layer G, it appears that the resistivity has slightly increased during the flooding operations. This may be due to re-saturation or it may possibly reflect a local change in the stratigraphy.

In Figures 4.2-6, 7 and 8 we show the resistivity cross-section derived from the crosswell EM data between wells OB-C1 and OB-C2. Figure 4.2-6 is the final crosswell resistivity section; in Figure 4.2-7 we have placed the induction logs 11-8W and 11-8WR within the section for reference, and in Figure 4.2-8 we have adjusted the color scale to magnify the contrast between higher and lower resistivity units. The figures clearly show a roughly flatlying multilayered section throughout much of the image, although there is a clear lateral boundary near well OB-C1 in the deeper parts of the section. Note that the shallower layers seem to clearly dip north to south whereas in the deeper layers this dip is much less obvious. It may be that resistivity changes due to the waterflood have obscured the dip in the deeper layers.

Note the difference in resistivity between the borehole induction logs on either side of the image. Well OB-C1 is considerably higher in resistivity than OB-C2, especially at the basal section below 1650 ft. The crosswell section in Figure 4.2-6 clearly shows some kind of lateral resistivity change near 15 feet on the section; and it is particularly evident in the adjusted image in Figure 4.2-8. This probably marks the lateral boundary in the waterflood in layer J. Lateral boundaries are less evident in layers F and H although there are indication of lateral changes at 15ft at depths near 1620 ft and 1700 ft on the section. These boundaries are less clear above and below these depths indicating that in some sub-layers within units F and H the water moves at a different velocity than in other layers. This is supported by an examination of the logs.

The implication from this image is that the existing waterflood has mainly penetrated into the deeper diatomite rich layers in the section. In these layers it has reduced the resistivity by up to 50 percent. It also suggests that the edge of the waterflood in these layers is roughly 35-40 feet north of the injector, 15-20 feet south of well OB-C1, and it has already moved past well OB-C2. Note that the position of this lateral boundary in some sub-layers of F and H is roughly the same as in J. This suggests that there is some variation among the individual sub-layers and evidently poor communication between sub-layers.

In Figure 4.2-9 we display the color-coded logs from well 11-8W, 11-8WR and that part of crosswell resistivity section adjacent to the wellbore. The figure indicates a close correspondence in resistivity as well as the position of vertical boundaries between the crosswell section and the borehole log for well 11-8WR. This implies that the crosswell data would be useful in calculating saturations. Although the crosswell section is somewhat smoothed, compared to the logs, the crosswell EM could clearly resolve layers as thin as 10 feet.

Conclusions and Future Work:
The crosswell EM surveys provided an excellent baseline resistivity distribution prior to the CO_2 flood. We can clearly see in which layers the water has penetrated and also deduce what rates it is moving. The survey also clearly indicates the effect of the waterflood on the section showing that it has concentrate largely in the diatomite units and has largely bypassed the silts. It is also clearly more effective in deeper horizons indicating that the penetration is probably a function of the pressure.

The section suggests that the present waterflood penetrates quite slowly and could be effectively monitored by one or two measurements per year at most. Of course the effect of the CO_2 flooding is unknown and perhaps the first repeat measurement should be six months after full-scale injection has begun.

References:
Alumbaugh, D. L., and Newman, G. A., "3D Massively Parallel Electromagnetic Inversion Part B: Analysis of a Cross-Well EM Experiment," *Radio Science* (1996).

Stosur, J. J., and David, A., "Petrophysical Evaluation of the Diatomite Formation of the Lost Hills Field, California," *Journal of Petroleum Technology* (1976) 1138.

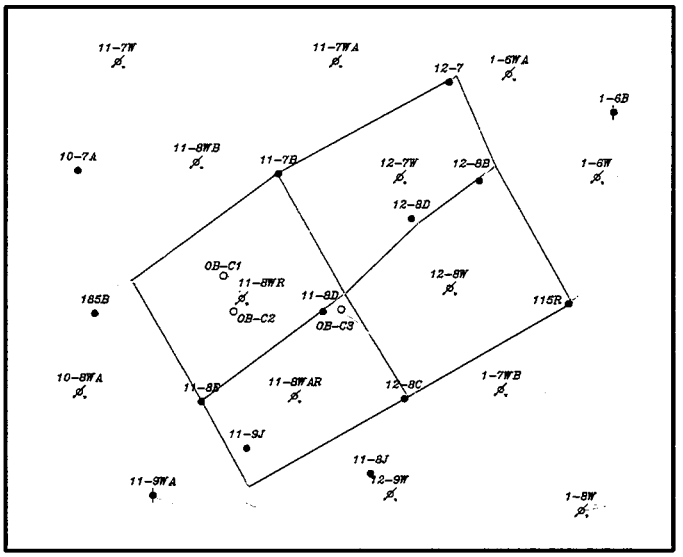

Figure 4.2-1. Base map for the EM survey at the CO_2 pilot.

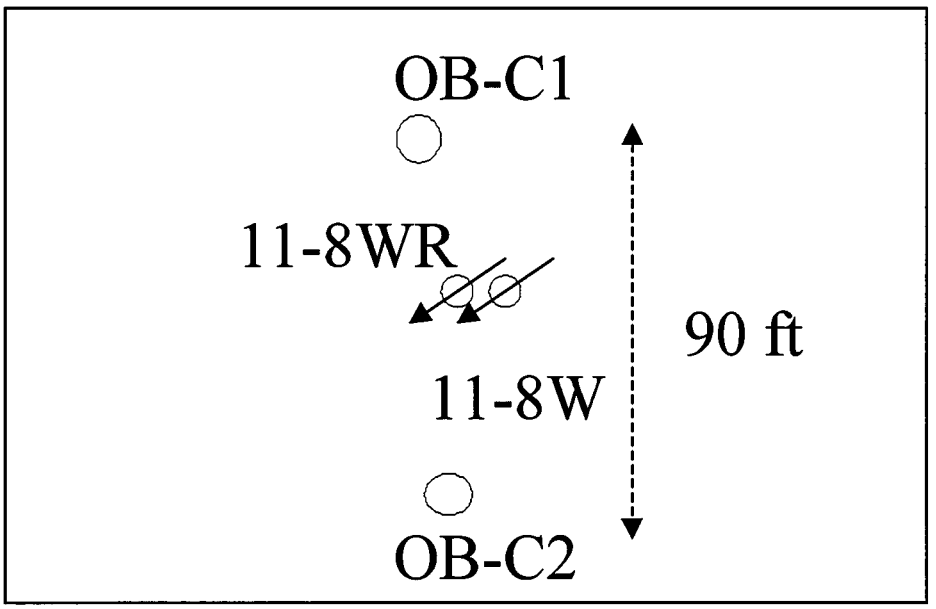

Figure 4.2-2. Well configuration at the CO_2 pilot. 11-8W, an abandoned water injector, has been replaced by 11-8WR.

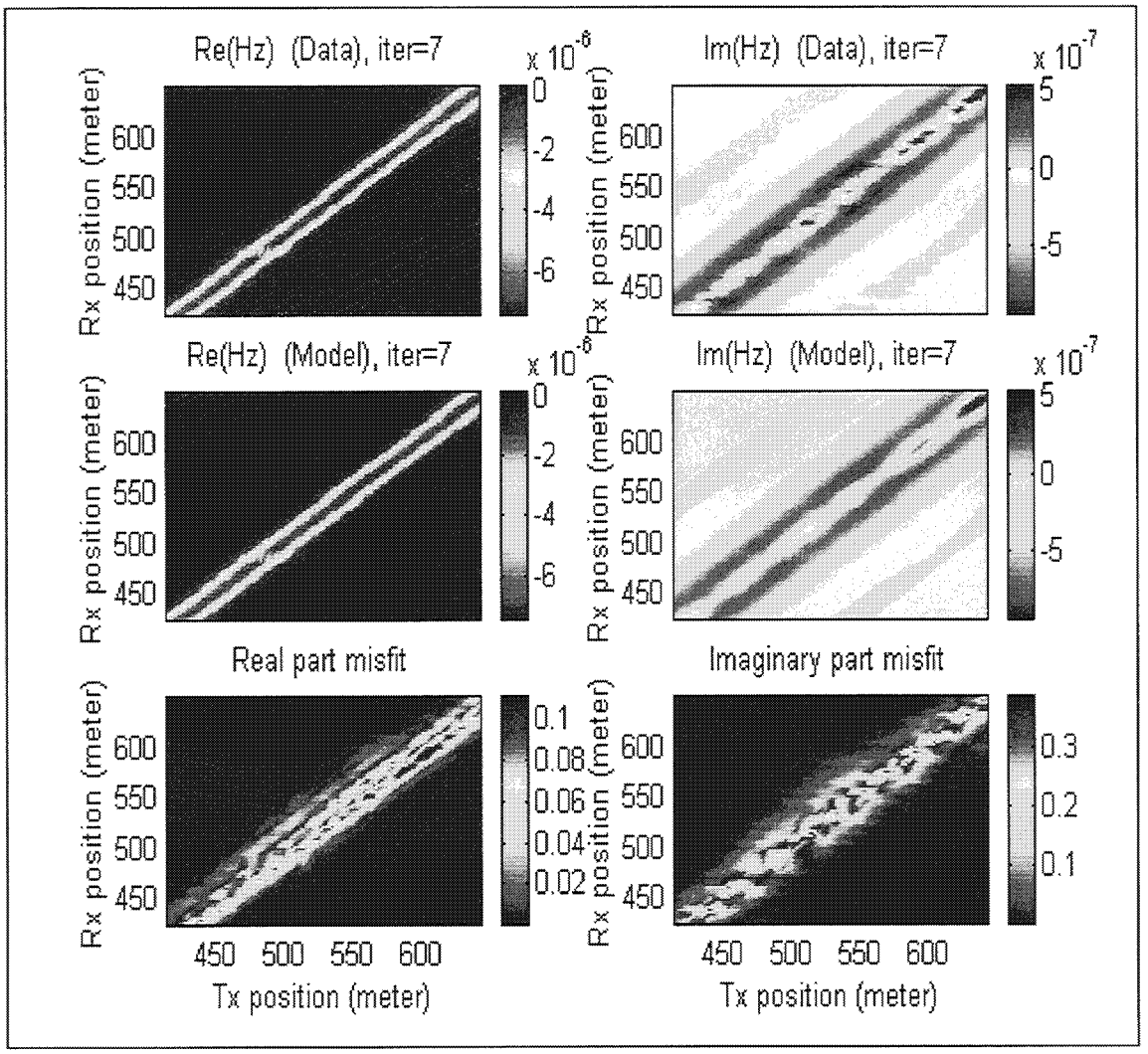

Figure 4.2-3. Combined data set for OB-C1 and OB-C2.

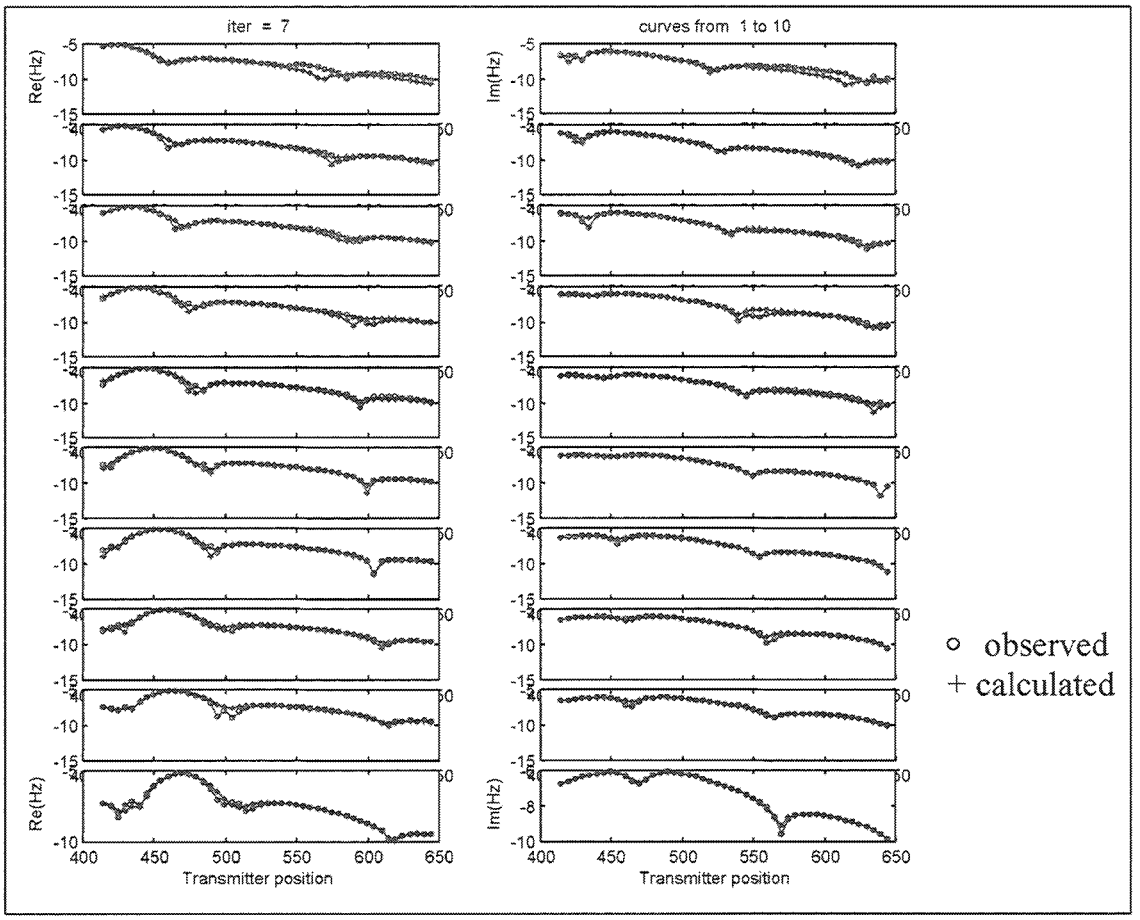

Figure 4.2-4. Sample observed and calculated data profiles.

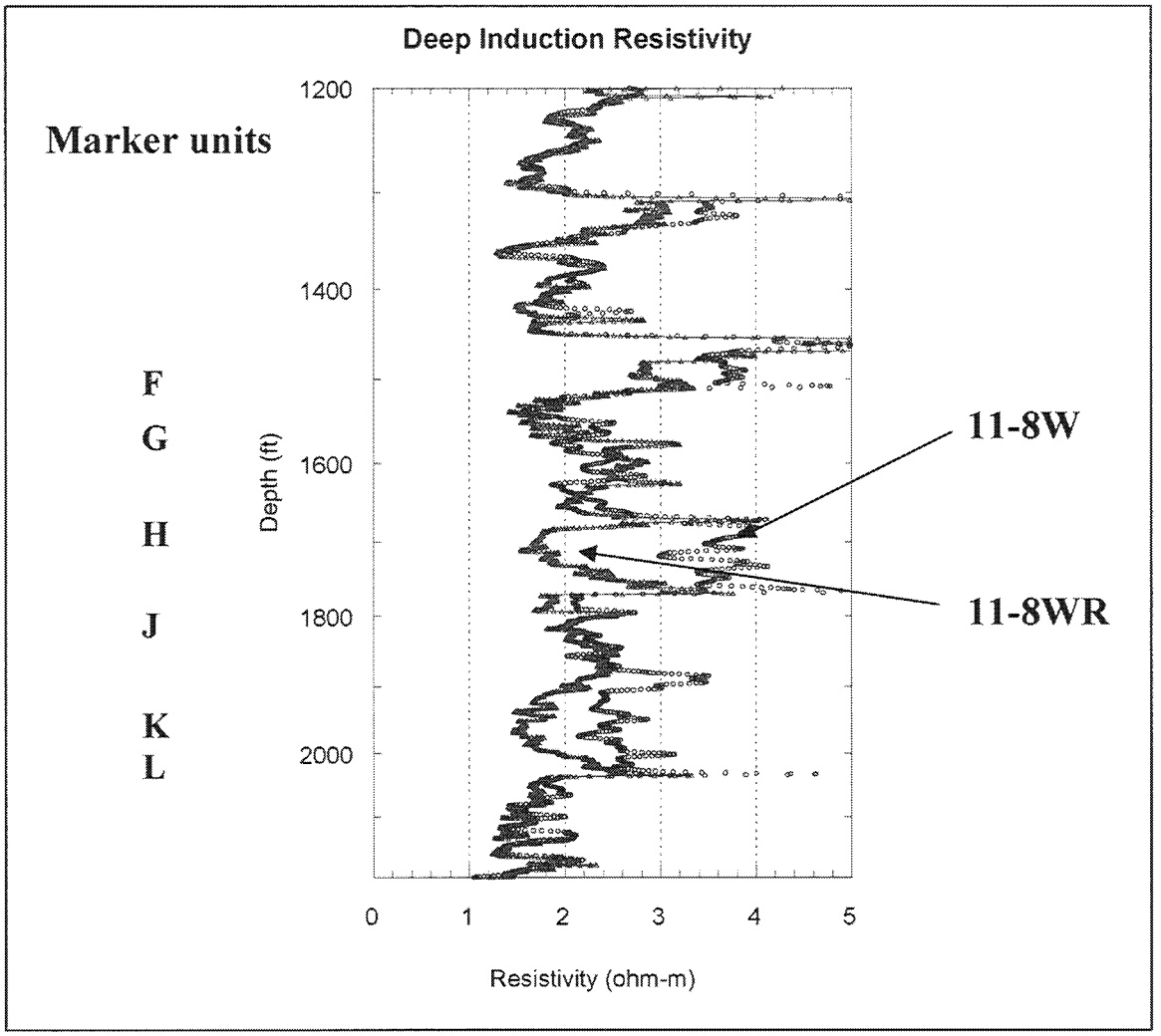

Figure 4.2-5. Comparison of well logs 11-8W and 11-8WR.

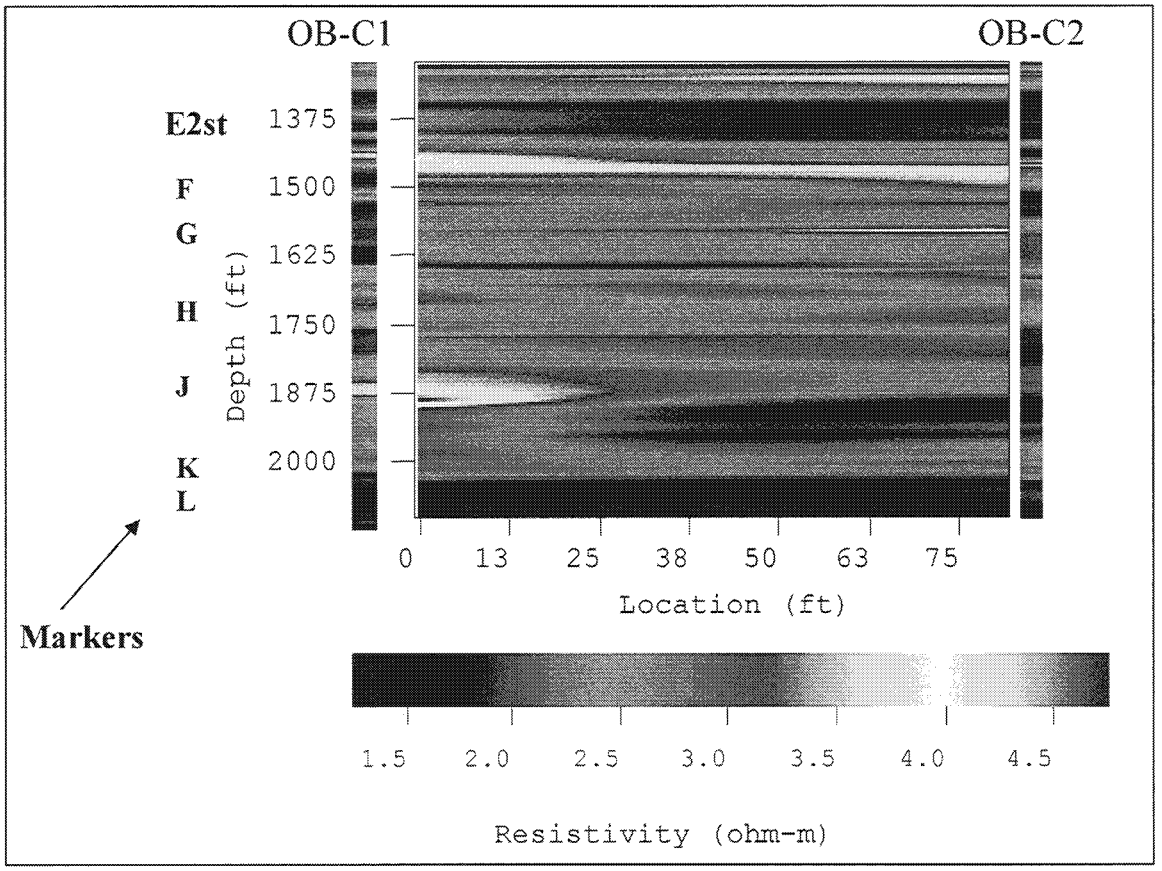

Figure 4.2-6. Crosswell resistivity distribution between OB-C1 and OB-C2.

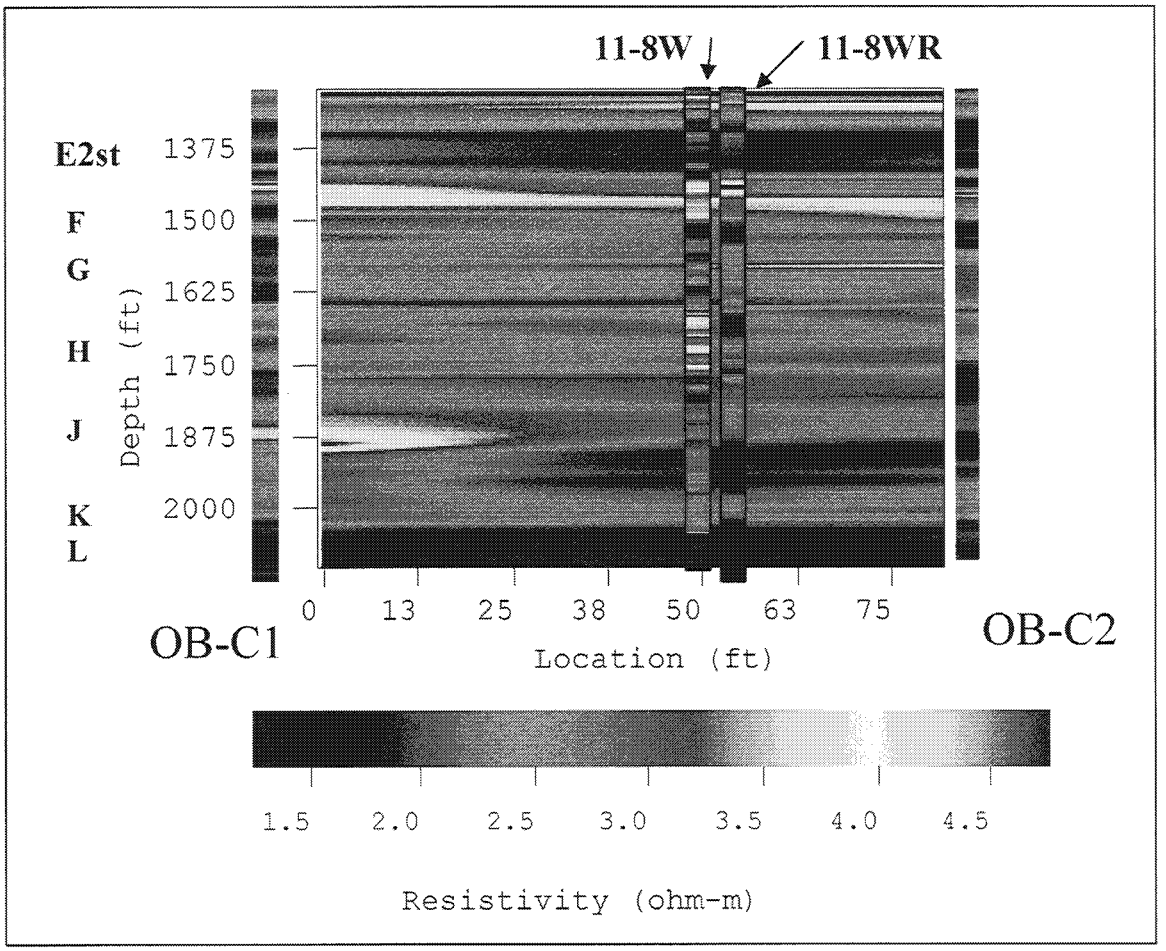

Figure 4.2-7. Crosswell resistivity distribution between OB-C1 and OB-C2.

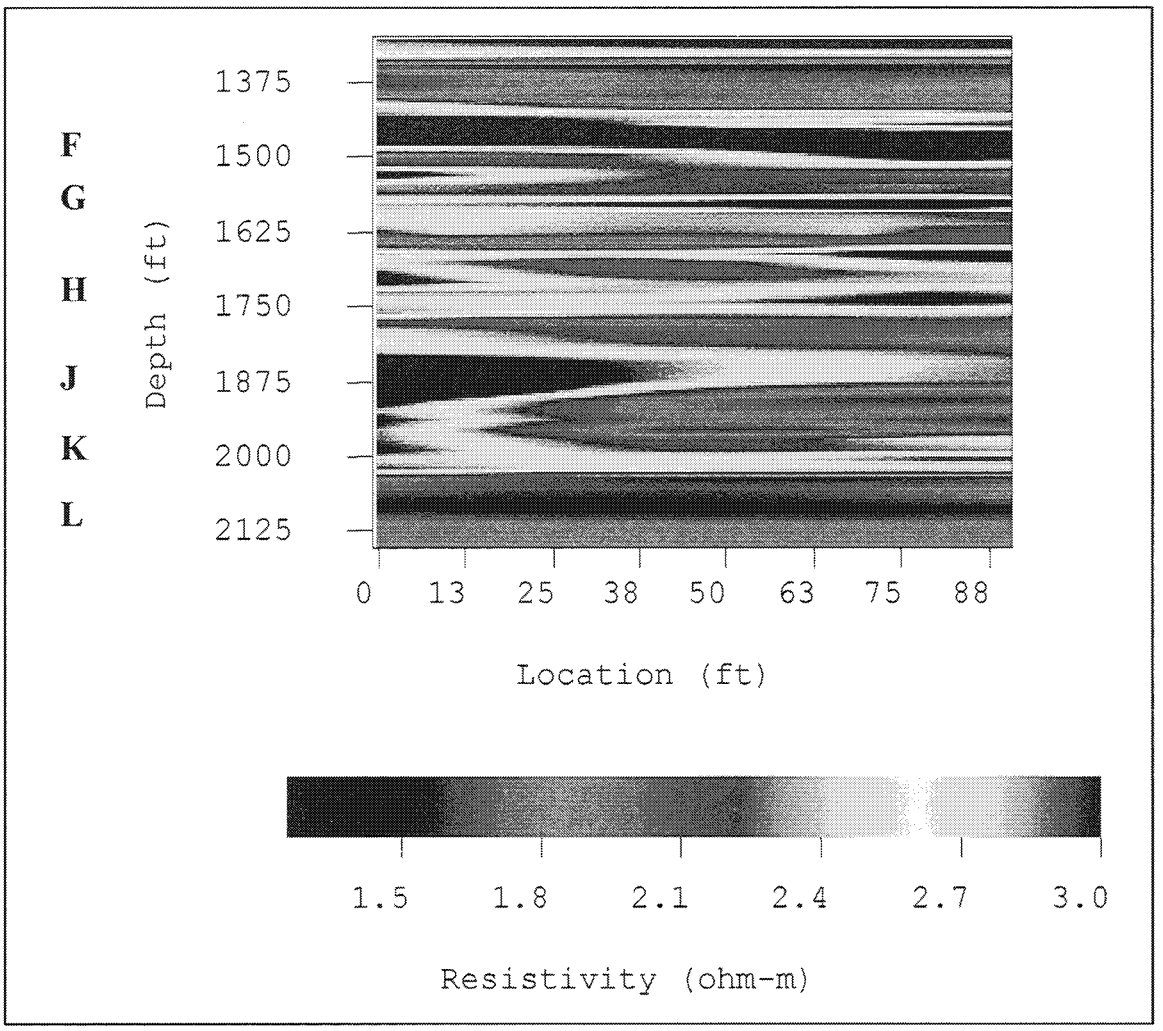

Figure 4.2-8. Crosswell resistivity distribution between OB-C1 and OB-C2 with adjusted color scale.

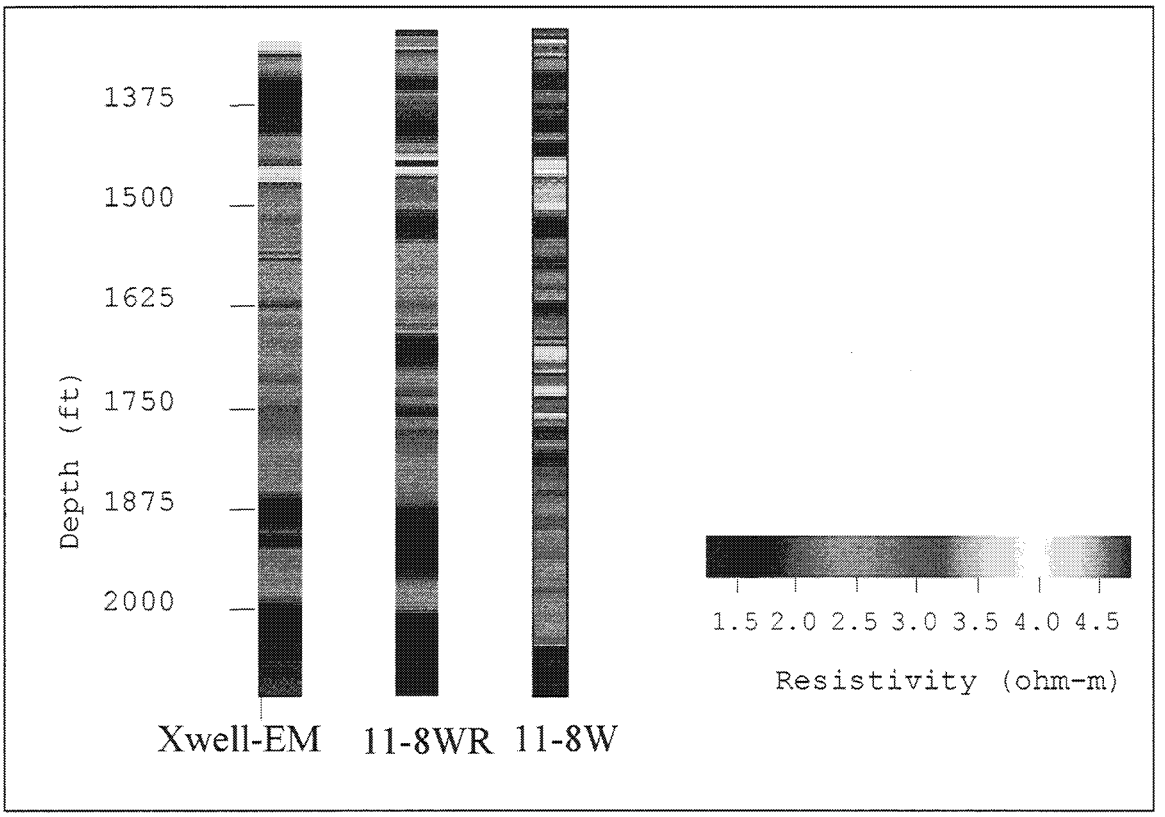

Figure 4.2-9. Comparison of logs and crosswell EM results at the well location.

4.3 CROSSWELL ELECTROMAGNETIC IMAGING OF CO_2 SEQUESTARTION

Barry Kirkendall and Jeff Roberts
Division of Geophysics and Global Security
Lawrence Livermore National Laboratory

Introduction:
The impetus for this proposed research project is to develop the ability to image subsurface injected CO_2 during EOR processes while simultaneously discriminating between pre-existing petroleum and water deposits. We are currently combining laboratory and field methods to image a pilot CO_2 sequestration EOR site using the cross-borehole electromagnetic (EM) technique, improve the inversion process in CO_2 studies by coupling results with petrophysical laboratory measurements, and focus on new gas interpretation techniques. Field and laboratory results can provide information on subsurface CO_2 detection, CO_2 migration tracking, and displacement of petroleum and water over time. This project directly addresses energy issues in two ways: 1) the development of field and laboratory techniques to improve in-situ analysis of oil and gas enhanced recovery operations and 2) provides a tool for in-situ analysis of CO_2 sequestration, a technical issue of growing importance.

Laboratory Electrical Properties of Rocks During CO_2 Injection:
We propose to measure the electrical properties of rocks from the site at conditions of full liquid saturation with oil and as they are invaded with liquid and gaseous CO_2. Measurements will be performed at temperatures and pressures appropriate to field conditions in a specially constructed device specifically aimed at these types of measurements. The system (Figure 1) consists of an externally heated fluid pressure vessel capable of confining pressures up to 500 MPa and temperatures up to 300°C. Pressure is controlled by three different pressure systems, one each for confining pressure, and upstream and downstream pore pressure control. Electrical measurements will be performed using two systems, a Hewlett-Packard HP4282 impedance bridge and a Solartron 1260 impedance analyzer. The HP4284 is used to monitor the sample at specific frequencies during periods of heating, pressure changes, and fluid injection. The impedance analyzer is used to make broadband measurements during (10^{-3} to 10^{6} Hz) periods when the sample is at stable experimental conditions. The device and measurement methodology has been tested on oil-filled diatomite samples from the Lost Hills that were injected with brine during EOR. These preliminary measurements showed some unexpected electrical behavior, resistivity increasing during brine injection, that helped interpret the Chevron well-logs and the LLNL crosswell inversions.

The experimental method will be adapted for the CO_2 injection process. A well-characterized water- or oil-saturated sample will be placed in the vessel for electrical measurements at the temperature of the formation (~38-45 C) and a variety of confining and pore pressures. Then, liquid CO_2 will be forced into the sample and the electrical properties monitored as the liquid water is pushed out. This will be easily accomplished at room temperature, as the critical pressure for CO_2 at 18°C is ~7.3 kPa (CRC, 1983), well within the

operating parameters of the device. Changes in the electrical properties will be noted. Next the pore pressure will be lowered so that the liquid CO_2 flashes to the gas phase. The electrical properties will be again be monitored for a period of time as the sample is held at static conditions to determine if there is a long-term effect. It is important that there is some knowledge of surface conduction mechanisms in the rocks so that any changes in electrical properties because of different surface tensions and wetting behavior can be discerned and understood.

A second type of experiment involves the injection of gaseous CO_2. As above, electrical properties will be monitored as the sample undergoes invasion of CO_2. It may be necessary to pump to relatively high pressures to obtain displacement of water. We will attempt to match reservoir characteristics whenever possible.

Samples undergoing boiling or CO_2 invasion may change geochemically. The nature of the geochemical change will be dependent on a number of factors, including rock chemistry, temperature, pressure, water/rock ratios, and fluid chemistry. These changes can affect measured electrical properties, in particular the surface conductance. While this research is not intended to be a full geochemical study of such chemical interactions, care will be taken to be aware of such changes and their importance to observed geophysical measurements. When necessary, our analyses will include a geochemical component.

Electromagnetic Imaging of CO_2 Injection:
Electromagnetic techniques are sensitive to rock pore fluids within the subsurface, which makes them the ideal method for addressing the problems of EOR in a heavy oil environment. In EOR applications, it is also important to discern between injection steam and gases, injection fluids, and formation fluids. The high sensitivity of electromagnetic energy to these physical processes, as well as recent advances in computational ability, inversion code resolution, and field instrumentation, make borehole EM techniques an important tool for such subsurface imaging problems.

During CO_2 sequestration, the high pressure of the injection forces the CO_2 to remain in a liquid state. After delivery to the subsurface formation, however, a volume increase creates a pressure drop which vaporizes the CO_2 to a gaseous state. It is this gaseous state that forces miscibility with the water and oil in the subsurface formation.

In this complex scenario, EM imaging must address the gaseous CO_2, the liquid water leftover from secondary recovery, and the original liquid petroleum in the formation. Based on initial forward model calculations, we expect a large contrast between the formation water and the petroleum / CO_2, but a small contrast between the CO_2 and the petroleum due to the similar inherent electrical conductivities of each component. Resolution of this small contrast will be possible with laboratory results and with improved gas interpretation techniques which are currently being developed based on higher resolution inversion techniques.

August 2000 Deployment:
A crosswell EM survey was acquired by Lawrence Livermore National Laboratory (LLNL) across OB-C1 and OB-C2 in August, 2000. The purpose of this survey was to produce baseline electrical conductivity map of the two-dimensional plane intersecting wells OB-C1 and OB-C2 at multiple frequencies (2.0 kHz and 4.0 kHz) prior to CO_2 injection. Both wells are deviated significantly and this deviation must be taken into account during processing using gyroscopic information acquired in August 2000. Future surveys will be compared with this pre-sequestration baseline survey. Figures 3 and 4 display the data acquired in the August 2000 deployment. In the next deployment, April 2001, both data sets will be inverted for both source frequencies, in order to develop a multi-frequency approach to interpreting CO_2 sequestration imaging.

Current Status and Future Research:
The initial deployment was acquired in August 2000 which consisted of multi-frequency (2.0 and 4.0 kHz) source measurements between the interval 1500 feet and 2100 feet. In April 2001, this deployment will be duplicated and the data will be processed and compared to show any change in the subsurface between the two dates. Additionally, laboratory analysis of core samples provided from the area began in January 2001. It was necessary to amend the laboratory device displayed in Figure 1 to accommodate the corrosive effects of CO_2. After the April 2001 deployment, we will be able to compare laboratory and field data to suggest an initial procedure to interpreting CO_2 sequestration with electromagnetic induction techniques.

Acknowledgements:
The authors would like to thank Mike Morea at Chevron for providing access to the wells in addition to tangible well information such as gyroscopic data and induction logs. We would also like to thank Steve Carlson, Pat Lewis, and Duane Smith at Lawrence Livermore National Laboratory for providing field and laboratory support to this point.

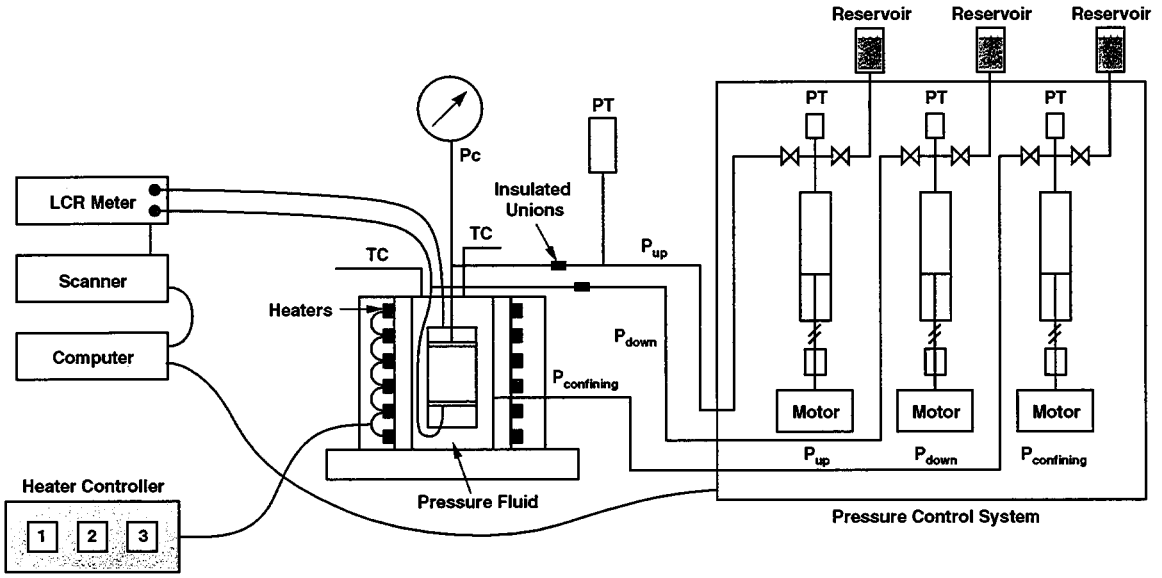

Figure 4.3-1. Schematic of the newly constructed device to be used to measure electrical properties of rocks at high pressure and temperature. System was designed to enable the investigation of electrical properties of porous media under a variety of conditions. There are three separate pressure control systems, stable temperature control up to 300°C, and computer data acquisition of electrical data and experimental parameters. The system can generate pore pressures up to 50 MPa and is easily adaptable for the use of CO_2 as a pore fluid.

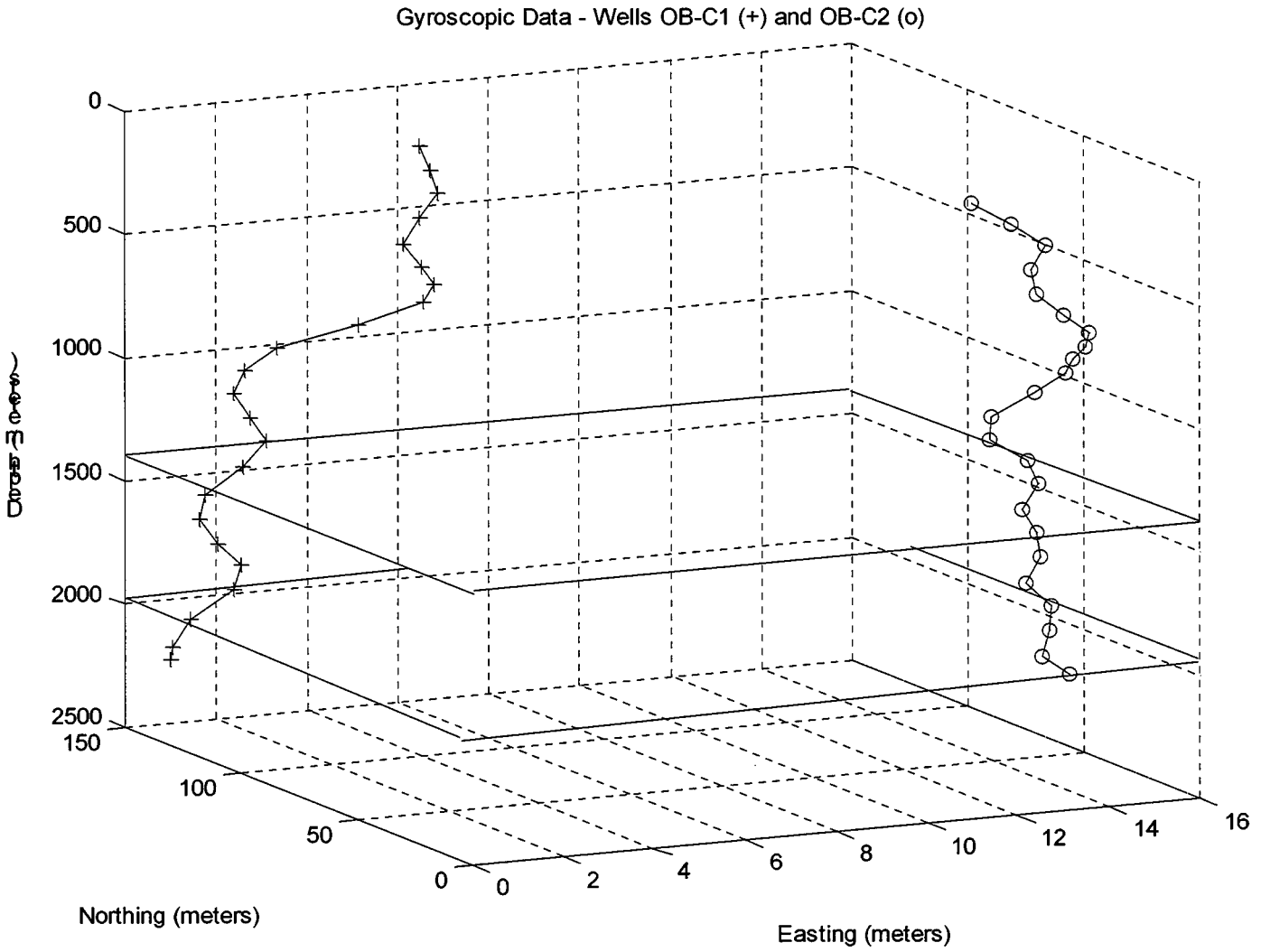

Figure 4.3-2. Gyroscopic information for wells OB-C1 and OB-C2. The surface distance between the two wells is 80 ft. 11-8 WR is the new replacement injector that will be used on the CO2 pilot. The region between the two planes (depth 1400 – 2000 m) is the region of interest in this study. The inversion routine has been adapted to account for this deviation, which is necessary to prevent artifacts in the inverted data.

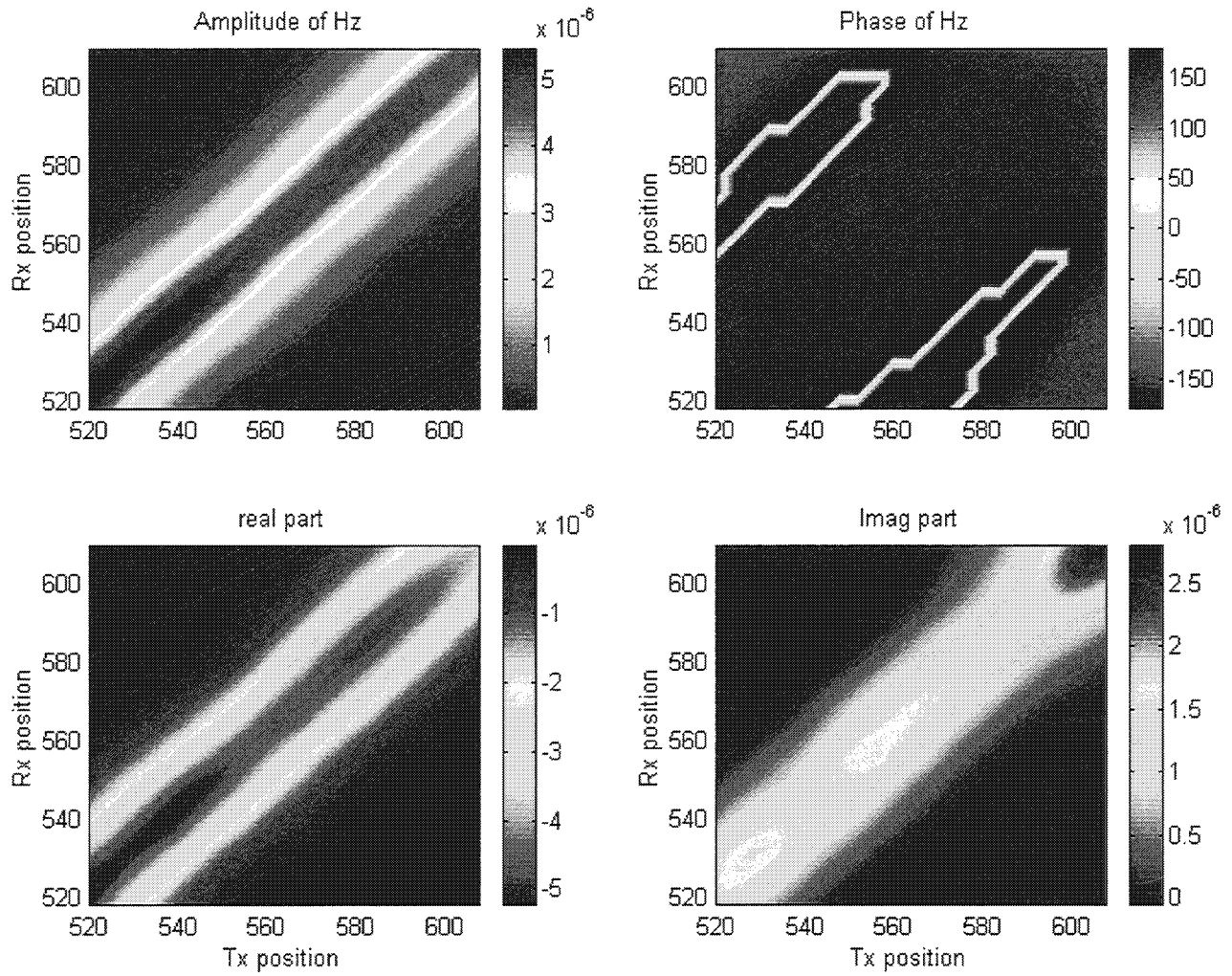

Figure 4.3-3. Data acquired in August 2000 at CO_2 site. These plots show the amplitude (top left), phase (top right), real (bottom left), and imaginary (bottom right) components of the data acquired. The purpose of such plots is for data integrity and to view any calibration errors. This data will be compared to data acquired in April 2001 – the second deployment to the site.

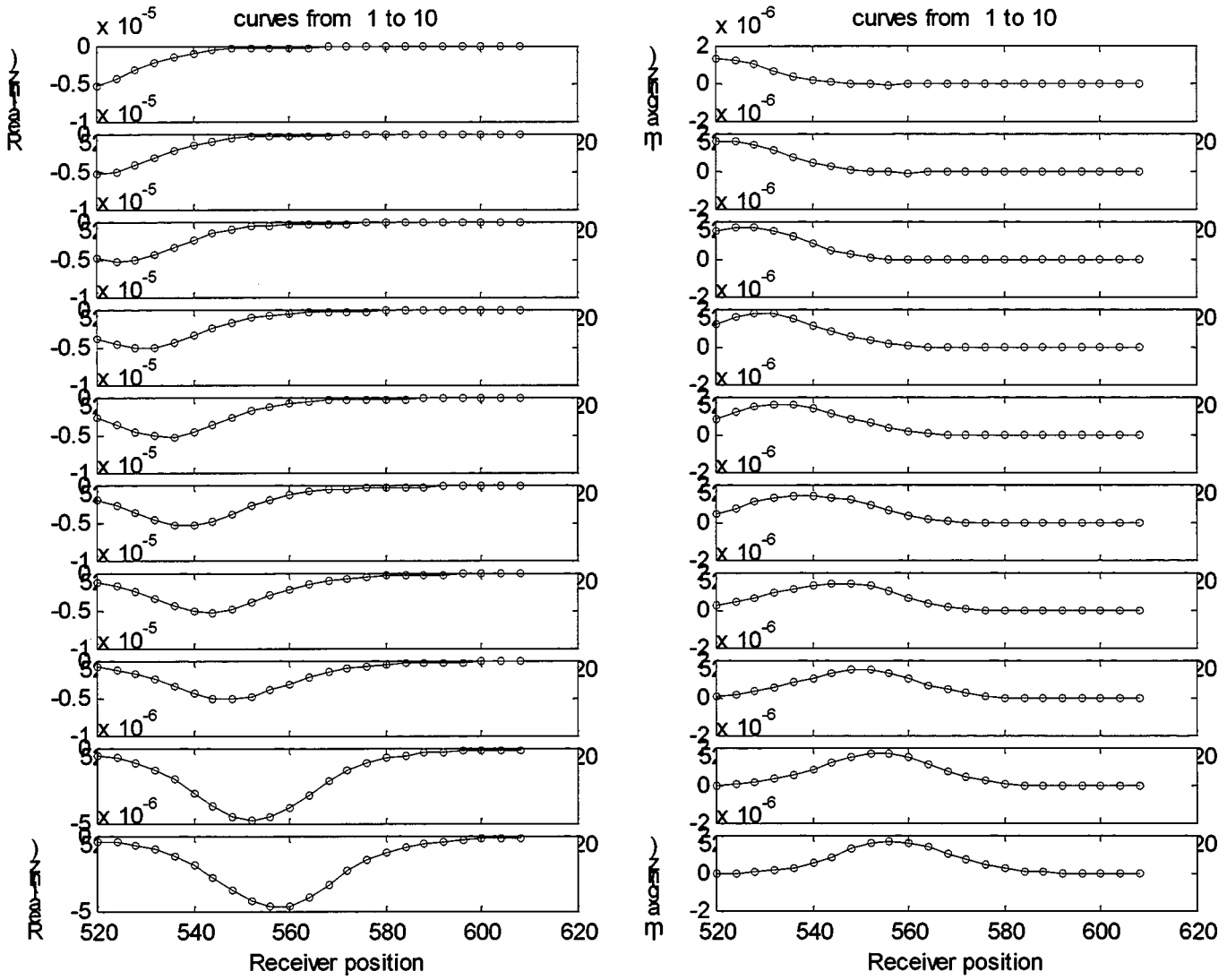

Figure 4.3-4. Data curves from August 2000 deployment. These curves are a preliminary attempt at processing the data. The left column represents the real component of the data, while the right column represents the imaginary component. This method of display is important when comparing two different deployments, such as August 2000 and April 2001, in order to provide confidence on calibration factors.

4.4 MONITORING SULFUR AND HYDROCARBON CHEMISTRY OF LOST HILLS OILS DURING CO_2 FLOODING

Rong J. Hwang
Chevron Research Technology Company

SUMMARY AND CONCLUSIONS:

Geochemical characterization has been conducted on produced oils that were sampled periodically from selected producing wells located in the CO_2 flood pilot area of the Lost Hills field. The objective is to determine if formation of solids, specifically elemental sulfur, has been induced by CO_2 injection to the reservoir. The analytical results of the recent oil samples (second set) taken in December 2000 and in January 2001 are comparable to those of the earlier samples (first set) taken in August 2000 shortly before the start of CO_2 injection. Little changes in bulk properties of the oils including API gravity, total sulfur %, and asphaltene % indicate that there are no significant changes in oil chemistry caused by CO_2 injection for over 3 months.

Elemental sulfur is absent in all the oils produced from wells in the pilot area prior to CO_2 injection. No elemental sulfur was found in the second set of oil samples either. Thus, CO_2 injection has so far not caused formation of elemental sulfur. The results indicate that the oils in the pilot area, based on bulk properties, have remained virtually unchanged after CO_2 injection for over three months. This suggests the interaction between oil and CO_2 in the reservoir has been fairly weak.

However, the oil from one of the monitoring wells, 11-8D, has experienced some measurable changes in molecular properties (more sensitive indicators), hydrocarbon and sulfur fingerprints, suggesting a significant interaction between this oil and CO_2, and proximity of this well to the CO_2 flow in the reservoir.

INTRODUCTION:

Enhanced oil recovery processes involving reservoir injection of gases, such as light hydrocarbons and CO_2, are known to often induce organic deposits that plug rock pores and thus reduce rock permeability (Shelton and Yarborough, 1977; Monger and Fu 1987) and well injectivity. The deposition of organic solids, mostly asphaltic components of crude oils, can lead to reduction in oil recovery and hence operational profits. In addition to asphaltics, heavy hydrocarbons can also segregate from the oil phase and precipitate in the reservoir, contributing to solid deposition (Hwang and Ortiz, 1998). Less known is CO_2 flooding may cause formation of elemental sulfur in the reservoir that enhances the deposition of solids (Hwang and Ortiz, 1998; Mathis, 1998). Elemental sulfur is insoluble in water and has limited solubility in oil. It would greatly contribute to the reduction of rock permeability once it is formed in the reservoir.

A DOE sponsored field trial to study the effect of CO_2 flood on oil and gas production has been underway in the Lost Hills CO_2 pilot area since August 2000. The field project includes a CO_2 pilot-monitoring plan designed to understand what would happen in the reservoir. As

a part of the overall monitoring plan, the oil chemistry monitoring during CO_2 flood is likely to provide insightful information for understanding and managing the CO_2 flood process.

The objectives of monitoring oil chemistry include (1) evaluating the impact of CO_2 flood on in-reservoir asphaltene precipitation, and (2) determining if elemental sulfur is formed in the reservoir during CO_2 flood. The results of oil geochemistry monitoring would provide the basis for the planning on remediation or mitigation. Further, defining the spatial and temporal changes in oil composition in the study would provide the clue on the flow direction of injected CO_2 in the reservoir, facilitating reservoir management and injection strategy for the CO_2 flood process.

SAMPLES AND METHODS:

The sampling plan is to take oil samples about quarterly from well heads of selected producers in the CO_2 pilot area during the lifetime of the CO_2 flood for geochemical characterization. The first set of samples was taken in August 2000, prior to CO_2 injection (Table 4.4-1). These samples would provide the baseline data. Two oil samples of the second set (wells 12-7 and 12-8D) were taken in December 2000, about three month after the start of CO_2 injection. The sample from the third well, 11-8D, was not taken until January 2001. The sampling delay was caused by the sand production problem associated with the 11-8D well.

Bulk properties such as API gravity and wt % asphaltenes were determined by standard geochemical procedures. Wt % sulfur of the oils was measured by ASTM method, D2622, using X-ray. Gas chromatography-atomic emission detector (GC-AED) was used to determine the elemental sulfur content of the oils. Gas chromatography was performed with an HP5890A Series II chromatograph equipped with HP7673A autosampler and HP 5921A atomic emission detector. The chromatograph was fitted a 15m x 0.25 mm DB-1 capillary column. Helium was used as carrier gas. After injection the column oven temperature was programmed from 50 to 300 °C at 3.5 °C/min. The sulfur emission line at 181 nm was used for detecting sulfur compounds and the carbon emission line at 179 nm for detecting hydrocarbons. The samples were also analyzed by GC-AED for sulfur and hydrocarbon fingerprints to profile sulfur and hydrocarbon species.

RESULTS AND DISCUSSION:

Bulk Properties

The bulk compositions of two sets of the oils produced at different times from 3 wells located in the pilot CO_2 flood area of Lost Hills are listed in Table 4.4-1. The analytical results of the recent oil samples (second set) taken in December 2000 and January 2001 are comparable to those of the earlier samples (first set) taken in August, 2000 shortly before the start of CO_2 injection. Little changes in bulk properties of the oils including API gravity, total sulfur %, and asphaltene % indicate these is no significant change in oil chemistry caused by CO_2 injection for over 3 months.

Elemental sulfur was not detected in the pre-CO_2 flood oil samples (first set) indicating elemental sulfur is absent in the oils or present in the trace level (< 10 ppm) not detected by the instrument. No elemental sulfur was found in the second set of oil samples either. Thus,

CO_2 injection has so far not caused formation of elemental sulfur. The results indicate that the oils have remained virtually unchanged after CO_2 injection for over three months.

The observations suggest that injected CO_2 has not had significant interaction with the reservoir oil resulting in little changes in physicochemical properties of the oil. This is contrary to the results of an earlier study of the McElroy CO_2 flood. In the McElory field, CO_2 injection caused an increase in oil API gravity and reduction in asphaltics and heavy hydrocarbon content within three months of CO_2 injection (Hwang and Ortiz, 1998). The differences in oil responses to CO_2 flood between the Lost Hills and McElory may lie in differences in reservoir conditions and oil properties. Alternatively, no contact between injected CO_2 and oil in the reservoir would account for little change in Lost Hills oil. However tracer and production data show CO_2 has been in contact with these wells.

Molecular Properties

Molecular properties of the oils such as hydrocarbon fingerprints (composition) derived from gas chromatographic analysis are generally more sensitive to the changes (perturbation) in recovery processes than bulk properties. To detect the early impact of the CO_2 flood on oil chemistry, the oils were analyzed by gas chromatograph-atomic emission detector (GC-AED) to monitor the changes, if any, in composition of hydrocarbon and sulfur species. Gas chromatograms of the oils are shown in Figures 4.4-1-6.

Hydrocarbon Fingerprints

The oils produced from the three monitoring wells are badly biodegraded. Paraffinic hydrocarbons and isoprenoids are absent in all the samples indicating the oils have undergone significant biodegradation in the reservoir. Hydrocarbons of the oils mainly consist of naphthenics and aromatics that are more resistant to biodegradation than paraffins and isoprenoids. Distributions of these hydrocarbons (hydrocarbon profiles) in the oils are illustrated in Figure 4.4-1 showing the dominance of light hydrocarbons ($\leq$ C10) despite the very moderate API gravity of the oils. The intermediate (C11~ C25) and heavy (> C25) hydrocarbons are relatively low in abundance. These hydrocarbon distributions remain pretty much the same for all the oils produced from monitoring wells even after CO_2 injection for three months (Figure 4.4-1). It appears no heavy hydrocarbons have dropped out from the oil phase in the Lost Hills reservoirs despite CO_2 injection. The observation is again consistent with that no strong interaction between the reservoir oil and injected CO_2 has occurred.

However, close examinations of chromatograms for detailed comparison of hydrocarbon fingerprints of oils produced before and after the start of CO_2 injection have revealed a slightly different story on the effect of CO_2 flood so far on oil chemistry. While it is true that hydrocarbon fingerprint remains virtually unchanged for some oils, it shows significant changes for the oil from well 11-8D (Figure 4.4-2). Hydrocarbon peak ratios selected for grouping to show similarity or dissimilarity in composition among the oils are listed in Table 4.4-2. The peak ratios that are chosen to maximize the differences among the oils are the basis for multi-variant statistic analysis, yielding the cluster diagram. Figure 4.4-3 shows the most dissimilar oil is the January 2001 sample from well 11-8D that clusters apart from the oils from other wells but also from the early sample of the same well. For wells 12-7D and 12-8D, the oils sampled before and after the start of CO_2 group together, respectively. The

results suggest that the well 11-8D has probably seen more CO_2 than other wells implying the well is located closer to pathways of CO_2 flow.

Quantitatively, the magnitude of compositional differences between the oils sampled before and after the start of CO_2 flood from well 11-8D is very significant and has an average difference of ~ 12 % for 9 ratios (Table 4.4-2). Analytical precision of the chromatographic analysis presented in peak ratios is generally 3 % or less. Thus, peak ratio differences of 5 % or more represent real compositional differences among the oils.

In comparison, the oils from other two wells, 12-7D and 12-8D, have little changes ($\leq$ ~ 1 %) since the start of CO2 injection.

Sulfur Fingerprinting

Oils in the offshore California and San Joaquin Valley sourced from the Monterey Formation and its equivalent shale are known rich in sulfur. With different physicochemical properties, sulfur compounds and their distribution in the oils have potential to enhance hydrocarbon based oil grouping for characterizing reservoirs and monitoring production processes.

Sulfur fingerprints of the oils, illustrated in Figure 4.4-5, are characterized by high abundances of well resolved C2-, C3-, and C4- alkyl substituted benzothiophenes although the parent compound, benzothiophene, is low in abundance. Moderate amounts of dibenzothiophene and its alkyl derivatives are also present. High abundances in benzothiophenes relative to dibenzothiophenes indicate the oils are low in thermal maturity. An increase in thermal maturity generally results in a decrease in abundances of benzothiophenes relative to those of dibenzothiophenes (Ho et al., 1974). All the oils display a huge hump of unresolved complex mixtures (UCM) of heavy organic sulfur compounds that are dominated by compounds heavier than C2-dibenzothiophenes, consistent with low maturity of the oils.

Unlike hydrocarbons, sulfur compounds in the Lost Hills oils have not suffered from biodegradation related depletion due to their higher resistance to biodegradation. Sulfur fingerprints can thus possibly provide information that may not be available from studying hydrocarbon composition. The oils from the three monitoring wells were analyzed for sulfur fingerprints, as shown in Figures 4.4-5, 6, and 7. Comparing sulfur fingerprints of the oils produced before and after the start of CO_2 flood, they are highly similar for the oils from well 12-7 and significantly different for the oils from 11-8D (Figures 4.4-5 and 6), which are consistent with the observations on hydrocarbon fingerprints of the oils. For the oils from well 12-8D, sulfur fingerprints show subtle changes while hydrocarbon fingerprints exhibit little changes (Figure 4.4-7).

Sulfur peak ratios selected for grouping to show similarity or dissimilarity in composition among the oils are listed in Table 4.4-3. Cluster analysis of the sulfur data yielded an oil grouping (Figure 4.4-8) similar to that based on hydrocarbons with one exception. The oils from well 12-8D do not group as closely because of larger differences seen in sulfur fingerprints than those indicated by hydrocarbon fingerprints. Inconsistency in grouping 12-

8D oils suggests the CO_2 effect on this well is very marginal. The magnitude of composition differences between the produced oils from well 12-8D has an average difference of ~ 6 % again suggesting the oil in this well has been slightly perturbed by CO_2 injection (Table 4.4-3).

REFERENCES:

Ho, T.Y., Rogers, M. A., Drushel, H. V., and Koons, C. B. (1974) Evolution of sulfur compounds in crude oils. AAPG Bull., 58, 2338-2348.

Hwang, R. J. and Ortiz, J. (1998) Effect of CO_2 flood on geochemistry of McElroy oil. In *Advances in Organic Geochemistry* 1997 (Edited by Horsfield B., Radke M., Schaefer R. G., and Wilkes H.), 485-503.

Mathis, L (1998) Deposition of elemental sulfur during CO_2 flood in the Goldsmith Field, personal communication.

Monger, T. G. and Fu, J. C. (1987) "The Nature of CO_2-Induced Organic Deposition", Society of Petroleum Engineers, SPE 16713.

Shelton, J. L. and Yarborough, L. (1977) "Multiple Phase Behavior in Porous Media During CO_2 or Rich-gas Flooding", Journal of Petroleum Technology, 1171-1178.

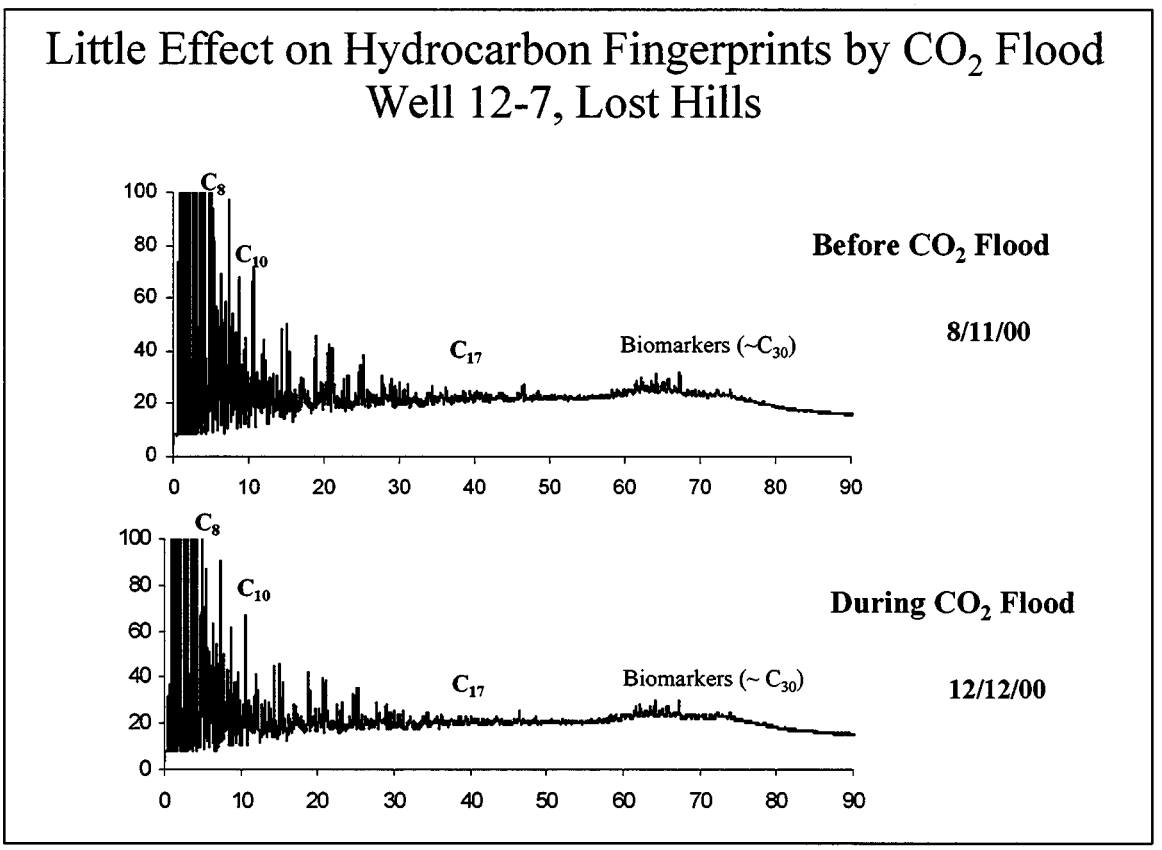

Figure 4.4-1. Hydrocarbon fingerprints are highly similar for the oils from well 12-7D, produced before and after the start of CO_2 flooding.

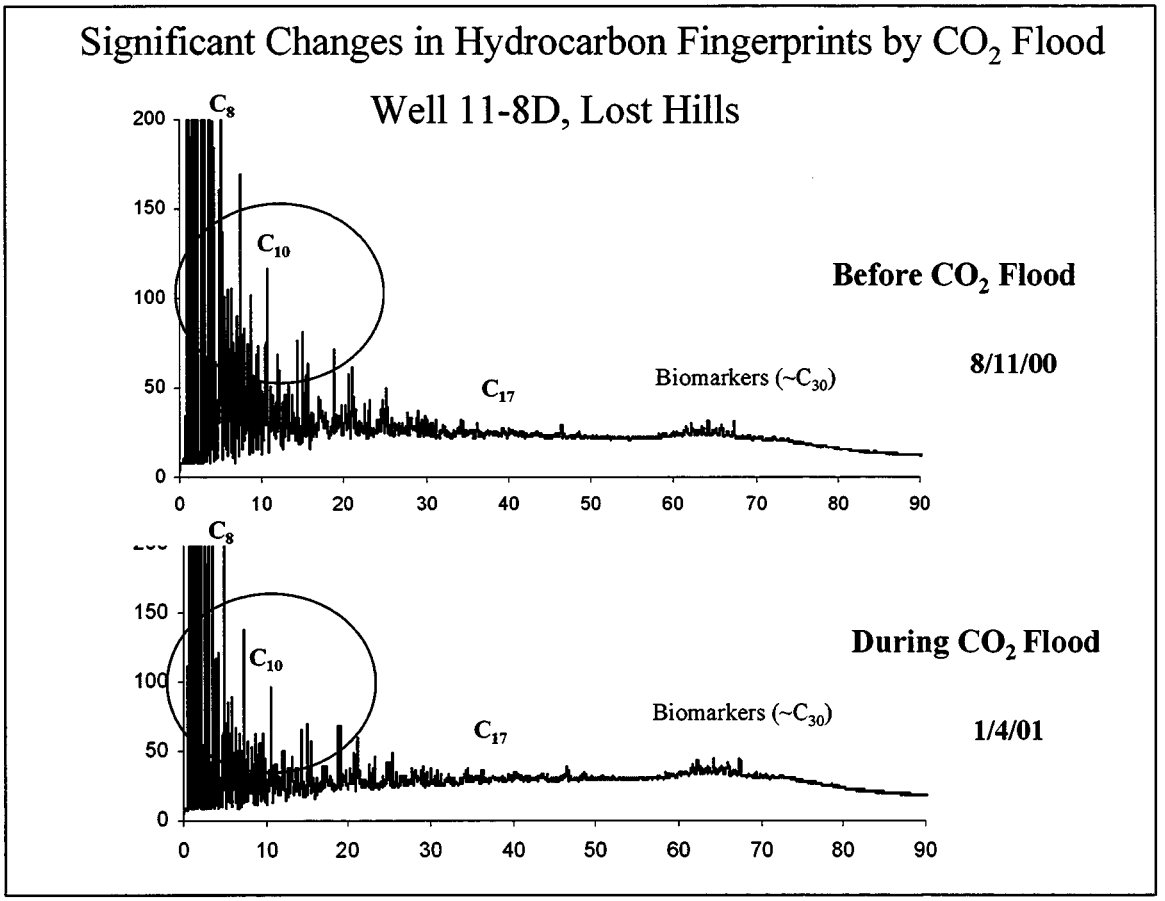

Figure 4.4-2. Hydrocarbon fingerprints are significantly different in the light ends for the oils from well 11-8D, produced before and after the start of CO_2 flooding.

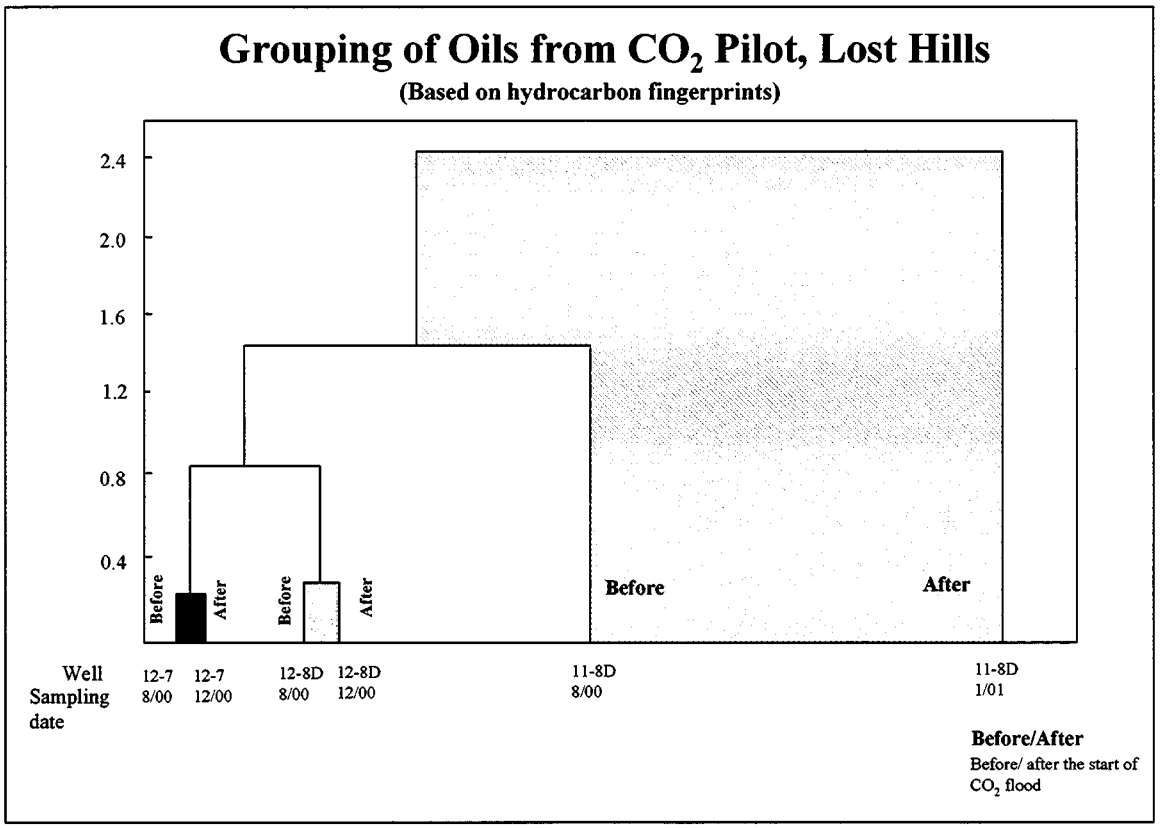

Figure 4.4-3. Cluster analysis showing well 11-8D has the most significant changes in hydrocarbon fingerprint after the start of CO_2 flooding.

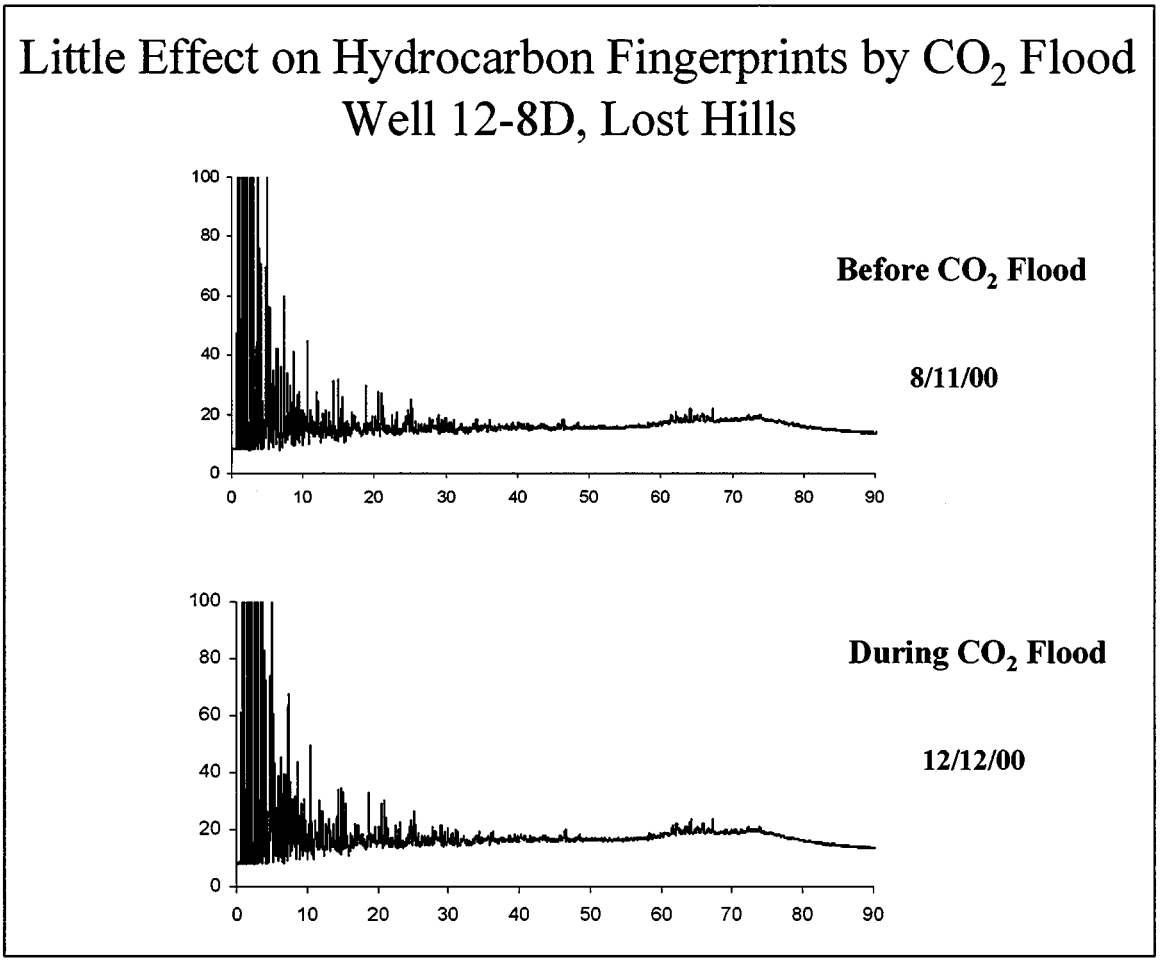

Figure 4.4-4. Hydrocarbon fingerprints are similar for the oils from well 12-8D, produced before and after the start of CO_2 flooding.

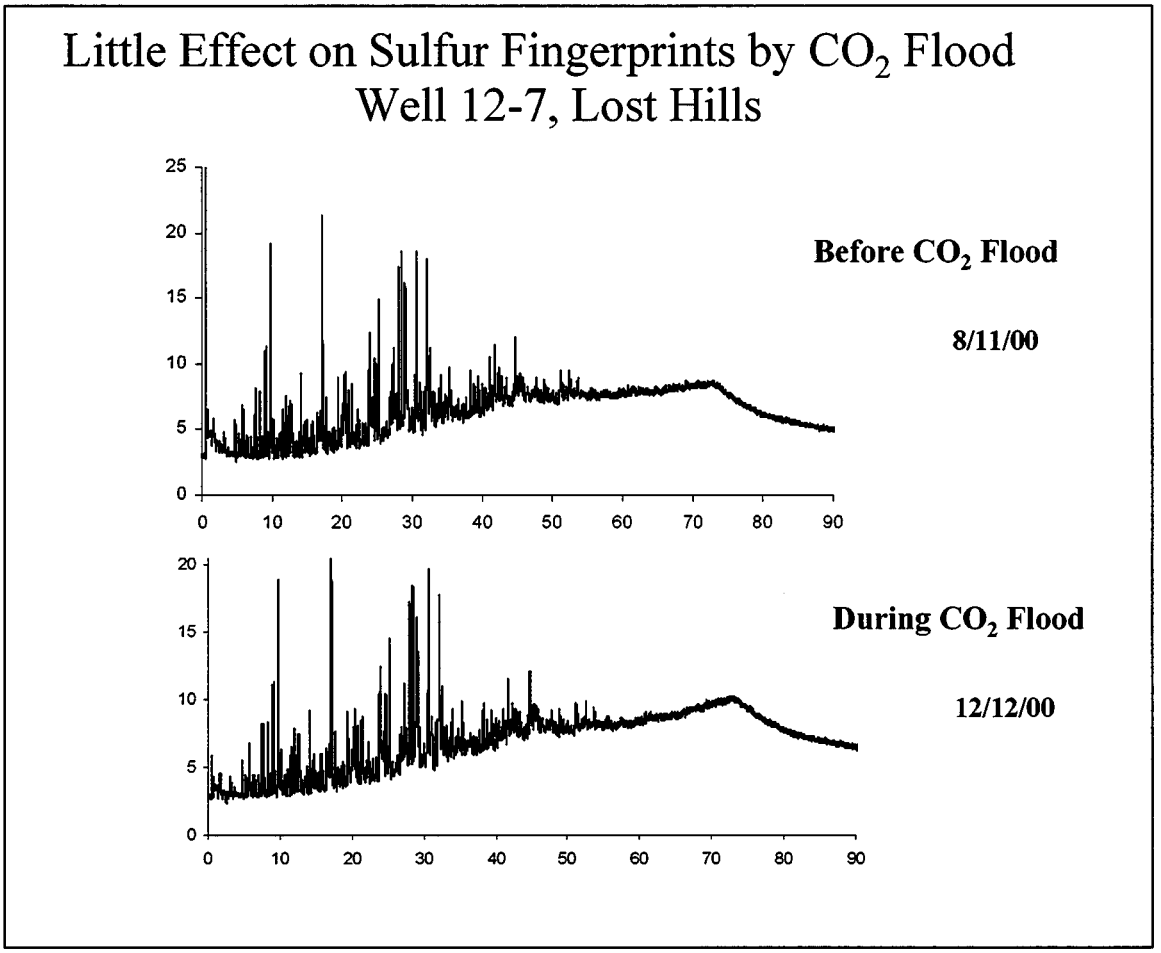

Figure 4.4-5. Sulfur fingerprints are highly similar for the oils from well 12-7, produced before and after the start of CO_2 flooding.

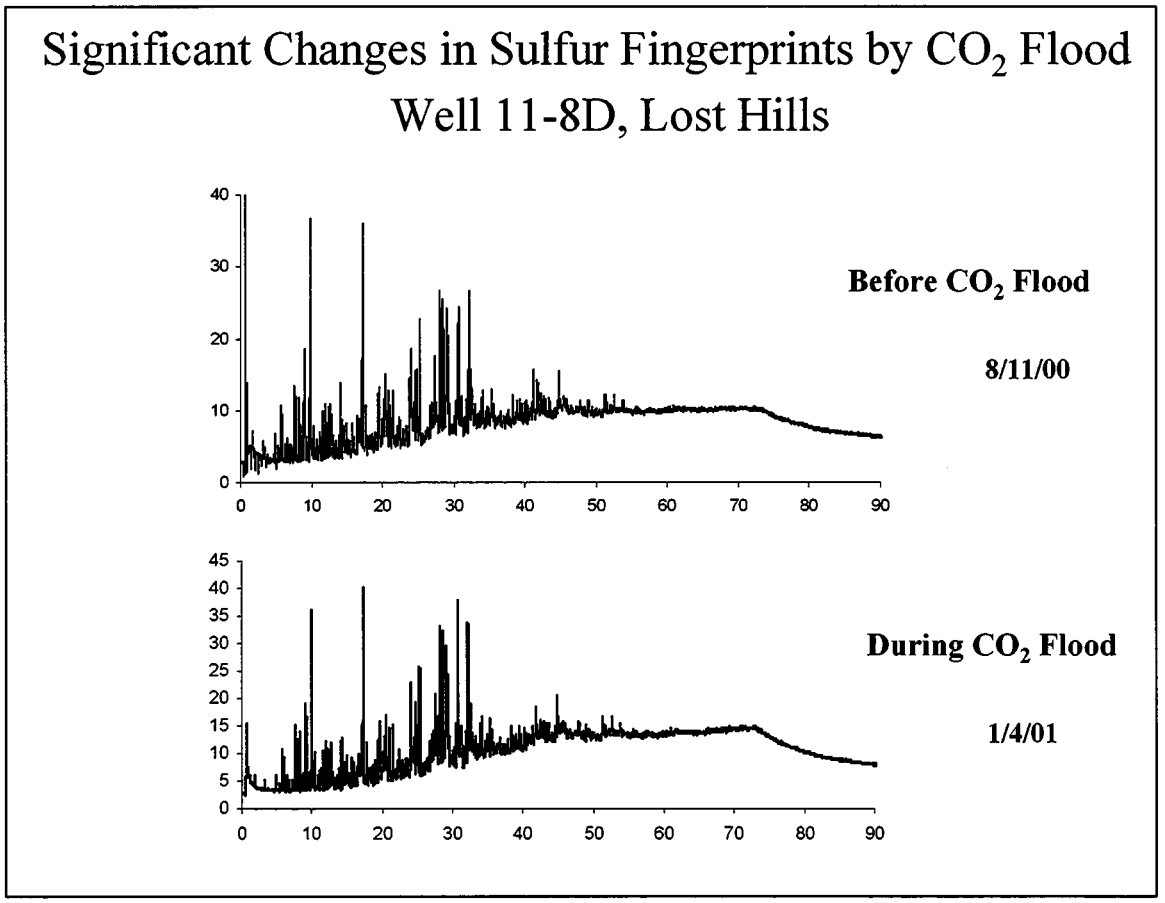

Figure 4.4-6. Sulfur fingerprints are significantly different for the oils from well 11-8D, produced before and after the start of CO_2 flooding.

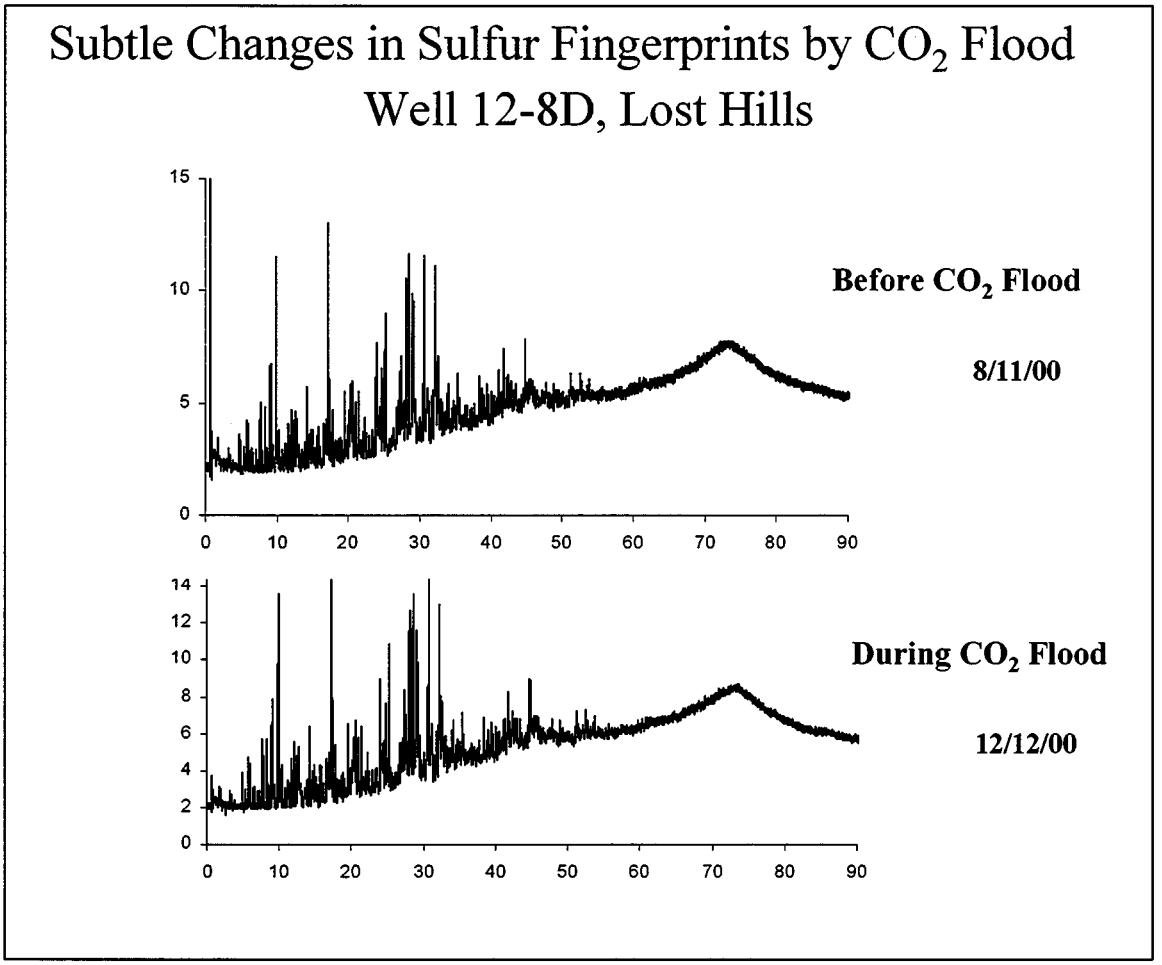

Figure 4.4-7. Sulfur fingerprints are slightly different for the oils from well 12-8D, produced before and after the start of CO_2 flooding.

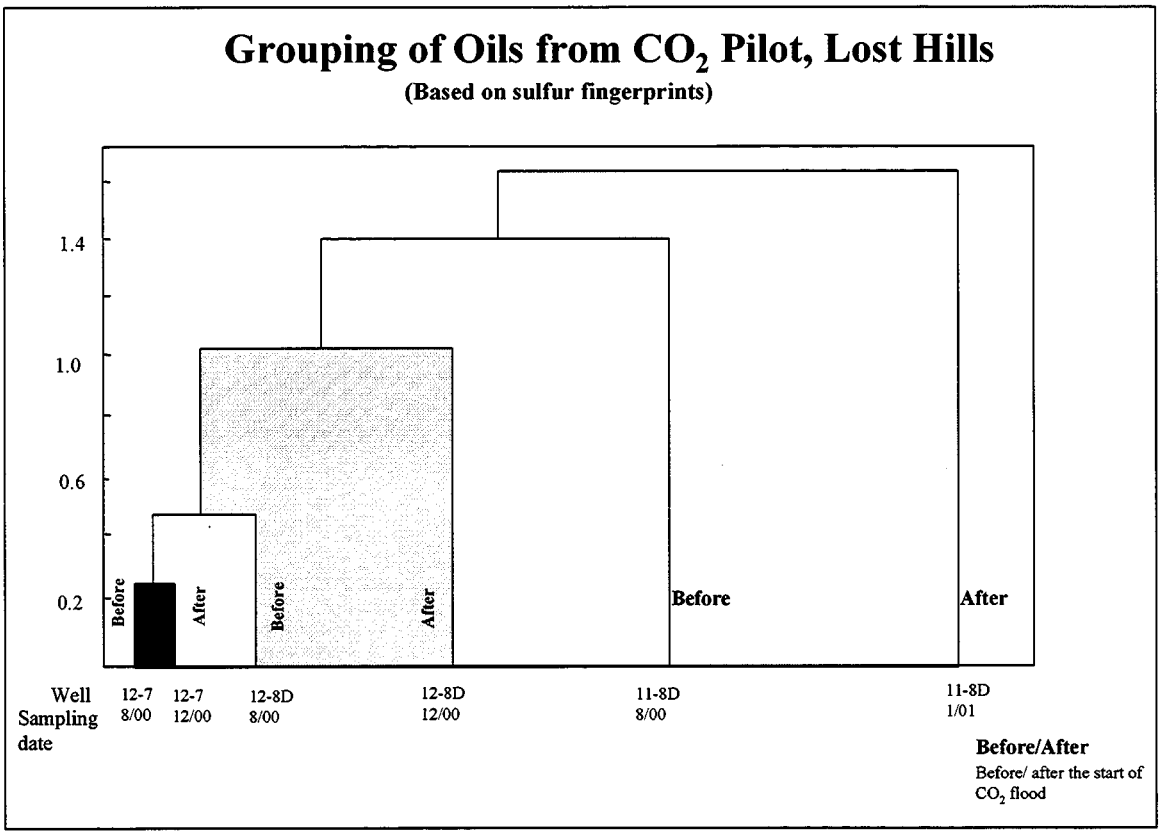

Figure 4.4-8. Cluster analysis showing the most significant changes for well 11-8D and moderate changes for well 12-8D in sulfur fingerprint after the start of CO_2 flood.

Table 4.4-1. Analysis of oils from CO_2 pilot area.

CRC	Well	Sampling Date	API Gravity	Total Sulfur %	Asphaltenes %	Elemental Sulfur
57422-1	11-8D	8/11/2000	21.8	1.10	3.2	ND
57423-1	12-7	8/11/2000	23.6	1.03	4.3	ND
57424-1	12-8D	8/11/2000	23.1	1.00	3.3	ND
57422-2	11-8D	1/4/2001	21.2	1.23	3.8	ND
57423-2	12-7	12/12/2000	23.7	0.94	3.1	ND
57424-2	12-8D	12/12/2000	22.4	1.04	2.7	ND

Wt % of Crude oils

ND, not detected; detection limit 10 ppm (GC-AED).

Table 4.4-2. Selected hydrocarbon peak ratios of oils from CO_2 pilot area.

CRC	Well	Sampling Date	Hydrocarbon Peak Ratios									
			86/ 89	101/ 98	82/ 77	119/ 122	149/ 146	99/ 94	75/ 74	242/ 241	68/ 72	Avg. % Diff.
57422-1	11-8D	8/11/2000	2.066	1.28	1.067	2.399	0.972	2.096	1.167	1.14	0.73	
57422-2	11-8D	1/4/2001	2.556	1.341	1.156	2.828	1.082	2.685	1.414	1.281	0.729	
% Diff.			19.2%	4.5%	7.7%	15.2%	10.2%	21.9%	17.5%	11.0%	0.1%	11.9%
57423-1	12-7	8/11/2000	1.668	1.212	0.932	2.216	0.955	1.742	0.97	0.945	0.695	
57423-2	12-7	12/12/2000	1.665	1.211	0.928	2.202	0.957	1.754	0.969	0.952	0.695	
% Diff.			0.2%	0.1%	0.4%	0.6%	0.2%	0.7%	0.1%	0.7%	0.0%	0.3%
57424-1	12-8D	8/11/2000	1.719	1.191	0.92	2.213	0.971	1.822	0.992	1.068	0.732	
57424-2	12-8D	12/12/2000	1.726	1.192	0.92	2.212	0.967	1.859	1.027	1.039	0.74	
% Diff.			0.4%	0.1%	0.0%	0.0%	0.4%	2.0%	3.4%	2.8%	1.1%	1.1%

Table 4.4-3. Selected sulfur peak ratios of Lost Hills oils from the CO_2 pilot area.

CRC	Well	Sampling Date	Sulfur Peak Ratios										
			135/ 130	64/ 67	125/ 123	136/ 140	92/ 96	65/ 66	208/ 205	116/ 119	57/ 56	183/ 185	Avg. % Diff.
57422-1	11-8D	8/11/2000	0.424	1.055	0.7	1.165	0.653	0.959	0.74	1.665	0.865	0.217	
57422-2	11-8D	1/4/2001	0.536	1.012	0.721	1.156	0.709	1.188	0.682	1.828	0.79	0.251	
% Diff.			20.9%	4.2%	2.9%	0.8%	7.9%	19.3%	8.5%	8.9%	9.5%	13.5%	9.6%
57423-1	12-7	8/11/2000	0.458	0.84	0.647	1.038	0.665	0.955	0.64	1.711	0.769	0.223	
57423-2	12-7	12/12/2000	0.461	0.841	0.641	1.002	0.661	0.995	0.645	1.71	0.762	0.225	
% Diff.			0.7%	0.1%	0.9%	3.6%	0.6%	4.0%	0.8%	0.1%	0.9%	0.9%	1.3%
57424-1	12-8D	8/11/2000	0.46	0.854	0.641	0.997	0.67	0.99	0.626	1.659	0.784	0.21	
57424-2	12-8D	12/12/2000	0.472	0.999	0.721	0.821	0.695	1.069	0.622	1.72	0.782	0.212	
% Diff.			2.5%	14.5%	11.1%	21.4%	3.6%	7.4%	0.6%	3.5%	0.3%	0.9%	6.6%

4.5 CO_2 CHEMISTRY MONITORING EFFORTS

D. R. Cole and G. R. Moline
Oak Ridge National Laboratory

Purpose:
Oak Ridge National Laboratory (ORNL) participates in the GEO-SEQ project funded jointly by NETL to LBNL, LLNL, and ORNL. The overall goal of the ORNL effort is to provide methods that utilize the power of natural and introduced tracers to decipher the fate and transport of CO_2 injected into the subsurface. The resulting data will be used to calibrate and validate predictive models used for (1) estimating CO_2 residence time, reservoir storage capacity, and storage mechanisms; (2) testing injection scenarios for process optimization; and (3) assessing the potential leakage of CO_2 from the reservoir.

Approach:
The basic approach is to utilize a combination of natural and applied gas tracers to delineate the subsurface movement of injected CO_2. The injected CO_2 will undergo a number of mass transfer processes as it interacts with the subsurface materials (e.g., rock, brine, hydrocarbons). These processes can enhance the reservoir's capacity for long-term storage of CO_2 and are, thus, important for both predicting and optimizing the effectiveness of geological sequestration of CO_2.

As the injected CO_2 interacts with the subsurface, its isotopic signature changes, thus making it an obvious natural tracer if: (1) the injection gas stream can be isotopically characterized, (2) the isotopic changes are significant enough to be detected during transport, and (3) the changes can be interpreted in the presence of multiple carbon sinks and sources in the subsurface. The first condition is straightforward, but the second and third are unknown and require modeling and laboratory testing to determine the feasibility of use of the CO_2 alone as a tracer.

Results:
In order to use the stable isotope compositions of carbon and oxygen in CO_2 as effective tracers during the injection tests we need to understand how these isotopes partition as a consequence of different process pathways (e.g., mineral reactions; sorption; aqueous dissolution). We investigated one important isotopic partitioning pathway, that of CO_2 interacting with hydrocarbon-saturated rock (an EOR injection scenario). We obtained hydrocarbon-bearing core from Chevron's Lost Hills field (Well OB-7). Four samples were selected for study: two taken in a horizontal orientation (sandy diatomites -H-1450.8 and H-1460.7) and two with a vertical orientation (diatomites:V-1685.8 and V-1706.0). Approximately 1.5 gms from each core were disaggregated, loaded into a two zone reaction vessel and reacted with a small quantity (2.33E-5 moles, ~0.001gms) of dry CO_2 (initial $\delta^{13}C_{PDB}$ = 50.4‰ and $\delta^{18}O_{PDB}$ = -13.47‰). CO_2 was also loaded into a fifth vessel (control) containing no core sample to measure possible partitioning between CO_2 and the vessel walls. These systems were allowed to react for 72 hours at 25°C. A small aliquot of CO_2 was isolated from the solid in the upper portion of each vessel and analyzed isotopically. The CO_2 from the control vessel showed no isotopic variation from the starting composition.

Without exception, the CO_2 sampled in the presence of the solid was isotopically enriched in both carbon and oxygen relative to CO_2 lost to the solid (sorption?). CO_2 reacted with sandy diatomites (horizontal orientation) was heavier in $\delta^{13}C$ by between 3.5 and 4‰ relative to "fixed" CO_2, whereas enrichments of between 4.0 and nearly 7‰ were observed for CO_2 reacted with diatomite. The $\delta^{18}O$ enrichments in CO_2 relative to "fixed" CO_2 were similar in magnitude regardless of lithology – ranging from 17 to as high as 35‰. The magnitude of the carbon isotope partitioning is comparable to what others have observed for CO_2 interaction with aqueous solutions. The preliminary conclusion to draw here is that a light isotopic component of CO_2 may be retained in the reservoir leading to progressively heavier isotopic CO_2 farther down the flow path. Clearly, more effort is needed to quantify how these isotopes fractionate as a function of temperature, PCO_2, surface area, hydrocarbon composition, mineral composition, solid to volatile mass ratios, and presence of H_2O.

Model calculations were conducted in order to assess the magnitude of carbon isotope change in CO_2 as it reacts with potential reservoir phases. The calculations assumed reaction in a closed system where CO_2 is allowed to interact with at varying portions with either a HCO_3^- bearing brine, calcite or hydrocarbon-rich rock (HC; Lost Hills, CA) of unspecified composition. Equilibrium isotope fractionation (taken from Friedman and O'Neil, 1977) is assumed in all calculations except one set where we used experimental batch-sorption isotope partition data obtained in at ORNL on Lost Hills core. Calculations were conducted for 20 and 100°C except for the sorption process which was based on our 20°C data. The initial carbon isotope value ($\delta^{13}C_{PDB}$) of the CO_2 was set at – 35‰, typical for CO_2 generated from coal-burning power plants. The initial carbon isotope values for the HCO_3^- fluid and calcite were set at -5 and 0 ‰, respectively, and are typical of what is observed in carbonate-hosted brine reservoirs. The HC carbon isotope value (-23‰) is based on what we measured for the Lost Hills core.

The results of these calculations are shown in Figure 4.5-1 where the $\delta^{13}C_{PDB}$ values for CO_2 are plotted against the atomic % carbon ratio between CO_2 and the interacting phase of interest (i.e., HCO_3^-, calcite, HC). In a simplistic way, one can think of the extreme left-hand side of the figure as the injection point for the CO_2, which undergoes reaction with progressively more and more of a particular carbon source during transport through the reservoir (left to right across the figure). In all cases the carbon isotope values of CO_2 become less negative through reactions with aqueous HCO_3^-, calcite or HC. The carbon isotope trajectory is determined by temperature that fixes the fractionation factor between CO_2 and any coexisting phase and the relative proportion of carbon in CO_2 to the carbon in the interacting phase. All of the cases shown are for binary systems (e.g., CO_2 – calcite; CO_2 – HCO_3^-). However, carbon isotope trajectories for CO_2 interacting with both HCO_3^- and calcite would lie between the respective binary curves for any given temperature scenario. Note that the carbon isotope trajectories for CO_2 interacting with HC-bearing rock vary considerably depending on whether the process is controlled by equilibrium isotope exchange or sorption; the latter being perhaps more realistic for low temperatures involving CO_2 injection into EOR or CBM systems.

Through careful selection based on their physical and chemical properties, a combined suite of applied tracers can act as a surrogate for the injected CO_2, providing information about the

mass transfer processes involving CO_2 by their differential transport behaviors. Batch reactor and flow-through column tests are planned that utilize a range of reservoir materials and temperature/pressure conditions to evaluate a suite of applied tracers and to quantify mass transfer coefficients relative to reservoir conditions (e.g., porosity, mineralogy, water saturation, hydrocarbon saturation, temperature, pressure). Additional tests will be conducted using these same materials and conditions to measure CO_2 isotopic changes. Initially, the natural and applied tracers will be evaluated separately to determine their respective transport behaviors. Later, we will combine them in flow-through column tests and determine correlations between the CO_2 and applied tracers. These experiments will provide a basis for designing and interpreting the results of a pilot field-scale CO_2 injection test. They will also provide key parameters for reservoir modeling and geophysical data interpretation being conducted by others on the project team.

After evaluating the results of published laboratory and field tracer studies, we have selected a suite of gas tracers that appear to have the physical and chemical properties that would make them appropriate for field use for tracking injected CO_2. The important selection criteria include: (a) low to zero concentration in the subsurface; (b) detectable at very low concentrations (parts per trillion or less); (c) stable under reservoir conditions; (d) environmentally safe; (e) subject to some of the same mass transfer processes as the injected CO_2; and (f) amenable to analysis using a single sample and a single method for the entire suite. Based on published studies, we have selected SF_6 and a suite of perfluorocarbons (PFC's) for our initial column studies. Results of these studies will be the basis for final determination of the tracers to be used for the field-scale CO_2 injection test and evaluation of the results of that test. Additionally, we have completed the basic design for a flow-through column apparatus that will allow us to test the relative interactions of the gas tracers with a variety of reservoir materials and under a range of pressure and temperature conditions appropriate for proposed injection scenarios (Figure 4.5-2).

The column setup relies on the use of a long, thin tube filled with reservoir materials placed within an oven to provide temperature control. In addition, a backpressure valve is built into the column outlet to allow experiments under increased pressure conditions. The column outflow is shunted to a gas chromatograph equipped with and electron capture device (ECD) by way of two columns, a carbopack column for perfluorocarbon separation and a molecular sieve for SF6 separation. The PFC's are stripped by the carbopack column, allowing the remaining gas stream to pass through the molecular sieve and be injected into the GC without the clogging effects of the PFC's. The PFC's then elute from the carbopack column and are injected into the GC, allowing all gases to be analyzed from a single sample. The design is similar to that used by Dugstad and others (1992) to test gas tracers for reservoir use.

Future Directions:

Future research efforts year will focus on five main areas:

(a) Construction of flow-through column tracer apparatus and its initial testing using a select group of rock types and gas tracers.

(b) Evaluation of the gas tracers to measure the relationship between variations in breakthrough behavior and specific transport processes

(c) Completion of core-gas-fluid isotope exchange experiments, emphasizing both the Lost Hill samples and more generic minerals representative of common reservoir lithologies, such as quartz (sandstone analogue), calcite (limestone analogue), and montmorillonite (mudstone analogue)

(d) Completion of model isotope calculations involving more complex reaction-path scenarios. This activity will also involve an assessment of isotopic studies of gas-bearing reservoir systems that may qualify as analogues for various CO_2 injection scenarios (e.g., brine formations, EOR, CBM, etc.)

(e) Initiation of combined injection of tracers and CO_2 to quantify the relationship between CO_2 partitioning and gas tracer partitioning.

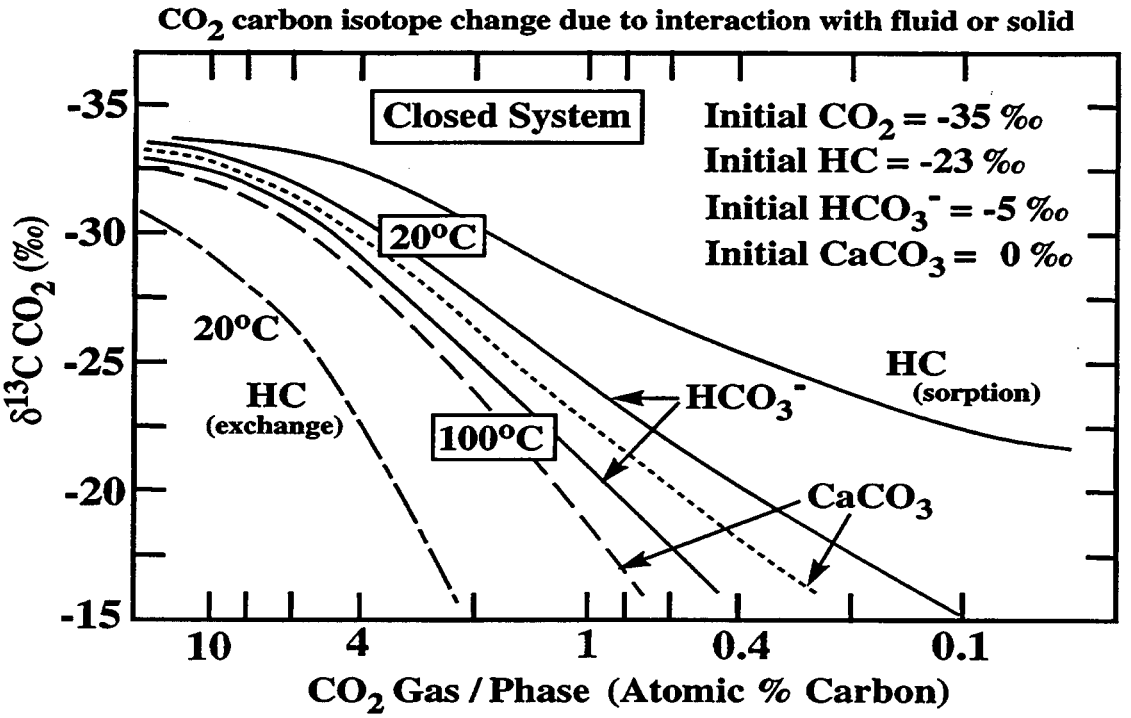

Figure 4.5-1. Changes in CO_2 isotopic composition due to interaction with fluids and solids. Movement along the x-axis from left to right can be considered analogous to changes during subsurface transport.

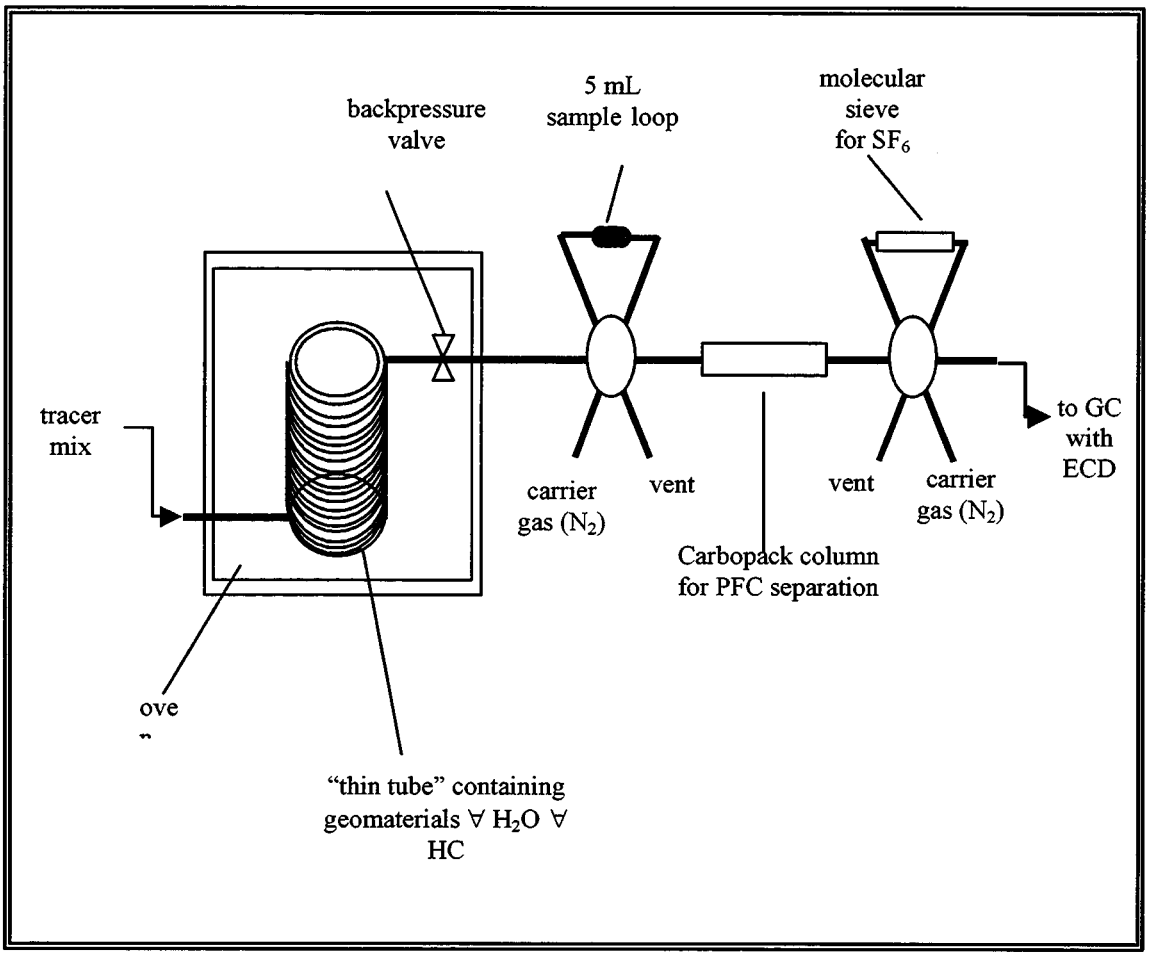

Figure 4.5-2. Column apparatus for flow-through gas tracer experiments.

4.6 INJECTION PROFILE MONITORING RESULTS

Michael F. Morea
Chevron USA Production Company

Injection profiles were run in all four injectors in September 2000 to determine vertical conformance of CO_2. Profiles indicate where CO_2 is exiting the wellbore. An "excellent" profile would be one that had CO_2 exiting all the perforations in equal amounts of CO_2. A "poor" injection profile would be one that had uneven distribution or portions of the wellbore receiving no CO_2.

Figures 4.6-1 and 4.6-2 show injection profiles for the four injectors in the CO_2 pilot. The figures illustrate the following curve tracks, starting from the left: percent water injection (0-50%, in blue); percent CO_2 injection (0-50%, pink); percent clay, silt/sand, biogenic silica (0-100%); depth and markers; completion interval, and deep resistivity (1-10 ohm-m). The water injection profile represents the pre-CO_2 injection baseline survey. Wells 11-8WR and 11-8WAR (Figure 4.6-1) are hydraulically propped fractured with limited, clustered perforations, whereas wells 12-7W and 12-8W (Figure 4.6-2) are hydraulically propped fractured with more extensive, evenly spaced wellbore perforations.

Wells 11-8WR (Figure 4.6-1, left) and 12-8W (Figure 4.6-2, right) have poor injection profiles with most of the CO_2 exiting the upper perforations. 11-8WR has 65% of the CO_2 exiting out of the top perforations. 12-7W has the best injection profile (Figure 4.6-2, left). This well was part of the CO_2 injection test that was performed in 1999 prior to the pilot. 12-7W has two CO_2 profiles: one for the 1999 injectivity test (center profile) and one for September 2000 (profile on the right). 12-7W clearly shows that CO_2 has no preference for silt-rich or diatom-rich lithologies. The poorer injection profiles in the other wells could be due to blocked perforations, preference for lower pressure zones, or poor hydraulic fractures.

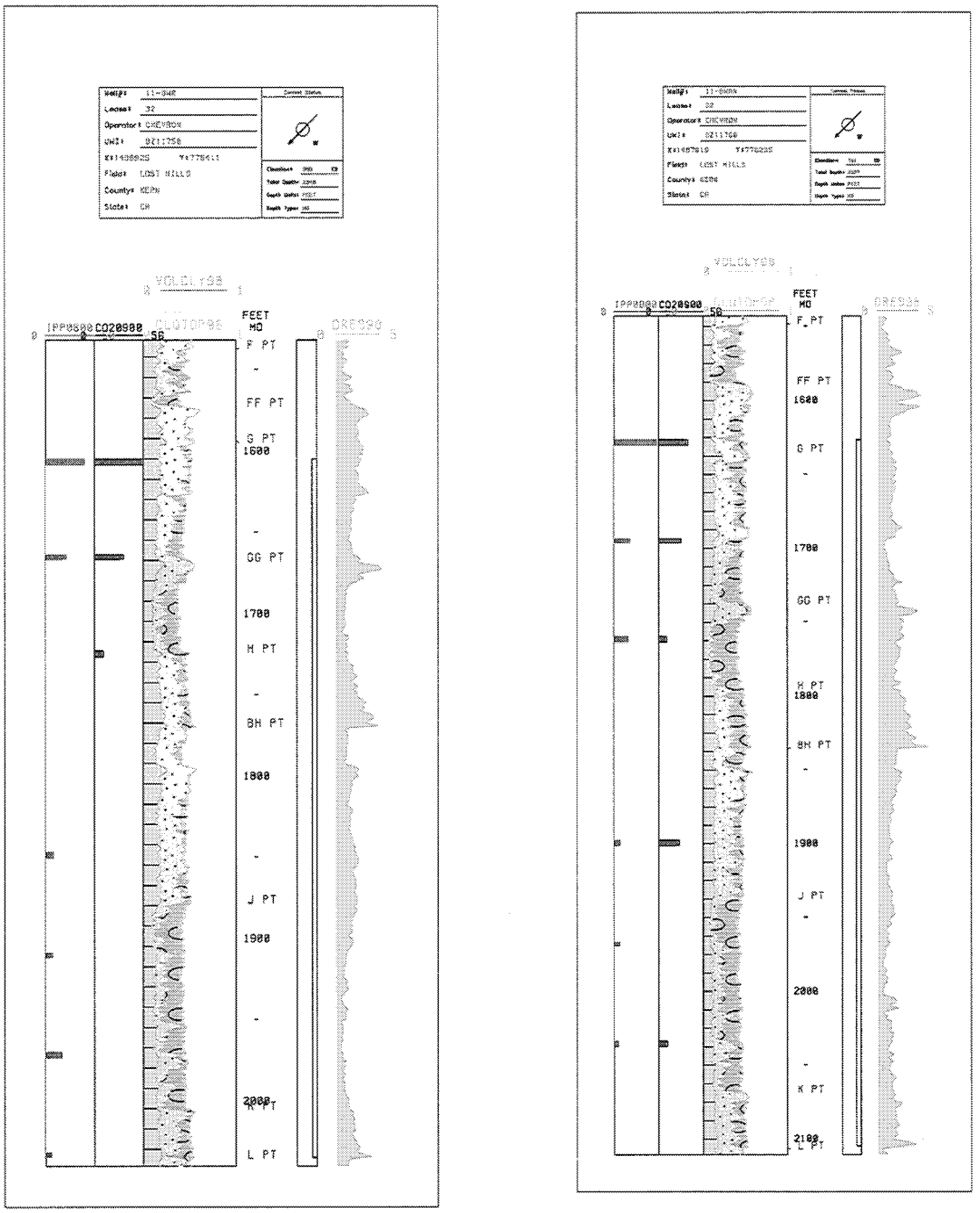

Figure 4.6-1. Injectivity profiles of 11-8WR (left) and 11-8WAR (right). See text for description of logs. 11-8WR has 65% of the CO_2 exiting out of the top perforations. 11-8WAR shows a better profile and is more comparable to the baseline water injection survey.

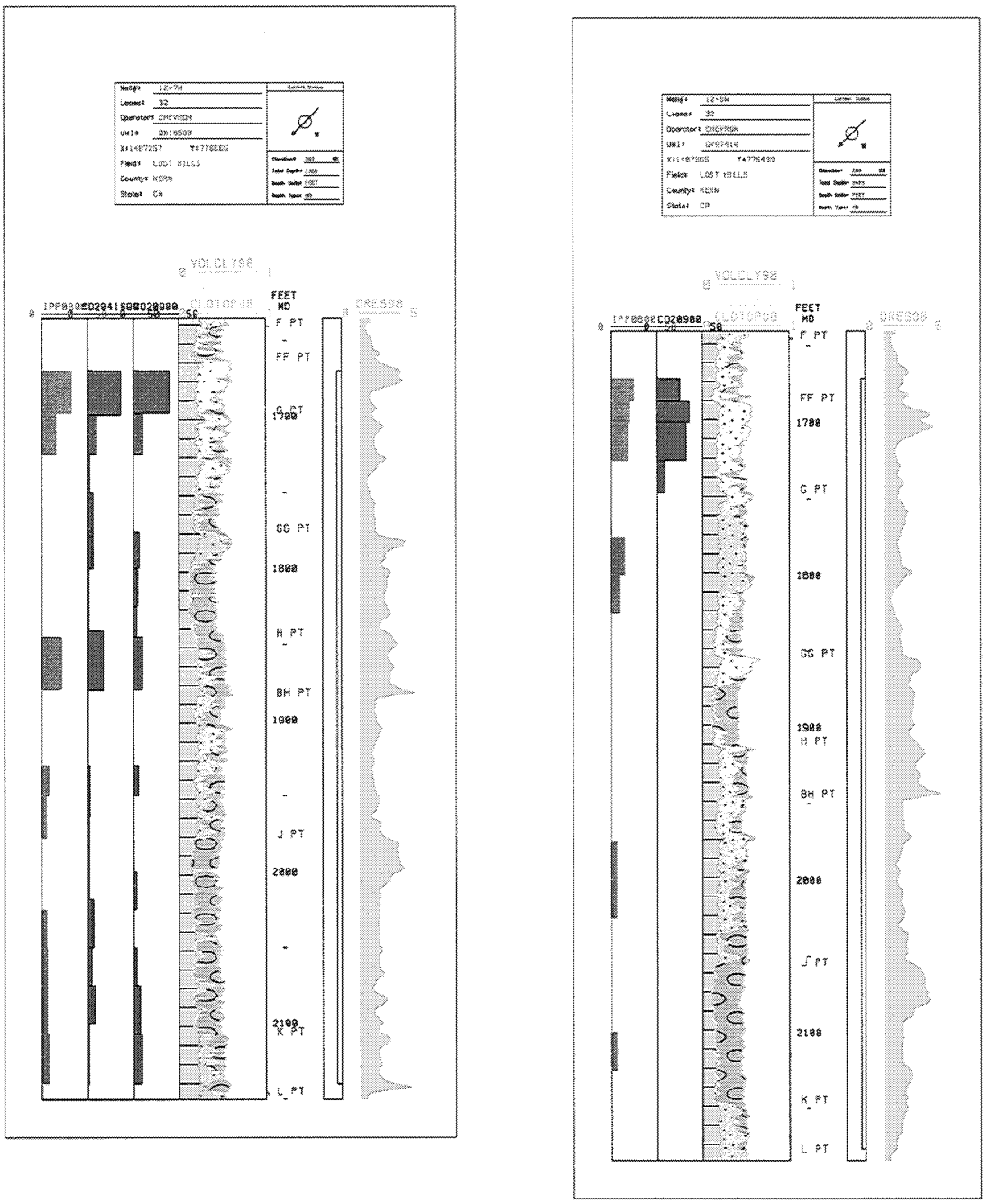

Figure 4.6-2. Injectivity profiles of 12-7W (left) and 12-8W (right). See text for description of logs. 12-7W was the injector used in the initial injectivity test. Baseline profile, CO_2 injectivity test profile, and monitoring profile all show water and CO_2 to have no preference for lithology (sandy diatomite vs. diatomite). This is the best profile of all 4 pilot injectors. 12-8W has a poor profile that shows all the CO_2 exiting the upper perforations.

4.7 CASED HOLE RESISTIVITY LOGGING IN CO_2 OBSERVATION WELLS

Michael F. Morea
Chevron USA Production Company

In January 2001 resistivity logs were run in the fiberglass cased OB-C1 and OB-C2 observation wells. The purpose of this logging was to compare these logs with the baseline surveys that were taken in both wells prior to CO_2 injection, and to monitor changes in resistivity due to CO_2 injection. For the baseline surveys, open hole logs (spontaneous potential, gamma ray, resistivity, neutron, density) were run in OB-C1 but could not be run in OB-C2 because the well was flowing back to surface during drilling. Therefore cased hole resistivity, gamma ray and neutron logs were run prior to CO_2 injection to act as a baseline survey. The OB-C1 is located 60 feet (bottom hole location), and the OB-C2 is located 30 feet (bottom hole location) on either side of the 11-8WR injector. Both wells are situated perpendicular to 11-8WR's hydraulic propped fracture azimuth.

A comparison of the open and cased hole logs in OB-C2 showed that there had been a subtle change in resistivity (~1 unit reduction in oil saturation) due to CO_2 injection. A similar comparison using open and cased hole logs in OB-C1 showed that there were larger changes in the deep resistivity curves in some intervals (Figures 4.7-1 to 4). These changes in resistivity equate to oil reductions in the 1 to 4 saturation unit range. Two preliminary observations that can be made from these figures are: 1) CO_2 has reduced the oil saturation in both diatomite and sandy diatomite, and 2) CO_2 has made its way out of the injection interval (FF – L) and migrated up into the C unit (Figure 4.7-1).

What is interesting about the log monitoring surveys in the two observation wells is that OB-C1 is twice as far away from the injector 11-8WR as OB-C2, and CO_2 has caused a greater oil saturation reduction in OB-C1 than OB-C2. As discussed in a previous section of this report, only a very small amount of injection tracer material has been detected in the surrounding producing wells. This quick, tracer travel time from injector to producer is due to the presence of natural fractures. However the small amount of recovered tracer indicates that most of the non-recovered tracer has probably moved into the reservoir matrix. The cased hole log data also indicates that CO_2 has moved into the reservoir matrix. In addition and more importantly, the cased hole log data indicates that CO_2 is displacing oil. Subsequent monitoring efforts (cased hole logs, electromagnetics, etc.) will help to further understand the distribution pattern of CO_2 in the reservoir.

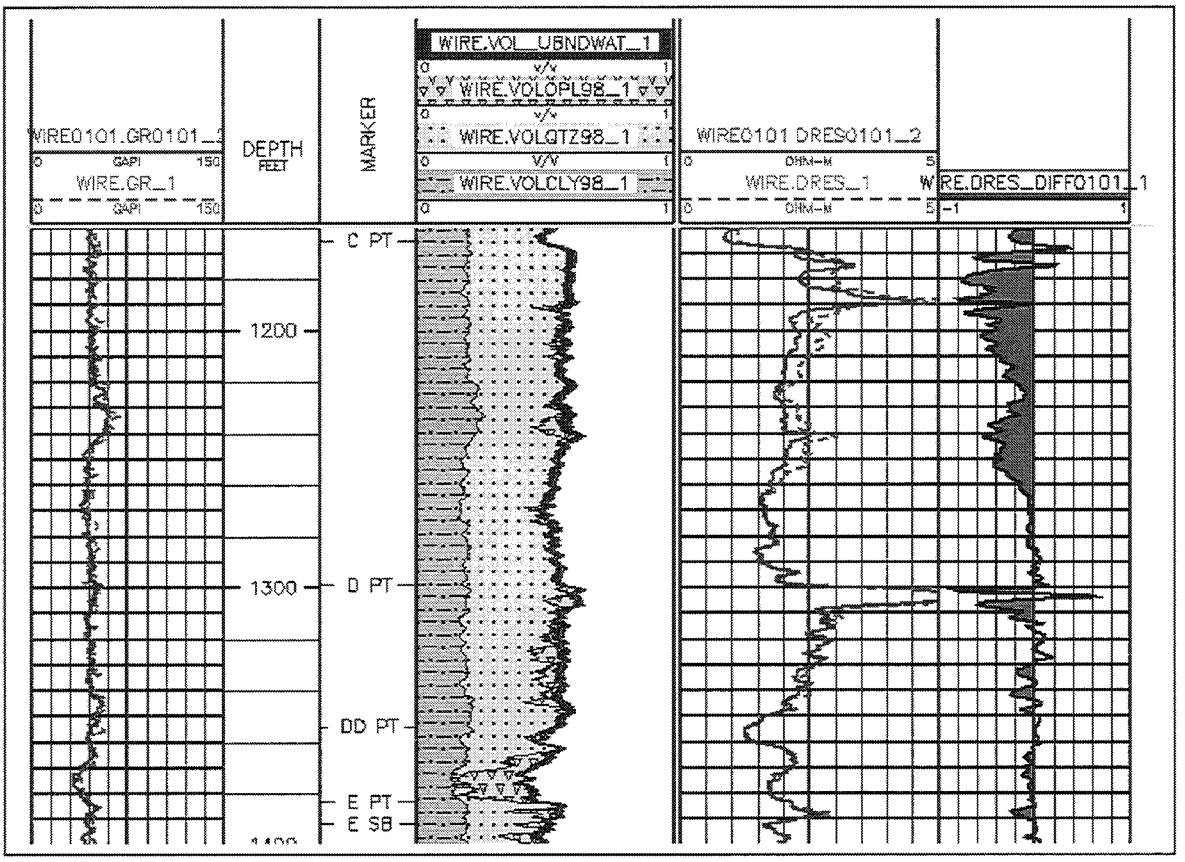

Figure 4.7-1. Comparison of baseline and January 2001 monitoring survey in the C – E interval in OB-C1. The curve tracks are, from left to right, gamma ray (blue, dashed curve – open hole baseline; red, solid curve – cased hole); measured depth; geologic markers; lithology (clay, silt/sand, and opal A); deep resistivity (blue, dashed curve – open hole baseline; red, solid curve – cased hole), and deep resistivity difference (-1 – 1 ohm m) between baseline and cased hole surveys. Note slight reduction in resistivity in the sandy diatomite of the C unit. Average oil reduction due to CO_2 across the 1165-1299' interval equals approximately 4 saturation units.

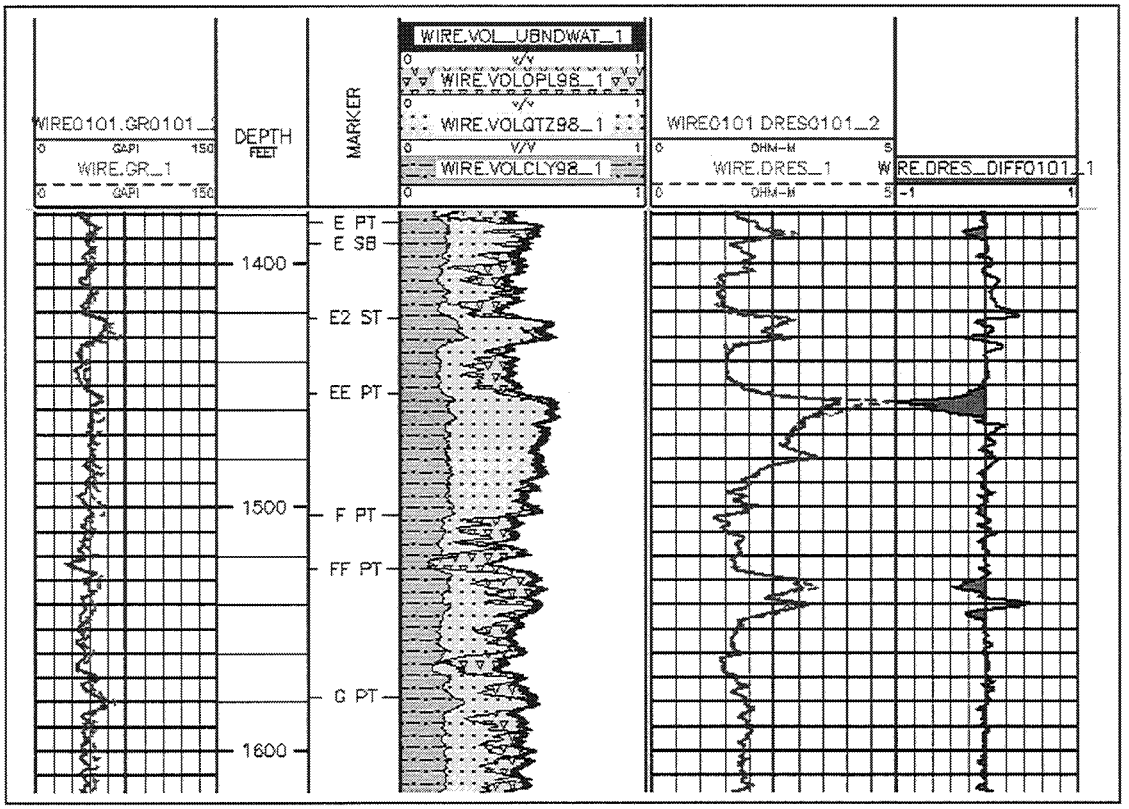

Figure 4.7-2. Comparison of baseline and January 2001 monitoring survey in the E – G interval in OB-C1. Curves the same as Figure 4.7-1. Note slight reduction in resistivity at the top of the sandy diatomite of the EE unit.

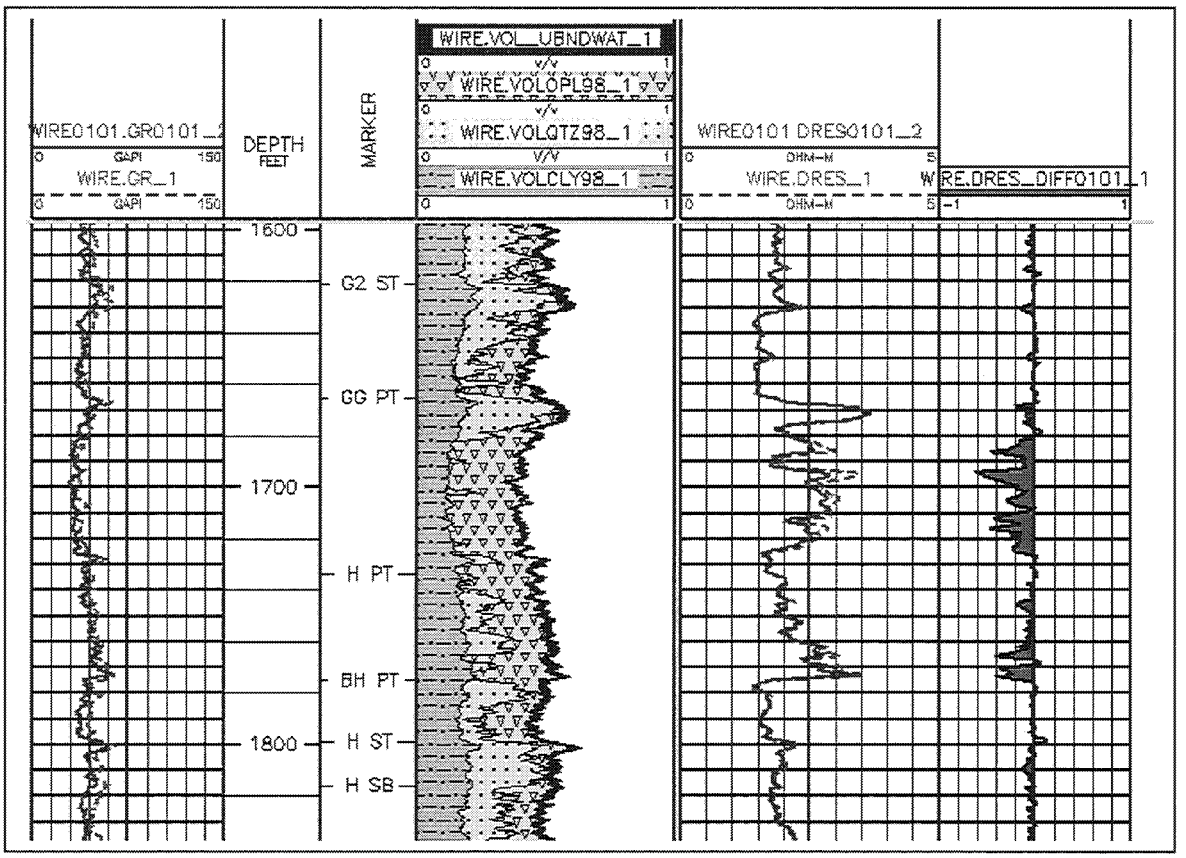

Figure 4.7-3. Comparison of baseline and January 2001 monitoring survey in the G – H interval in OB-C1. Curves the same as Figure 4.7-1. Note slight reduction in resistivity in the diatomite of the GG unit. Average oil reduction due to CO_2 across the 1680-1776' interval equals approximately 2 saturation units.

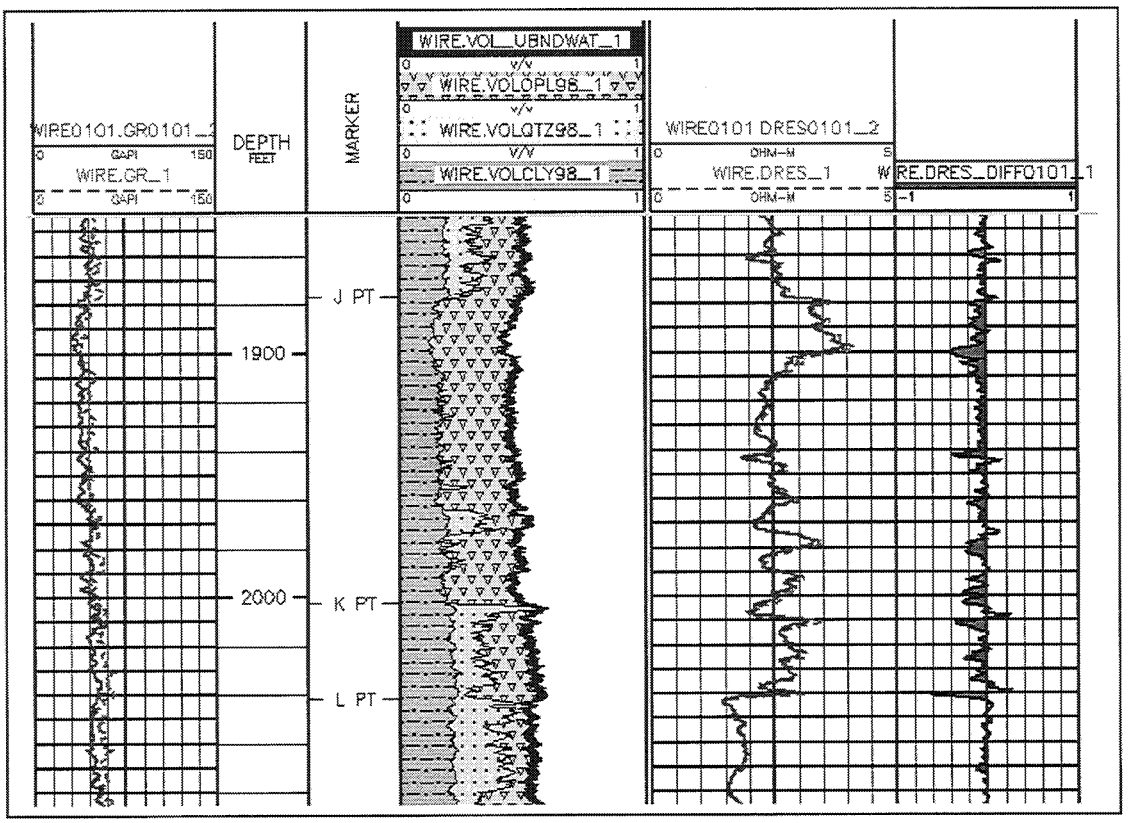

Figure 4.7-4. Comparison of baseline and January 2001 monitoring survey in the J – L interval in OB-C1. Curves the same as Figure 4.7-1. Note slight reduction in resistivity in the diatomite of the J unit. Average oil reduction due to CO_2 across the 1898-2044' interval equals approximately 1 saturation unit.

4.8 BOREHOLE SEISMIC MONITORING OF CO_2 INJECTION IN A DIATOMITE RESERVOIR

Thomas M. Daley, Ernest L. Majer, Roland Gritto, Sally M. Benson
Lawrence Berkeley National Laboratory, Earth Science Division

Background:

Chevron USA Production Company is currently operating a CO_2 injection pilot program in the Lost Hills, California oil field. This pilot program, which is partially funded by the U.S. Department of Energy (DOE) as an enhanced oil recovery project, is ideally suited for design and testing of geologic sequestration concepts including subsurface monitoring techniques. Our goal is to demonstrate through field testing, techniques for imaging subsurface CO_2 and for monitoring geologic sequestration. Other investigators are studying electromagnetic (EM) and electrical methods and we plan to integrate the geophysical results. CO_2 has been used by the oil industry for many years to enhance oil production. Previous studies in carbonate reservoirs have shown that seismic velocity changes are caused by CO_2 injection and that these changes can be spatially mapped using crosswell seismic surveys (Wang and others, 1998). The seismic velocity change can be up to 10%, which is easily detectable and mappable with modern crosswell seismic surveys. Therefore, borehole seismic surveys hold great promise for mapping and long term monitoring of sequestered CO_2. The quantity and quality of CO_2 sequestration will, of course, vary greatly depending of the reservoir properties. The diatomite reservoir at Lost Hills has unusually high porosity (avg. 50%) and low permeability (0.1 - 10 millidarcies). Because of the low permeability, the diatomite reservoir is developed with 1.25 acre well spacing or less. Despite this small well spacing, only 5% of the estimated 2.2 billion barrels of oil in place have been produced since discovery in 1910.

The diatomite at Lost Hills is composed of biogenic silica, clay and silt/sand. While the percentage of clay (20-30%) is fairly constant vertically in the reservoir, the percentages of silt/sand and biogenic silica vary. This variation of lithologic composition affects the reservoir's porosity and permeability distribution: biogenic silica rich beds have higher porosity (due to diatom structure) but lower permeability than silt/sand beds.

Field Site and CO_2 Injection Information:

The CO_2 injection pilot is being operated by Chevron USA in Lost Hills field. The pilot covers 10 acres. It is divided into four injector-centered, 2.5-acre patterns. The reservoir volume around one injection well (11-8WR) is being monitored by crosswell seismic studies using two observation wells (OB-C1 and OB-C2). The reservoir depth is about 1400 feet (425 m) to 2100 feet (640 m) below ground level. The injection well was hydraulically fractured over the reservoir interval prior to injection. This part of the Lost Hills field has also had previous enhanced production using water flood. The CO_2 injection began in August 2000 at a relatively low flow rate of 125 million cubic feet (Mcf) per day. The rate has been gradually increased to the current rate of 425 Mcf/day per injection well. The injection pressure is held at 800-900 psi. The reservoir temperature is about 108° F. At this pressure and temperature, the CO_2 is expected to be in gas phase. The expected effect of the CO_2 is to swell the oil and lower reservoir fluid viscosity. Tracers have been placed in the

CO_2 injectors and to date (in the early stages of injection) about 1-2% of the tracer has been detected in some of the production wells. The CO_2 is being transferred, by BOC Gases, from Chevron's El Segundo, CA refinery using 4 trucks per day to supply this 4 well injection program. The CO_2 is stored locally in tanks and distributed to the injection wells with surface pipes.

Seismic Properties of CO_2:
The seismic properties of CO_2 (velocity and density) vary with pressure and temperature. In particular, the transition from liquid phase to gas phase has a dramatic effect on seismic properties as shown in Figure 4.8-1. This is a key point at the Lost Hills site where the injection is at 800 to 900 psi and temperature is about 108 0F, so we expect the CO_2 to have a subsurface gas phase. If there is a subsurface gas phase, the seismic visibility and mappability will be greatly enhanced. Previous crosswell and singlewell seismic studies have shown the ability to detect a single gas-bearing fracture such as the CO_2 filled hydrofracture at Lost Hills (Majer and others, 1997).

Borehole Seismic Acquisition:
LBNL has collected three borehole seismic data sets using the observation wells OB-C1 and OB-C2. Two crosswell surveys used OB-C1 for a source well and OB-C2 for a receiver well (Figure 4.8-2). The first survey used a piezoelectric source while the second used an orbital vibrator source. Both used 3-component wall-locking accelerometer sensors. The third survey was a single well imaging experiment (source and receivers in the same well) in OB-C1 using the piezoelectric source and both the 3-component accelerometers and hydrophone sensors. The surveys had 5 foot (1.5 m) interval spacing between source and receiver depths. The distance between wells is approximately 80 feet (24 m). The piezoelectric crosswell survey obtained high frequency data (>2000 Hz) giving wavelengths of about 1 m. A 3-component receiver gather is shown in Figure 4.8-3. This data set is notable for being narrow band. Spectral analysis (Figure 4.8-4) shows narrow spectral peaks at about 1500, 1700 and 2200 Hz. One implication is a "ringy" waveform that has been previously observed in diatomite studies (Wilt and others, 1997). The spectral content and amplitude also vary with depth as shown in Figure 4.8-4 and this may represent material property variations within the diatomite beds. The orbital vibrator source is lower frequency (70-350 Hz) providing a separate scale of investigation (wavelengths of about 6 m). The orbital vibrator is a recently developed borehole source and it is notable for generating two components of source motion, in-line and cross-line, and thereby generating both P- and S-waves (Daley and Cox, 2000). The measurement of P- and S-wave velocities allows greater understanding of subsurface material properties, especially in gas and liquid saturated porous material. Figure 4.8-5 shows a 6-component receiver-gather for the orbital vibrator data (2-components of source and 3-components of receiver). The wavefield shows P-waves generated by the in-line source and a combination of S-wave and tube-wave energy generated by both sources. We believe the slow S-velocity in the diatomite allows generation of a "Mach" wave, i.e., a formation shear-wave generated by the borehole tube-wave. In general, the diatomite has a fairly complicated seismic wave propagation due to the high porosity and mixed pore fluid (oil, water and gas). The detection and delineation of CO_2 will be combined with understanding the overall wave propagation properties of diatomite.

Current Results:
We have obtained preliminary 2-D tomographic images of velocity for both pre-injection seismic crosswell experiments. These results are shown in Figures 4.8-6a and 4.8-6c with an interpreted cross section provided by Chevron USA in Figure 4.8-6b. The high frequency piezoelectric data set has higher resolution as expected. A low velocity zone is seen in Figure 4.8-6c between 1600 and 1700 feet. The apparent dip of this zone may be indicating the faulted offset seen in the cross-section. Lower velocities are measured from the longer wavelength (lower frequency) orbital vibrator data (Figure 4.8-5) which may be an indication of different scales of heterogeneity being measured in the diatomite. It is not unusual to see frequency dependent measurements of seismic velocity. No sonic logs are yet available in these wells, however sonic logs, which are about 10,000 Hz, often have higher velocities than surface seismic data which are about 100 Hz. Borehole tomography falls in between these scales of measurement. The most important aspect of these data sets is that they represent a baseline measurement of reservoir properties before CO_2 injection. The complexities of the diatomite reservoir make direct measurement of one property (such as CO_2 concentration) very difficult. However, time-lapse changes measured against this baseline survey, should be controlled by CO_2 injection and flow properties. The post-injection surveys should begin in spring of 2001. It is the time-lapse changes in seismic properties that should be most useful in monitoring and mapping CO_2 in the subsurface.

Acknowledgments:
This work was supported by the GEO-SEQ project of the DOE National Energy Technology Laboratory (NETL) under contract DE-AC03-76SF000098. Data processing was performed at the Center for Computational Seismology, which is supported by the Office of Basic Energy Sciences. Thanks to Mike Morea and Chevron USA Production for their generous help with field information.

References:
Daley, T.M., and Cox, D., 1999, Orbital vibrator seismic source for simultaneous P- and S-wave crosswell acquisition, Lawrence Berkeley National Laboratory Report LBNL-43070, Berkeley, CA (submitted to Geophysics).

Majer, E.L., Peterson, J.E., Daley, T.M., Kaelin, B., Queen, J., D'Onfro, P., and Rizer, W, 1997, Fracture Detection using Crosswell and Single Well Surveys, Geophysics, v. 62.

Wang, Z., Cates, M.E., and Langan, R.T., 1998, Seismic monitoring of a CO_2 flood in a carbonate reservoir: A rock physics study, Geophysics, v. 63.

Wilt, M., Schenkel, C., Daley, T., Peterson, J., Majer, E., Murer, A.S., Johnston, R.M., Klonsky, L., 1997, Mapping Steam and Water Flow in Petroleum Reservoirs, Society of Petroleum Engineers Symposium, Bakersfield, CA.

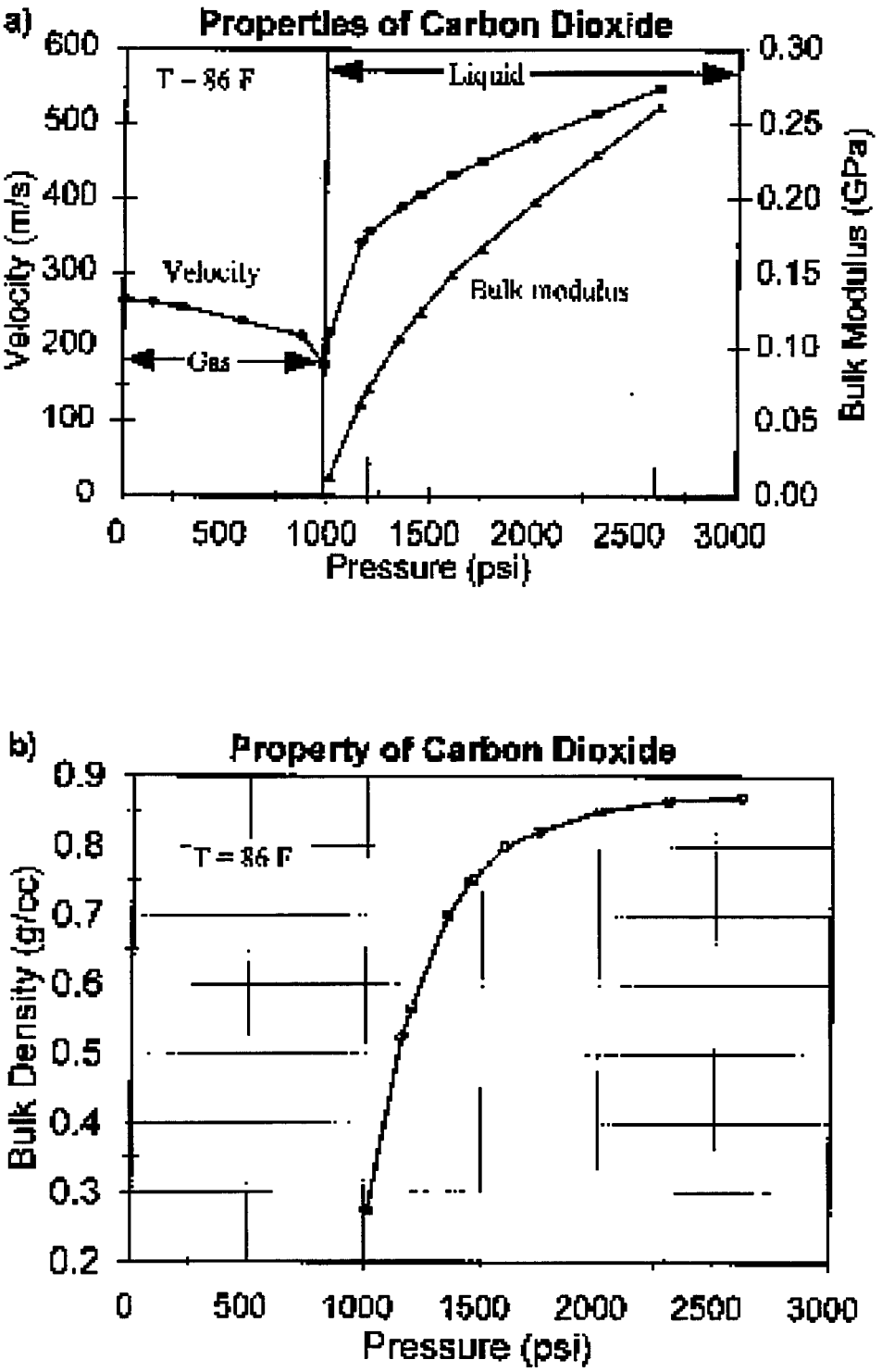

Figure 4.8-1. Effect of CO_2 on seismic P-wave velocity (top, a) and bulk density (bottom, b). From Wang and others, 1998.

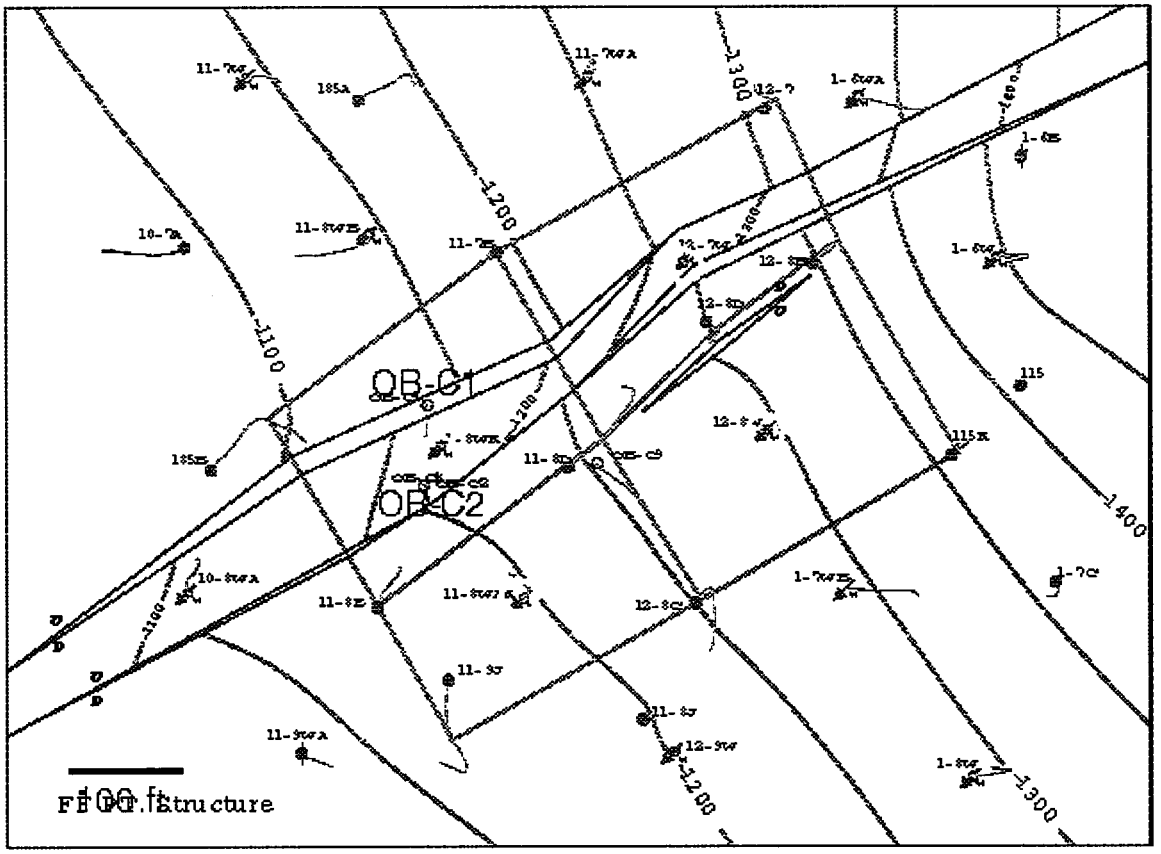

Figure 4.8-2. CO_2 Injection site (blue lines) with contoured top of reservoir (green lines) and interpreted faults (red lines). Our study is in wells OB-C1 and OB-C2 for injector 11-8WR. Each blue square contains one of the four CO_2 injection wells (yellow circle). This is a 2.5 acre pattern. Figure from M. Morea (Chevron, USA).

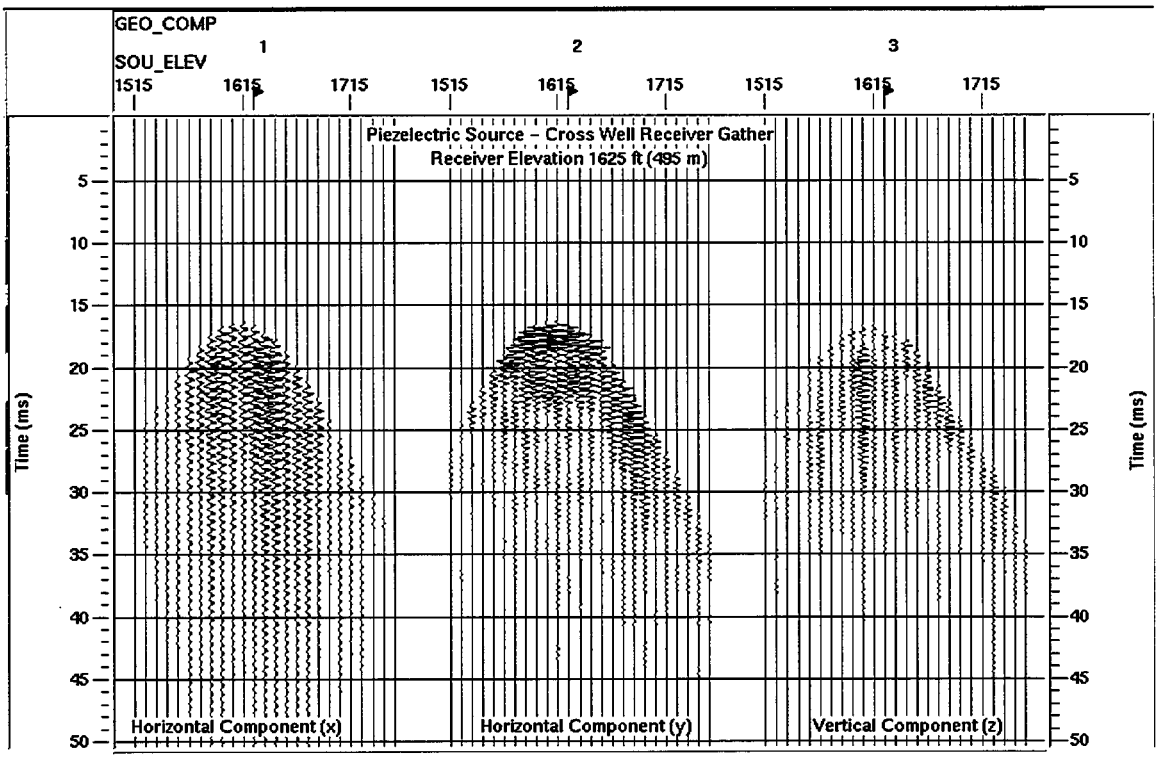

Figure 4.8-3. Piezoelectric source data for 3-component sensor. A strong P-wave arrival is observed.

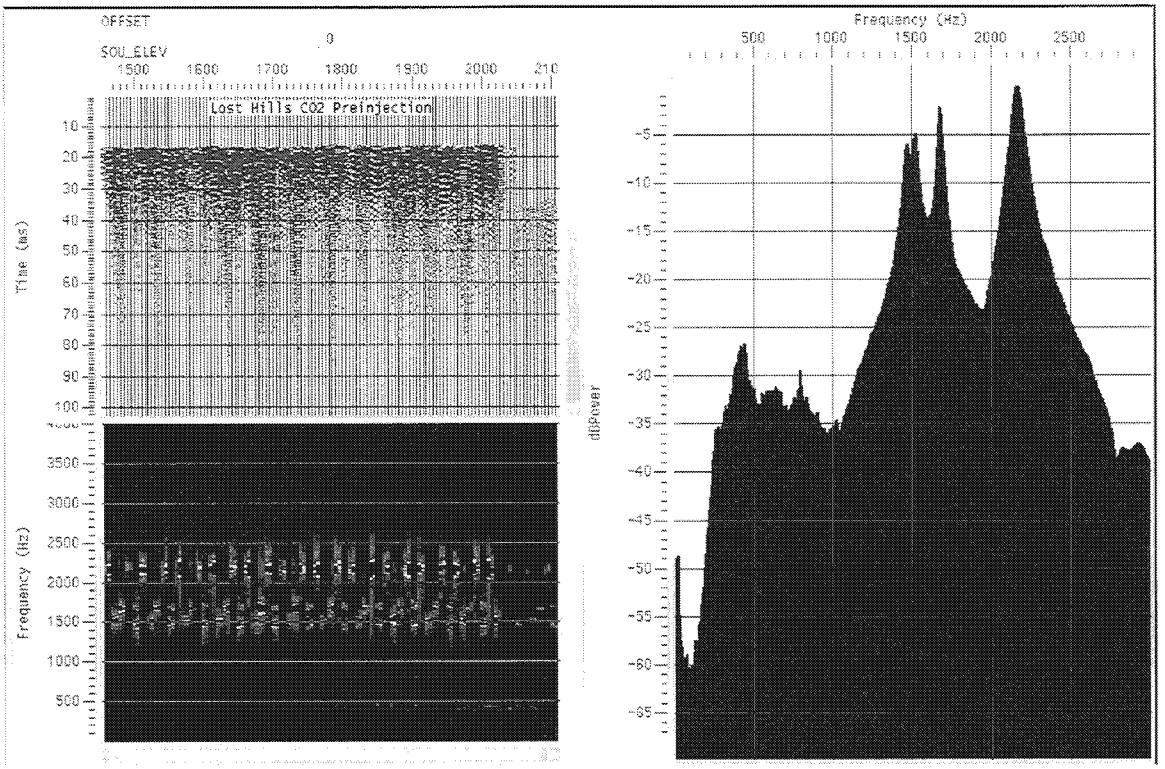

Figure 4.8-4. Spectral analysis of piezoelectric source data for zero-offset propagation. Seismograms (top left), frequency vs. depth (bottom left) and total frequency content (right) are shown. The narrow band frequency peaks (right) and the depth stratification of frequency content (bottom left) are presumed to be caused by subsurface heterogeneity.

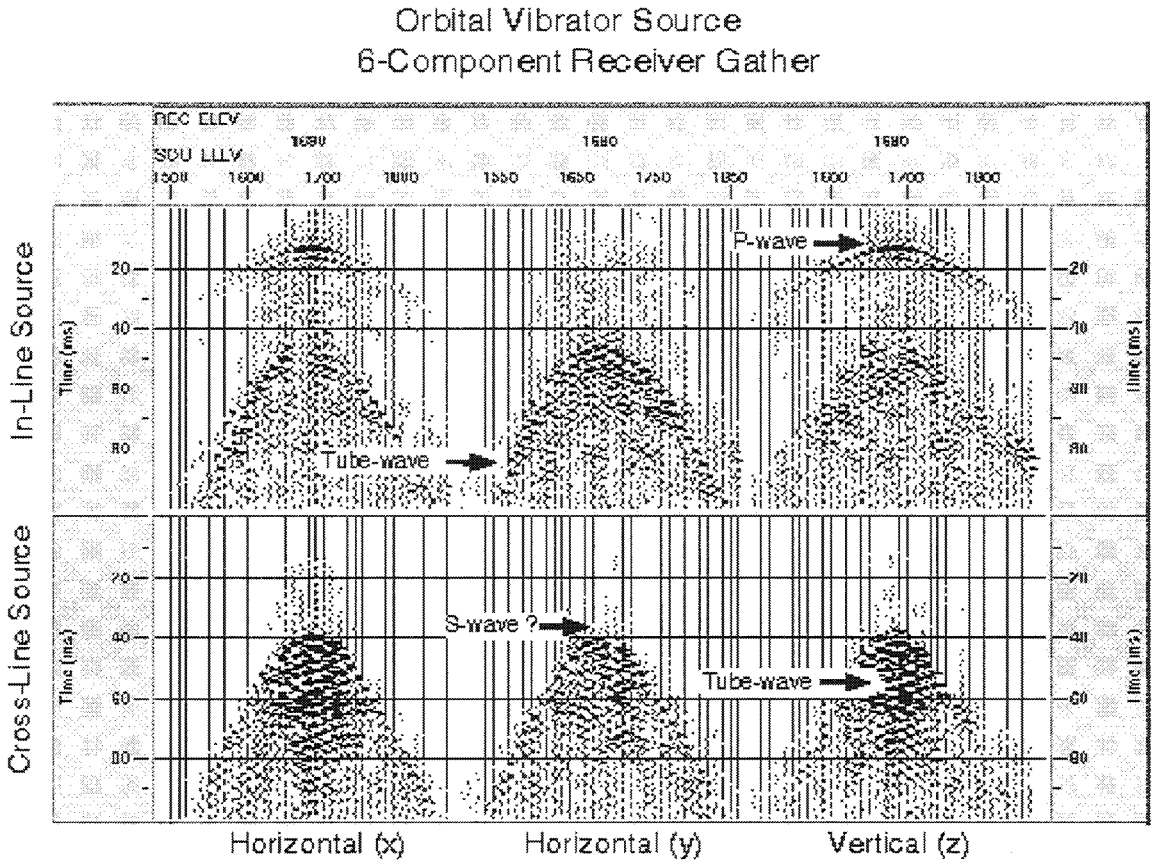

Figure 4.8-5. 6-component data from orbital vibrator source (2-components) and 3-component receivers. P-waves and tube-waves are strong. S-wave is inferred from travel time.

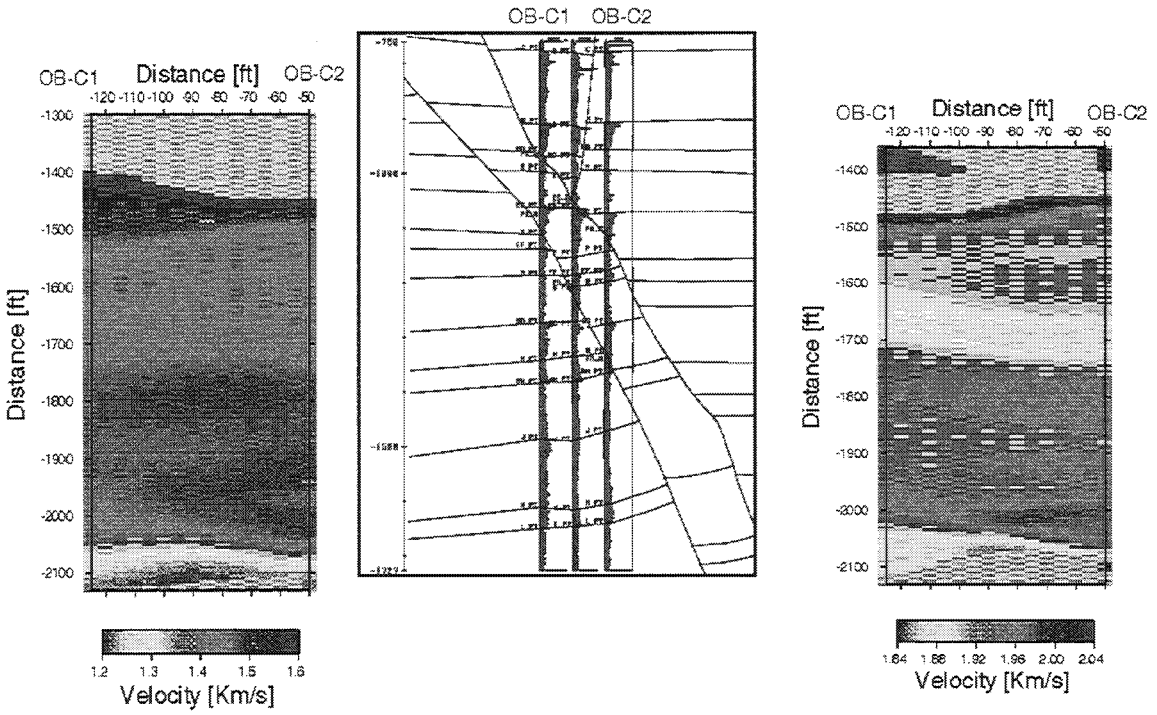

Figure 4.8-6. 6a (left) is a P-wave velocity tomogram for the orbital vibrator source showing the low frequency response. 6b (center) is the interpreted cross section for wells OB-C1, 11-8WR, and OB-C2 (left to right) with diatomite horizons and interpreted fault zone from (Chevron USA). 6c (right) is the velocity tomogram for the piezoelectric source showing the high frequency response.

4.9 NUMERICAL MODELING FOR CROSSWELL SEISMIC

G. Michael Hoversten
Lawrence Berkeley National Laboratory

Introduction:

As part of LBNL's work on carbon sequestration in geologic formations we are conducting numerical modeling and field data acquisition of crosswell seismic and electromagnetic (EM) data at Chevron's Lost Hills CO_2 injection pilot. Numerical forward models have been generated from reservoir flow simulations provided by Chevron. The objective of the modeling works is to provide an understanding of the relationships between the reservoir parameters, the fluid and CO_2 saturations and the observed geophysical data that will be used to monitor the injection process. The relationships developed through forward modeling will then be used to interpret the field data in terms of fluid saturations and CO_2 content. We are only in the initial stages of forward and inverse modeling. So far we are working with the pre-injection model to explore the relations between the reservoir flow simulations and the geophysical data taken prior to injection. Future work will include modeling the geophysical response to CO_2 injection.

Numerical model of the Pilot Area:

We have begun work with a flow simulation that modeled the waterflood of the area of the OB-C1 and OB-C2 wells up to the beginning of CO_2 injection. Figure 4.9-1 shows the well locations and the area of the field covered by the flow simulation.

The flow simulation parameters of interest for the geophysical modeling are porosity, pressure and fluid saturation. In order to convert these to seismic velocity and electrical conductivity log data, data from Well 166 was used for seismic velocities and data from the OB-C1 was used for electrical conductivity. A model published by Dvorkin & Nur (1996) for unconsolidated sand grains coupled with Gassmann's equation (Gassmann 1951) was used to relate the porosity, pressure and fluid saturations to velocity. A simple mixing law for porosity and fluid saturations is used to predict density. While the Dvorkin & Nur model is not specifically for diatomite it does a good job of predicting the observed p-wave velocity and density simultaneously for the available logs given the logged porosity and saturations, and assuming a hydrostatic pressure gradient. The velocities are not to sensitive to pressure and will be refined with pressure data from the flow simulations later. Figure 4.9-2 shows the regression fit for the 166 well velocity and density logs.

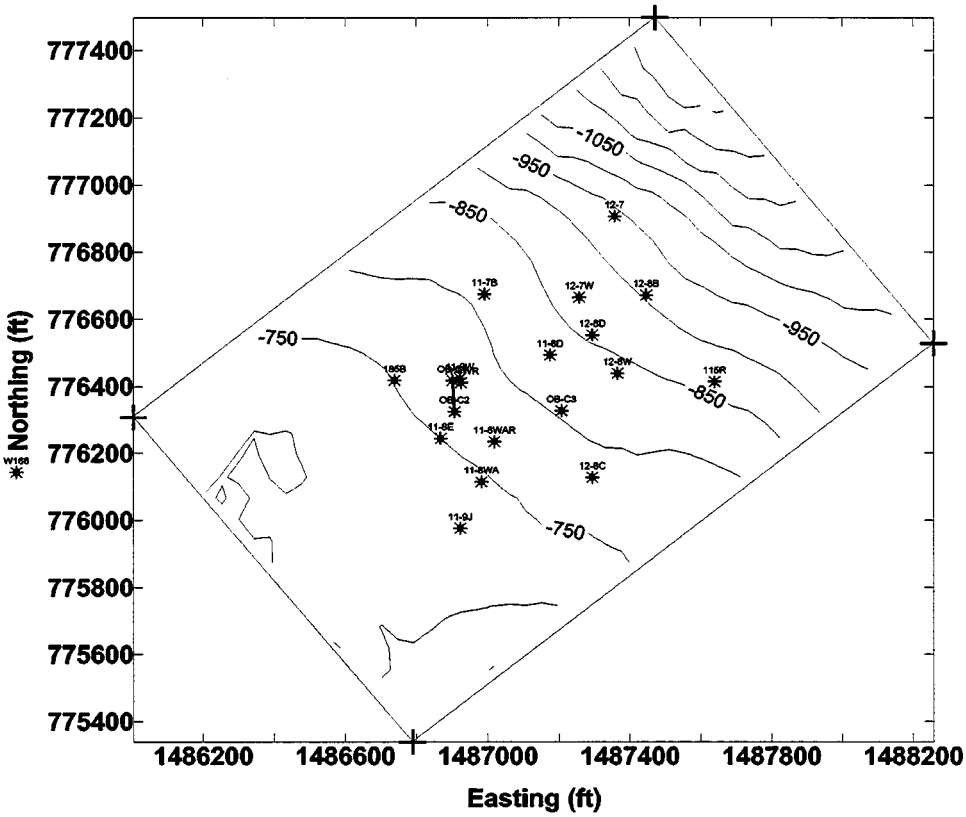

Figure 4.9-1: The area covered by the flow simulation is surrounded by the rectangle with red crosses at the corners. The cross well seismic and EM data was acquired between OB-C1 and OB-C2 shown as the red line near the center of the figure. The 166 well used for developing the velocity model is to the west just below the vertical axis annotation. Contours show structure on the top of the reservoir interval.

It is observed that the largest errors in matching the 166 well velocity log occur where there is significant gas saturation. We are currently considering other models to address this and will be doing further modeling to determine a model with better performance in the presence of gas. This will be supported by on going laboratory measurements of the sonic velocity and electrical resistivity in diatomite cores during CO_2 flood.

In order to calculate electrical resistivity in the 3-D model the water saturation and porosity were used in an Archie's law regression. Figure 4.9-3 shows the results of fitting the OB-C1 resistivity log. The models illustrated in Figures 4.9-2 and 3 were used to construct a 3-D velocity, density and electrical resistivity cube. Figure 4.9-4 shows the porosity cube from the model.

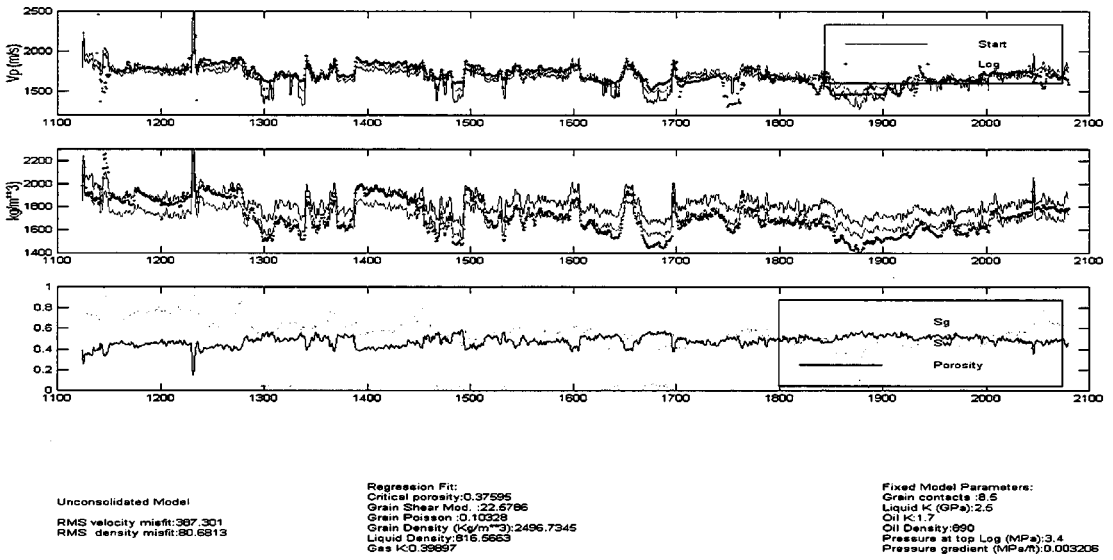

Figure 4.9-2: Log p-wave velocity, density, porosity, Sw and Sg used in multi-parameter minimization for Dvorkin & Nur model parameters. Upper panel: Observed Vp - red curve, Starting Vp - blues curve, Final Vp - magenta curve. Middle panel: Observed density - red curve, Starting density - blue curve, Final density - magenta curve. Bottom panel: green curve - water saturation, light blue curve - gas saturation, black curve - porosity.

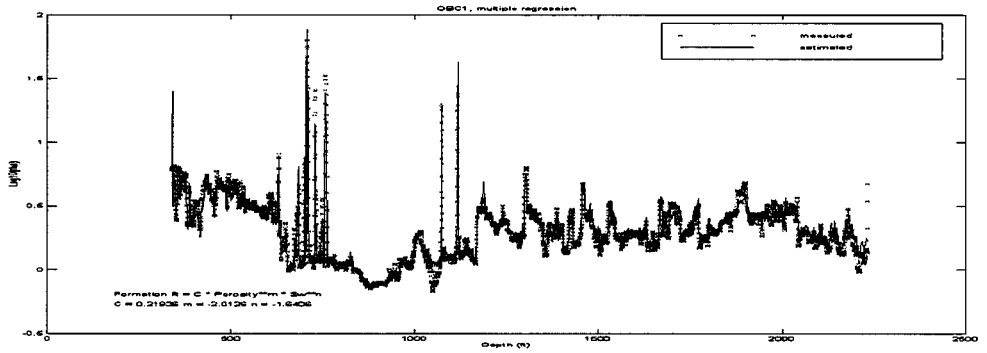

Figure 4.9-3: OB-C1 deep induction resistivity log (RED) compared to the Archie's Law regresion (BLUE).

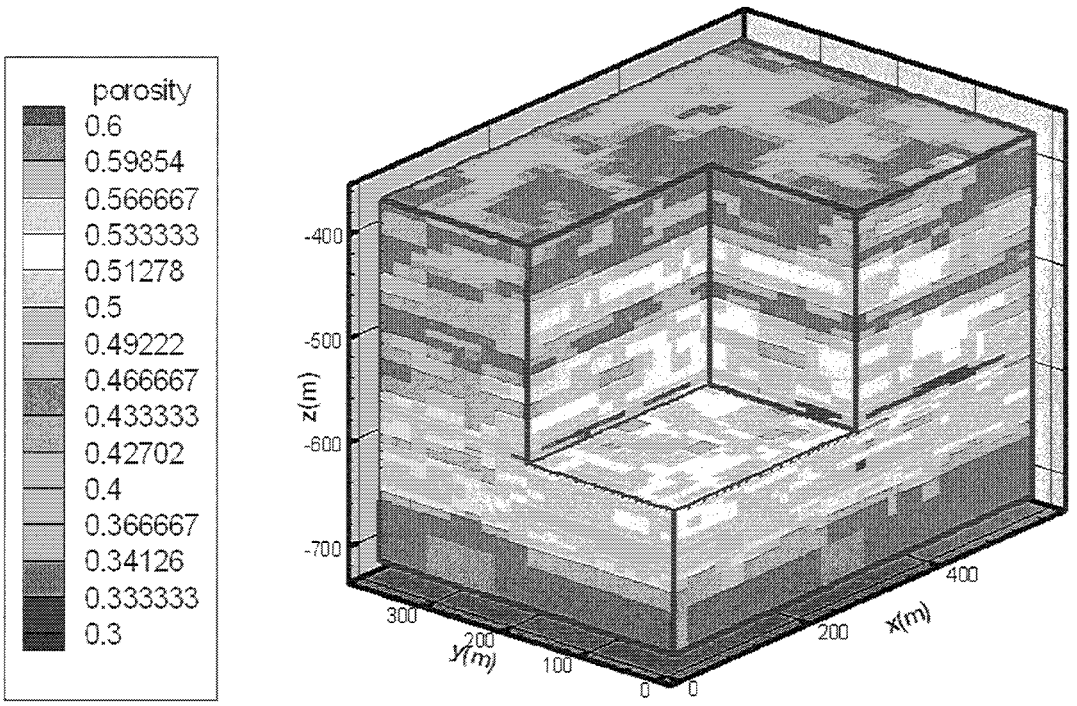

Figure 4.9-4: 3-D porosity cube viewed from the southwest. Northwest face of cutout section corresponds to approximate location of the OB-C1 well.

A two-dimensional cross section between the OB-C1 and OB-C2 wells was extracted from the 3-D model for use in initial 2-D forward modeling. Forward 2-D and 3-D elastic and EM modeling has been done. As a first pass to check velocities the 2-D elastic simulation used a pressure source. The field data was acquired with an orbital vibrator so the wave fields are not the same. However, this comparison does show that are model velocities are roughly 10% to low. Figure 4.9-5 shows the 2-D elastic response for a single shot at a depth of 567 m compared to the field data for this shot location.

We are currently setting up the 3-D velocity model with the proper orbital vibrator source for simulation and examining why the velocities converted from the reservoir simulation are to low.

Initial Field Data Inversion

The before injection field data has been inverted using first break travel time tomography and 2-D electromagnetic inversion. Figure 4.9-6 shows the velocity tomogram and the inverted electrical conductivity sections. These initial images both have features, which seem inconsistent with the local geology. The velocity section shows apparent dips that are to high where as the electrical conductivity section contains horizontally elongated "bulls eye" features in the center of the section. In addition there seems to be little spatial correlation between the velocity and electrical conductivity. We are working to understand these images and attempting to improve them.

Work is continuing on the data sets taken prior to injection so that our modeling and inversion tools will be ready when the first time-lapse measurements are taken just after CO_2 break through.

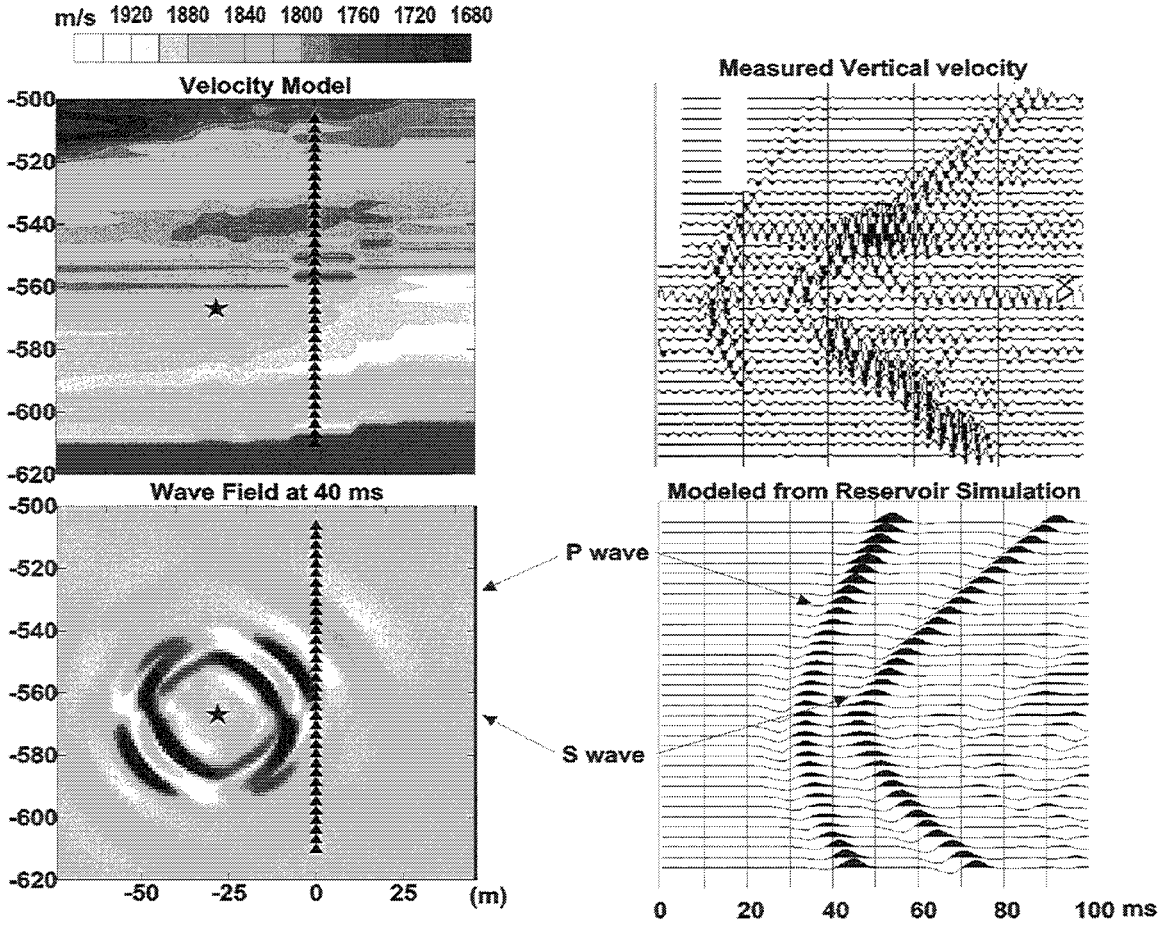

Figure 4.9-5: Two-dimensional elastic forward model based on reservoir simulation. Velocity was converted from reservoir parameters using the relations illustrated in Figure 2. The measured field data is compared to the calculated data showing a time shift that indicates our model velocities are on the order of 10% to low.

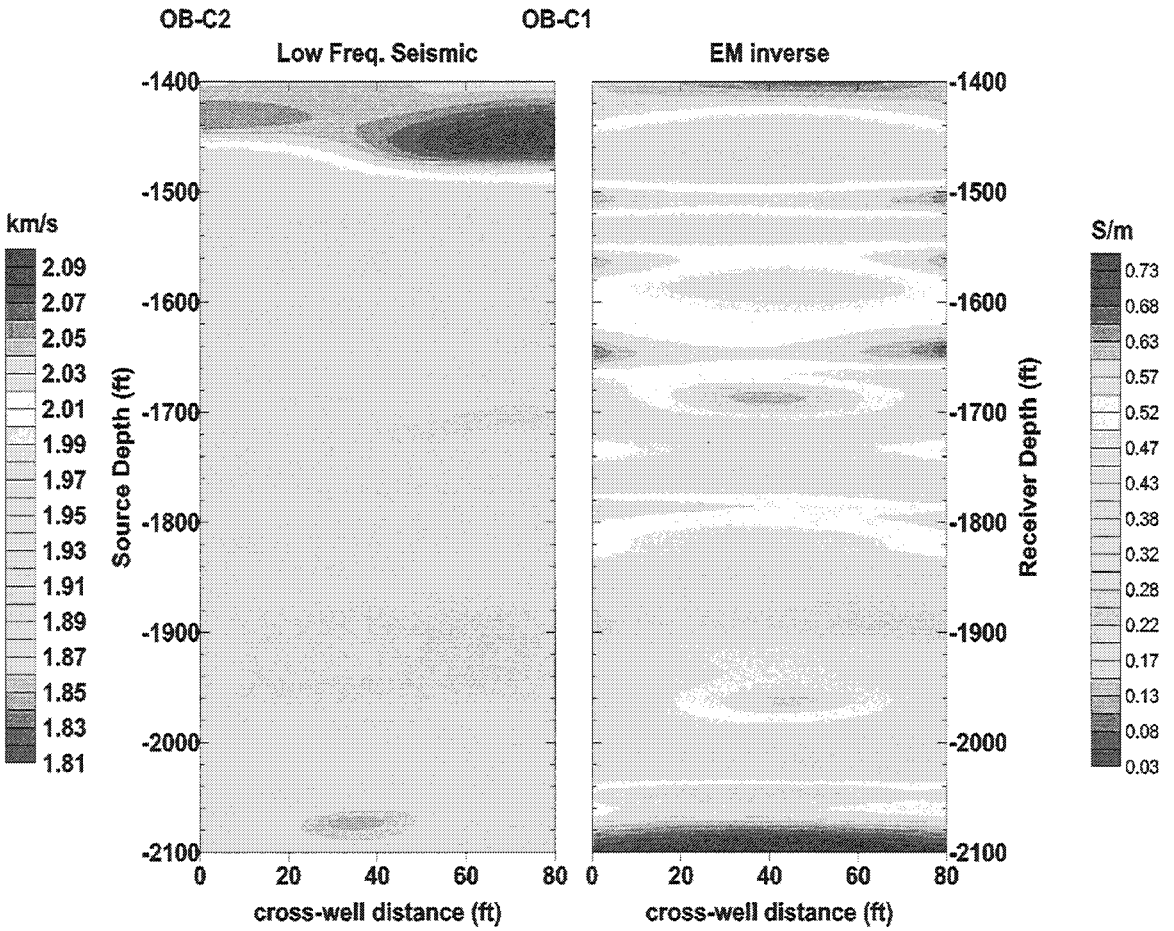

Figure 4.9-6: Left panel - first break travel time tomogram. Right panel - crosswell EM inverted conductivity using only the vertical magnetic field.

4.10 PRESSURE OBSERVATIONS

Pasquale R. Perri
Chevron USA Production Company

A dedicated pressure observation well was drilled and completed for the CO_2 pilot. It contains a "short string" (1749 ft mid-perf depth) and a "long string" (1920 ft mid-perf depth) to monitor average reservoir pressure changes during the pilot. Figure 4.10-1 is a plot of the short string and long string measurements since commencing CO_2 injection on August 31, 2000. We are perplexed why the short string (shallower) reads higher that the long string (deeper). In addition, the pressure observation well readings are significantly lower than RFT pressure data taken from pilot producer 12-8D in 1999 (see Figure 4.10-2).

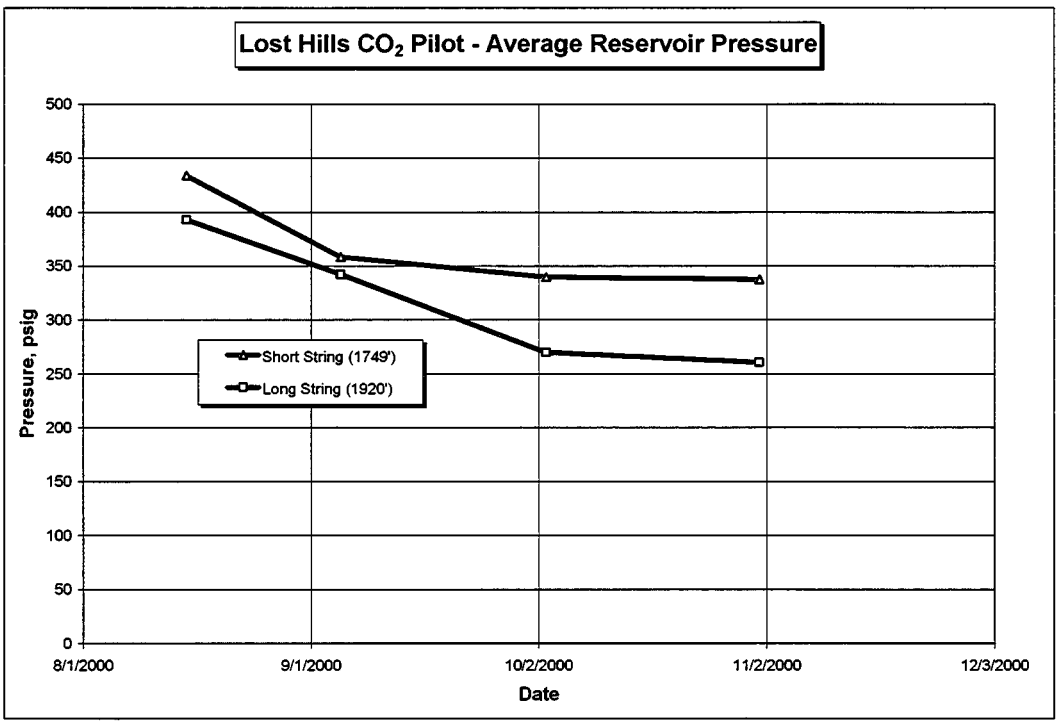

Figure 4.10-1. Average Reservoir Pressure for CO_2 Pilot.

A recent tracer injection test into the pressure observation well indicated the possibility of a poor cement bond. We hope to substantiate these results and possibly implement cement-squeezing techniques to rectify the problem. In late December 2000, the four CO_2 injectors were shut-in after experiencing sanding problems in four pilot producers.

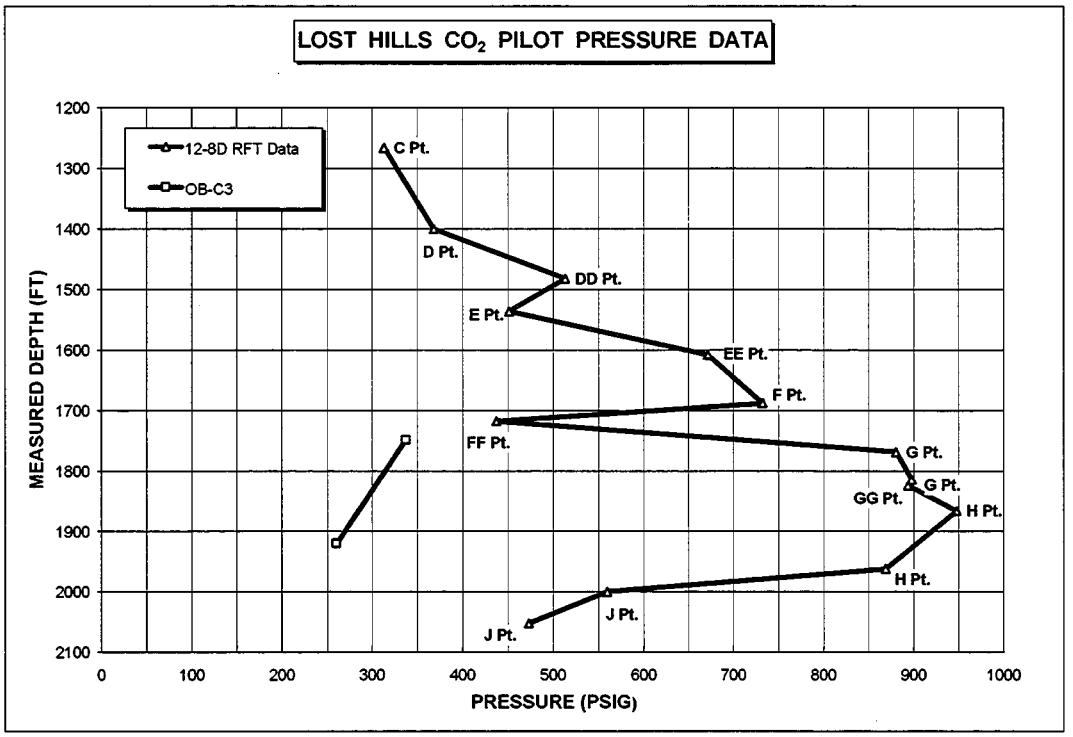

Figure 4-10-2. RFT Pressure Data Compared to Observation Well Data.

Table 4.10-1 is a summary of the static bottomhole pressure surveys run on each of the four injectors after they had been shut-in for approximately three weeks. The shut-in bottomhole pressure measurements are substantially higher than the pressure observation well data and are more in line with the recent RFT measurements (Figure 4-10-2).

Table 4-10-1. Shut-In Bottomhole Pressure for Pilot Injectors.

Injector	Shut-In BHP (psi)
11-8WR	901
11-8WAR	1283
12-7W	1026
12-8W	1222

4.11 SURFACE TILTMETER FRACTURE MAPPING IN THE CO_2 INJECTION PILOT

Eric Davis
Pinnacle Technologies, Inc.

This report discusses surface tiltmeter fracture mapping results for the CO_2-injection pilot in section 32 of the Lost Hills Field at a target depth between 1600 and 2100 ft. CO_2-injection was conducted for several months in 4 wells, 11-8WR, 11-WAR, 12-8W and 12-7W, after conducting propped fracture treatments in all wells. To determine the CO_2-injection induced fracture orientation, the "negative image" of the fracture was mapped by conducting a shut-in on each of the four well on subsequent days with the goal to determine the change in tilt signal from the individual closing fractures.

Although surface tilt mapping of CO_2-injections has been successfully conducted in the past, results in this project are not as clear-cut as we would like. The main reason for the high uncertainty in the surface tilt mapping results lies in power outages throughout the Lost Hills Field that occurred very quickly after all of the four shut-ins. These power outages, where all injection and production activities in the field suddenly stop, largely "overwhelm" the changes in surface tilt signals that are induced by the shut-in at individual CO_2-injection wells. As a result, the azimuth and dip uncertainties generated by these power outages are much larger than normal.

Background and Past Surface Tilt Mapping of CO_2 Injections:
Chevron currently utilizes many processes to recover its reserves: primary recovery (stimulation), secondary recovery (water flooding), and tertiary recovery (steam flooding). In an effort to increase reserve recovery and lower operating costs, Chevron is investigating another tertiary process, CO_2-injection.

Surface tiltmeters were mobilized into the CO_2-injection pilot in section 32 of the Lost Hills Field area in February 2000, and were first utilized to determine the fracture orientation of propped fracture treatments in wells 11-8WR and 11-WAR. Wells 12-8D and 12-7W in section 32 were propped fracture treated in 1999. Results of the propped fracture treatments in the two newer wells are consistent with typical high-rate propped fracture orientations in this area of the Lost Hills, with an average fracture azimuth of N 68° E and an average fracture dip of 89° down-to-the-SE.

Past surface tilt mapping on wells 12-8D and 12-7W clearly showed two preferred fracture orientations for low-rate CO_2-injections at orientations that were roughly 45° different from the propped fracture azimuth. SPE 54079 (co-authored by Mark Emanuele and John Broussard from Chevron) discusses a similar phenomena that was observed during steam injections, where fractures grow predominantly along two distinct planes rotated roughly 45° with respect to the preferred fracture plane – the planes of maximum shear stress. It is believed that the fracture growth direction for low injection rates (including CO_2-injections)

may differ from the direction for high injection rates if enhanced leakoff through shear fractures increases the pore pressure ahead of the fracture tip.

Following the propped fracture treatments, low-rate water injection was conducted on all four wells in the pilot in May 2000. Although mapping of low-rate water, steam and CO_2 injections have been successful in the past, mapping results were inconclusive due to ongoing propped fracturing activities in nearby wells that overwhelmed the tilt signals induced by these low-rate water fractures.

Discussion of CO_2 Injection Mapping Results:

In December of 2000 a series of shut-ins were conducted on each of the four wells to determine the tilt signal that would be induced by a closing fracture system. This type of analysis requires that all activities in other wells continue as normal, so that the "background signal" from these other activities remains the same. If only one CO_2-injection well is shut-in at the time, the change in tilt signal will reflect the "image" of the closing fracture.

Unfortunately, these conditions were NOT met due to accidental power outages that occurred quickly after each of the four shut-ins, which is the period used for background data. These power outages result in a change in tilt response from more than the single well that was targeted for shut-in. As a matter of fact, a power outage causes ALL of the field injection and production activity to suddenly stop. As shown in Figure 4.11-2, the change in tilt signal from the power outage is much larger than the change in tilt from the shut-in, and greatly overwhelms this response. Therefore, there is higher uncertainty in the tilt induced from the shut-in in the individual well. As a result, the vector maps, which comprise the tilt from multiple surface tilt sites, do not show the familiar pattern associated with hydraulic fracture growth.

Figure 4.11-3 shows an example of a vector map, and one of the things that jumps out is that some of the largest tilt signals occur far away from the wellbore, indicating that deformation is occurring farther away from the well.

Table 4.11-2 and Figure 4.11-1 show the fracture orientation results from the shut-in cycles in each of the 4 wells. Note that azimuth uncertainties are of order 45°, which is much higher than our typical 3° for propped fractures at this depth or the typical uncertainty of ~8-10° for low-rate injections. Although the data quality is rather poor due to power outages, some of the CO_2 fractures appear to grow along shear planes at roughly a 45° angle with the local preferred fracture plane, especially in wells 11-8WR and 11-8WAR that were recently propped fracture treated. This is consistent with earlier CO_2-injection tilt mapping results in wells 12-8D and 12-7W. In well 12-7W and 12-8W, however, this pattern is not so obvious.

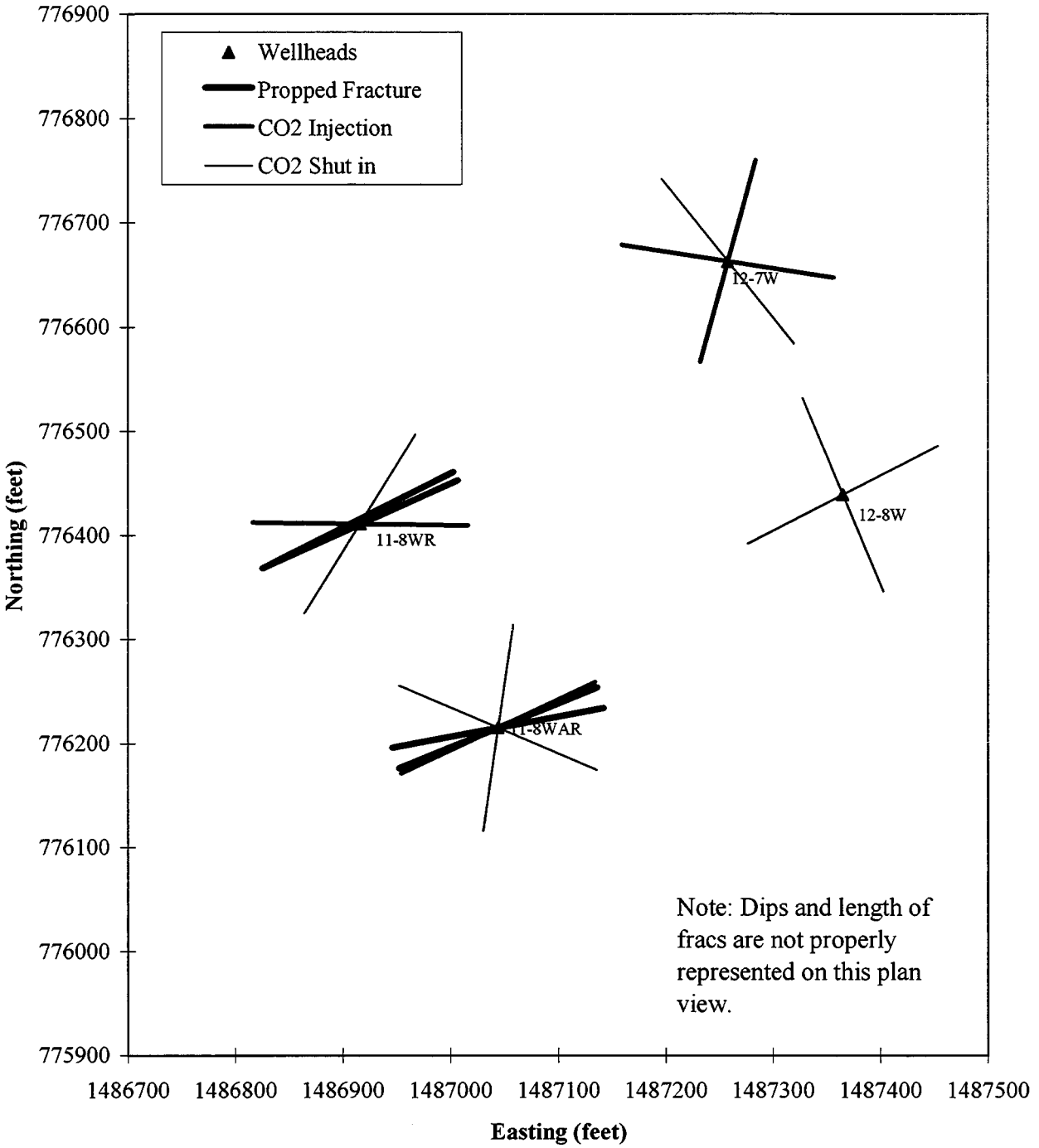

Figure 4.11-1. Map showing fracture orientation that were measured for several propped fracture treatments and CO_2-injection cycles in 4 wells in the section 32 CO_2-pilot in the Lost Hills Field. The propped fracture orientations are consistent with the local field average, but CO_2-induced fracture systems are significantly different. Although the data quality is rather poor due to power outages, some of the CO_2 fractures appear to grow along shear planes at roughly a 45° angle with the preferred fracture plane.

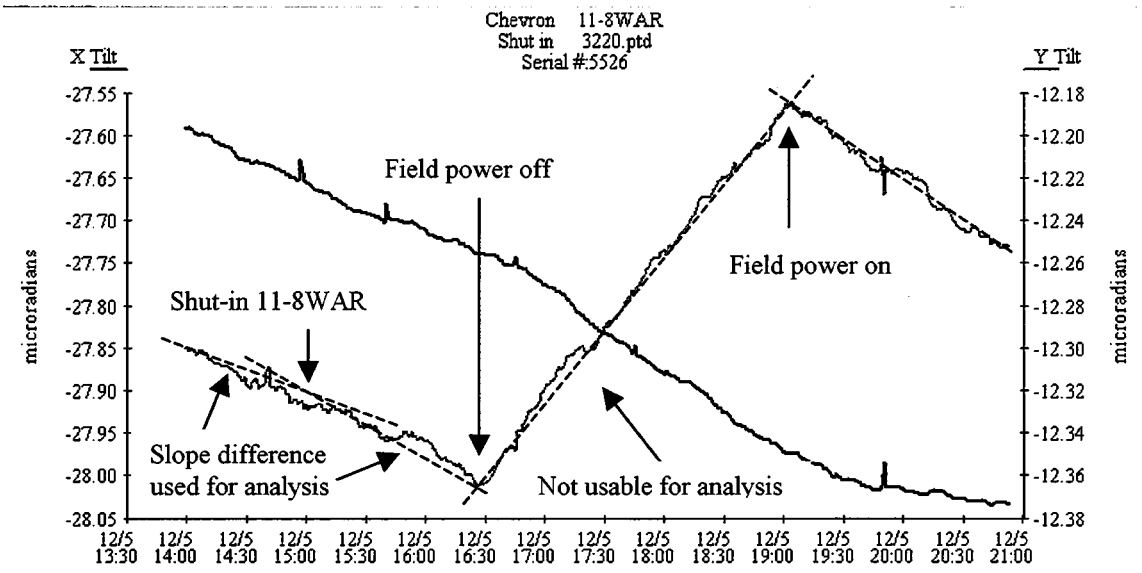

Figure 4.11-2. Signal plot showing shut-in of well 11-8WAR and power shut down on 12/05/00. The difference in slope in tilt response just before and just after the shut-in is used to determine the total tilt response. For a normal analysis and more accurate analysis, however, we would also use the change in slope once the CO_2-injection starts back up. This data became not unusable for the analysis due to the power outage that occurred early after the shut-in.

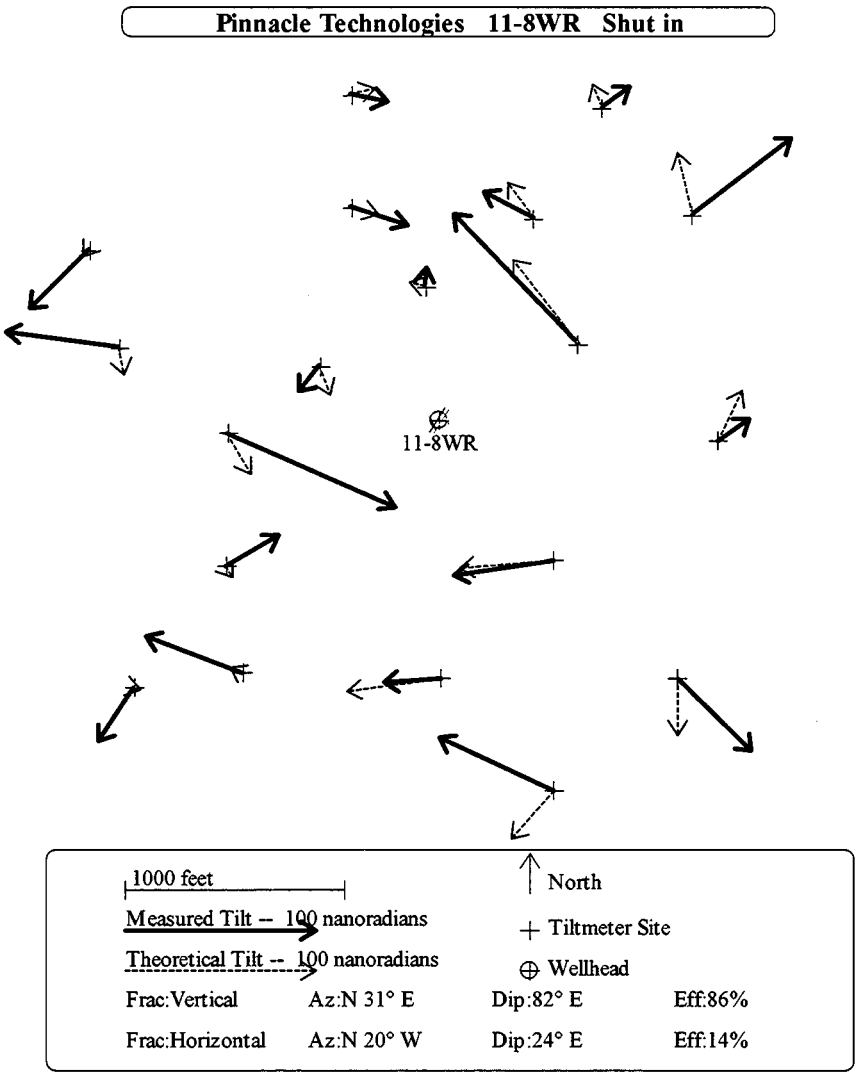

Figure 4.11-3. Vector plot for well 11-8WR on 12/04/00 (shut in).

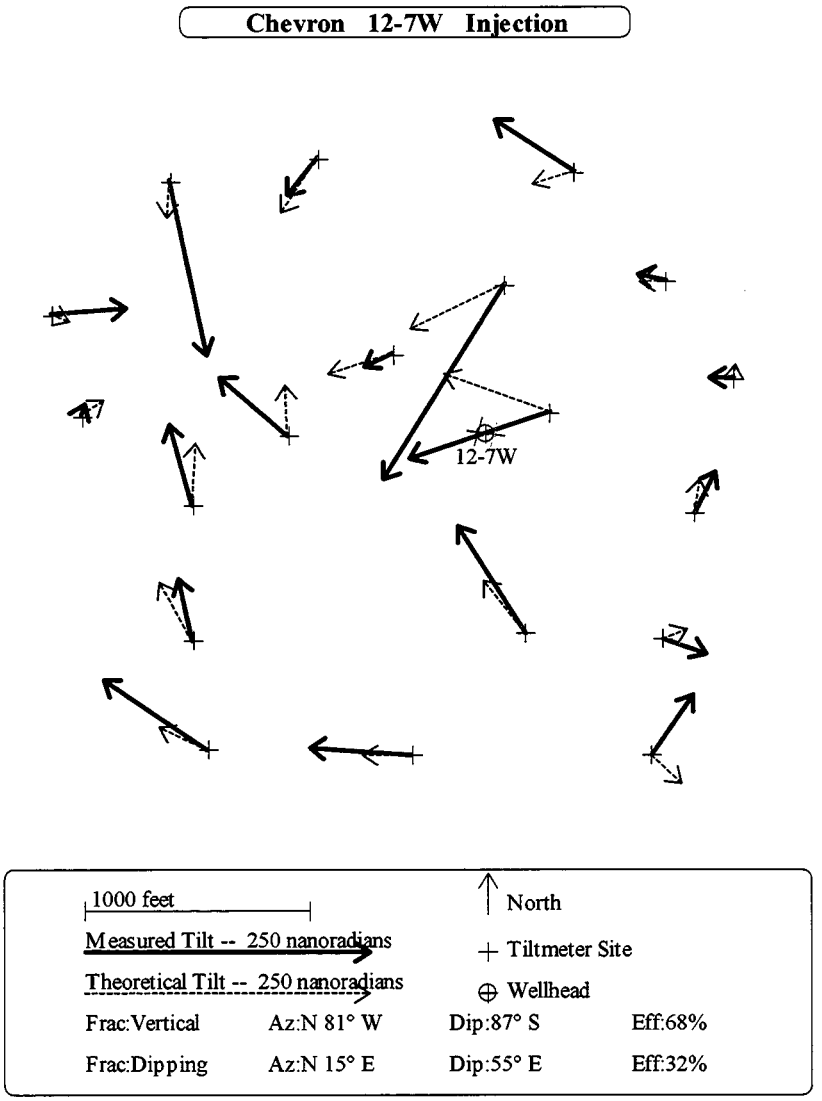

Figure 4.11-4. Vector plot for well 12-7W on 12/08/00 (injection).

Table 4.11-1. Surface tiltmeter fracture mapping results for propped fracture treatments in wells 11-8WAR and 11-8WR.

Well Name	Stage #	Job Date mm/dd/yy	Perforation Interval (ft)	Fracture Azimuth	Fracture Dip	Vol % Horizontal Component
11-8WAR	1	07/15/00	1898 - 2105	N 67° E ± 3°	88° down to the SE ±2°	24%
	2	07/15/00	1605 - 1785	N 79° E ±2°	88° down to the NW ±2°	35%
11-8WR	1	07/15/00	1847 - 2035	N 65 E ± 2°	85° down to the NW ±2°	24%
	2	07/15/00	1605 - 1785	N 60 E ± 2°	80° down to the SE ± 2°	21%
Average				**N 68°E**	**89° down to the SE**	**26%**

Table 4.11-2. Injection/Shut-in Summary and Fracture Orientation Results for Chevron CO_2-injection wells 11-8WR, 11-8WAR, 12-8W, and 12-7W.

Well	Date	Time	Description	Azimuth	Dip	Vol % of Component
11-8WR	Indefinite		Injection			
	12/04/00	15:12	Shut in	N31°E±45°	82° down to SE ±30°	86%
				-	Horizontal	14%
	12/04/00	17:00 – 19:50	Power shut down			
	12/05/00	08:45	Starting injection	N89°W±45°	85° down to SW ±30°	68%
				-	Horizontal	32%
11-8WAR	Indefinite		Injection			
	12/05/00	15:00	Shut in	N8°E±35°	80° down to NW ±25°	85%
				N66°W±45°	Dipping	15%
	12/05/00	16:20 – 19:00	Power shut down			
	12/06/00	07:36	Starting injection	N64°E±45°	77° down to SE ±30°	74%
				-	Horizontal	26%
12-8W	Indefinite		Injection			
	12/06/00	15:05	Shut in	N62°E±45°	80° down to SE ±30°	49%
				N22°W±35°	Dipping	51%
	12/06/00	16:30 – 21:00	Power shut down		-	-
	12/07/00	7:30 – 8:30	Power shut down	No injection is analyzed	-	-
12-7W	Indefinite		Injection			
	12/07/00	15:00	Shut in	N38°W±45°	80° down to SW ±25°	87%
				-	Horizontal	13%
	12/07/00	16:30 – 20:30	Power shut down			
	12/08/00	07:25	Starting injection	N81°W±30°	87° down to SW ±25°	77%
				N15°E±35°	Dipping	23%

4.12 CORROSION MONITORING

John F. Cooney
Chevron USA Production Company

General Description:

The intent of the corrosion monitoring program is to determine the impact of produced CO_2, in higher concentrations, on our existing facilities. It will help us determine what facilities and flowlines would need to be replaced or upgraded, due to CO_2 corrosion, if the pilot is successful. If excessive corrosion is detected, we will attempt to mitigate it utilizing chemicals. If necessary, some flowlines and facilities will be replaced. Mitigation measures will be scaled up to evaluate facility costs (capital and operating expenditures) for full-field CO_2 development.

Benchmarking:

Producing Wells & Flowlines

Baseline iron and hardness samples were taken on each of the 10 producing wells in the CO_2 flood every day from August 14, 2000 to August 18, 2000. The corrosion rate was also measured prior to commencing CO_2 injection. In addition, a total water analysis was also run on each producing well.

Production Facilities

Corrosion rates were monitored on the pool lines leaving the CO_2 gauge setting, and on the main pool line coming from an adjacent production facility.

Continuos Monitoring

Iron loss and hardness at each well are being monitored weekly. Corrosion coupons are measured every two weeks. If and when breakthrough occurs at a well, a LPR probe (resistivity probe that correlates to corrosion rate) is installed to replace the corrosion coupon in order to monitor corrosion rate in a shorter time frame. The oil/water pool line leaving the gauge setting is being continuously monitored with a LPR probe. In December 2000 and January 2001, LPR probes were added to the wells that have seen a significant amount of CO_2 tracer. New data from these LPR probes will not be compiled until March 2001.

Results for Well Flowline Corrosion:

For the first few months of the pilot, only well 11-8E had a LPR probe (due to their high cost). The orange line in Figure 4.12-1 shows these LPR readings. Corrosion coupons were being utilized to monitor the other 9 wells. Even though the monitoring shows signs of increased corrosion, the increase is not significant enough to require chemical or facility changes for protection.

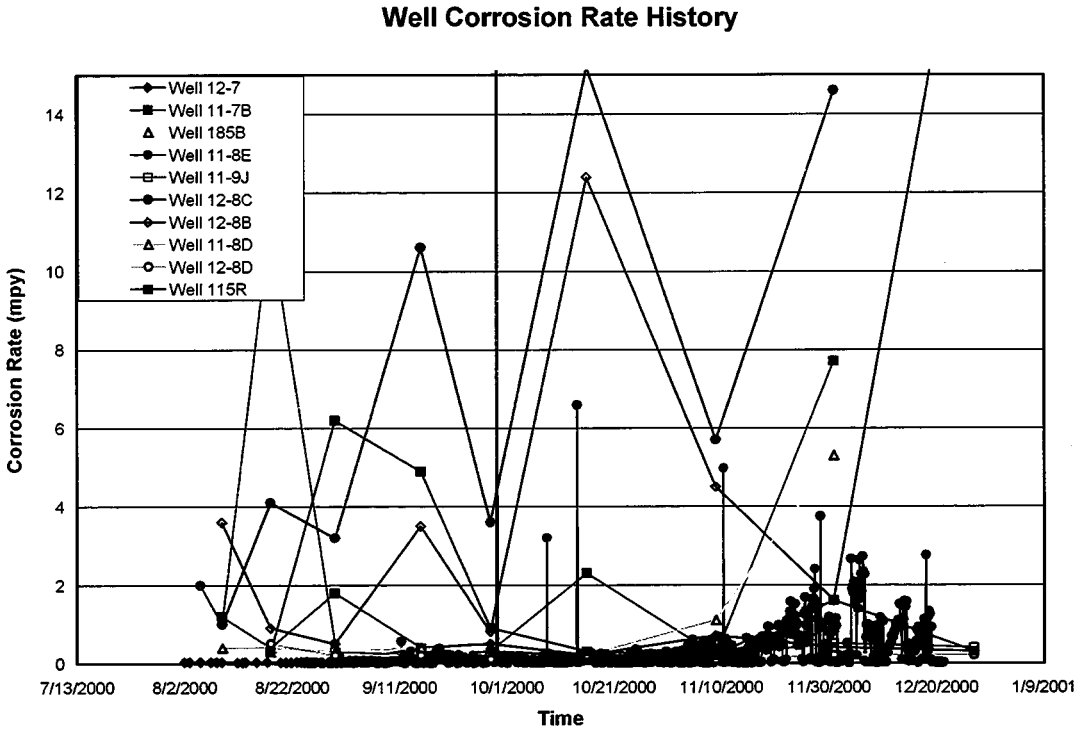

Figure 4.12-1: Well Corrosion Rate History Chart

LPR Probe Results:
The LPR readings at 11-8E correlated very well to breakthrough of CO_2 in this producing well. Readings started to climb slightly only a few weeks after CO_2 injection started (early September 2000). The LPR readings increased significantly in November 2000, which is also when we started to measure significant CO_2 production from this well.

Corrosion Coupons:
Data from corrosion coupons has a large amount of error. As you can see from Figure 4.12-1 above (the Well Corrosion Rate History Chart), it is very difficult to draw any conclusions. Of the three wells that saw a large CO_2 flow rate increase (12-8D, 11-8D, and 12-7), only 11-8D showed any signs of flowline corrosion increases. This happens to be the center pilot producer. The uncertainty in the corrosion coupons resulted in another four LPR probes being installed on producers that are starting to see CO_2 breakthrough.

Iron Loss Counts from Wells:
Iron loss counts are an indication of how much iron loss is occurring in the well. There have been no measurable changes in the iron loss counts for the producing wells in the pilot.

Production Line / Facility Corrosion:
No conclusions can be reached from corrosion data taken at critical points in the production system. Changes in the LPR probe, dark blue line in Figure 4.12-2, do not correlate to changes

in CO_2 concentrations. The data from the corrosion coupons has too much error to detect the subtle changes.

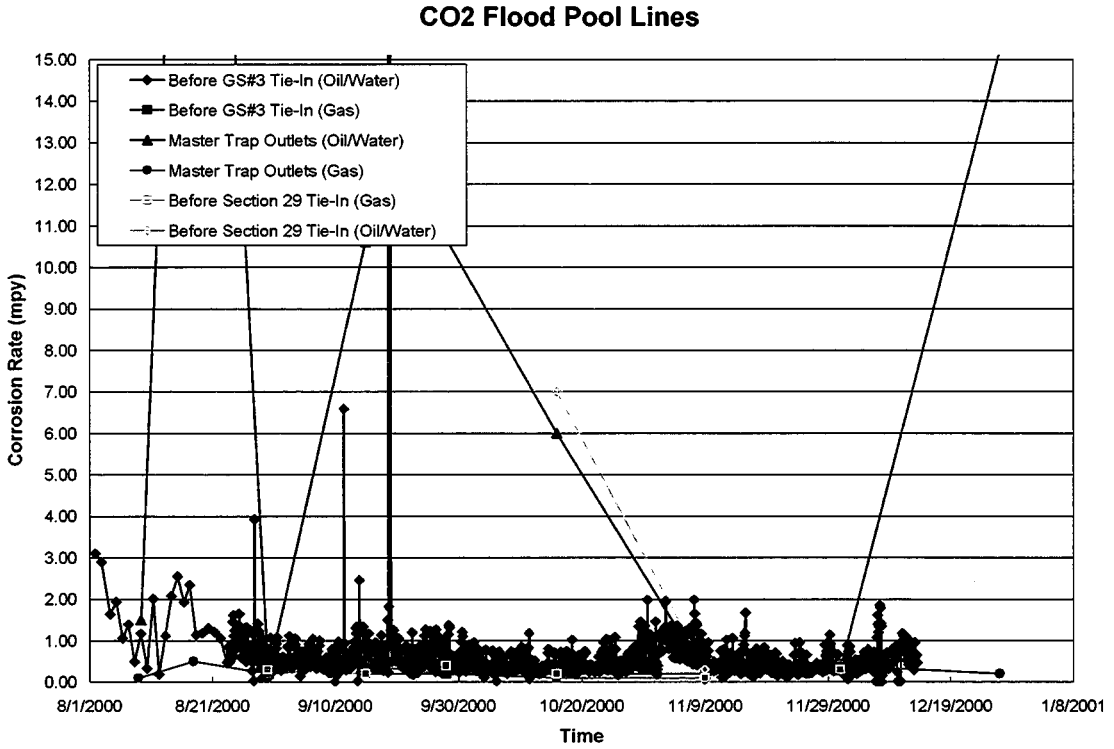

Figure 4.12-2: Production Lines/Facilities Corrosion Rate History Chart

SECTION 5

TECHNOLOGY TRANSFER

5.1 TECHNOLOGY TRANSFER

Aydin, A., 1997, Fault Control on Hydrocarbon Migration and Fluid Flow in Neogene Basins and Related Reservoirs of Central and Coastal California, USA: An Overview, in, Pollard, D. D. and Aydin, A. eds., Proceedings of the Rock Fracture Project Workshop, Stanford University, Stanford, CA.

Aydin, A., Dholakia, S. K., Antonellini, M., and Lore, J., 1996, Fault Control on Hydrocarbon Migration in Neogene Basins in Central and Coastal California, USA, Faulting, Fault Sealing and Fluid Flow in Hydrocarbon Reservoirs, Conference, University of Leeds.

Bilodeau, B. J., and Smith, S. C., 1997, Session Chairmen for Reservoir Characterization and Improving Recovery in Monterey-type Siliceous Shales, Pacific Section AAPG/SEPM Annual Convention, Bakersfield, CA.

Bilodeau, B. J., Smith, S. C., and Julander, D. R., 1997, Comprehensive Reservoir Characterization Using Open-Hole Wireline Logs, Core, and Downhole Video, Buena Vista Hills Field, California, Pacific Section AAPG/SEPM Annual Convention, Bakersfield, CA.

Britton, A.W., Smith, J. L., and Chapman, D., 1997, Continuous Permeability and Porosity Determinations in the Chevron 653Z-26B Well, Buena Vista Field, Kern County, CA, Pacific Section AAPG/SEPM Annual Convention, Bakersfield, CA.

Britton, A. W., and Morea, M. F., 1998, Acoustic Anisotropy Measurements in the Siliceous Shale, 653Z-26B Well, Buena Vista Hills Field, California, AAPG Annual Convention, Salt Lake City, UT.

Campagna, D. J., Amos, J. F., and Mamula, N., 1998, Influence of Structure, Reservoir Compartments, and Natural Fractures on Oil and Gas Production in the Southern San Joaquin Basin, California, AAPG Annual Convention, Salt Lake City, UT.

Carpenter, A. B., and Moore, T. S., 1997, Origin of Boron-Rich Pore Water in the Monterey Formation, San Joaquin Valley, CA, Pacific Section AAPG/SEPM Annual Convention, Bakersfield, CA.

Daley, T.M., Majer, E.L., Gritto, R., Benson, S.M., 2000, Borehole Seismic Monitoring of CO_2 Injection in a Diatomite Reservoir, AGU, EOS, v. 81, n. 48.

Decker, D. and Bilodeau, B. J., 1997, Antrim Shale Resource and Reservoir Characterization as an Analog for Diffusion Controlled Gas Production from the Monterey Formation Pacific Section AAPG/SEPM Annual Convention, Bakersfield, CA.

Dholakia, S. K., 1995, An Integrative Study of Fractures and In Situ Stress in the Antelope Shale, Monterey Formation, Stanford Rock Fracture Project, Stanford University, Stanford, CA.

Dholakia, S. K., 1996, Outcrop to Reservoir: Importance of Faulting to Hydrocarbon Migration in the Monterey Formation, CA, Stanford Rock Fracture Project, Stanford University, Stanford, CA.

Dholakia, S. K., Aydin, A. Pollard, D. D., and Zoback, M. D., 1995, Relationship between Hydrocarbon Transport and Shearing Deformation in the Antelope Shale, Monterey Formation, San Joaquin Valley, California, GSA Annual Convention.

Dholakia, S. K., Aydin, A., Pollard, D. D., and Zoback, M. D., 1996, Hydrocarbon Transport and Shearing Processes in the Antelope Shale, Monterey Formation, San Joaquin Valley, California, AAPG Annual Convention San Diego, CA.

Dholakia, S. K., Aydin, A., Pollard, D. D., and Zoback, M. D., 1998, Development of Fault-controlled Hydrocarbon Pathways in the Monterey Formation, California, AAPG Bulletin, v. 82, no. 8, p. 1551-1574.

Dholakia, S. K., Aydin, A., Pollard, D. D., Zoback, M. D., and Barton, C., 1996, Integration of Geological and Borehole Image Data for the Interpretation of Conductive Structural Inhomogeneities in the Monterey Formation, California, Geological Application of Borehole Imaging Conference, Houston, TX.

Dholakia, S. K., Aydin, A, Pollard, D. D., Zoback, M. D., Barton, C., and Bilodeau, B. J., 1997, Integration of Surface Geology and Borehole Geophysics for Reservoir Characterization in the Monterey Siliceous Shales for the Purpose of Facilitating Improved Recovery Designs, Pacific Section AAPG/SEPM Annual Convention, Bakersfield, CA.

Dholakia, S. K., Aydin, A., Zoback, M. D., and Pollard, D. D., 1995, Plan for an Integrative Study of Fractures and In Situ Stress in the Antelope Shale, Monterey Formation, Stanford Rock & Borehole Geophysics Project Annual Report, Stanford University, Stanford, CA.

Dholakia, S. K., Lore, J., Brankman, C. M., and Roznovsky, T., 1996, Fault Control on Hydrocarbon Migration in the Monterey Formation, CA, Proceedings of the Stanford Rock Fracture Project Field Workshop, Stanford University, Stanford, CA.

Dholakia, S. K., Zoback, M. D., and Aydin, A., 1996, Stress State, Shearing Deformation and Implications for Hydrocarbon Transport in the Monterey Formation, California, Stanford Rock & Borehole Geophysics Project Annual Report, Stanford University, Stanford, CA.

Dholakia, S. K., Zoback, M. D., Barton, C., Aydin, A. and Pollard, D. D., Active Faults and Hydrocarbon Migration and Production in the Monterey Formation, California, Geophysics (in prep).

Fargo, D., 1997, Advanced Coring and Wellsite Handling Add Pizazz to Buena Vista Hills Core, Pacific Section AAPG/SEPM Annual Convention, Bakersfield, CA.

Fargo, D., 1997, Advanced Coring and Wellsite Case Study of Chevron/DOE Well 653Z-26B, Core Technology Meeting, Anchorage, AK.

Fargo, D., 1997, Case Study: Chevron/DOE Buena Vista Field Core Project, Technology Meeting, AERA Energy, Bakersfield, CA.

Jacobs, J. L., 1997, Characterization and Formation of En Echelon Fracture Arrays in the Monterey Formation, California. In, Pollard, D. D. and Aydin, A., eds., Proceedings of the Rock Fracture Project Workshop, Stanford University, Stanford, CA.

Kuuskraa, V., 1997, Incorporating Reservoir Characterization into Optimized Production of Siliceous Shales and Other Gas Bearing Shales, Pacific Section AAPG/SEPM Annual Convention, Bakersfield, CA.

Langan, R. T., 1997, Crosswell Reflection Imaging in the San Joaquin Valley: Buena Vista Hills, Society of Exploration Geophysicists, Development and Production Forum, Vail, CO.

Langan, R. T., 1997, Crosswell Seismology, Where We've Been and Where We're Going, Producers Executive Committee, Gas Research Institute, Chicago, IL.

Langan, R. T., 1997, Crosswell Imaging in West Texas and the San Joaquin Valley, Geosciences Department, Princeton University, Princeton, NJ.

Langan, R. T., Julander, D. R., Morea, M. F., Addington, C. M., and Lazaratos, S. K., 1998, Crosswell Seismic Imaging in the Buena Vista Hills, San Joaquin Valley: A Case Study, Annual International Meeting, Society of Exploration Geophysicists, New Orleans, LA.

Langan, R.T., Julander, D.R., Morea, M.F., Addington, C.M., and Lazaratos, S.K., 2000, Crosswell Seismic Imaging in the Buena Vista Hills, San Joaquin Valley: A Case History, Pacific Section Convention, AAPG, Long Beach.

Mamula, N., and Campagna, D. J., 1997, Determination of Reservoir Compartmentalization Using Mesoscopic Scale Fracture Analysis in the Buena Vista Hills Area of the Southern San Joaquin Valley, CA, Pacific Section AAPG/SEPM Annual Convention, Bakersfield, CA.

Montgomery, S.L., Morea, M.F., Perri, P.R., and Emanuele, M.A., 2000, New Effort to Evaluate EOR Possibilities in Monterey Formation, San Joaquin Basin, Oil and Gas Journal, September 25.

Montgomery, S.L., and Morea, M.F., in press, Antelope Shale (Monterey Formation), Buena Vista Hills Field: Advanced Reservoir Characterization to Evaluate CO_2 Injection for Enhanced Oil Recovery, AAPG.

Morea, M. F., 1997, Advanced Reservoir Characterization in the Antelope Shale to Establish the Viability of CO_2 Enhanced Oil Recovery in California's Monterey Formation Siliceous Shales, Oil Technology and Gas Environmental Program Review Meeting, Houston, TX.
Morea, M. F., 1998, Advanced Reservoir Characterization in the Antelope Shale to Establish the Viability of CO_2 Enhanced Oil Recovery in California's Monterey Formation Siliceous Shales, DOE/BC/14938-8, (DE98000484), 1997 Annual Report, National Petroleum Technology Office, US Department of Energy, Tulsa, OK.

Morea, M. F., 1999, Advanced Reservoir Characterization in the Antelope Shale to Establish the Viability of CO_2 Enhanced Oil Recovery in California's Monterey Formation Siliceous Shales, DOE/BC/14938-12, (OSTI ID: 5127), 1998 Annual Report, National Petroleum Technology Office, US Department of Energy, Tulsa, OK.

Morea, M. F., Julander, D. R., Zalan, T. A., and Beeson, D. C., 1998, Advanced Reservoir Characterization of the Siliceous Shale, Buena Vista Hills, California, Pacific Section AAPG Convention, Ventura, CA.

Morea, M. F., Zalan, T. A., and Jacobs, J. L., 1997, Buena Vista Hills Reservoir Characterization Study, Chevron/DOE Class III Reservoir Project. In, Advances in Reservoir Description Techniques as Applied to California Oil and Gas Fields Workshop, Pacific Section AAPG/SEPM Annual Convention, Bakersfield, CA.

Morea, M. F., Zalan, T. A., Julander, D. R., Beeson, D. C., and Britton, A. W., 1998, Advanced Reservoir Characterization of the Siliceous Shale, Buena Vista Hills, California: Integration of Geological, Geochemical, and Petrophysical Data, AAPG Annual Convention, Salt Lake City, UT.

Morea, M. F., and Zalan, T. A., in press, Chapter 3, Buena Vista Hills Field, California, Borehole Imaging, DOE/AAPG Advanced Logging Volume, Tulsa, OK.

Morea, M. F., and Zalan, T. A., in press, Chapter 4, Buena Vista Hills Field, California, Advanced Logging Tools, DOE/AAPG Advanced Logging Volume, Tulsa, OK.

Perri, P. R., 2000, Advanced Reservoir Characterization in the Antelope Shale to Establish the Viability of CO_2 Enhanced Oil Recovery in California's Monterey Formation Siliceous Shales, DOE/BC/14938-12, (OSTI ID: 5127), 1999 Annual Report, National Petroleum Technology Office, US Department of Energy, Tulsa, OK.

Perri, P.R., Emanuele, M.A., Morea, M.F., and Fong, W.S., 2000, Lost Hills CO_2 Pilot: Evaluation, Design, Injectivity Test Results, and Implementation, Western Regional Meeting, SPE, Long Beach, n. 62526.

Perri, P.R., Emanuele, M.A., Morea, M.F., and Fong, W.S., "Lost Hills CO_2 Pilot: Evaluation, Design, Implementation and Early Results," Sixth Annual Permian Basin CO_2 Flood Conference, Midland, TX, December 6, 2000.

Tang, R. W., Zhou, D., Beeson, D. C., Ulrich, R. L., and Morea, M. F., 1998, Immiscible CO_2 Floods in Low Permeability Reservoirs, International Energy Agency, Collaborative Project on Enhanced Oil Recovery, 19th Workshop and Symposium, Carmel, CA.

Toronyi, R. M., 1997, Advanced Reservoir Characterization in the Antelope Shale to Establish the Viability of CO_2 Enhanced Oil Recovery in California's Monterey Formation Siliceous Shales, DOE/BC/14938-7, (DE98000460), 1997 Annual Report, National Petroleum Technology Office, US Department of Energy, Tulsa, OK.

Wang, G. Y., 1997, 3-D Attenuation Imaging, Annual International Meeting, Society of Exploration Geophysicists, Dallas, TX.

Wang, G. Y., Harris, J. M., Magalhaes, C. G., Julander, D. R., and Morea, M. F., 1998, Buena Vista Hills 3-D Attenuation and Velocity Tomography, Annual International Meeting, Society of Exploration Geophysicists, New Orleans, LA.

Wilt, M., Zhang, P., Morea, M., Julander, D., and Mock, P., in press, Using Crosswell Electromagnetics to Map Water Saturation and Formation Structure at Lost Hills, SPE, Bakersfield, no. 68802.

Zalan, T. A., Morea, M. F., Julander, D. R., and Denoo, S. A., 1998, Applying Integrated Formation Evaluation to Advanced Reservoir Characterization in California's Monterey Formation Siliceous Shales, DOE/BDM OK/ PTTC Class Project Logging Workshop, Advanced Applications of Wireline Logging for Improved Oil Recovery, Denver, CO.

Zalan, T. A., Morea, M. F., Julander, D. R., and Denoo, S. A., 1998, Integrated Formation Evaluation in California's Monterey Formation Siliceous Shales, Buena Vista Hills Field, California, 1998, SPE Western Regional Meeting, Gems Session, Bakersfield, CA.

Zalan, T. A., Morea, M. F., Julander, D. R., and Denoo, S. A., 1998, Applying Integrated Formation Evaluation to Advanced Reservoir Characterization in California's Monterey Formation Siliceous Shales, Society of Professional Well Log Analysts, 39th Annual Logging Symposium, Keystone, CO.

Zoback, M. D., Barton, C., Finkbeiner, T., and Dholakia, S. K., 1996, Evidence for Fluid Flow along Critically-Stressed Faults in Crystalline and Sedimentary Rock, Faulting, Fault Sealing and Fluid Flow in Hydrocarbon Reservoirs, Abstracts, Conference, University of Leeds.

Data from this project has been given to Southwest Research Institute, San Antonio, TX and included in their project:

Parra, J. O., Characterization of Fracture Reservoirs using Static and Dynamic Data: From Sonic and 3D Seismic to Permeability Distribution, BDM Subcontract No. G4S51-731, and Prime Contract No. DE-AC22-94PC91008.